

**Enzymatic synthesis of selected amino acid
esters of sugars**

A thesis submitted to the

**University of Mysore
Mysore, India**

**for the degree of
Doctor of Philosophy**

in

CHEMISTRY

By

K. Lohith M.Sc.,

Fermentation Technology and Bioengineering Department
Central Food Technological Research Institute
Mysore- 570020, INDIA

August 2006



K. LOHITH
Senior Research Fellow
Fermentation Technology and Bioengineering
Central Food Technological Research Institute
Mysore – 570 020, India

Declaration

I hereby declare that the thesis entitled, “**Enzymatic synthesis of selected amino acid esters of sugars**”, submitted for the degree of **Doctor of Philosophy in Chemistry** to the **University of Mysore** is the result of the work carried out by me under the guidance of Dr. S. Divakar in the Department of Fermentation Technology and Bioengineering, Central Food Technological Research Institute, Mysore, during the period 2003-2006.

I further declare that the results of this work have not been submitted for the award of any other degree or fellowship.

Mysore
Date:10.08.2006



(K. Lohith)

Website : <http://www.cftri.com>

Grams : FOODSEARCH, Mysore

☎ : 0821- 2514760, 2516802, 2514306 ; Fax : 0821 - 2517233



केन्द्रीय खाद्य प्रौद्योगिक अनुसंधान संस्थान, मैसूर - 570 020, भारत
Central Food Technological Research Institute
Mysore - 570 020, India

cftri

Dr. S. Divakar
Fermentation Technology and Bioengineering
Central Food Technological Research Institute
Mysore - 570 020
E-mail: divakar643@gmail.com

Certificate

I hereby declare that the thesis entitled, "Enzymatic synthesis of selected amino acid esters of sugars", submitted by Mr. K. Lohith for the degree of **Doctor of Philosophy in Chemistry** to the **University of Mysore** is the result of the work carried out by him under my guidance in the Department of Fermentation Technology and Bioengineering, Central Food Technological Research Institute, Mysore, during the period 2003-2006.

Mysore
Date: 10-8-2006

S. Divakar
(S. Divakar)
PRD GUIDE

Acknowledgements

I express my deep sense of gratitude to my research supervisor, **Dr. Soundar Divakar** Scientist, Fermentation Technology and Bioengineering Department for giving me this wonderful opportunity to work under his personnel supervision. I am indubitably grateful for his suggestions, valuable guidance, highly constructive criticism, constant encouragement and support throughout the investigation.

I wish to express my deep sense of gratitude to Dr. N. G. Karanth, former Head, FTBE and Dr. M.C. Misra, Head, FTBE for their constant support and encouragement during my stay at the department.

My sincere thanks to Dr. V. Prakash, Director CFTRI, for providing an opportunity to work in this esteemed institute.

I would like to express my heartfelt thanks to Mr. B. Manohar, Scientist, Food Engineering department for his help in statistical analysis of my work.

I extend my sincere thanks to all scientists and technical staff of the FTBE department for their kind co-operation and support during my research work.

Help from the members of the Central Instrumentation Facilities and Services, Library and health center is greatly acknowledged.

My special thanks to staff of Nuclear Magnetic Resonance Research Centre, Indian Institute of Science, Bangalore for recording NMR spectra.

I am indebted to all my research colleagues of my lab Mr. G.R. Vijayakumar, Mr. B.R. Somashekar and Mr. R. Sivakumar for their support and friendship.

I would also like to acknowledge my other colleagues of FTBE and other departments for their kind co-operation and timely help.

Award of Junior Research Fellow and Senior Research Fellow by Council of Scientific and Industrial Research, New Delhi is gratefully acknowledged.

I consider myself very lucky to have highly motivating and supporting parents, brothers - Mr. Divakar and Mr. Sunil who were the guiding force behind all my success.

Kenchaiah Lohith

List of Patents and Publications

Patents

1. **K. Lohith**, G.R. Vijayakumar, B. Manohar and S. Divakar (2003). An improved method for the preparation of amino acyl esters of monosaccharides. PCT/IN03/00466, 498/DEL/2004
2. **K. Lohith**, B.R. Somashekar, B. Manohar and S. Divakar. (2005). An improved enzymatic process for the preparation of amino acyl esters of disaccharides. (Submitted to CSIR patent cell)

Papers

1. G.R. Vijayakumar, **K. Lohith**, B.R. Somashekar and S. Divakar. (2004). Lipase catalysed synthesis of L-alanyl, L-leucyl and L-phenylalanyl esters of D-glucose using unprotected amino acids. **Biotechnol. Lett.** 26, 1323-1328.
2. **K. Lohith** and S. Divakar. (2005) Lipase catalysed synthesis of L-phenylalanyl-D- glucose. **J. Biotechnol.** 117, 49-56.
3. V. Kamath, P.S. Rajini, **K. Lohith**, B.R. Somashekar and S. Divakar. (2006). Angiotensin Converting Enzyme inhibitory activity of amino acid esters of carbohydrates. **Int. J. Biol. Macromol.** 38, 89-93.
4. **K. Lohith**, B. Manohar and S. Divakar (2006) Response surface methodological study of *Rhizomucor miehei* lipase catalysed synthesis of L-phenylalanyl-D-glucose. **Eur. Food Res. Technol.** In Press.
5. **Lohith K.**, Vijayakumar G. R., Somashekar B. R., Sivakumar R. and Divakar S. (2006) Glycosides and amino acyl esters of carbohydrates as potent inhibitors of Angiotensin Converting Enzyme. **Eur. J. Med. Chem.** In press.
6. **Lohith K.**, Manohar B. and Divakar S. (2006). Competitive inhibition by substrates in *Rhizomucor miehei* and *Candida rugosa* lipases catalysed esterification reaction between L-phenylalanine and D-glucose. Submitted for publication.
7. **Lohith K.** and Divakar S. (2006). Syntheses of L-prolyl, L-phenylalanyl, L-tryptophanyl and L-histidyl esters of carbohydrates using *Candida rugosa* lipase. Submitted for publication.

CONTENTS		Page No.
Chapter 1		
Introduction		
1.1. Enzymes as biocatalysts		1
1.2. Lipases		1
1.2.1. Porcine pancreas lipase		3
1.2.2. <i>Rhizomucor miehei</i> lipase		4
1.2.3. <i>Candida rugosa</i> lipase		4
1.3. Reactions catalyzed by lipases		5
1.4. Mechanism of lipase catalyzed esterification in organic solvents		6
1.5. Advantages of lipase catalysis over chemical catalysis		9
1.6. Important factors influencing the lipase activity in organic solvents		16
1.6.1. Nature of substrate		16
1.6.2. Nature of solvent		17
1.6.3. Thermal Stability		19
1.6.4. Role of water in lipase catalysis		21
1.6.5. Immobilization		24
1.7. Strategies employed in lipase catalyzed esterification		25
1.7.1. Esterification in reverse micelles		25
1.7.2. Esterification in supercritical carbon dioxide		26
1.7.3. Esterification in micro wave assisted reactions		27
1.7.4. Kinetic studies of lipase catalyzed esterification reactions		28
1.7.5. Response Surface Methodology in lipase catalysis		29
1.7.6. Lipase catalyzed resolution of racemic esters		30
1.8. Scope of the present work		31
Chapter 2		
Materials and methods		
2.1. Materials		34
2.1.1. Lipases		34
2.1.2. L-Amino acids		34
2.1.3. Carbohydrates		35
2.1.4. Other chemicals		35
2.1.4. Solvents		35
2.2. Methods		36
2.2.1. Lipase activity		36
2.2.1.1. Hydrolytic activity		36
2.2.1.2. Esterification activity		37
2.2.2. Protein estimation		38

2.2.3. Preparation of buffers	39
2.2.4. Esterification procedure	39
2.2.5. Isolation of esters	40
2.2.6. High Performance Liquid Chromatography	40
2.2.7. UV-Visible spectroscopy	41
2.2.8. Infra Red spectroscopy	41
2.2.9. Nuclear Magnetic Resonance spectroscopy	42
2.2.9.1. ¹ H NMR	42
2.2.9.2. ¹³ C NMR	42
2.2.9.3. Two-dimensional HSQCT	42
2.2.10. Mass spectroscopy	43
2.2.11. Polarimetry	43
2.2.12. Critical micellar concentration determination	43
2.2.13. Water activity	44
2.2.14. Preparation of N-acetyl phenylalanine	44
2.2.15. Extraction of Angiotensin Converting Enzyme from pig lung	45
2.2.16. Angiotensin Converting Enzyme inhibition assay	45
2.2.17. Extraction of porcine pancreas lipase	46
2.2.18. Identification of lipases and ACE by SDS-PAGE	47
Chapter 3	
Synthesis of L-phenylalanyl-D-glucose and L-phenylalanyl-lactose	
3.1. Introduction	50
3.2. Present work	51
Synthesis of L-phenylalanyl-D-glucose	
3.2.1. Selection of organic solvents	52
3.2.2. Reaction profile	53
3.2.3. Effect of lipase concentration	54
3.2.4. Effect of substrate concentration	55
3.2.5. Effect of buffer salt	55
3.2.6. Reusability of lipases	57
3.3. Synthesis of L-phenylalanyl-lactose	57
3.3.1. Reaction profile	57
3.3.2. Effect of substrate concentration	58
3.3.3. Effect of PPL and CRL concentration	59
3.3.4. Effect of buffer salt	60
3.4. Determination of Critical Micellar Concentration	61
3.5. Discussion	61
3.6. Optimization of L-phenylalanyl-D-glucose synthesis using Response Surface Methodology	66
3.7. Experimental	73

Chapter 4

***Candida rugosa* lipase catalysed syntheses of L-prolyl, L-phenylalanyl, L-tryptophanyl and L-histidyl esters of carbohydrates**

4.1. Introduction	75
4.2. Present work	76
Syntheses and characterization of L-prolyl, L-phenylalanyl, L-tryptophanyl and L-histidyl esters of carbohydrates	
4.2.1. L-Prolyl esters of carbohydrates	77
4.2.1.1. L-Prolyl-D-glucose 16a-c	84
4.2.1.2. L-Prolyl-D-galactose 17a-c	84
4.2.1.3. L-Prolyl-D-mannose 18a-e	85
4.2.1.4. L-Prolyl-D-fructose 19a-c	86
4.2.1.4. L-Prolyl-D-ribose 20a and b	87
4.2.1.6. L-Prolyl-lactose 21a and b	87
4.2.1.7. L-Prolyl-maltose 22a-c	88
4.2.1.8. L-Prolyl-D-sorbitol 23a and b	89
4.2.2. L-Phenylalanyl esters of carbohydrates	90
4.2.2.1. L-Phenylalanyl-D-glucose 24a-e	96
4.2.2.2. L-Phenylalanyl-D-galactose 25a-e	97
4.2.2.3. L-Phenylalanyl-D-mannose 26a-e	97
4.2.2.4. L-Phenylalanyl-D-fructose 27a and b	98
4.2.2.5. L-Phenylalanyl-D-arabinose 28a-c	98
4.2.2.6. L-Phenylalanyl-lactose 29a-c	99
4.2.2.7. L-Phenylalanyl-maltose 30a and b	100
4.2.2.8. L-Phenylalanyl-D-mannitol 31a and b	101
4.2.3. L-Tryptophanyl esters of carbohydrates	102
4.2.3.1. L-Tryptophanyl-D-glucose 32a-e	108
4.2.3.2. L-Tryptophanyl-D-galactose 33	109
4.2.3.3. L-Tryptophanyl-D-mannose 34	109
4.2.3.4. L-Tryptophanyl-D-fructose 35a and b	110
4.2.3.5. L-Tryptophanyl-lactose 36a and b	111
4.2.3.6. L-Tryptophanyl-maltose 37a-d	111
4.2.3.7. L-Tryptophanyl-sucrose 38	112
4.2.3.8. L-Tryptophanyl-D-sorbitol 39a and b	113
4.2.4. L-Histidyl esters of carbohydrates	114
4.2.4.1. L-Histidyl-D-glucose 40a-e	118
4.2.4.2. L-Histidyl-D-mannose 41a and b	119
4.2.4.2. L-Histidyl-D-fructose 42	120
4.2.4.4. L-Histidyl-maltose 43a-c	120
4.2.4.5. L-Histidyl-D-mannitol 44	121
4.3. NMR characterization of spectral data for L-prolyl, L-phenylalanyl, L-tryptophanyl and L-histidyl esters of carbohydrates	122

4.3.1. L-Prolyl esters of carbohydrates 16-23	122
4.3.2. L-Phenylalanyl esters of carbohydrates 24-31	123
4.3.3. L-Tryptophanyl esters of carbohydrates 32-39	124
4.3.4. L-Histidyl esters of carbohydrates 40-44	125
4.4. Discussion	125
4.5. Experimental	130
Chapter 5	
Competitive inhibition by substrates in <i>Rhizomucor miehei</i> and <i>Candida rugosa</i> lipases catalysed esterification of D-glucose with L-phenylalanine	
5.1. Introduction	133
5.2. Present work	134
5.2.1. <i>Rhizomucor miehei</i> lipase catalysis	134
5.2.2. <i>Candida rugosa</i> lipase catalysis	139
5.3. Discussion	142
5.3.1. <i>Rhizomucor miehei</i> lipase	142
5.3.2. <i>Candida rugosa</i> lipase	143
5.4. Experimental	144
Chapter 6	
Angiotensin Converting Enzyme inhibition activity of L-prolyl, L-phenylalanyl, L-tryptophanyl and L-histidyl esters of carbohydrates	
6.1. Introduction	146
6.2. Present work	148
6.3. Discussion	152
6.4. Experimental	153
6.4.1. Extraction of ACE from pig lung	153
6.4.2. Esterification Procedure	154
6.4.3. Angiotensin Converting Enzyme inhibition assay	155
Conclusions	157
Summary	161
Bibliography	167

List of Figures

Number	Captions
Fig. 2.1	Calibration curve for protein estimation by Lowry's method
Fig. 2.2	Calibration curve for hippuric acid estimation by spectrophotometric method
Fig. 2.3	Plot of R_f values of molecular marker verses log molecular weight
Fig. 2.4A	SDS-PAGE for lipases
Fig. 2.4B	SDS-PAGE for Angiotensin Converting Enzyme
Fig. 3.1	HPLC chromatograph for the reaction mixture of L-phenylalanine and D-glucose
Fig. 3.2	Reaction profile for L-phenylalanyl-D-glucose synthesis
Fig. 3.3	Effect of substrate concentration on synthesis of L-phenylalanyl-D-glucose
Fig. 3.4	Enzyme reusability in the synthesis of L-phenylalanyl-D-glucose
Fig. 3.5	Effect of substrate concentration on synthesis of L-phenylalanyl-lactose
Fig. 3.6	Three-dimensional surface plot showing the effect of L-phenylalanine and RML concentration on the extent of esterification
Fig. 3.7	Contour plot showing iso-esterification regions obtained due to the effect of RML and buffer concentration on the extent of esterification
Fig. 3.8	Three-dimensional surface plot showing the effect of RML concentration and buffer pH on the extent of esterification
Fig. 3.9	Three-dimensional surface plot showing the effect of RML concentration and incubation period on the extent of esterification
Fig. 3.10	Contour plot showing iso-esterification regions obtained due to the effect of L-phenylalanine concentration and buffer pH on the extent of esterification
Fig. 3.11	Contour plot showing iso-esterification regions obtained due to the effect of L-phenylalanine concentration and buffer concentration on the extent of esterification
Fig. 4.1	HPLC chromatogram for L-proline and D-galactose reaction mixture
Fig. 4.2	UV spectrum for L-prolyl-D-glucose
Fig. 4.3	Two-dimensional HSQCT NMR spectrum for L-prolyl-D-glucose
Fig. 4.4	Two-dimensional HSQCT NMR spectrum for L-prolyl-D-galactose
Fig. 4.5	Two-dimensional HSQCT NMR spectrum for L-prolyl-D-mannose
Fig. 4.6	UV spectrum for L-prolyl-D-ribose
Fig. 4.7	A typical mass spectrum for L-prolyl-D-ribose
Fig. 4.8	A typical IR spectrum of L-prolyl-D-ribose

Fig. 4.9	Two-dimensional HSQCT NMR spectrum for L-prolyl-D-ribose
Fig. 4.10	Two-dimensional HSQCT NMR spectrum for L-prolyl-D-fructose
Fig. 4.11	Two-dimensional HSQCT NMR spectrum for L-prolyl-lactose
Fig. 4.12	A typical mass spectrum for L-prolyl-maltose
Fig. 4.13	Two-dimensional HSQCT NMR spectrum for L-prolyl-maltose
Fig. 4.14	A typical IR spectrum of L-prolyl-D-sorbitol
Fig. 4.15	Two-dimensional HSQCT NMR spectrum for L-prolyl-D-sorbitol
Fig. 4.16	UV spectrum for L-phenylalanyl-D-glucose
Fig. 4.17	A typical IR spectrum of L-phenylalanyl-D-glucose
Fig. 4.18	A typical mass spectrum of L-phenylalanyl-D-glucose
Fig. 4.19	Two-dimensional HSQCT NMR for L-phenylalanyl-D-glucose
Fig. 4.20	^{13}C NMR spectrum of L-phenylalanyl-D-galactose
Fig. 4.21	^{13}C NMR spectrum of L-phenylalanyl-D-mannose
Fig. 4.22	A typical IR spectrum of L-phenylalanyl-D-fructose
Fig. 4.23	^{13}C NMR spectrum of L-phenylalanyl-D-fructose
Fig. 4.24	Two-dimensional HSQCT NMR spectrum of L-phenylalanyl-D- arabinose
Fig. 4.25	Two-dimensional HSQCT NMR spectrum of L-phenylalanyl-lactose
Fig. 4.26	A typical mass spectrum of L-phenylalanyl-maltose
Fig. 4.27	^{13}C NMR spectrum of L-phenylalanyl-maltose
Fig. 4.28	Two-dimensional HSQCT NMR spectrum of L-phenylalanyl-D-mannitol
Fig. 4.29	HPLC chromatogram for reaction mixture of L-tryptophan and D-glucose
Fig. 4.30	Two-dimensional HSQCT NMR of L-tryptophanyl-D-glucose
Fig. 4.31	Two-dimensional HSQCT NMR of L-tryptophanyl-D-mannose
Fig. 4.32	UV spectra for L-tryptophanyl-D-galactose
Fig. 4.33	Two-dimensional HSQCT NMR for L-tryptophanyl-D-galactose
Fig. 4.34	UV spectrum for L-tryptophanyl-D-fructose
Fig. 4.35	A typical IR spectrum of L-tryptophanyl-D-fructose
Fig. 4.36	A typical mass spectrum of L-tryptophanyl-D-fructose
Fig. 4.37	Two-dimensional HSQCT NMR for L-tryptophanyl-D-fructose
Fig. 4.38	Two-dimensional HSQCT NMR for L-tryptophanyl-lactose
Fig. 4.39	Two-dimensional HSQCT NMR for L-tryptophanyl-maltose

Fig. 4.40	A typical mass spectrum of L-tryptophanyl-sucrose
Fig. 4.41	Two-dimensional HSQCT NMR for L-tryptophanyl-sucrose
Fig. 4.42	A typical IR spectrum of L-tryptophanyl-D-sorbitol
Fig. 4.43	Two-dimensional HSQCT NMR for L-tryptophanyl-D-sorbitol
Fig. 4.44	HPLC chromatogram for reaction mixture of L-histidine and maltose esterification reaction
Fig. 4.45	A typical mass spectrum of L-histidyl-D-glucose
Fig. 4.46	Two-dimensional HSQCT NMR for L-histidyl-D-glucose
Fig. 4.47	Two-dimensional HSQCT NMR for L-histidyl-D-mannose
Fig. 4.48	Two-dimensional HSQCT NMR for L-histidyl-D-fructose
Fig. 4.49	Two-dimensional HSQCT NMR for L-histidyl-maltose
Fig. 4.50	UV spectrum for L-histidyl-D-mannitol
Fig. 4.51	A typical IR spectrum of L-histidyl-D-mannitol
Fig. 4.52	A typical mass spectrum for L-histidyl-D-mannitol
Fig. 4.53	Two-dimensional HSQCT NMR for L-histidyl-D-sorbitol
Fig. 5.1	Initial rate (v) plots of L-phenylalanyl-D-glucose synthesis
Fig. 5.2	Double reciprocal plots for RML catalysed L-phenylalanyl-D-glucose reaction: $1/v$ versus $1/[D\text{-glucose}]$
Fig. 5.3	Double reciprocal plots for RML catalysed L-phenylalanyl-D-glucose reaction: $1/v$ versus $1/[L\text{-phenylalanine}]$
Fig. 5.4	Replot of slopes of $1/[L\text{-phenylalanine}]$ versus $[D\text{-glucose}]$ from Fig. 5.3 from RML catalysed reaction
Fig. 5.5	Replot of slopes of $1/[D\text{-glucose}]$ versus $[L\text{-phenylalanine}]$ from Fig. 5.2 from RML catalysed reaction
Fig. 5.6	Double reciprocal plots for CRL catalysed L-phenylalanyl-D-glucose reaction: $1/v$ versus $1/[D\text{-glucose}]$
Fig. 5.7	Double reciprocal plots for CRL catalysed L-phenylalanyl-D-glucose reaction: $1/v$ versus $1/[L\text{-phenylalanine}]$
Fig. 5.8	Replot of slopes of $1/[L\text{-phenylalanine}]$ versus $[D\text{-glucose}]$ from Fig. 5.7 from CRL catalysed reaction
Fig. 6.1	A typical ACE inhibition plot for captopril
Fig. 6.2	ACE inhibition plots for L-prolyl esters of carbohydrates
Fig. 6.3	ACE inhibition plots for L-phenylalanyl esters of carbohydrates
Fig. 6.4	ACE inhibition plots for L-tryptophanyl esters of carbohydrates
Fig. 6.5	ACE inhibition plots for L-histidyl esters of carbohydrates

List of Tables

Number	Title	Page No.
Table 1.1	Industrial applications of lipases	3
Table 1.2	List of some commercially important esters produced by lipases	10
Table 2.1	List of lipases and their suppliers	34
Table 2.2	List of chemicals and suppliers	35
Table 2.3	Esterification and hydrolytic activities of different lipases	37
Table 2.4	Protein content of different lipase preparations	38
Table 2.5	Water activities for different organic solvents by Karl-Fischer method	45
Table 3.1	Effect of solvent mixtures on the synthesis of L-phenylalanyl-D-glucose	53
Table 3.2	Effect DMF volume on the synthesis of L-phenylalanyl-D-glucose	53
Table 3.3	Effect of lipase concentration on the synthesis of L-phenylalanyl-D-glucose	54
Table 3.4	Effect of buffer salts (pH and concentration) on the synthesis of L-phenylalanyl-D-glucose	56
Table 3.5	Effect of incubation period on the synthesis of L-phenylalanyl-lactose	58
Table 3.6	Effect of lipase concentrations on the synthesis of L-phenylalanyl-lactose	59
Table 3.7	Effect of buffer salts (pH and buffer volume) on the synthesis of L-phenylalanyl-lactose	60
Table 3.8	Coded values of the variables and their corresponding actual values used in the design of experiments	66
Table 3.9	Experimental design with experimental and predicted yields of L-phenylalanyl-D-glucose based on the response surface equation	68
Table 3.10	Analysis of variance of the response surface model along with coefficients of the response equation.	69
Table 3.11	Validation of experimental data	72
Table 4.1	Retention times and R_f values of L-prolyl esters of carbohydrates	79
Table 4.2	NMR data of free carbohydrates	80
Table 4.3	Syntheses of L-prolyl esters of carbohydrates	81
Table 4.4	Retention times and R_f values of L-phenylalanyl esters of carbohydrates	91
Table 4.5	Syntheses of L-phenylalanyl esters of carbohydrates	93
Table 4.6	Retention times and R_f values of L-tryptophanyl esters of carbohydrates	103
Table 4.7	Syntheses of L-tryptophanyl esters of carbohydrates	105

Table 4.8	Retention times and R_f values of L-histidyl esters of carbohydrates	115
Table 4.9	Syntheses of L-histidyl esters of carbohydrates	116
Table 4.10	Percentage yields and proportions of L-prolyl, L-phenylalanyl, L-tryptophanyl and L-histidyl esters of carbohydrates	127
Table 5.1	Apparent values of kinetic parameters for RML catalysed synthesis of L-phenylalanyl-D-glucose.	137
Table 5.2	Experimental and predicted initial rate values for the synthesis of L-phenyl alanyl -D-glucose by RML	138
Table 5.3	Apparent values of kinetic parameters for CRL catalysed synthesis of L-phenylalanyl-D-glucose	140
Table 5.4	Experimental and predicted initial rate values for the synthesis of L-phenylalanyl-D-glucose by CRL	141
Table 6.1	Protease inhibition assay for D-glucose ester	149
Table 6.2	IC_{50} values for ACE inhibition by amino acyl esters of carbohydrates	150

List of Schemes

Number	Title	Page No.
Scheme 1.1	Types of reactions catalysed by lipases	6
Scheme 1.2	Mechanism of lipase mediated esterification.	9
Scheme 1.3	Various equilibria involved at the microaqueous inter-phase	23
Scheme 3.1	Lipase catalysed synthesis of L-phenylalanyl-D-glucose esters in anhydrous organic solvents	51
Scheme 4.1	<i>Candida rugosa</i> lipase catalysed syntheses of L-prolyl esters of carbohydrates	78
Scheme 4.2	<i>Candida rugosa</i> lipase catalysed Syntheses of L-phenylalanyl esters of carbohydrates in anhydrous organic solvents	91
Scheme 4.3	<i>Candida rugosa</i> lipase catalysed syntheses of L-tryptophanyl esters of carbohydrates	103
Scheme 4.4	<i>Candida rugosa</i> lipase catalysed syntheses of L-histidyl esters of carbohydrates	115
Scheme 5.1	Ping-Pong Bi-Bi mechanism of RML catalysed synthesis of L-phenylalanyl-D-glucose showing inhibition by both D-glucose and L-phenylalanine	136
Scheme 5.2	Ping-Pong Bi-Bi mechanism of CRL catalysed synthesis of L-phenylalanyl-D-glucose showing inhibition by D-glucose.	139
Scheme 6.1	Role of angiotensin converting enzyme (ACE) in blood pressure regulation	146
Scheme 6.2	Schematic representation of ACE inhibition by captopril to the active sites	147
Scheme 6.3	Schematic representation of ACE active sites and binding of inhibitors	147

List of abbreviations and symbols

A	Absorbance
α	Alpha
ANOVA	Analysis of variance
ACE	Angiotensin Converting Enzyme
Å	Angstrom
β	Beta
BSA	Bovine serum albumin
CRL	<i>Candida rugosa</i> lipase
^{13}C	Carbon-13
CCRD	Central Composite Rotatable Design
J	Coupling constant
CMC	Critical Micellar Concentration
$^{\circ}\text{C}$	Degree centigrade
δ	Delta
DMSO-d ₆	Deuteriated Dimethyl sulfoxide
CH ₂ Cl ₂	Dichloromethane
DMSO	Dimethyl sulfoxide
eV	Electron volt
EC	Enzyme commission
γ	Gamma
g	Gram
Hz	Hertz
HMQCT	Heteronuclear Multiple Quantum Coherence Transfer
HSQCT	Heteronuclear Single Quantum Coherence Transfer
HPLC	High Performance Liquid Chromatography
h	Hour
IR	Infra Red
K _i	Inhibitor constant
v	Initial velocity
KDa	Kilodalton
MS	Mass Spectroscopy
V _{max}	Maximum velocity
MHz	Mega hertz
K _M	Michelis Menton constant
μg	Microgram
μL	Microlitre
mg	Milligram
mL	Milliliter
mmol	Millimole
min	Minute
M	Molarity
mol	Mole
[M] ⁺	Molecular ion
nm	Nanometer

N	Normality
NMR	Nuclear Magnetic Resonance
[α]	Optical rotation
ppm	Parts per million
%	Percentage
π	Pi
PAGE	Polyacrylamide gel electrophoresis
PPL	Porcine pancreas lipase
KBr	Potassium bromide
^1H	Proton
RSM	Response Surface Methodology
R_f	Retention factor
RT	Retention time
RML	<i>Rhizomucor miehei</i> lipase
σ	Sigma
SDS	Sodium dodecyl sulfate
TEMED	N, N, N', N'-Tetramethylethylenediamine
TMS	Tetra methyl silane
TLC	Thin layer chromatography
2D	Two-Dimensional
UV	Ultra Violet
v/v	Volume by volume
a_w	Water activity
cm^{-1}	Wave per centimeter
w/w	Weight by weight

Chapter 1
Introduction

1.1. Enzymes as biocatalysts

Synthetic chemistry involving chemical routes require drastic conditions, like use of acids or alkali, high temperature, hazardous chemicals, toxic metals and catalysts leading to high energy consumption, coloring of products, low selectivity and environmental pollution. It is also tedious to synthesize regio and stereo selective compounds, as they require continuous protection and deprotection steps. Thus chemical syntheses include multi step processes and result in number of byproducts and hence economically inefficient. Some chemically synthesized products also require exhaustive purification steps.

Enzymes give better solutions to all these problems. Enzymes act as biocatalysts, which can function under milder reaction conditions, without requiring high temperatures, use of hazardous chemicals and they are totally 'eco friendly' in nature. Enzymatic activity in non aqueous solvents offers a new methodology for the production of many useful compounds which are not feasible in aqueous media. Klivanov initiated this outstanding approach and the enzymes in non-aqueous media found large number of applications in organic synthesis (Klivanov 1986). Enzymes are employed in organic solvents for the synthesis of esters (Santaniello *et al.* 1993), chiral compounds (Orrenius *et al.* 1995), surfactants (Plou *et al.* 1999; Sarney *et al.* 1996; 1995), pharmaceutical intermediates (Duan *et al.* 1997), biotransformations of oils and fats (Bosley and Calyton 1994; Vulfson 1994) and sugar based polymers (Patil *et al.* 1991). Thus, the use of enzymes as biocatalysts in biotechnology has found potential applications in pharmaceutical, food, cosmetic, flavor and fragrance and beverage industries.

1.2. Lipases

Of the estimated 25,000 enzymes present in nature, only about 2800 have been characterized and about 400 enzymes, mainly hydrolases, transferases and oxido-

reductases have been identified as commercially potential ones. But only 50 different kinds of enzymes find application on an industrial scale (Winterhalter and Schreier 1993; Schreier and Winterhalter 1993; Berger 1995). The enzymes of commercial importance in food industry are amylases, proteases, pectinases, cellulases, hemicellulases, lipases and lactases.

Lipases (EC 3.1.1.3) normally catalyze hydrolysis of triglycerides at the oil/water interface. Their ability to form ester bonds under reverse hydrolytic conditions has enabled them to catalyze various other types of reactions like esterification, transesterification, polymerization and lactonization. Some of the industrial applications of lipases are listed in Table 1 (Vulfson 1994) The high selectivity and mild conditions associated with lipase mediated transformations have made them very attractive for the synthesis of a wide range of natural products, pharmaceuticals, fine chemicals, food ingredients (Schreier, 1997) and bio-lubricants (Dorm *et al.* 2004). For example, lipases are employed to get poly unsaturated fatty acids (PUFAs) which are then used along with their mono- and diglycerides for the synthesis of nutraceuticals, pharmaceuticals like anticholesterolemics, antiinflammatories and thrombolytics (Gill and Valivety 1997; Belarbi *et al.* 2000). *Candida rugosa* lipase is employed in the paper industry to remove the pith from the pulp (Sharma *et al.* 2001). The main reason for the use of lipases is the growing interest and demand for the products prepared through natural means, which are environmentally compatible. Because of their versatility in application, lipases are regarded as enzymes with high commercial potential. Lipase catalyzed esterification in organic solvents offers synthetic challenges, which if dealt with successfully, can result in the generation of several useful compounds.

Table 1. Industrial applications of lipases (Vulfson 1994)

Industry	Action	Product or application
Detergents	Hydrolysis of fats	Removal of oil stains from fabrics
Dairy	Hydrolysis of milk fat, cheese ripening, modification of butter fat	Development of flavoring agents in milk, cheese, and butter
Bakery	Flavor improvement	Shelf-life prolongation
Beverages	Improved aroma	Beverages
Food	Quality enhancement Transesterification	Mayonnaise, dressings, and Whippings, health foods
Meat and fish	Flavor development	Defatting
Fats and oils	Transesterification, hydrolysis	Cocoa butter, margarine, fatty acids, glycerol, mono and diglycerides
Chemicals and Pharmaceuticals	Enantioselectivity, synthesis, transesterification, hydrolysis	Chiral building blocks, chemicals digestive aids
Cosmetics	Synthesis	Emulsifiers, moisturizers
Leather	Hydrolysis	Leather products
Paper	Hydrolysis	Paper with improved quality by dewaxing.

1.2.1. Porcine pancreas lipase (PPL)

Pancreatic lipases exhibit high molecular activity and under optimal conditions one molecule of lipase can cleave nearly 7000 ester bonds per second (Scharpe *et al.* 1997). Most of the work on pancreatic lipase has been conducted with lipase from porcine pancreas. Porcine pancreas is the richest source for pancreatic lipases and it was the first purified lipase (Peschke 1991). Pancreatic lipase contains a single chain glycoprotein of about 48 KDa molecular weight and it is a serine hydrolase (Winkler and Gubernator 1994). From pH titration and photo oxidation studies, histidine residue was

found to responsible for the catalytic activity (Winkler *et al.* 1990), the catalytic triad consisting of Ser-152, His-263 and Asp-176. Donner (1976) purified and released co-lipase activity by reduction with beta-mercaptoethanol in the presence of guanidine chloride and measured some of the physical parameters: Molecular weight 52 KDa, sedimentation coefficient (s degrees 20, w) 4.0 S, diffusion coefficient (D degrees 20, w) $6.7 \times 10^{-7} \text{ cm}^2 \text{ s}^{-1}$, Stokes' radius (r) 30.3 Å, partial specific volume (v) $0.72 \text{ cm}^3 \text{ g}^{-1}$, frictional ratio (f/f₀) 1.23 and isoelectric point (pI) 5.18 (Donner 1976).

1.2.2. *Rhizomucor miehei* lipase (RML)

The crystallographic study of *Rhizomucor miehei* lipase (RML) has explained that RML is made up of a single polypeptide chain with 269 amino acid residues and the molecular weight is 29.4 KDa (Brady *et al.* 1990, Brzozowski *et al.* 1991). Brady *et al.* (1990) identified that RML is an α / β type protein with three disulphide bonds which are responsible to stabilize the two terminal strands. The catalytic triad contains Ser-144, His-257 and Asp-203, which is buried under a single 17 residue long surface loop (82-96 residue) called lid, that occludes the active site in the native structure (Derewenda *et al.* 1992). Brzozowski *et al.* (1991) studying an atomic model of inhibitor-RML complex, showed a direct covalent bond formation between nucleophilic O_γ of Ser 144 and substrate. Carbonyl oxygen of the substrate may be stabilized by the interaction of amide nitrogen and the hydroxyl of Ser 82 (Leu 145 may also be involved in amide interaction) through hydrogen bonding and this Ser 82 has favorable conformation for oxy-anion interaction.

1.2.3. *Candida rugosa* lipase (CRL)

Candida rugosa lipase is the first example of a native interface- activatable lipase in 'open' form. CRL is a single domain protein belonging to the family of α / β hydrolase proteins. In CRL, the active triad contains Ser-209, Glu-341 and His-449 and

nearer to this active site, three surface loops (62-92, 122-129 and 294-305) are present which are very important for catalytic activity. Hence the interfacial activation of these lipases is associated with conformational rearrangement of surface loops (Grochulski *et al.* 1993). The oxyanion hole O_{γ} is formed by the backbone amide of Gly-123, Gly-124 and Ala-210, which are involved in formation of hydrogen bonds with the substrates. Presence of two acyl binding ‘pockets’ in the active site of CRL depicts the substrate specificity of carbon chain length, a small pocket which can bind well with short chain acids and the bigger pocket, which can bind well with longer chain acids (Parida and Dordick 1993). This was experimentally proved by showing that the mechanism depends on the chain length of acyl moiety and independent of the type of reaction catalysed and this behaviour is similar when the reaction was carried out in different solvents also.

1.3. Reactions catalyzed by lipases

The ranges of substrates with which lipases react and also the range of reactions they catalyze are probably far more than any other enzymes studied till date.

Lipases catalyze three types of reactions (**Scheme 1**):

1.3.1. Hydrolysis:

In aqueous media when there is large excess of water, ester hydrolysis is the dominant reaction.

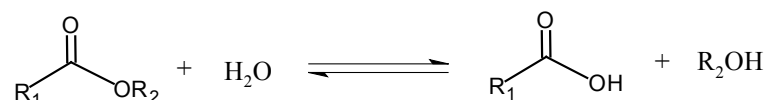
1.3.2. Esterification:

Under low water conditions such as in nearly anhydrous solvents, esterification can be achieved. If the water content of the medium is controlled, relatively better product yields can be obtained.

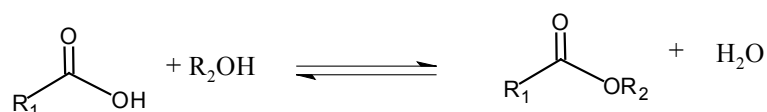
1.3.3. Transesterification:

The acid moiety of an ester is exchanged with another one. If the acyl donor is a free acid, the reaction is called **acidolysis** and if the acyl donor is an ester, the reaction is called **interesterification**. In **alcoholysis**, the nucleophile alcohol acts as an acyl acceptor.

1. Hydrolysis

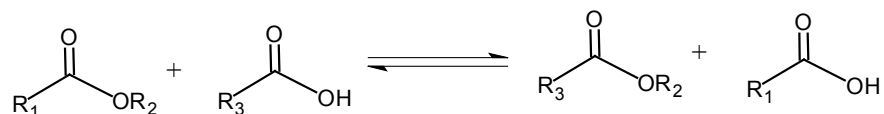


2. Esterification

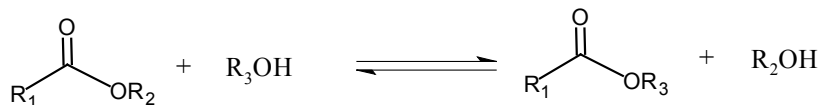


3. Transesterification

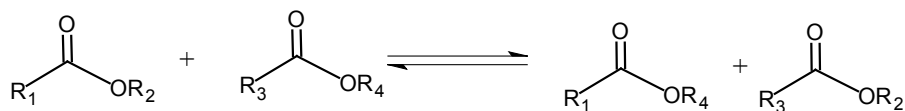
a. Acidolysis



b. Alcoholysis



c. Interesterification



Scheme 1.1. Types of reactions catalysed by lipases

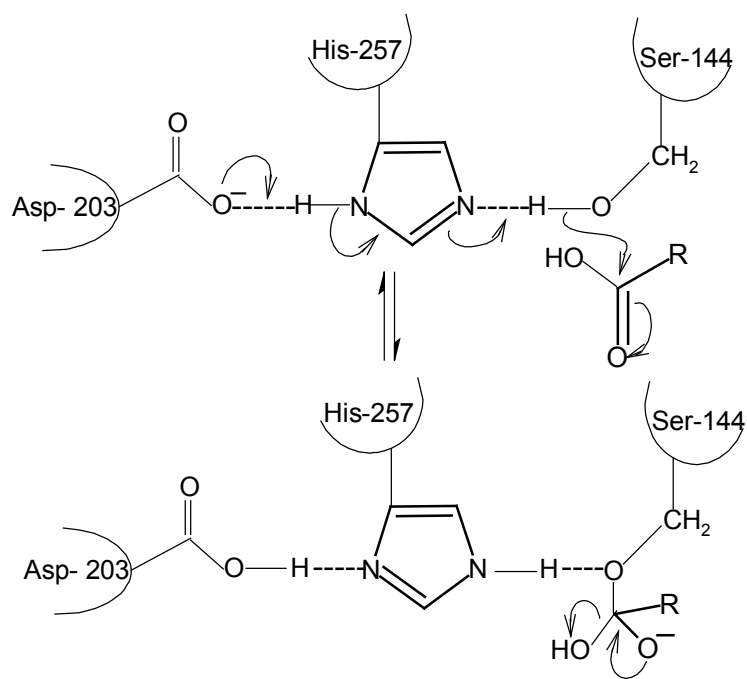
1.4. Mechanism of lipase catalysed esterification in organic solvents

Lipases show lipid splitting nature and the mechanism is same as that of serine proteases (Pleiss *et al.* 1998). Catalytic triad in lipases contains Ser, His and Asp/ Glu residues. The serine residue in active center is activated by histidine and aspartic acid / glutamic acid residues. The substrate acid forms a tetrahedral acyl-enzyme

intermediate by reaction with the OH group of the catalytic serine residue. The resulting excess of negative charge that develops on the carbonyl oxygen atom is stabilized by the oxyanion hole (Brzozwski *et al.* 1991). The tetrahedral intermediate I, forms a serinate ester with elimination of water molecule. Subsequent nucleophilic attack of alcohol to the acyl-enzyme intermediate leads to tetrahedral intermediate II. Finally, the product ester is released and enzyme is free for the next molecule to attack. Grochulski *et al.* (1994), Cygler *et al.* (1994) and Schrag and Cygler (1997) proposed this mechanism for the ester formation in case of RML (**Scheme 1.2**).

Step 1. Acylation step

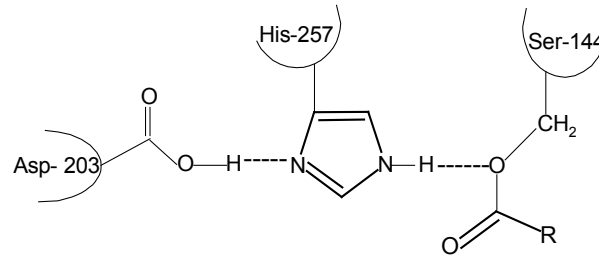
Initially serine hydroxyl group forms a tetrahedral intermediate complex I with acyl donor, the negative charge that is formed in tetrahedral intermediate is stabilized by forming hydrogen bonds with amino acid residues, which are responsible for the oxyanion hole formation



Tetrahedral complex I

Step 2. Formation of acyl enzyme complex

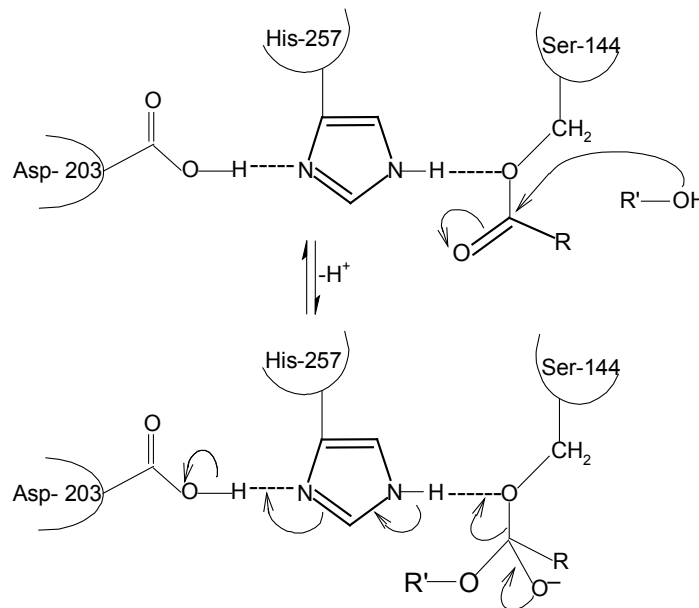
After the formation of tetrahedral intermediate I, an acyl-enzyme complex is formed through covalent bond with Ser residue by losing one molecule of water.



Acyl enzyme complex

Step 3. Nucleophilic attack by alcohol

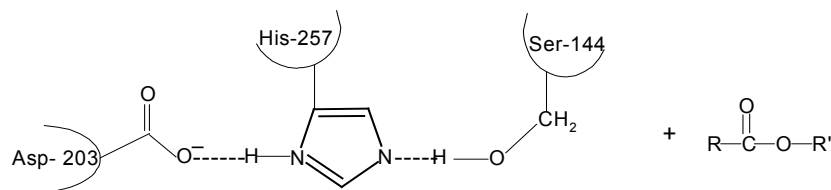
Nucleophile alcohol, attacks the carbonyl center of the tetrahedral intermediate forming a tetrahedral complex II forming enzyme-acid-alcohol complex.



Tetrahedral complex II

Step 4. Release of ester

Finally, the ester is released leaving enzyme free which will be ready for next molecule to attack.



Scheme 1.2. Mechanism of lipase mediated esterification.

1.5. Advantages of lipase catalysis over chemical catalysis

There are many advantages of using lipases as biocatalysts

1. Specificity of the reaction.
2. Milder reaction conditions under which the lipolytic process can be operated.
3. Non-generation of by-products associated with the use of several chemical procedures.
4. Improved product-yield and better product quality.
5. Exploitation of the stereo and regio-specificities shown by lipases to produce high value chiral synthons.
6. Success in immobilization techniques that have enabled the reuse of lipases leading to economically viable processes.
7. Good conversion yields.
8. Lipases are highly thermostable, exhibiting activity at 100 °C.
9. Use of non-polar solvents which impart stability to lipase rather than in water, renders insolubility of the enzyme, solubility of substrates and products in organic solvents resulting in homogenous reaction conditions, easy product workout procedures and easy removal of water formed as a by-product.

Table 2 lists some of the commercially important flavour, fragrance, surfactant and sweetener esters prepared through lipase catalysis.

Table 2. Lists of some commercially important esters produced by lipases

Name of the compound	Use	Lipase	References
A. Flavour Esters			
Isoamyl acetate	Banana flavour	<i>Pseudomonas fluorescense</i> <i>Candida antarctica</i> <i>Rhizomucor miehei</i> <i>Rhizomucor miehei</i> <i>Candida cylindraceae</i> , PPL, <i>Aspergillus niger</i> Novozyme 435 <i>Rhizomucor miehei</i> , <i>Candida antarctica</i> <i>Rhizomucor miehei</i> , <i>Candida antarctica</i> <i>Pseudomonas pseudomallei</i> Porcine liver lipase	Takahashi <i>et al.</i> 1988 Langrand <i>et al.</i> 1990 Rizzi <i>et al.</i> 1992; Chulalaksananukul <i>et al.</i> 1993; Razafindralambo <i>et al.</i> 1994; Divakar <i>et al.</i> 1999 Harikrishna <i>et al.</i> 2000; 2001 Welsh <i>et al.</i> 1990 Gubicza <i>et al.</i> 2000 Afife Guvenc <i>et al.</i> 2002 Romero <i>et al.</i> 2005a, 2005b Kanwar and Goswami 2002 Ngrek 1947 Kumar <i>et al.</i> 2005
Isoamyl butyrate	Banana flavour	<i>Candida antarctica</i> <i>Rhizomucor miehei</i> <i>Candida cylindraceae</i> , PPL, <i>Candida antarctica</i> , Geotrichum sp. and <i>Rhizopus</i> sp.	Langrand <i>et al.</i> 1988; Langrand <i>et al.</i> 1990 Mestri and Pai 1994b Welsh and Williams 1990 Gubicza <i>et al.</i> 2000; Macedo <i>et al.</i> 2004
Isomayl propionate	Banana flavour	<i>Candida antarctica</i>	Langrand <i>et al.</i> 1988
Isoamyl isovalerate	Apple flavour	<i>Rhizomucor miehei</i>	Chowdary <i>et al.</i> 2002
Isobutyl isobutyrate	Pineapple flavour	<i>Rhizomucor miehei</i>	Hamsaveni <i>et al.</i> 2001
Methyl propionate	Fruity flavour	<i>Rhizomucor miehei</i>	Perraud and Laboret 1989
Ethyl butyrate	Pineapple flavour	<i>Candida cylindraceae</i>	Gubicza <i>et al.</i> 2000; Gillies <i>et al.</i> 1987

Butyl isobutyrate	Sweet fruity odor	<i>Candida cylindracea</i> , PPL and <i>Aspergillus niger</i>	Yadav and Lathi 2003 Welsh and Williams 1990
Protocatechuic aldehyde		<i>Rhizomucor miehei</i> , PPL	Divakar 2003
Short chain alcohol esters of C ₂ - C ₁₈ acids	Fruity odor	<i>Staphylococcus warneri</i> <i>Staphylococcus xylosus</i>	Talon <i>et al.</i> 1996
Short chain fatty acid esters	Fruity odor		Mestri and Pai 1994a Macedo <i>et al.</i> 2003; Xu <i>et al.</i> 2002
Long chain alcoholic esters of lactic acids	Flavour	<i>Candida antarctica</i> Novozym435 <i>Rhizomucormiehei</i>	From <i>et al.</i> 1997; Torres and Otero 1999; Parida and Dordick 1991 Bousquet <i>et al.</i> 1999
Methyl benzoate	Exotic fruity and berries flavour	<i>Candida rugosa</i>	Leszczak and Minh 1998
Tetrahydrofurfuryl butyrate	Fruity favor	Novozym 435	Yadav and Devi 2004
Cis-3-hexen-1-yl acetate	Fruity odor	<i>Rhizomucor miehei</i>	Chiang <i>et al.</i> 2003
B. Fragrance Esters			
Tolyl esters	Honey note	<i>Rhizomucor miehei</i> , PPL	Burdock 1994 Suresh-Babu <i>et al.</i> 2002, Manohar and Divakar 2002
Anthranilic acid esters of C ₂ – C ₁₈ alcohols.	Flowery odor of jasmine	<i>Candida cylindracea</i> PPL	Kittleson and Pantaleone 1994 Suresh Babu and Divakar 2001
4-t-Butylcyclohexyl acetate	Woody and intense flowery notes	PPL	Manohar and Divakar 2004a Manohar and Divakar 2004b
Geranyl methacrylate	Floral fruity odor	<i>Rhizomucor miehei</i> , PPL, <i>Pseudomonas cepacia</i>	Athawale <i>et al.</i> 2002

Citronellyl acetate	Fruity rose odor	<i>Candida antarctica</i> SP435	Claon and Akoh 1994b
Citronellyl propionate		<i>Pseudomonas fragi</i>	Mishio <i>et al.</i> 1987
Citronellyl valerate			Marlot <i>et al.</i> 1985
Geranyl butyrate			
Geranyl propionate			
Geranyl valerate			
Farnesol butyrate	Fruity odor	<i>Candida rugosa</i>	Akoh <i>et al.</i> 1992; Shieh <i>et al.</i> 1996
Farnesol propionate			
Farnesol valerate			
Phytol butyrate			
Phytol propionate			
Phytol valerate			
Citronellyl laurate	Fruity, characteristic lavendar and bergamot-like fragrance	Novozym SP	Yadav and Lathi 2004
α -Terpinyl acetate		<i>Rhizomucor miehei</i>	Rao and Divakar 2002
α -Terpinyl propionate			
α -Terpinyl esters of fatty acids		<i>Rhizomucor miehei</i>	Rao and Divakar 2001
α -Terpinyl esters of short chain acids		<i>Aspergillus niger</i> , <i>Rhizopus delemar</i> , <i>Geotrichum candidum</i> , <i>Pencillium cyclopium</i>	Iwai <i>et al.</i> 1980
Terpinyl esters of triglycerols			Claon and Akoh 1994a
Butyl oleate	Surfactants	<i>Rhizomucor miehei</i>	Knez <i>et al.</i> 1990
2-O- Alkanoyl lactic acid esters of C ₂ -C ₁₈ alcohols	Surfactants	<i>Rhizomucor miehei</i> , PPL	Kiran and Divakar 2001; Kiran <i>et al.</i> 1998

C. Surfactant and Sweeteners

N-Acetyl-L-leucyl-D-glucose N-Acetyl-L-methionyl-D-glucose N-Acetyl-L-tyrosinyl-D-glucose N-Acetyl-L-tryptophnyl-D-glucose N-Acetyl-L-phenylalanyl-D-glucose N-Acetyl-L-phenylalanyl-D-galactose	Surfactants	<i>Mucor javanicus</i> , <i>Pseudomonas cepacia</i> , Subtilisin,	Maruyama <i>et al.</i> 2002
N-Acetyl-L-phenylalanyl-D-fructose N-Acetyl-L-phenylalanyl-D-mannose N-Acetyl-L-phenylalanyl-lactose N-Acetyl-L-methionyl-methyl- β -D-galactopyranoside N-t-Boc-L-phenylalanyl-D-glucose N-t-Boc-L-phenylalanyl-D-galactose N-t-Boc-L-phenylalanyl-D-fructose N-t-Boc-L-phenylalanyl-Methyl α -D-glucopyranoside N-t-Boc-L-phenylalanyl-D-sorbitol		Subtilisin	Maruyama <i>et al.</i> 2002; Riva <i>et al.</i> 1988
		Optimase M-440, Proleather, APG 380	Park <i>et al.</i> 1996

N-t-Boc-L-phenylalanyl-cellobiose		Optimase M-440	Park <i>et al.</i> 1999
N-t-Boc-L-phenylalanyl – trehalose			
N-t-Boc-L-phenylalanyl – maltose			
N-t-Boc-L-phenylalanyl – lactose			
N-t-Boc-L-leucyl-sucrose			
N-t-Boc-L-tyrosinyl-sucrose			
N-t-Boc-L-methionyl-sucrose			
N-t-Boc-L-aspartyl–sucrose			
N-t-Boc-L-phenylalanyl-xylitol		Optimase M-440	Jeon <i>et al.</i> 2001
N-t-Boc-L-phenylalanyl-arabitol			
N-t-Boc-L-phenylalanyl-D-mannitol	Surfactants, Sweeteners	<i>Rhizomucor miehei</i> , PPL	Vijayakumar <i>et al.</i> 2004; Lohith <i>et al.</i> 2003
L-Alanyl-D-glucose			
L-Leucyl–D-glucose			
2-O-ester			
3-O- ester			
6-O- ester			
2, 6-di-O- ester			
3,6-di-O- ester	Surfactants	<i>Rhizomucor miehei</i> , PPL	Vijayakumar <i>et al.</i> 2004; Lohith and Divakar 2005; Lohith <i>et al.</i> 2003
L-Phenylalanyl esters of D-glucose			
2-O-ester			
3-O- ester			
6-O- ester			
2, 6-di-O- ester			

N-Acetyl-L-alanyl-methyl-β-D-galactopyranoside 6-O- ester 4-O- ester 3-O- ester 2-O- ester	Surfactants, Sweeteners	Subtilisin <i>Rhodotorula lactosa</i>	Riva <i>et al.</i> 1988 Suzuki <i>et al.</i> 1991
6-O- Butyl glucose 6-O- Acetyl glucose 6-O- Capryloyl glucose 6-O- Acetyl galactose 6-O- Acetyl maltose 6-O- Acetyl fructose 1-O- Acetyl fructose Fructose oleate	Surfactants Surfactant	PPL Subtilisin Lipozyme, <i>Rhizomucor miehei</i> ,	Therisod and Klivanov 1986 Kirk <i>et al.</i> 1992 Zaks and Dodds 1997 Klivanov 1986 Dordick 1981 Schlotterbeck <i>et al.</i> 1993 Boyer <i>et al.</i> 2001. Khaled <i>et al.</i> 1991
Fatty acid esters of glycosides		<i>Candida antarctica</i>	Adlerhorst <i>et al.</i> 1990
Butyl oleate Oleyl butyrate Oley oleate	Surfactants	<i>Candida rugosa</i>	Zaidi <i>et al.</i> 2002
6- O- Lauroyl sucrose 6-O-Lauroyl glucose 6-O-Lauroyl maltose 6-O-Palmitoyl maltose 6,1-di-O-Lauroyl sucrose 6,6-di-O-Lauroyl sucrose 6'-O- Palmitoyl maltose	Surfactants	<i>Humicola lanuginosa</i> <i>Candida antarctica</i>	Ferrer <i>et al.</i> 1999; Ferrer <i>et al.</i> 2005
β-Methylglucoside methacrylate / acrylate	Surfactants	<i>Candida antarctica</i>	Kim <i>et al.</i> 2004

1.6. Important factors influencing the lipase activity in organic solvents

1.6.1. Nature of substrate

Lipases are known to display varying degrees of selectivities towards the substrates with which they interact (Bloomer 1992). Steric hindrance (branching, unsaturation and chain length) and electronic effects of the substrates are the two major forces that determine selectivity (Bevinakatti and Banerjee 1988). In esterification reactions, many lipases display high selectivities on long and medium chain fatty acids than the short chain and branched ones (Alhir *et al.* 1990). Most lipases display selectivities towards carboxylic acids. *Geotrichum candidum* lipase reacts only with fatty acids containing a *cis* bond at the 9th position (Schrag *et al.* 1996). Generally alcohols like ethanol and geraniol have been reported to be inhibitory in esterification and transesterification reactions (Chulalaksananukul *et al.* 1990; 1992; Miller *et al.* 1988). Molar ratio of the substrates plays an important role in esterification, which can be improved by increasing either alcohol or acid but in most of the cases, alcohols may be inhibitory and acids may cause acidification of microaqueous interface resulting in inactivation of lipases (Dorm *et al.* 2004; Guvenc *et al.* 2002; Zaidi *et al.* 2002). It is difficult to generalize the effect of chain length on esterification, because it depends on lipase preparation and the specificity of the enzymes. Esterification increased with increase in chain length when reaction was catalysed with lipases from *Staphylococcus warneri* and *Staphylococcus xylosus* (Talon *et al.* 1996). In case of Lipolase 100T, esterification decreased with increase in chain length and found to be independent of chain length when esterification was catalysed with Novozyme 435 (Kumar *et al.* 2005).

Use of acetic acid as an acyl donor was attempted with little or no success (Takahashi *et al.* 1988) in the preparation of acetates. Compared to its higher homologous (propionates, butyrates), acetic acid is a potent inhibitor by preferentially

reacting with the serine residue at the active site of lipase (Huang *et al.* 1998). Iwai *et al.* (1980) did not observe any reaction between acetic acid and geraniol using lipases from four different microorganisms. Langrand *et al.* (1988) showed that acetic acid esters were difficult to synthesize in high yields due to lipase inactivation by acid. Although, few researchers have focused their attention on transesterification to obtain high yields of acetates (Langrand *et al.* 1990, Rizzi *et al.* 1992; Chulalaksananukul *et al.* 1993), reports on maximizing acetate production by direct esterification are scanty. Also, low molecular weight substrates are more water-soluble and as such may react differently than do high molecular weight (less water soluble) substrates in non aqueous systems.

1.6.2. Nature of solvent

Most information regarding enzyme catalysis like reaction rates, kinetics and mechanistic aspects have been derived from studies conducted in aqueous solutions (Dixon and Webb 1979; Welsh and Williams 1990). But, when enzymes are directly dispersed in organic solvents, they exhibit remarkable changes in their properties (Klibanov 1986). Organic solvents employed influence reaction rate, maximum velocity (V_{\max}) or specific activity (K_{cat}), substrate affinity (K_M), specificity constants (K_{cat}/K_M) (Zaks and Klibanov 1986), enantio-selectivity (Sakurai *et al.* 1988), lipase stability (Kung and Rhee, 1989) and stereo and regio-selectivities (Parida and Dordick 1991; 1993; Nakamura *et al.* 1991; Rubio *et al.* 1991). Several efforts have also been made to correct the kinetic affinity parameters for substrate-solvent interactions (Van Tol *et al.* 1992; Reimann *et al.* 1994). The enzyme activity in different solvents could be due to variable degree of enzyme hydration imposed by the solvents and not to their direct effect on the enzyme or substrates. Generally use of organic solvents in enzyme catalysed synthesis exhibit more advantages than aqueous media (Klibanov 1986).

The advantages are:

1. Non polar / hydrophobic substrates can be employed for the reaction.
2. Enhances the reaction rate
3. Shifting of thermodynamic equilibria towards ester synthesis by maintaining low water activity.
4. Easy product recovery in low boiling organic solvents.
5. Since enzymes are insoluble in organic solvents, can be easily recovered from the reaction mixture by simple filtration.
6. Water dependent reactions such as hydrolysis, polymerization and racemization can be avoided.
7. Enzymes, especially lipases, may not be active in highly polar solvent which can cause denaturation due to strong hydrogen bonding interactions.
8. Inhibition of enzymes by hydrophobic substrates or products minimized due to the dispersion throughout the organic solvents, which again minimizes substrate concentration at enzyme surface.
9. Microbial contamination resulting in enzyme inhibition as well as degradation/ modification of required products.

Investigations on quantification of solvent effects on enzyme catalysis were carried out (Brink and Tramper 1985; Laane *et al.* 1987). Brink and Tramper (1985) tried to explain the influence of many water immiscible solvents on biocatalysis by employing the Hildebrand parameter, δ , as a measure of solvent polarity. They concluded that enhanced reaction rates could be expected when the polarity of the organic solvents was low ($\delta \approx 8$) and its molecular weight > 150 . But later, it was demonstrated that δ was a poor measure of solvent polarity. Laane *et al.* (1987) quantified solvent polarity on the basis of log P values. The log P value of a solvent could be defined as the logarithmic value of the partition coefficient of the solvent in *n*-octanol/water two-phase system.

Generally, biocatalysis is low in solvents of $\log P < 2$, is moderate in solvents with a $\log P$ value between 2 and 4 and high in non-polar solvents of $\log P > 4$. *Rhizomucor miehei* lipase was shown to follow these rules when esterification reactions were conducted in different solvents (Laane *et al.* 1987). In presence of hydrophilic solvents ($\log P < 2$) lipozyme has showed no esterification. Hence, polar solvents may remove the essential water from the enzyme and disrupt the active confirmation (Gargouri *et al.* 2002; Adachi and Kobayashi 2005). They also probably form hydrogen bonds between solvent molecule and surface amino acids of the enzyme. Solvents whose $\log P$ values were > 2 , dissolve to a lesser degree in water, leaving the enzyme suitably hydrated in its active conformation and so are able to support product synthesis (Soo *et al.* 2003). But a lipase which exhibits increasing activity with increased DMSO content (a polar solvent) has also been isolated (Bloomer 1992). Effect of $\log P$ values of organic solvents was studied by correlating to K_{cat} and K_m . K_{cat} showed strong correlation with $\log P$ but not K_m . K_{cat} was not affected by different solvent composition with constant $\log P$ whereas K_m was reported to change remarkably (Hirakawa *et al.* 2005). Most of the lipases readily undergo inactivation in presence of polar solvents, which is very much essential to dissolve certain substrates like sugars, hence the idea of solvent mixtures of non polar solvents with small amount of polar solvents was also employed in lipase catalysis (Ferrer *et al.* 1999). While it is generally accepted that non-polar solvents are better than polar ones for lipase catalyzed esterification reactions, a clear consensus is yet to be reached regarding the issue of solvent effects on enzyme catalysis in general.

1.6.3. Thermal Stability

Many factors govern the catalytic activity and operational stability of lipases at higher temperatures in non-aqueous media (Bloomer 1992). Zhu *et al.* (2001) reported

that thermal stability of a lipase is obviously related to its structure. Thermal stability is also influenced by environmental factors such as pH, solvent and the presence of metal ions. At least in some cases, thermal denaturation appears to occur through intermediate states of unfolding of the polypeptide chain (Zhu *et al.* 2001). Other factors such as the nature of the organic medium employed and water content in the microenvironment of the enzyme (Halling 1994) also affect thermal stability. There are a few reports on the thermostability of lipases in aqueous media. Lipase from *Pseudomonas fluorescens* 33 was found to retain 10-20 % higher activity in the presence of casein and Ca^{2+} at higher temperatures (60°C-90°C) at only 10 min of incubation (Kumura *et al.* 1993). Thermostabilities of some serine esterases like chymotrypsin and lipase from *Candida rugosa* and *Rhizomucor miehei* have been studied as a function of hydration of the enzymes using differential scanning calorimetry (Turner *et al.* 1995). It was found that the denaturation temperature (T_m) was 30°C–50°C higher in anhydrous environments than in aqueous solutions. Volkin *et al.* (1991) reported that enzymes are more thermostable in hydrophobic solvents rather than in hydrophilic solvents, because in hydrophobic solvents enzymes are inert with respect to their interaction with protein even at higher temperature and in hydrophilic solvents stripping of water from the enzyme leads to denaturation. Porcine pancreas lipase was reported to retain higher esterification activity in dry organic environment (2M heptanol solution in tributyrin) at a temperature of 100°C when a low concentration of water (0.015%) was maintained in the reaction system (Zaks and Klivanov 1984). Half-life for the enzyme was found to be more than 12 h at 100 °C. However, when concentration of water was increased to 3 %, loss of activity was almost instantaneous (half life = 2 min). Porcine pancreas lipase (PPL) in non-aqueous media showed that longer periods of incubation of PPL, especially at 80°C, did not affect the active conformation of PPL even after incubation

for a period upto 10 days (Kiran *et al.* 2001) at very low water content. Immobilization of the enzyme and addition of salt hydrates are known to enhance the thermostability of lipases in organic media (Kvittengen *et al.* 1992; Halling 1992). Thermal stability can also be improved by making surfactant-lipase complex (Goto *et al.* 2005; Maruyama *et al.* 2002; Wu *et al.* 2002). It is a common practice now to carry out lipase catalyzed esterification reactions at around 80°C - 90°C (Trani *et al.* 1991). Noel and Combes (2003) conducted series of experiments at different temperatures to study the thermal effect of *Rhizomucor miehei* (RML) and concluded that thermal deactivation occurs due to the formation of aggregates rather than protein unfolding.

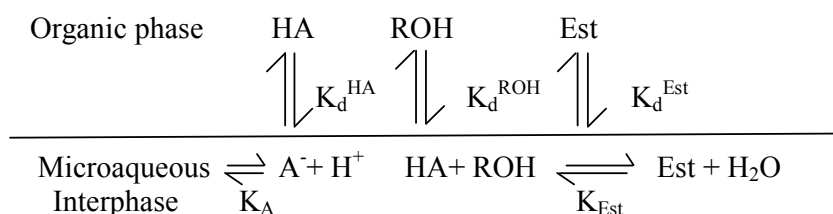
1.6.4. Role of water in lipase catalysis

Water plays a crucial role in the reversible reaction catalyzed by lipase, involving hydrolysis and esterification (Hahn-Hägardal 1986; Gayot *et al.* 2003). While a critical amount of water is necessary for maintaining the active conformation of the enzyme, excess water facilitates hydrolysis (Halling 1989; 1994; Zaks and Klivanov 1985; 1988; Valivety *et al.* 1993; Cameron *et al.* 2002). The bound water structure is very important in stabilizing the conformation of a lipase in non-aqueous media. There are 22 buried water molecules in case of *Rhizomucor miehei* lipase (Brady *et al.* 1990), where water on the enzyme is bound to charged and polar residues on the surface as a monolayer (Tramper *et al.* 1992; Kvittengen 1994; Halling 1994; Carrea *et al.* 1995; Vermue and Tramper 1995; Zaks and Klivanov 1988; Gorman and Dordick 1992). Presence of excess water decreases the catalytic activity from both kinetic and thermodynamic points of view (Chulalaksananukul *et al.* 1990; Marty *et al.* 1992). The concentration of water in organic solvents is inversely proportional to thermostability of lipases (Zaks and Klivanov 1984). It was shown that for PPL, hydrophobic solvents served better than hydrophilic ones for catalysis (Zaks and Klivanov 1988; Parida and Dordick 1991).

Substrate concentrations and water activity can control the product distribution, hence only monoester of ethylene glycol can be prepared by using either a low water activity or by employing higher concentrations of alcohols and *vice versa* for diesters (Chand *et al.* 1997). Presence of certain amount water (optimum water, 5%) with crude lipase from horse liver enhanced reaction rate by three fold and also stereoselectivity increased by 50% (Gutman *et al.* 1991). Humeau, *et al.* (1998) and Osorio *et al.* (2001) reported that beyond the critical water concentration, esterification decreases because the size of the water layer which is formed around the enzyme retards the transfer of acyl donor to active site of the enzyme. Yadav and Devi (2004) conducting experiments at various speed of agitation found that there is no effect of speed of agitation (Guvenc *et al.* 2002) on esterification. The water layer surrounding the enzyme makes the enzyme to be more flexible (act as molecular lubricant) by forming multiple hydrogen bonds and interacting with the organic solvent, causing denaturation. Organic substrates and products with poor solubility in aqueous medium diffuse with difficulty through the intra-particle water layer to the active centers of the enzyme. Thus the activity of the enzyme would depend on water-induced inactivation or partition of components between the bulk solvent and the microenvironment (Yadav and Devi 2004, Yadav and Lathi 2004). Almost all lipases are active at low water activity but there is large difference in optimal water activity between the lipases (Ma *et al.* 2002; Gargouri *et al.* 2002).

There are several methods available to monitor water activity like Karl-Fischer titration (Halling 1994) and specialized sensors (Blanco *et al.* 1989). In esterification reactions, water formed can be removed from the reaction mixture leading to higher yields (Bloomer *et al.* 1992) by passing the reaction mixture through a bed of desiccants (Halling 1990; Gubicza *et al.* 2000). In non-polar solvents, excess water adds to the

already existing hydration shell on the enzyme constituting the microaqueous inter-phase. Partitioning of the acid, alcohol and product between microaqueous inter-phase and solvent phases plays a significant role in regulating esterification. The solubility of the acid and its dissociation, result in a proton build-up at the inter-phase. In lipase catalyzed esterification, the various equilibria involved at the microaqueous inter-phase are shown in **Scheme 1.3** (Aires-Barros *et al.* 1989).



Scheme 1.3

where HA = acid, ROH = alcohol, Est = ester, K_d^{HA} , K_d^{ROH} and K_d^{Est} = distribution coefficients of acid, alcohol and ester respectively; K_A = dissociation constant of acid, K_{Est} = equilibrium constant of esterification. Since water is present in micro-quantities and is inaccessible, direct measurement of microaqueous pH is not possible (Valivety *et al.* 1990). Attempts have been made to measure the pH in non-aqueous systems by Cambou and Klivanov (1984a), who reported the use of an indicator, which changed colour with pH. A reliable method has been developed by Valivety *et al.* (1990) in which an hydrophobic indicator (fluorescein ester with 3,7,11- trimethyldodecanol) is used, which remains completely in the organic phase, but responds to pH changes in an adjacent aqueous phase. Thermodynamic factors operating at the microaqueous enzyme-water-solvent phase in non-polar solvents were also investigated in terms of the water of reaction, partitioning of acid between the microaqueous phase and the organic solvent,

dissolution and dissociation of the acid, the resultant number of H^+ present in the microaqueous phase and the extent of esterification (Kiran *et al.* 2002).

1.6.5. Immobilization

Immobilization of lipase facilitates large area of inter-phase for the reaction to occur. The advantages of immobilizing lipases are repetitive use of a given batch of enzymes, better process control, enhanced stability, enzyme - free products (Welsh and Williams 1990; Rahman *et al.* 2005), increased stability of polar substrates, shifting of thermodynamic equilibria to favour ester synthesis over hydrolysis, reduction in water dependent side reactions such as hydrolysis, elimination of microbial contamination and potential to be used directly within a chemical process. In presence of organic solvents, immobilized lipase showed enhanced activity (Ye *et al.* 2005). Ye *et al.* (2005) reported that at lesser water content, free lipase preparation showed increase in activity than the immobilized lipase preparation. With the increment of the amount of water added, conformational limitation on the enzyme as a result of covalent bond formation between the enzyme and the matrix, led to increase in activity due to immobilization.

Immobilization of lipases has been performed by various methods such as adsorption, entrapment and covalent binding, using different supports. For covalent immobilization, usually, support matrices like silica beads are activated with glutaraldehyde (Ulbrich *et al.* 1991). In case of non-covalent immobilization, lipases can be adsorbed with very good activity to a weak anion exchange resin (Eigtved 1989; Ison *et al.* 1990). For non-covalent immobilization, both ionic and hydrophobic interactions between lipase and surface are important (Malacata *et al.* 1990). Polymers such as poly vinyl alcohol (PVA), carboxymethyl cellulose (CMC), poly ethylene oxide (PEO) and CMC: PVA blends can also be used for lipase immobilization (Vecchia *et al.* 2005). Morphology of films surfaces analyzed by scanning electron microscopy indicated that

lipases were preferentially located on the polymer surface (Crespo *et al.* 2005). Vecchia *et al.* (2005) have immobilized 10 different lipases on PVA, CMC and PVC: CMC blend (50:50% m/m) and among them *Mucor javanicus* (MJL) or *Rhizopus oryzae* (ROL) exhibited highest activity. This immobilized enzyme can be reused at least 10 times for a span of 80 days. *Candida antarctica* B (Novozym 435) was immobilized on mesoporous silica with octyltriethoxysilane and it retained its activity even after 15 reaction cycles (Blanco *et al.* 2004). Calcium carbonate was found to be the most suitable adsorbent when crude *Rhizopus oryzae* lipase was immobilized on different supports and it exhibited long-chain fatty acid specificity (Ghamgui *et al.* 2004). Lipase from *Pseudomonas cepacia* was gel-entrapped by polycondensation of hydrolyzed tetramethoxy silane and iso-butyltrimethoxy silane and it was subjected to repeated use without losing much activity (Noureddini *et al.* 2005).

1.7. Strategies employed in lipase catalyzed esterification

1.7.1. Esterification in reverse micelles

Enzymatic reactions in reverse micelles (water-in-oil) offer many advantages over those in micelles (oil-in-water) impart solubilization of lipases and hydrophobic/hydrophilic substrates at higher concentrations, better control over water activity and large interfacial area leading to enhanced reaction rates in a thermodynamically stable single phase (Stamatis *et al.* 1999). Various reactions like synthesis of flavour esters (Borzeix *et al.* 1992), macrocyclic lactones (Rees *et al.* 1995), and resolution of chiral alcohols (Rees and Robinson 1995) have been attempted in reverse micelles. Krieger *et al.* (2004) highlighted some of the recent developments on the use of lipases in reverse micelles. There have been some efforts to continuously recover the product as well as enzyme for reuse, which, are the major problems of enzyme catalysis in reverse micelles. Reverse micelles can exchange biocatalyst, water,

substrates and products with the bulk organic solvent (Krieger *et al.* 2004). Murakata *et al.* (1996) have reported high esterification activity of entrapped lipases on lipophilic substrates. The effective diffusion coefficient of lauric acid varied with the lecithin microemulsion-based organogel (MBGs) compositions, while that of butyl alcohol remained constant in the esterification of lauric acid with butyl alcohol catalyzed by *Candida rugosa* lipase (Nagayama *et al.* 2002). High initial reaction rate was obtained in extremely low water content when the esterification of oleic acid with octyl alcohol catalyzed by *Rhizopus delemar* lipase was investigated in reverse micellar system of sugar ester DK-F-110 (Naoe *et al.* 2001). Kinetic studies were carried out to study the esterification of octanoic acid with 1-octanol, catalyzed by *Candida lipolytica* (CL) lipase, in water-in-oil microemulsions formed by water/ bis-(2-ethylhexyl) sulfosuccinate sodium (AOT)/isooctane (Zhou *et al.* 2001). An esterification reaction of hexanol and hexanoic acid in the cyclohexane/dodecylbenzenesulfonic acid (DBSA)/water microemulsion system using *Candida cylindracea* lipase demonstrated that DBSA itself can act as a kind of acid catalyst (Han and Chu 2005).

1.7.2. Esterification in supercritical carbon dioxide

Use of super critical carbon dioxide (SCCO₂) as a solvent and reaction medium is growing rapidly in recent years. Super critical carbon dioxide has several advantages over organic solvents: it is cheap, non-toxic, non-inflammable, used at near ambient critical temperature (31.1⁰ C) and moderate critical pressure (Srivastava *et al.* 2003). The solvent properties of SCCO₂ can be readily modified by adjusting the pressure and temperature, the diffusivity of solutes in CO₂, which is higher than in organic solvents and easy recovery of CO₂ from the reaction products minimizing the need for costly downstream processing. When CO₂ is used along with organic solvents, it offers an additional advantage of being an environment-friendly process (Clifford 1994).

Fatty acid methyl esters were prepared from methanol and seed oils in flowing CO₂ by employing immobilized *Candida antartica* lipase (Holmberg *et al.* 1989). Transesterification of soybean oil with glycerol, 1,2-propanediol and methanol by immobilized *Candida antartica* lipase for the synthesis of monoglycerides have also been reported (Jackson and King 1997). Isoamyl acetate was synthesized using lipases from *Candida antartica* and *Rhizomucor miehei* in SCCO₂ where *Rhizomucor miehei* gave 100% esterification with acetic anhydride (Romero *et al.* 2005a). Enantioselective enzymatic hydrolysis of 3-hydroxy-5-phenyl-4-pentenoic acid ethyl ester in a biphasic buffer/SCCO₂-system was also carried out (Hartmann *et al.* 2001) where one ester enantiomer was preferably hydrolyzed, the other remained in the supercritical phase. *Candida cylindracea* lipase catalyzed enantioselective esterification of racemic 2-(6-methoxy-2-naphthyl) propionic acid in microaqueous isooctane showed that alcohol concentration influences enzyme performance (Wu and Liu 2000). Production of ethyl esters from ethanol and cod liver oil by an immobilized lipase from *Candida antartica*, in SCCO₂ has also been described (Gunnlaugsdottir *et al.* 1998).

1.7.3. Esterification in micro wave assisted reactions

From the last decade the use of microwave technology in organic synthesis is enormously developed because of short reaction time, purity of the resulting products and enhancement of reaction yields (Loupy *et al.* 1998). Adelhorst *et al.* 1990 synthesized monoesters of glucopyranosides in large scale using lipases from *Candida antartica* and *Rhizomucor miehei* in dry media. Immobilized *Candida antartica* was employed for the esterification of methyl-D-glucopyranoside, D-glucose and α,α -trehalose with dodecanoic acid in dry media under focused microwave irradiation (Gelopujic *et al.* 1996). In this technology enzyme maintains selectivity and also retains its activity without loss of much activity.

1.7.4. Kinetic studies of lipase catalyzed esterification reactions

Kinetics of lipase catalyzed esterification reactions help in not only quantifying a reaction but also bring out some intricate details of enzyme inhibition and mechanism which have quite a lot of bearing on the industrial application of lipases (Vulfson 1994). When lipases were used in organic solvents, it was found that they followed a complex two-substrate Ping-Pong Bi-Bi mechanism (Zaks and Klibanov 1985). A Ping-Pong Bi-Bi mechanism, which stands for two-substrate two-product reaction, is a sequential one i.e., both substrates bind to the enzyme successively before the product is formed. The amount of lipase available and the rate of breakdown of the enzyme-substrate complex govern the overall rate of reaction. If the organic acid employed is inhibitory in nature, then it remains bound to the enzyme strongly and no acyl transfer occurs. In some cases, even if the acyl transfer occurs, product formed may remain bound to the enzyme resulting in inhibition.

Lipase-catalyzed esterification between oleic acid and ethanol (Chulalaksananukul *et al.* 1990) and transesterification between geraniol and propyl acetate (Chulalaksananukul *et al.* 1992) were found to follow Ping-Pong Bi-Bi mechanism where both ethanol and geraniol were found to be inhibitory. Similar Ping-Pong Bi-Bi mechanism was found to be followed in the kinetics of esterification of lauric acid by (-)-menthol catalyzed by lipase from *Penicillium simplicissium* with (-) menthol being inhibitory (Stamatis *et al.* 1993). In a transesterification reaction between isoamyl alcohol and ethyl acetate catalyzed by Lipozyme IM20, the substrates, ethyl acetate and isoamyl alcohol and one of the products (ethanol) were found inhibitory. Of the three alcohols, ethanol was found to be more inhibitory (Rizzi *et al.* 1992) than the others.

A kinetic model has also been proposed, taking into account, the effect of solvent (γ_s – substrate solvation) and a_w , which are thermodynamic parameters. In this model, the

hydration state of the enzyme molecule was examined and equilibrium kinetic constants were expressed in terms of thermodynamic activity. Predictions based on this model were found to be in good agreement with experimental observations (Lee 1995; Janssen *et al.* 1999). Mathematical analyses of experimentally observed initial rates yielded various parameters, $K_{m(\text{lactic acid})}$, $K_{m(\text{stearic acid})}$, V_{\max} and $K_{i(\text{lactic acid})}$ in the kinetic study of the reaction between stearic acid and lactic acid (Kiran and Divakar 2002). Thus, with improved kinetic models being proposed, one can predict the enzyme behaviour in a more efficient manner.

1.7.5. Response Surface Methodology (RSM) in lipase catalysis

Response surface methodological analysis provides an important tool for optimizing reaction conditions. This methodology has been applied to several esterification reactions also. Most of the RSM studies have centered on working out the optimization conditions for a particular lipase catalysed esterification reaction (Sheih *et al.* 1995; 1996; Claon and Akoh 1994a; Kiran *et al.* 1999; 2000; 2001; Harikrishna *et al.* 1999). Thus, optimum conditions for the enzymatic synthesis of geranyl butyrate using lipase AY from *Candida rugosa* was worked out by Sheih *et al.* (1996). Similarly, the effect of reaction parameters on SP 435 lipase catalysed synthesis of citronellyl acetate in organic solvents was carried out by Claon and Akoh (Claon and Akoh 1994b). Optimisation of conditions for the synthesis of 2-O-palmitoyl lactic acid, 2-O-stearoyl lactic acid and 2-O-lauroyl lactic acid using lipases from *Rhizomucor miehei* and porcine pancreas was studied by Kiran *et al.* (Kiran *et al.* 1999; 2000; 2001). RSM was also employed to optimize the synthesis of flavors using lipases (Nogales *et al.* 2005; Macedo *et al.* 2004; Buzzini *et al.* 2003). *Rhizomucor miehei* lipase catalysed synthesis of bio diesel from soybean oil and methanol was optimized using RSM and the optimum conditions were determined by rigid matrix analysis which also indicated that methanol

was inhibitory (Shieh *et al.* 2003). Shaw *et al.* (2003) optimized the synthesis of propylene glycol monolaurate using RSM and a 3-level-4-factor fractional factorial design was adopted to evaluate the optimum conditions.

Usefulness of several statistical designs in experimental optimization including Box-Behnken, Central Composite Rotatable and Plackett-Burman designs in lipase catalysed esterification reactions have also been described (Manohar and Divakar 2004a). Analyses of several response surface plots obtained by employing statistical designs in lipase catalysed esterification reactions have indicated that such plots could be grouped into four types to explain the esterification behaviour in the presence of different kinds of substrates and reaction conditions. Similarly, a Plackett-Burman design helps in the selection of the most probable organic acid or alcohol in a mixture, in a facile esterification reaction. Predominant acid binding in preference to alcohol gives rise to dome-shaped response surface plots. The competitive and inhibitory nature of substrates is brought out clearly in response surface plots. Rate plots show linear relationships between time and substrate with smooth surfaces within the limits of the variables employed. There are other uneven plots, which reflect the effect of variables like buffer pH, buffer concentration and temperature on the activity of lipase employed. The stability of lipases under drastic esterification conditions of temperature and solvents could also be studied.

1.7.6. Lipase catalyzed resolution of racemic esters

There is an increasing demand for preparing optically active pure compounds in pharmaceutical industry. Various methods are available to synthesize the optically active compounds. Among them enzymatic are more attractive (Sheldon 1996). Lipases have also been extensively used in the resolution of racemic alcohols and carboxylic acids through asymmetric hydrolysis of the corresponding esters (Cambou and Klivanov

1984b). Chirally pure hydroxyalkanoic acids which find wide applications as drug intermediates have been obtained from racemic (\pm)-hydroxyalkanoic esters (Scilimati *et al.* 1988; Feichter *et al.* 1989; Engel *et al.* 1991). Molecular modelling studies have revealed that enzyme behaviour towards racemic substrates can be predicted (Hult and Norin 1993). Rantwijk and Sheldon (2004) critically reviewed resolution of chiral amines through enantioselective acylation by three different serine hydrolases such as lipases, subtilisin and *Penicillin* acylase and recommended *Candida antarctica* lipase because of its high enantioselectivity and stability. Resolution of some enantiomeric alcohols like (*R,S*)-2-octanol, (*R,S*)-2-(4-chlorophenoxy) propionic and (*R,S*)-2-bromo hexanoic acids were carried out using lipases from *Candida rugosa* and *Pseudomonas* sp., where *R*-alcohol was obtained with an enantiometric excess of about 98% (Crespo *et al.* 2005). Optically active (*S*)- α -cyano-3-phenoxybenzyl (CPB) acetate was obtained from racemic cyanohydrins by transesterification using lipase from *Alcaligenes* sp. in organic media (Zhang *et al.* 2005). Lipase like enzyme isolated from porcine pancreas immobilized in DEAE - Sepharose gave pure (*S*)-(-) glycidol from (*R*)-(-)-glycidyl butyrate when the reaction was carried out in pH 7.0 and 10% dioxane at 25 °C (Palomo *et al.* 2003).

1.8. Scope of the present work

The above described features have clearly established that, as one of the most thoroughly studied hydrolyzing enzymes in synthetic reactions, lipases have come a long way in establishing themselves as an important synthetic tool to bio-organic reactions. The main scope of the present work described in this thesis is to use the lipases in esterification reactions to prepare commercially important esters. Amino acyl esters of carbohydrates, exhibit a large number of applications. They can be used as antibiotics, detergents, sweetening agents, microcapsules in pharmaceutical reagents, in delivery of

biological active amino acid esters, anti tumor agents and antiviral nucleoside amino acid esters.

Literature survey indicates that lipase catalysed synthesis of amino acyl esters of carbohydrates are very few (Park *et al.* 1999; 1996; Boyer *et al.* 2001; Maruyama *et al.* 2002; Vijyakumar *et al.* 2004; Lohith and Divakar 2004). The available literature deals with N-protected and carboxyl group activated amino acids and carbohydrates. The reported protocols exhibit some severe limitations. Most of researchers have employed proteases for their work (Boyer *et al.* 2001; Park *et al.* 1999; 1996; Riva *et al.* 1986). Protected and carboxyl group activated amino acids and carbohydrates have been employed (Park *et al.* 1999; 1996). Reactions were carried out with health hazardous solvents like dimethyl sulphoxide, pyridine and dimethylformamide. Most of the reports are from experiments carried out in shake flask levels with large amount of enzyme being employed in such reactions (Riva *et al.* 1986). Lipases have been reported to give insignificant results in preparing amino acyl esters of carbohydrates (Park *et al.* 1996).

The experimental protocols developed in the present work described in this thesis have efficiently dealt with the above mentioned disadvantages. Commercially available lipases, which are also economically viable were employed in the present work. Use of unprotected and unactivated amino acids and carbohydrates have been employed for the reactions, which effectively reduce the number of acylation and deacylation steps. Low boiling solvents were employed for the reactions such that solvents can be recovered by distilling. The work out procedures were easy and the product recovery involved very few unit operations. Smaller amounts of enzyme and larger amounts substrates were employed to obtain high yields than the reported. All the reactions were carried out in presence of solvent mixtures using an experimental set up, which maintained a very low

water activity, very much essential for high enzyme activity and for carrying out reactions in a large-scale level as well.

The present work describes synthesis of L-phenylalanyl, L-tryptophanyl, L-histidyl and L-prolyl esters of aldohexoses (D-glucose, D-galactose and D-mannose), ketohexose (D-fructose), pentoses (D-arabinose and D-ribose), disaccharides (lactose, maltose and sucrose) and sugar alcohols (D-sorbitol and D-mannitol) using lipases from *Rhizomucor miehei*, porcine pancreas and *Candida rugosa* in organic solvents. Various effects of enzyme, substrate and buffer concentrations, pH, enzyme reusability, kinetics, regio and stereo selectivity were investigated. The isolated product esters were also tested for probable pharmaceutical activity as well. Thus the full potentialities of lipases are brought out in this study which describes the synthesis of several amino acyl esters of carbohydrates for the first time using lipases from *Rhizomucor miehei*, porcine pancreas and *Candida rugosa*.

Chapter 2

Materials and Methods

2.1. Materials

2.1.1. Lipases

In the present work, three different lipases were employed - two from fungal sources, *Rhizomucor miehei* lipase (RML) and *Candida rugosa* lipase (CRL) and one from animal source, porcine pancreatic lipase (PPL).

Table 2.1. List of lipases and their suppliers

Lipase	Manufacturer	Amino acyl esters synthesized
Porcine pancreas lipase (Type II, Steapsin, crude preparation)	Sigma Chemical Co., St. Louis. MO, USA.	Preparation of L-phenylalanyl, L-tryptophanyl, L-histidyl esters of D-glucose and L-phenylalanyl esters of lactose
<i>Rhizomucor miehei</i> lipase (Lipozyme IM20 immobilized on weak anion exchange resin)	Novo-Nordisk, Bagsvaerd, Denmark and Boehringer Mannheim, Germany.	Preparation of L-phenylalanyl-D-glucose (Response Surface Methodology and kinetic studies).
<i>Candida rugosa</i> lipase	Sigma Chemical. Co. MO, USA.	Preparation of L-prolyl, L-phenylalanyl, L-tryptophanyl, and L-histidyl esters of D-glucose, D-galactose, D-mannose, D-fructose, D-arabinose, D-ribose, lactose, maltose, sucrose, D-sorbitol and D-mannitol.

2.1.2. L-Amino acids

L-Proline, L-phenylalanine, L-tryptophan and L-histidine were purchased from Hi-Media Ind. Ltd. and were used as such.

2.1.3. Carbohydrates

D-Glucose and sucrose from SD fine chemicals (Ind.) Ltd., D-galactose and D-fructose from Hi-Media Ind. Ltd., D-mannose, D-arabinose, D-ribose and D-mannitol from LOBA Chemie Pvt. Ltd. India, maltose from Sigma Chemical. Co. MO, USA, lactose from SISCO Research Laboratories Pvt. Ltd. India and D-sorbitol from Rolex Laboratory Reagent India Ltd. were employed for the reactions.

2.1.4. Other chemicals

Table 2.2. List of chemicals and suppliers

Chemicals	Supplier
Sodium acetate (CH_3COONa), Sodium dihydrogen phosphate (Na_2HPO_4)	Ranbaxy Laboratories Ltd. India,
Di-sodium tetraborate ($\text{Na}_2\text{B}_4\text{O}_7 \cdot 10\text{H}_2\text{O}$), sodium chloride, sodium hydroxide, hydrochloric acid, sulphuric acid, iodine resublimed, molecular sieves 4\AA , copper sulphate, silica gel and sodium potassium tartarate.	SD fine Chemicals (Ind.) Ltd.
Ninhydrin, 1-naphthol, hippuric acid, triton x-100 Brilliant blue R 250, β -mercaptoethanol, trichloro acetic acid	LOBA Chemie Pvt. Ltd. India.
Hippuryl-L-histidyl-L-leucine tetrahydrate, bovine serum albumin, Sephadex G-10 and Sephadex G-25	Sigma Chemical. Co. MO, USA
Bio Gel P-2	Bio-Rad Laboratories, USA.
KBr, Folin-Cicolteau reagent, and HEPES buffer (N-[2-hydroxyethyl] piperazine-N'-[2-Ethanesulphonic acid]).	SISCO Research Laboratories Pvt. Ltd. India

2.1.4. Solvents

Solvents: dichloromethane, chloroform, n-hexane, n-heptane, pyridine, dimethylformamide, n-butanol, acetic acid, butyric acid, acetone, diethyl ether purchased from SD fine Chemicals (Ind.) Ltd. were employed after distilling once. Acetonitrile and methanol of HPLC grade were purchased from Qualigens fine chemicals (India) Ltd. and were used as such.

2.2. Methods

2.2.1. Lipase activity

Both esterification as well as hydrolytic activities of the lipases were determined.

2.2.1.1. Hydrolytic activity

Hydrolytic activity of lipase is defined as μmol of butyric acid released per min per mg of immobilized lipase preparation. The specific activity is expressed as μmol of butyric acid released per min per mg of protein present in the lipase (Table 2.3). Hydrolytic activities of different lipases were determined by the tributyrin method (Vorderwulbecke *et al.* 1993).

A stock solution containing 10 mL of tributyrin, 90 mL of 0.01 M pH 7.0 sodium phosphate buffer, 0.2 g sodium benzoate, 0.5 g of gum acacia and 50 μL 10% SDS was prepared. It was emulsified by stirring and the pH was adjusted to 7.0 with concentrated NaOH. From this stock solution, 4 mL was pipetted out into stoppered conical flasks (S), containing 8 mL, 0.01 M pH 7.0 sodium phosphate buffer to obtain a solution with a final concentration of 0.113 M tributyrin. Known quantities of lipases (5 –15mg) were added to this solution and incubated at 37 °C in a Heto-Holten shaker water bath for different intervals of time. After incubation, the pH of the reaction mixture in the flask was adjusted to 9.5 with standard 0.04 N NaOH. A blank (B) was also performed without adding enzyme. The hydrolytic activity was evaluated by using the following equation.

$$\text{Hydrolytic activity} = \frac{(\text{S}-\text{B}) \times \text{N}}{1000 \times \text{E} \times \text{T}} \quad \begin{array}{l} \mu\text{mol}/\text{min}.\text{mg of lipase} \\ \text{preparation or protein} \end{array}$$

Where, (S-B) = difference in volume of NaOH in mL between sample (S) and blank (B), N= normality of NaOH, E = amount of lipase preparation or protein taken in mg and T= incubation period in min.

2.2.1.2. Esterification activity

Esterification activities of four different lipases were determined by butyl butyrate method (Kiran *et al.* 2000). A stock solution containing 0.33M butanol and 0.16M butyric acid was prepared. In a 25 mL stoppered conical flask, 3 mL of the stock solution was dispersed in 5 mL of n-heptane. The reaction mixtures were incubated with known quantities of lipases for different intervals (30, 60, 90 and 120 min) in a Heto-Holten shaker water bath at 50 °C. After incubation, the contents of the flasks were titrated with standard 0.02 N NaOH. A blank (without the enzyme) was also performed. Table 2.3 shows the esterification activities of four different lipases. The esterification activity was evaluated by using the following equation.

$$\text{Esterification activity} = \frac{(\text{B-S}) \times \text{N}}{1000 \times \text{E} \times \text{T}} \begin{array}{l} \mu\text{mol}/\text{min}.\text{mg of lipase} \\ \text{preparation or protein} \end{array}$$

Where (B-S) = difference in volume of NaOH in mL between blank (B) and sample (S), N= normality of NaOH, E= actual amount of the lipase preparation or protein taken in mg and T= incubation period in min.

Table 2.3. Esterification and hydrolytic activities of different lipases ^a.

Lipase	Esterification activity ^b		Hydrolytic activity ^c	
	Activity $\mu\text{mol}/\text{min}.\text{mg}$ of lipase preparation	Specific activity $\mu\text{mol}/\text{min}.\text{mg}$ of enzyme protein	Activity $\mu\text{mol}/\text{min}.\text{mg}$ of lipase preparation	Specific activity $\mu\text{mol}/\text{min}.\text{mg}$ of enzyme protein
PPL	0.06	0.17	0.32	0.97
RML	0.46	7.27	0.10	1.59
CRL	0.03	7.64	-	-
Chirozyme	0.35	0.32	-	-

^aFor each enzyme the activity results were obtained from an average of three individual experiments for different time intervals. Error in activity measurements were \pm 5-10%. ^b Butyl butyrate method, lipase employed – 5, 10 and 15 mg, Incubation temperature – 50 °C. ^c Tributyrin method, lipase employed – 5, 10 and 15 mg, Incubation temperature – 37 °C.

2.2.2. Protein estimation

Protein content of all the four lipases were determined by using Lowry's method (Lowry *et al.* 1951). In order to leach out the protein from the immobilized matrix or carrier, 20 mg lipase preparations were stirred in 50 mL, 0.5 M NaCl at 4 °C for 12 h and from this, known volumes of the samples were taken for protein estimation.

Solution **A** – 1% of copper sulphate in water, solution **B** – 1% of sodium potassium tartarate in water and solution **C** – 2% of sodium carbonate solution in 0.1 N NaOH were prepared. Working solution **I** was prepared by mixing one part each of solution **A** and **B** and 98 parts of **C**. A 1:1 diluted solution of commercially available Folin- Cicolteau reagent with distilled water served as working solution **II**. To the protein sample in 1 mL water, 5 mL of working solution **I** was added and incubated for 10 min at room temperature. A 0.5 mL of working solution **II** was then added followed by incubation at room temperature for 30 min and absorbance was measured at 660 nm using a Shimadzu UV – 1601 spectrophotometer. Calibration curve for protein concentration was prepared by employing bovine serum albumin (BSA) in the concentration range 0 -100 µg in 6.5 mL of the sample (Fig. 2.1). Using this calibration plot protein content of four different lipases were determined and values are shown in Table 2.4.

Table 2.4. Protein content of different lipase preparations ^a

Lipase	Protein content (%)
Porcine pancreas lipase (PPL)	32.8
Rhizomucor miehei lipase (RML)	6.3
Candida rugosa lipase (CRL)	35.3
Chirazyme	3.2

^aLowry's method, lipase employed -20mg in 50 mL 0.5 M NaCl, Absorbance measured at 660 nm. Values are an average from three different concentrations of lipases. Errors in measurement will be ± 3-5%.

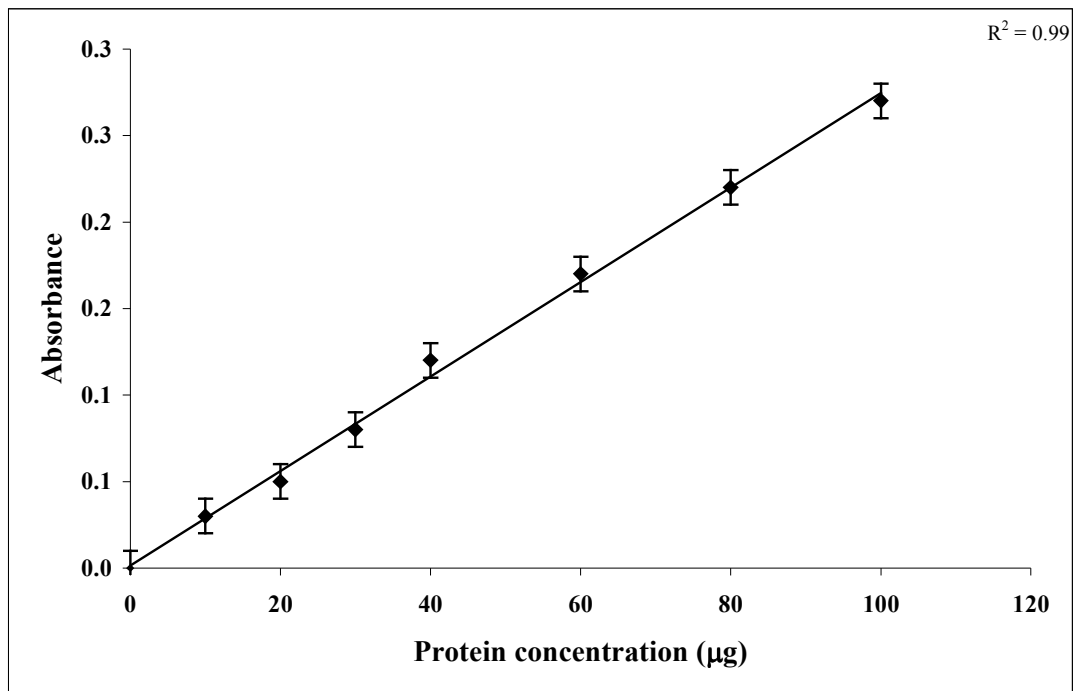


Fig. 2.1. Calibration curve for protein estimation by Lowry's method. A stock solution of 300 µg/ 3mL BSA solution was prepared. From the stock solution 0.2, 0.3, 0.4, 0.6, 0.8, 1.0 mL solutions were pipetted out and the total volume was made upto 1 mL with distilled water. Absorbance was measured at 660 nm.

2.2.3. Preparation of buffers

Decimolar concentrations of CH₃COONa buffer for pH 4.0 and 5.0, Na₂HPO₄ for pH 6.0 and 7.0 and Na₂B₄O₇·10H₂O for pH 8.0 buffers were prepared by dissolving appropriate amount of respective salts in distilled water and the pH was adjusted with dilute HCl or NaOH using Controlled Dynamics pH meter, model – APX175 E/C, India.

2.2.4. Esterification procedure

A bench-scale level procedure (Divakar *et al.* 1999) was adapted for the preparation of amino acyl esters of carbohydrates. Reactants such as unprotected L-amino acids (0.001- 0.005 mol) and carbohydrates (0.001 – 0.005 mol) were taken in a flat bottomed two necked flask along with 100 mL CH₂Cl₂: DMF (90:10 v/v) or hexane: CHCl₃: DMF (45:45:10 v/v) in presence of 0.018 - 0.225 g of lipases (expressed as % w/w based on the carbohydrate employed) and refluxed for a period of 3 - 120 h. The condensed vapours of solvents which formed an azeotrope with water was passed through a desiccant (molecular sieves of 4Å were used as desiccants) before being returned into the reaction mixture, thereby facilitating complete removal of water of reaction (Divakar *et al.* 1999; Lohith *et al.* 2003; Lohith and Divakar 2004). This experimental setup maintained a very low water activity of $a_w = 0.0054$ throughout the reaction period. The reaction mixture after distilling off the solvent was then added to 20 mL of water, stirred and filtered to remove the lipase. The filtrate was evaporated on a water bath to get the unreacted carbohydrate, unreacted L-amino acids and the product esters which were then analyzed by HPLC. In reactions, which involved use of buffer salts, known volumes of 0.1 M buffer solutions at specified pH were added to the reaction mixture to impart ‘pH memory’ to the enzyme. Decimolar concentrations of CH₃COONa buffer for pH 4.0 and 5.0, Na₂HPO₄ for pH 6.0 and 7.0 and Na₂B₄O₇ ·10 H₂O for pH 8.0 buffers were employed. The amino acids employed were L-

phenylalanine, L-tryptophan, L-histidine and L-proline. The carbohydrates employed were D-glucose, D-mannose, D-galactose, D-fructose, D-arabinose, D-ribose, lactose, maltose, sucrose, D-sorbitol and D-mannitol.

2.2.5. Isolation of esters

The esters formed were separated by size exclusion chromatography using Sephadex G-10 and Sephadex G-25 and Bio Gel P-2. Column of size 100 cm x 1.0 cm was employed. About 30g of gel (Bed volume of 70-80 mL) was packed and 200 mg of the reaction mixture was dissolved in distilled water and loaded onto these columns and eluted with water at a flow rate of 2 mL/h. Separation was monitored by thin layer chromatography (silica plates were prepared by dissolving 8 g of silica gel mesh 60-120 in 20 mL of water and spreaded uniformly over 20 x 20 cm glass plate and air and oven dried) using n-butanol: acetic acid: water (70:20:10 v/v/v) as mobile phase. The spots were detected by spraying ninhydrin (for amine group detection) and 1-naphthol (reducing sugar detection). The isolated product esters subjected to characterization.

2.2.6. High Performance Liquid Chromatography

Amino acyl esters of carbohydrates prepared using lipases were analyzed by high performance liquid chromatography (HPLC). A Shimadzu LC10AT instrument connected to a μ -Bondapak aminopropyl column (10 μ m particle size, 3.9 x 300 mm length) was employed. Mixture of acetonitrile: water (80:20 v/v) was used as mobile phase at a flow rate of 1.0 mL/ min and detected using Refractive Index detector. Retention times: D- glucose – 5.5 min, L-phenylalanine – 6.2 min and L-phenylalanyl-D-glucose – 9.2 min. The reaction mixture was also monitored by using LiChrosorb RP-18 column (5 μ m particle size, 4.6 x 150 mm length). Peaks were detected using an UV detector at 254 nm and 210 nm in case of L-proline reactions. Eluted with acetonitrile: water (20:80 v/v) as mobile phase at a flow rate of 1.0 mL/min. Retention times are

(min): L-proline – 3.0, L-prolyl-D-glucose – 3.8, L-prolyl-D-galactose – 3.9 and 4.4, L-prolyl-D-mannose – 3.2 and 4.0, L-prolyl-D-fructose – 3.9, L-prolyl-D-ribose – 3.2 and 3.8, L-prolyl-lactose – 3.8, L-prolyl-maltose – 3.8, L-prolyl-D-sorbitol – 3.1 and 4.1, L-phenylalanine- 2.2, L-phenylalanyl-D-glucose- 2.9 and 3.1, L-phenylalanyl-D-galactose – 3.3 and 3.8, L-phenylalanyl-D-mannose – 3.0 and 3.5, L-phenylalanyl-D-fructose – 3.4 and 4.1, L-phenylalanyl-D-arabinose – 4.6, L-phenylalanyl-lactose – 3.1, L-phenylalanyl-maltose – 4.5, L-phenylalanyl-D-mannitol – 2.9, L-tryptophan – 4.9, L-tryptophanyl-D-glucose – 6.9, L-tryptophanyl-D-galactose – 6.2, L-tryptophanyl-D-mannose – 6.2, L-tryptophanyl-D-fructose – 7.1, L-tryptophanyl-lactose – 5.3, L-tryptophanyl-maltose – 5.2, L-tryptophanyl-sucrose – 5.8, L-tryptophanyl-D-sorbitol – 5.8, L-histidine – 4.2, L-histidyl-D-glucose – 4.7, L-histidyl-D-mannose – 4.7, L-histidyl-D-fructose – 4.8, L-histidyl-maltose – 4.8 and L-histidyl-D-mannitol – 4.8. Since different equivalents of L-amino acids were employed, the conversion yields were determined based on the peak areas of amino acyl esters and that of L-amino acids. The ester yields were expressed in % esterification or mmol of ester formed based on the amino acid concentration employed.

2.2.7. UV-Visible spectroscopy

A Shimadzu UV – 1601 spectrophotometer was used for UV characterization of isolated esters. Samples were prepared in water at 0.1-3.0 mM range.

2.2.8. Infra Red spectroscopy

A Nicolet 5700 FTIR instrument was used for recording IR spectra for the isolated esters. A 2.0 to 3.0 mg of ester sample was prepared as KBr pellet and the IR spectrum was recorded.

2.2.9. Nuclear Magnetic Resonance Spectroscopy

2.2.9.1. ¹H NMR

A Brüker DRX-500 MHz spectrometer operating at 500.13 MHz was used to record ¹H NMR spectra in DMSO-d₆ with 40 mg of the sample dissolved in 0.5 mL of solvent. About 50-200 scans were accumulated with a recycle period of 2-3 seconds to obtain good spectra. The spectra were recorded at 35 °C with tetramethyl silane (TMS) as internal standard for measuring the chemical shift values to within ± 0.001ppm. A region from 0 –10 ppm was scanned for all the samples.

2.2.9.2. ¹³C NMR

A Brüker DRX-500 MHz spectrometer operating at 125 MHz was used to record ¹³C NMR spectra. A region from 0 - 200 ppm was scanned and about 500 – 6000 scans were accumulated for each spectrum. TMS was taken as an internal standard. Samples were dissolved in 0.5 mL of DMSO-d₆ and recorded at 35 °C.

2.2.9.3. Two-dimensional HSQCT

Two dimensional Heteronuclear Multiple Quantum Coherence Transfer spectra (2-D HMQCT) and Heteronuclear Single Quantum Coherence Transfer spectra (2-D HSQCT) were recorded at 500 MHz on a Brüker DRX-500 MHz spectrometer. Proton and carbon 90° pulse widths were 12.25 and 10.5 μs respectively. Chemical shift values were expressed in ppm relative to internal TMS standard. About 40mg of the sample dissolved in DMSO-d₆ was used for recording the spectra in magnitude mode with sinusoidal shaped z-gradients of strength 25.7, 15.42 and 20.56 G/cm with a gradient recovery delay of 100 μs to defocus unwanted coherences. t₁ was incremented in 256 steps with a computer memory size of 4K. The spectra were processed using unshifted and π/4 shifted sine bell window function in F₁ and F₂ dimensions respectively.

2.2.10. Mass spectroscopy

Mass spectra of the isolated esters were obtained using a Q-TOF Waters Ultima instrument (No.Q-Tof GAA 082, Waters corporation, Manchester, UK) fitted with an electron spray ionization (ESI) source. The data acquisition software used was version 4.0. The Spectra were recorded in positive ion mode using spray voltage at 3.5 kV and a source temperature of 80 °C. Mass spectra were recorded under electron impact ionization at 70 eV electron energy. Samples were prepared in the concentration range of 0.5-1.0 mg/mL in distilled water and injected by flow injection analysis at a flow rate of 10 µL/ min. The recorded mass of the sample was in the range of 100-1000.

2.2.11. Polarimetry

Specific rotation of the isolated esters were measured at 20 °C using Perkin-Elmer 243 polarimeter. A 0.2 – 1.5 % solution of the esters in distilled water was employed for the measurements. Specific rotations were determined from

$$[\alpha]_D^{20\text{ }^\circ\text{C}} = \frac{[\alpha]_{\text{obs}} \times 100}{C \times l}$$

Where $[\alpha]_D$ = specific rotation in degrees in a sodium 590 lamp, α_{obs} = observed rotation, C= concentration of esters in g/100 mL and l = path length in dm.

2.2.12. Critical micellar concentration (CMC) determination

Critical micellar concentration was determined by spectroscopic method (Beyaz *et al.* 2004). A 1 mL aliquot of ester solutions in the concentration range from 0 to 100 mM was prepared. The absorption of the solutions were recorded at 254 nm wavelength using quartz cuvette in a Shimadzu UV – 1601 spectrophotometer. The absorption values were plotted against concentrations of the ester. The concentration at which an abrupt change in the linearity of the plot was considered as critical micellar concentration.

2.2.13. Water activity

Water activity of the reaction media was measured using Mettler Toledo DL-50 auto titrator by Karl-Fischer reagent (Vogel 1961; Grünke 2003). Known amount of the solvents were titrated against the Karl-Fischer reagent. Karl-Fischer reagent contains mixture of pyridine, iodine and sulphur dioxide dissolved in methanol. The main reaction can be described by two steps. In the first step, formation of an intermediate 'pyridine sulphur trioxide', which was later converted into 'pyridine-N-sulphuric acid' by the action of pyridine, sulphur dioxide and methanol. In the second step, pyridine-N-sulphuric acid is oxidized by iodine in presence of water.

The endpoint of the KF titration in an auto titrator is indicated by polarising a double platinum electrode. The voltage between the platinum electrodes is measured as volume of titrant (Karl-Fischer reagent) added. As long as traces of water are present in the titration cell, all iodine molecules are immediately reduced to iodide by the KF reagent. The electrical resistance of the solution stays at a high level. After titrating all water molecules, a small excess of iodine molecules leads to a strong decrease in the resistance. Hence the decrease of the resistance is considered as the end point. The stoichiometry in the reaction is 1:1 (I_2 : H_2O). Hence one molecule of iodine is equivalent to one molecule of water. A 1 mL of Karl-Fischer reagent can react with 5 mL of water. Amount of water was determined by the amount of Karl-Fischer reagent consumed by the solvent. Table 2.5 shows the water activities of some organic solvents.

2.2.14. Preparation of N-acetyl phenylalanine

L-Phenylalanine (5.0g, 0.030 mol) of was dissolved in 8 mL (0.099 mol) of pyridine in 100 mL round bottomed flask. The reaction mixture was allowed to stir for 10 min. To this stirring solution 18 mL (0.188 mol) of acetic anhydride was added drop wise. The reaction mixture was allowed to react for 20 h and then the whole reaction

mixture was poured into ice. The solid product formed was separated by filtration and dried in air. Recrystallization was done with hot water using animal charcoal. The yellow crystals were filtered and air dried.

Table 2.5. Water activities for different organic solvents by Karl-Fischer method

Solvent ^a	Water activity (a _w)
Acetone	0.008
Benzene	0.142
Chloroform	0.028
Dichloromethane	0.054
Heptane	≈0
Hexane	0.183
Methyl isobutyl ketone	0.043

^a Volume of solvent taken – 40 mL; Errors in measurement ±5%.

2.2.15. Extraction of Angiotensin Converting Enzyme (ACE) from pig lung

ACE was extracted from pig lung by the method of Andjar-Sanchez *et al.* (2003). A 100 g of pig lung was minced and homogenized using a blender with 10 mM pH 7.0 HEPES buffer containing 0.4M NaCl at a volume ratio of 5:1 (v/w of pig lung). The temperature was maintained at 4 °C throughout the procedure. The homogenate was centrifuged at 9000 g for 60 min. The supernatant was discarded and the precipitate was washed twice with 200 mL of 10 mM pH 7.0 HEPES buffer containing 0.4M NaCl. The final precipitate was resuspended in 200 mL of pH 7.0, 10 mM HEPES buffer containing, 0.4M NaCl, 10 μM ZnCl₂, 0.5%(w/v) triton X 100 and stirred over night. The solution was centrifuged to remove the pellets. The supernatant was dialyzed against water using a dialysis bag of molecular weight cut off 10 kD and later lyophilized.

2.2.16. Angiotensin Converting Enzyme (ACE) inhibition assay

ACE inhibition assay for the esters prepared were performed by the Cushman and Cheung (1971) method. Aliquots of esters solutions in the concentration range 0.13 to

1.06 mM (0.1 mL to 0.8 mL of 2.0 mM stock solution) were taken and to this 0.1 mL of ACE solution (0.1% in 0.1 M phosphate buffer, pH 8.3 containing 300 mM NaCl) was added. To this solution, 0.1 mL of 5.0 mM hippuryl-L-histidyl-L-leucine (HHL) was also added and the total volume made upto 1.25 mL by adding phosphate buffer (0.95 mL to 0.25 mL of 0.1 M pH 8.3 containing 300 mM NaCl). The solution was incubated on a Heto-Holten shaking water bath for 30 min at 37 °C. Blanks were performed without the enzyme by taking only the ester solution (0.1 to 0.8 mL) along with 0.1 mL of 5.0 mM HHL. The total volume was made upto to 1.25 mL by adding same buffer (1.05 mL to 0.35 mL). The reaction was terminated by adding 0.25 mL of 1M HCl. Hippuric acid formed in the reaction was extracted with 1.5 mL of ethyl acetate. One mL of ethyl acetate layer was evaporated to dryness and treated with equal amount of distilled water and the absorbance was measured at 228 nm for hippuric acid. The hippuric acid formed in 1.5 mL of ethyl acetate was determined from a calibration curve prepared using a standard hippuric acid solutions of 0 – 400 nmol concentrations in 1mL of distilled water (Fig. 2.2). Specific activity was expressed as μmol of hippuric acid formed per min per mg of enzyme protein.

$$\text{Specific activity} = \frac{A_{ts} - A_{\text{blank}}}{T \times S \times E}$$

A_{ts} = absorbance of test solution, A_{blank} = absorbance of blank solution, T = incubation period in min, S = slope value of the calibration plot, E = amount of enzyme taken in mg protein.

2.2.17. Extraction of porcine pancreas lipase

Crude PPL was extracted by adopting the procedure of Verger *et al.* (1969). Local slaughter house pig pancreas was minced into small pieces. About 100 g pancreas

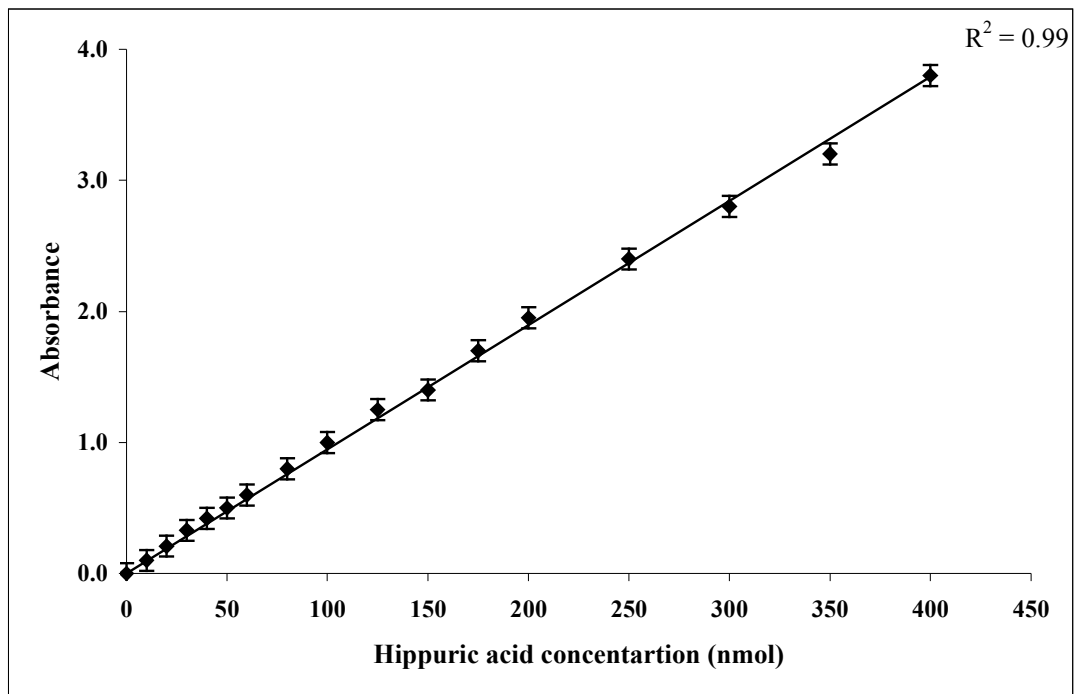


Fig. 2.2. Calibration curve for hippuric acid estimation by spectrophotometric method. A stock solution of 44.8 mg hippuric acid in 25 mL water was prepared, from which different aliquots of concentrations 0 to 350 nmol were pipetted out and made up to 1mL. Absorbance was measured at 228 nm.

was homogenized with 300 mL of chloroform: butanol mixture in the ratio of 9:1 (v/v) at 25 °C. The solvent was decanted and washed with 200 mL of a fresh solvent mixture of 4:1 (v/v) chloroform: butanol mixture and drained completely. The lipid free pellets were then washed with 200 mL of cold acetone and finally with 150 mL diethyl ether to get a fine powder which was then lyophilized. Hydrolytic and esterification activities were found to be 0.25 $\mu\text{mol}/\text{min. mg}$ of protein and 0.002 $\mu\text{mol}/\text{min. mg}$ of protein respectively.

2.2.18. Identification of lipases and ACE by SDS-PAGE

Sodium dodecyl sulphate - polyacrylamide gel electrophoresis (SDS-PAGE) was carried out to check the purity of lipases. SDS-PAGE at pH 8.3 was carried out according to the method described by Laemmli (1970) in a discontinuous buffer system. The following reagents were prepared.

- A. Acrylamide (29.2 g) and bis-acrylamide (0.8g) were dissolved in 100 mL water filtered and stored in a dark brown bottle at 4 °C (This amounts to 30% acrylamide solution).
- B. Separating gel buffer (18.1g) was dissolved in water and the pH of the solution was adjusted to 8.8 with HCl. Then the solution was made upto 100 mL and stored at 4°C.
- C. Stocking gel buffer – Tris-HCl (3.0g) was dissolved in water, pH of the solution was adjusted to 6.8 with HCl (6.0 N) and made upto 100 mL in water.
- D. Sodium dodecyl sulphate (SDS), 10g was dissolved in 100 mL water
- E. Ammonium persulphate was freshly prepared by dissolving 50 mg in 0.5 mL of distilled water.
- F. Tank buffer – Tris-HCl (0.3g), glycine (1.44g) and SDS (0.15g) were dissolved in 150 mL of water.

- G. Staining solution – A 0.2g of Coomassie brilliant blue R 250 was dissolved in a mixture of methanol: acetic acid : water (25: 15: 60 v/v/v). The reagent was filtered and stored in room temperature.
- H. Destaining solution – Methanol: acetic acid: water (25: 15: 60 v/v/v).
- I. Sample buffer was prepared in solution C diluted to 1:4 containing SDS (4% w/v), β -mercaptoethanol (10% v/v), glycerol (20% v/v) and bromophenol blue (0.1%).

Preparation of separating gel – A 3.2 mL of A, 0.92 mL of B, 2.71 mL of distilled water, 0.05 mL of D and 0.03 mL of solution E were mixed and then degassed which was then poured between the assembled glass plates sealed with agar (2% w/v). The gels were layered with 0.5 mL of distilled water and allowed to polymerize at room temperature for 30 min.

Stocking solution was prepared by mixing the solutions of 0.66 mL of A, 1.0 mL of C, 2.25 mL of distilled water, 0.05 mL of solution D, 0.01 mL of TEMED and 0.03 mL of E and poured above the polymerized gel. The gel thus prepared were of the size 10.5 x 9.0 cm and thickness 0.8 mm.

Lipase samples were prepared by dissolving 25 μ g of protein in solution 'I' (50 μ L). The samples were heated in a boiling water bath for 10 min, then samples were loaded into the wells immersed in solution F (tank buffer) and were run at a constant voltage of 40 Volts until the tracking dye, bromophenol blue was just (0.5 cm) above the lower end of the gel. Medium range protein markers phosphorylase (97.4 KDa), bovine serum albumin (66.3 KDa), ovalbumin (43.0 KDa), carbonic anhydrase (29.0 KDa) and soyabean trypsin inhibitor (20.0 KDa) were used. The markers were supplied as a solution having each protein at a concentration of 0.5 to 0.8 mg/mL. The markers were 1:1 diluted with solution I and boiled prior to use. Later the gel was stained for protein with reagent 'G' for 6 h at room temperature followed by destaining in reagent H.

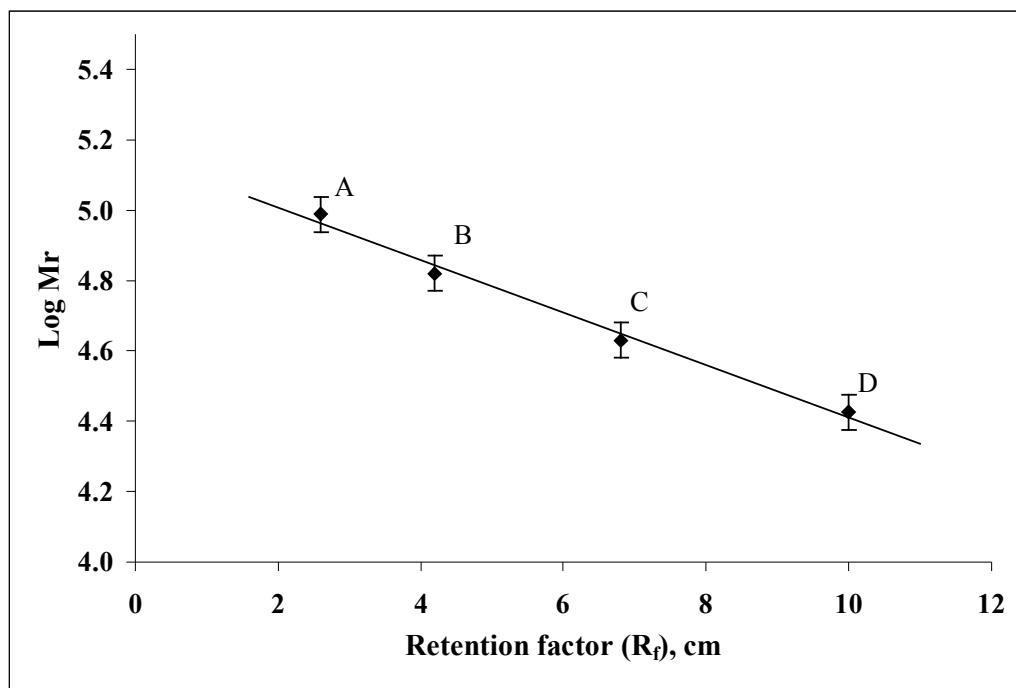


Fig. 2.3 Log M_r versus R_f plot . (A) Phosphorylase (97.4 KDa), (B) BSA (66.3 KDa), (C) Ovalbumin (43.0 KDa), (D) Carbonic anhydrase (29.0 KDa).

Plot was constructed by taking R_f values of molecular marker on X-axis and $\log M_r$ values of each molecular marker on Y-axis (Fig 2.3). From this plot molecular weight of the unknown protein was determined. Lipases from *Rhizomucor miehei*, porcine pancreas and *Candida rugosa* and molecular weight markers were subjected to SDS-PAGE and stained with Coomassie brilliant blue R 250 (Fig. 2.4A). Lane 1 is the crude porcine pancreas extracted from pig lung, showing large number of bands and one band corresponding to a molecular mass of 54.9 KDa along with other protein contaminants of different molecular masses. Lane 2 is a commercial PPL showing a major band of molecular mass 54.9 KDa, and also contains some protease of molecular masses less than 50 KDa. Lane 3 representing *Candida rugosa* lipase, showed a band corresponding the molecular mass of 57.5 KDa. The band with a molecular mass of 30.2 KDa was obtained for *Rhizomucor miehei* lipase in lane 4. Molecular masses of the all the three lipases showed good correspondence to literature reports (Pernas *et al.* 2002; Brady *et al.* 1990; Winkler and Gubernator 1994).

Angiotensin Converting Enzyme (ACE) showed a molecular mass of 152 KDa along with the other protein contaminations (Fig. 2.4B, Lane 1) and this band showed a good correspondence to the reported molecular mass of 147 KDa by Soffer *et al.* (1974).

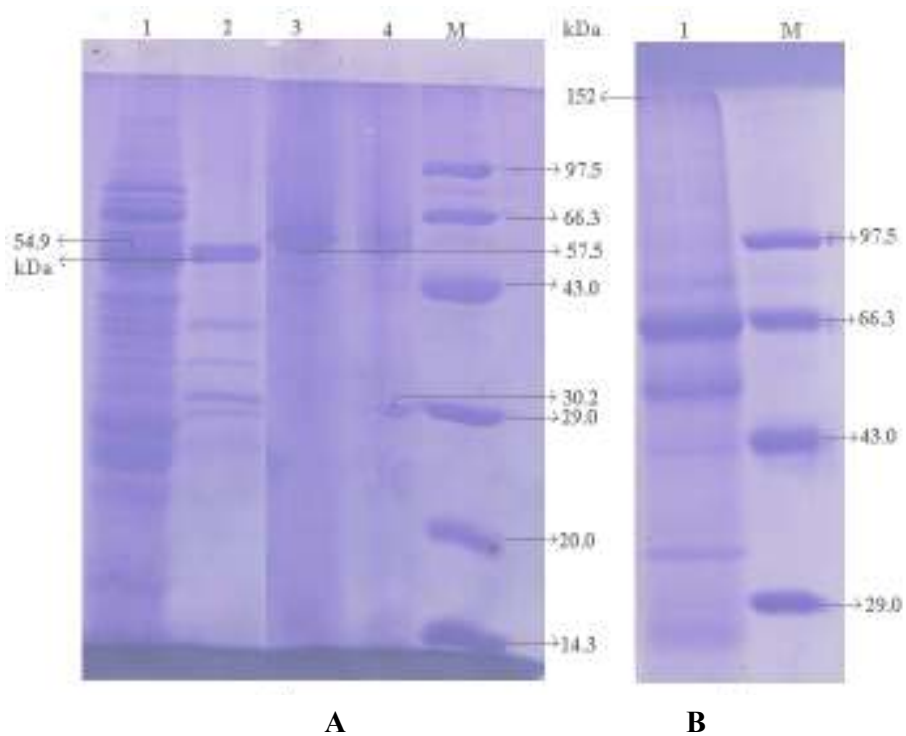


Fig. 2.4. SDS-PAGE for (A) lipases; Lane 1 –crude PPL isolated from porcine pancreas; Lane 2 – PPL from Sigma; Lane 3- CRL from Sigma; Lane 4 –RML from Novo-Nordisk; Lane M for M_r standard proteins: Phosphorylase (97.4 KDa), BSA (66.3 KDa), Ovalalbumin (43.0 KDa) and Carboxy anhydrase (29.0 KDa). (B) Lane 1 for ACE isolated from pig lung.

Chapter-3
Synthesis of L-phenylalanyl-D-glucose
and L-phenylalanyl-lactose

3.1. Introduction

Regioselective modification of carbohydrates is a tedious procedure due to the presence of multiple hydroxyl groups, which involves protection and deprotection (Haines 1981; Tamura *et al.* 1985). Use of lipases in the synthesis of sugar esters are industrially important due to regio and stereo selectivity imparted by them (Ferrer *et al.* 1999). Amino acyl esters of sugars are used as microcapsules in pharmaceutical preparations, in the delivery of biological active agents, antibiotics, sweeteners, emulsifiers, active nucleoside amino acid esters, anti-tumor agents and in the synthesis of biologically active peptides (Krik *et al.* 1992; Zaks and Dodds 1997; Kunz and Kullmann 1992). Few reports are available on the regioselective synthesis of sugar esters of amino acids in organic solvents using mostly proteases (Klibanov 1986; Park *et al.* 1996; 1999; Riva *et al.* 1988). The existing protocols for the synthesis of amino acyl esters of carbohydrates enzymatically deals with protected and activated amino acids. They exhibit defects like use of larger amount of enzymes, lesser amounts of substrates, enzymes which are not economically viable and processes (shake flask level) difficult to adopt industrially. Lipases from *Candida rugosa*, *Mucor javanicus*, *pseudomonas cepacia* and *pseudomonas fluorescens*, proteases from *Aspergillus melleus* (Maruyama *et al.* 2002) and other proteases like subtilisin (Riva *et al.* 1988, Boyer *et al.* 2001) and optimase M-440 (Park *et al.* 1996; 1999), catalysed the trans esterification of N-blocked L-phenylalanine ester and D-glucose regioselectively and that too preferably at the primary hydroxyl groups. Park *et al.* (1996) also reported that lipases from porcine pancreas and Lipozyme IM-20 gave insignificant results. Reactions were conducted in shake flasks using lesser quantity of substrates and larger quantity of enzymes.

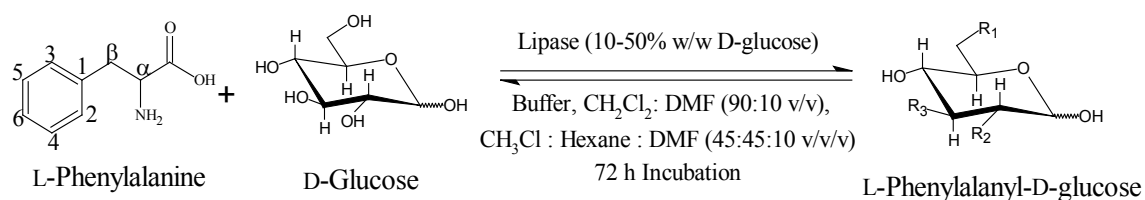
In the present investigation, N-acetyl-L-phenylalanine gave very low yields of esters with D-glucose when *Rhizomucor miehei* (RML) and porcine pancreas lipases (PPL) were employed. The present investigation describes the synthesis of amino acyl

esters of carbohydrates using unprotected and unactivated amino acids and carbohydrates catalysed by lipases. This chapter particularly describes synthesis of two representative amino acyl esters of carbohydrates namely L-phenylalanyl-D-glucose and L-phenylalanyl-lactose.

3.2. Present work

Synthesis of L-phenylalanyl-D-glucose

Esterification was carried out by incubating D-glucose and L-phenylalanine in an organic solvent using lipases (Scheme 3.1). Lipases from *Rhizomucor miehei* (RML) and porcine pancreas (PPL) were employed for the reaction. The extent of esterification was monitored by HPLC (Fig. 3.1).



2-*O*-ester: $R_2 = \text{L-C}_6\text{H}_5\text{CH}_2\text{CH(NH}_2\text{)COO}$, $R_1 = R_3 = \text{OH}$

3-*O*-ester: $R_3 = \text{L-C}_6\text{H}_5\text{CH}_2\text{CH(NH}_2\text{)COO}$, $R_1 = R_2 = \text{OH}$

6-*O*-ester: $R_1 = \text{L-C}_6\text{H}_5\text{CH}_2\text{CH(NH}_2\text{)COO}$, $R_2 = R_3 = \text{OH}$

2,6-*di-O*-ester: $R_2 = R_1 = \text{L-C}_6\text{H}_5\text{CH}_2\text{CH(NH}_2\text{)COO}$, $R_3 = \text{OH}$

3,6-*di-O*-ester: $R_3 = R_1 = \text{L-C}_6\text{H}_5\text{CH}_2\text{CH(NH}_2\text{)COO}$, $R_2 = \text{OH}$

Scheme 3.1. Lipase catalyzed synthesis of L-phenylalanyl-D-glucose esters in anhydrous organic solvents

Since different equivalents of L-phenylalanine were employed, the conversion yields were determined based on the peak areas under L-phenylalanine and that of L-phenylalanyl ester of D-glucose or lactose and expressed as mmol with respect to the free L-phenylalanine concentration employed. The errors in HPLC yields were $\pm 10 - 15\%$. Esters were separated by passing through Sephadex G-10 and Bio-Gel P-2 and eluting with water. The isolated esters were characterized by UV, IR, mass and 2D-NMR spectroscopy. Spectral characterization for L-phenylalanyl-D-glucose is shown in Section 4.2.2.1. Synthesis of L-phenylalanyl-D-glucose was studied in terms of effect of organic

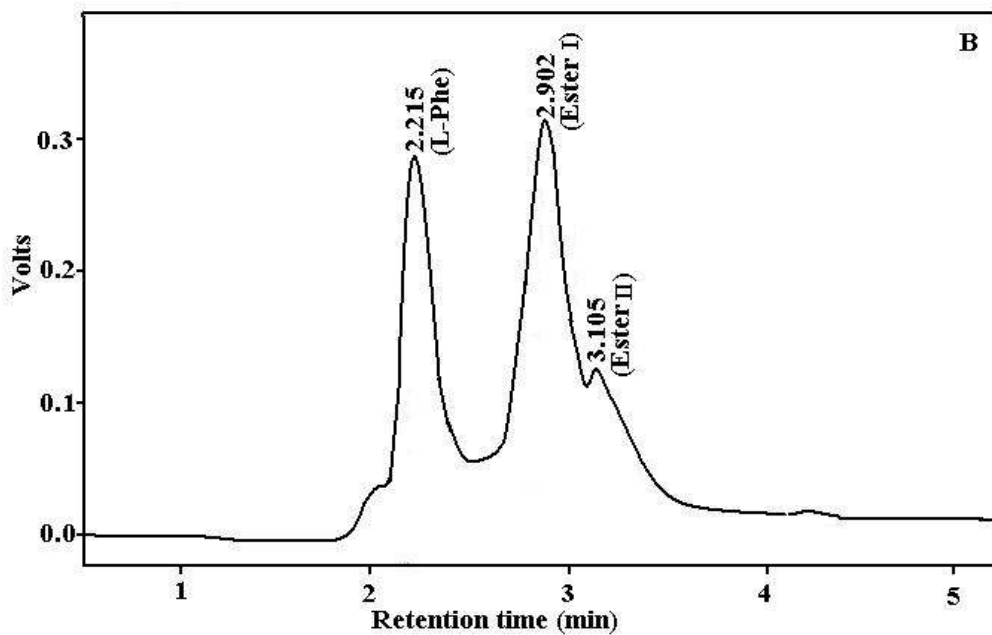
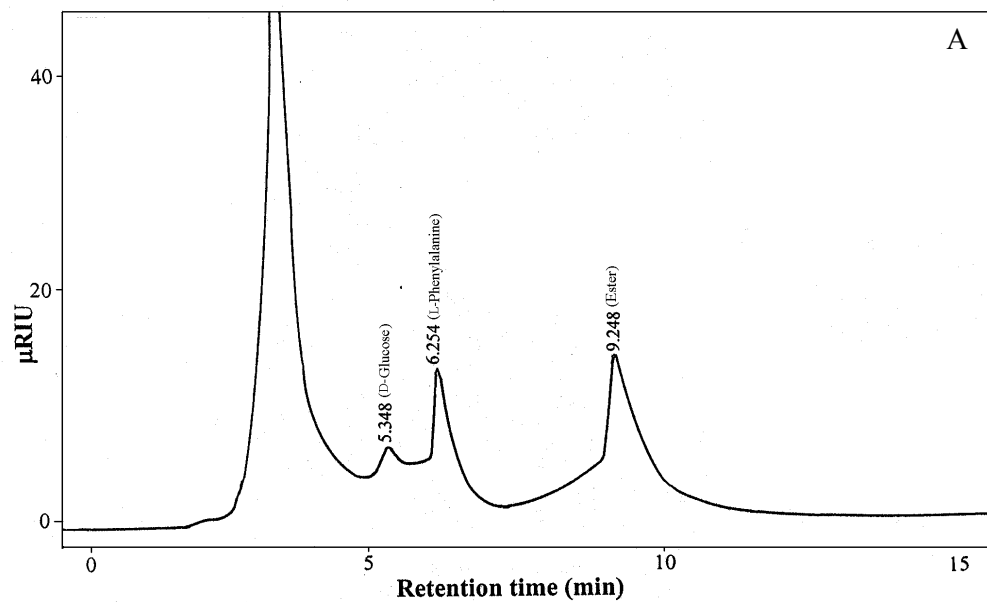


Fig. 3.1. HPLC chromatograph for the reaction mixture of L-phenylalanine and D-glucose. (A) column – aminopropyl, mobile phase – acetonitrile: water (80:20 v/v), flow rate- 1 mL/min, detector – Refractive Index. (B) column – C-18, mobile phase – acetonitrile: water (20:80 v/v), flow rate- 1 mL /min, detector – UV at 254nm. Errors in yields are \pm 10-15%.

solvents, incubation period, effect of lipase concentrations, effect of substrate concentrations, effect of buffer pH and its concentration and enzyme reusability. The esterification reactions described in present work did not occur without the use of enzymes.

3.2.1. Selection of organic solvents

Solvent effect of enzymatic synthesis is very difficult to generalize because three-dimensional structure of protein interacts differently with different solvents. Hence, some solvents are better media for enzyme-catalyzed processes than the other. Generally, non-polar organic solvents form poor multiple hydrogen bonds to generate conformational changes, which result in stronger electrostatic bonds inside protein molecule and stiffen its three dimensional structure (Antczak *et al.* 2004).

Both D-glucose and L-phenylalanine are insoluble in many organic solvents. They require solvents like pyridine or DMSO for complete solubility. Since these solvents more health hazardous and are also difficult to handle during work up, they were not employed. An attempt was made to choose the right solvent, which should dissolve enough substrate to carry out the reaction without affecting the enzyme activity or stability. Presence of small amount of DMF in dichloromethane improved the solubility of substrates employed (Table 3.1). Presence of dichloromethane and DMF (90:10 v/v) showed maximum yield of 98% (0.98mmol). Very low esterification (<5%) was observed with heptane: DMF (90:10 v/v) and Benzene: DMF (90:10 v/v).

Effect of increasing amounts of DMF from 5 to 50 mL was studied. The reaction was carried out by taking 1 mmol each of D-glucose and L-phenylalanine and 30% (w/w based on D-glucose) RML in the presence of 0.2 mM (0.2 mL, 0.1M) pH 4.0 acetate buffer at a constant total solvent volume of 100 mL. Table 3.2 shows that esterification increased with increasing DMF volume from 5 mL to 10 mL, thereafter it decreased

gradually. At higher volume of DMF (increasing polarity of the solvent mixture) enzyme may undergo denaturation due to stripping of water molecule from the enzyme surface, which is very much essential for maintaining the three-dimensional structural stability (Volkin *et al.* 1991). This could lead to lesser yields at higher volume of DMF.

Table 3.1 Effect of solvent mixtures on the synthesis of L-phenylalanyl-D-glucose ^a

Solvent (90: 10 v/v)	%Yield RML	%Yield PPL
Acetone: DMF	42	46
Benzene: DMF	<5%	<5%
Chloroform: hexane: DMF ^b	57	32
Dichloromethane: DMF	98	68
Hexane: DMF	49	10
Heptane: DMF	<5%	<5%

^a Conversion yields were from HPLC with respect to L-phenylalanine. Error in yield measurements will be $\pm 10-15\%$. This applies to all the yields given in the subsequent tables also. Reaction conditions: L-phenylalanine- 1mmol; D-glucose – 1mmol; RML/PPL – 90 mg; incubation period – 72h; Solvent: 90 mL solvent with 10 mL of DMF; ^b CH₂Cl₂: hexane: DMF (45:45:10 v/v/v).

Table 3.2 Effect DMF volume on the synthesis of L-phenylalanyl-D-glucose ^a

DMF volume in mL	Yield in % (mmol)
5.0	21 (0.21)
10.0	79 (0.79)
20.0	72 (0.72)
30.0	56 (0.56)
50.0	58 (0.58)

^a L-Phenylalanine – 1 mmol; D-glucose – 1 mmol; RML – 54 mg (30% w/w based on D-glucose); total volume of the solvent mixture – 100 mL; Buffer - 0.2 mM (0.2 mL of 0.1M) pH 4.0 acetate buffer; incubation period – 72 h.

3.2.2. Reaction profile

Effect of incubation period for the synthesis of L-phenylalanyl-D-glucose was carried out using 30% w/w D-glucose of RML. The conversion yields by HPLC showed

that esterification increased with increase in incubation period from 24 h (0.38 mmol, 38.2%), 48 h (0.50 mmol, 49.8%) to 72 h (0.79 mmol, 78.6%), which then decreased to 0.67 mmol (67.2%) at 96 h and 0.50 mmol (50.1%) at 120 h probably due to hydrolysis (Fig. 3.2). From the initial slope value, the rate of esterification was found to be 0.012 mmol h⁻¹.

3.2.3. Effect of lipase concentration

Effect of RML and PPL concentrations on esterification of L-phenylalanyl-D-glucose was studied in the enzyme concentration range 10–50% (w/w based on D-glucose). In case of RML, esterification increased steadily from 0.64 mmol (64%) at 10% of RML to 0.98 mmol (98%) at 40% of RML and decreased to 0.57 mmol (57%) at 50% RML concentration (Table 3.3). In case of PPL, esterification was the lowest at 30% enzyme concentration (1.04 mmol, 42%) and the highest at 50% enzyme concentration (1.89 mmol, 76%). Since, equimolar concentrations of L-phenylalanine and D-glucose were employed, competition between both the substrates for PPL could result in preferential D-glucose binding at lower (10–30%) enzyme concentrations leading to increase in free L-phenylalanine concentration with the concomitant decrease in the acyl-enzyme complex. Higher (>40%) PPL concentrations could increase the concentration of the acyl-enzyme complex leading to higher conversions.

Table 3.3 Effect of lipase concentration on the synthesis of L-phenylalanyl-D-glucose

Enzyme concentration (w/w based on D-glucose)	Esterification ^a	Esterification ^b
	% (mmol) RML	% (mmol) PPL
10%	64 (0.64)	62 (1.56)
20%	68 (0.68)	46 (1.15)
30%	67 (0.67)	42 (1.04)
40%	98 (0.98)	68 (1.70)
50%	57 (0.57)	76 (1.89)

^a D-Glucose- 1 mmol; L-phenylalanine - 1 mmol; Solvent – CH₂Cl₂ : DMF (90:10 v/v) at 40 °C; ^b D-glucose – 2.5 mmol; L-phenylalanine - 2.5 mmol; Incubation period - 72 h.

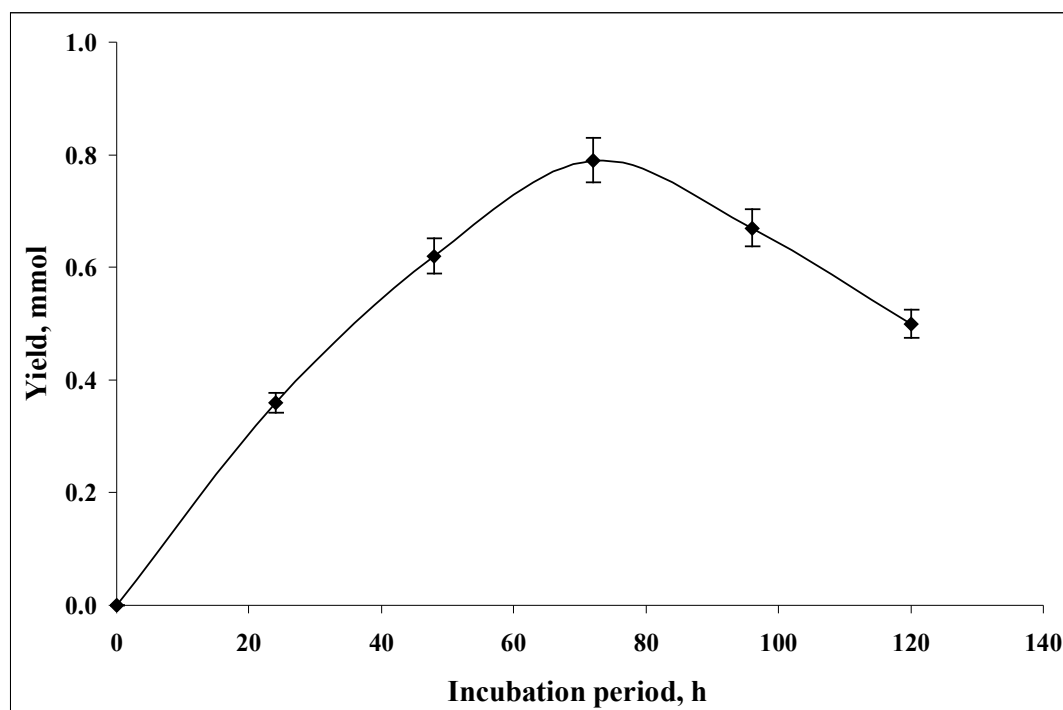


Fig. 3.2. Reaction profile for L-phenylalanyl-D-glucose synthesis. Reaction conditions: CH_2Cl_2 : DMF (90:10 v/v), RML -54 mg, L-phenylalanine - 1 mmol, D-glucose - 1.0 mmol, Buffer - 0.2 mM (0.2 mL) 0.1M pH 4.0 acetate buffer.

3.2.4. Effect of substrate concentration

Effect of L-phenylalanine concentration on esterification using 54 mg RML (30%, w/w based on D-glucose) at a constant 1 mmol D-glucose and the effect of D-glucose concentration using 72 mg RML at a fixed 1 mmol L-phenylalanine concentration were studied (Fig. 3.3). In both the cases, maximum esterification of 0.67 mmol (67%) and 0.71 mmol (71%) were observed at 1:1 molar ratios of D-glucose and L-phenylalanine, respectively. Esterification yields decreased from 2 equivalents of L-phenylalanine (0.38 mmol, 19%) to reach the lowest yield of 0.32 mmol (6%) at 5 equivalents. Between 2 and 4 equiv. of D-glucose concentrations, the extent of conversion remained almost constant around 53–56% and decreased to 0.47 mmol (47%) at 5 equiv. of D-glucose. This showed that higher concentrations of L-phenylalanine and D-glucose could be inhibitory to RML.

3.2.5. Effect of buffer salt

While earlier workers have not studied the effect of buffer salts on this esterification reaction, the present study investigated the same, both in connection with the stabilization of the enzyme in non-polar solvents and also due to the use of zwitter ionic amino acid in the reaction. Small amount of water, which is added in the form of buffer salts also acts as a lubricant or plasticizer, which renders conformational mobility to enzymes required for optimal catalysis (Gregory 1995).

A buffer of known pH and volume (concentration) was added to the reaction mixture and the effect of imparting ‘pH memory’ to the enzyme (Kiran *et al.* 2002) on this esterification was studied. Buffers of different pH ranging from pH 4.0 to 8.0 were employed (Table 3.4). In the presence of buffer salts, conversion increased. In the presence of 0.2 mM buffers (0.2 mL of 0.1M pH 4.0–8.0), 10% higher yields than those

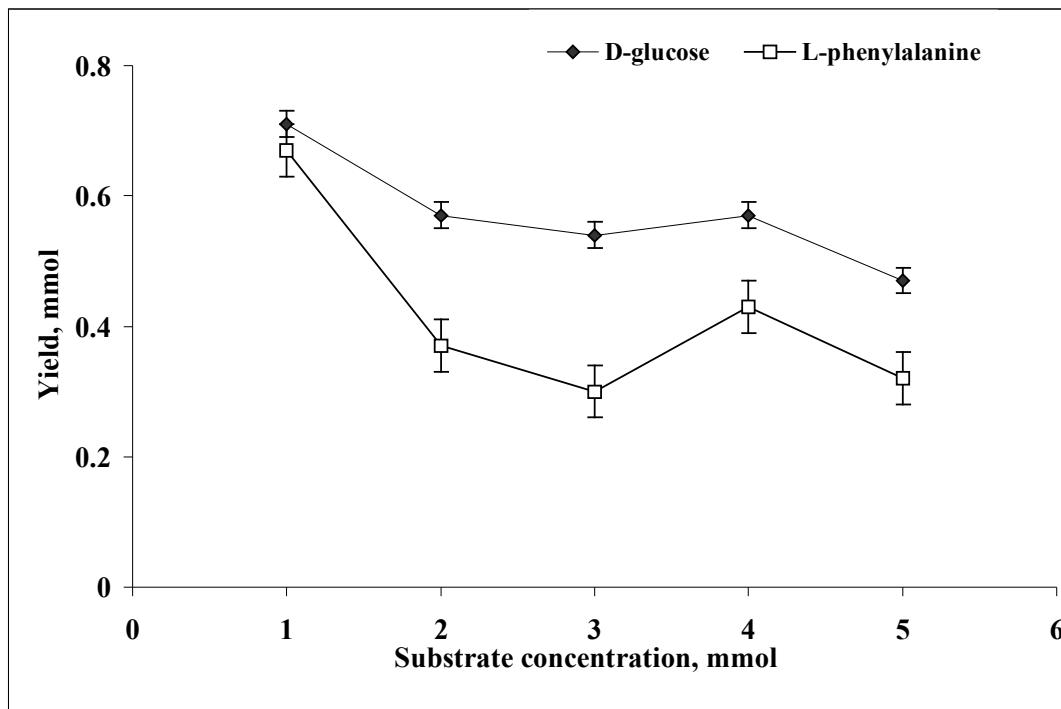


Fig 3.3. Effect of substrate concentration on synthesis of L-phenylalanyl-D-glucose. (□) L-phenylalanine-1mmol -5 mmol, D-glucose- 1mmol, RML-30% w/w based on D-glucose. (◆) D-glucose - 1mmol - 5mmol, L-phenylalanine –1mmol, RML- 40% w/w based on D-glucose, Reaction conditions: Temperature - 40⁰C, Incubation period - 72 h, Solvent - DMF and CH₂Cl₂ (10:90 v/v).

without buffers were obtained. Maximum esterification of 0.79 mmol (79%) with RML was achieved with pH 4.0 acetate buffer. However in case of PPL, maximum esterification of 0.63 mmol (63%) was achieved with pH 6.0 phosphate buffer.

Effect of buffer salt concentration was studied using acetate buffer (pH 4.0) for RML and phosphate buffer (pH 6.0) for PPL (Table 3.4) in the concentration range 0.05–0.5 mM. In case of RML, conversion yields increased from 0.54 mmol (54%) at 0.05 mM buffer salt to 0.79 mmol (79%) at 0.2 mM buffer salt and further increase in buffer salt concentration lowered the yield to 0.70 mmol (70%) at 0.5 mM buffer salt. In case of PPL, esterification increased from 0.23 mmol (23%) at 0.05 mM buffer salt to 0.65 mmol (65%) at 0.1 mM buffer salt and further increase in buffer salt concentration resulted in a reduced yield of 0.06 mmol (6%) at 0.5 mM buffer salt. Higher levels of enzyme hydration (in the form of water containing the buffer salt) could have altered the active three-dimensional structure of the enzyme reducing its esterification activity.

Table 3.4. Effect of buffer salts (pH and concentration) on the synthesis of L-phenylalanyl-D-glucose ^a

pH	RML	PPL	Buffer conc. (mM)	RML	PPL
	Esterification ^b % (mmol)	Esterification ^c % (mmol)		Esterification ^d % (mmol)	Esterification ^e % (mmol)
4.0	79 (0.79)	31 (0.31)	0.05	54 (0.54)	23 (0.23)
5.0	69 (0.69)	47 (0.47)	0.1	67 (0.67)	65 (0.65)
6.0	69 (0.69)	63 (0.63)	0.2	79 (0.79)	63 (0.63)
7.0	67 (0.67)	34 (0.34)	0.3	78 (0.78)	49 (0.49)
8.0	45 (0.45)	44 (0.44)	0.4	69 (0.69)	47 (0.47)
-	-	-	0.5	70 (0.70)	06 (0.06)

^a D-Glucose – 1 mmol; L-phenylalanine - 1 mmol; Incubation period - 72 h; Enzyme – 30% w/w based on D-glucose; Solvent - CH₂Cl₂ : DMF - (90:10 v/v) at 40 °C; ^b Buffer concentration – 0.2 mM (0.2 mL of 0.1M); Solvent - CHCl₃ : hexane : DMF – (45 : 45 : 10 v/v) at 60 °C; ^c Buffer concentration – 0.2 mM (0.2 mL of 0.1M); ^d Buffer - 0.1M of pH 4.0 acetate buffer; Solvent - CHCl₃: hexane: DMF - (45 : 45 : 10 v/v) 60 °C; ^e Buffer - 0.1M pH 6.0 phosphate buffer.

3.2.6. Reusability of lipases

Reusability of RML and PPL was studied at an equimolar (2.5 mmol) D-glucose and L-phenylalanine concentration with PPL (50%, w/w based on D-glucose) and RML (40%, w/w based on D-glucose). After completion of each reaction, the enzyme separated from the reaction mixture (as outlined in the Section 2.2.4) air dried and reused for the next reaction. After each cycle, total esterification activity ($\mu\text{mol}/\text{min}$) of the enzyme was determined. In case of RML, the enzyme loss after each cycle was about 20–30%, whereas in case of PPL it was 50–70% as PPL dissolved in water more readily than RML. Reusability was examined up to fourth cycle for RML, but in case of PPL, it was only up to two cycles (Fig. 3.4). RML activity decreased gradually from 91% (1st cycle: total enzyme activity - 99.0 $\mu\text{mol}/\text{min}$) to 10% (4th cycle- total enzyme activity – 9.6 $\mu\text{mol}/\text{min}$), esterification yields at second and third cycles are 80% (total enzyme activity - 86.4 $\mu\text{mol}/\text{min}$) and 23% (total enzyme activity – 24.1 $\mu\text{mol}/\text{min}$), respectively. However, PPL showed better activity in the second cycle also, 46% (total enzyme activity - 15 $\mu\text{mol}/\text{min}$) in the first cycle and 45% (total enzyme activity - 10 $\mu\text{mol}/\text{min}$) in the second cycle.

3.3. Synthesis of L-phenylalanyl-lactose

The enzymatic esterification between L-phenylalanine and lactose was studied in detail to understand the difference in the esterification between a monosaccharide and disaccharide.

3.3.1. Reaction profile

L-Phenylalanyl-lactose synthesis was studied in detail using lipases from porcine pancreas (PPL) and *Candida rugosa* (CRL). The reaction was carried out between equimolar (0.5 mmol) concentrations of L-phenylalanine and lactose with 50% CRL (w/w based on lactose) in presence of dichloromethane and DMF (90:10v/v) and 0.2 mM

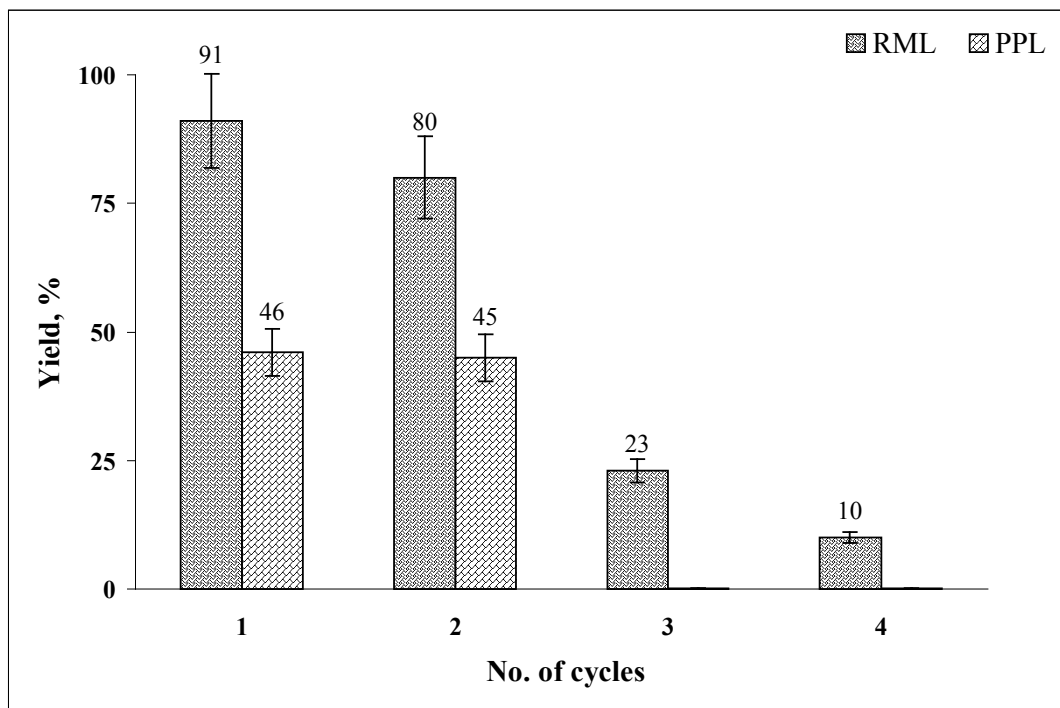


Fig. 3.4. Enzyme reusability in the synthesis of L-phenylalanyl-D-glucose. D-glucose and L-phenylalanine - 2.5 mmol each, temperature - 40 °C, incubation period - 72 h, RML amount - 1st cycle - 180 mg (total enzyme activity - 99.0 $\mu\text{mol}/\text{min}$), 2nd cycle - 173 mg (total enzyme activity - 86.4 $\mu\text{mol}/\text{min}$), 3rd cycle - 91 mg (total enzyme activity - 24.1 $\mu\text{mol}/\text{min}$), 4th cycle - 77 mg (total enzyme activity - 9.6 $\mu\text{mol}/\text{min}$), PPL amount - 1st cycle - 225 mg (total enzyme activity - 15 $\mu\text{mol}/\text{min}$), 2nd - cycle - 66 mg (total enzyme activity 10 $\mu\text{mol}/\text{min}$).

(0.2 mL of 0.1M) pH 4.0 acetate buffer. Table 3.5 shows that esterification increased with incubation period from 6 to 72 h and decreased at 96 h probably due to hydrolysis of the ester formed. From the initial slope value, the rate of esterification was found to be $0.005 \text{ mmol h}^{-1}$.

Table 3.5. Effect of incubation period on the synthesis of L-phenylalanyl-lactose ^a

Incubation period (h)	Yield in % (mmol)
6	14 (0.07)
12	21 (0.10)
18	50 (0.25)
24	24 (0.12)
48	57 (0.29)
72	61 (0.30)
96	47 (0.24)

^a L-Phenylalanine – 0.5 mmol; lactose – 0.5 mmol; CRL – 90 mg (50% w/w based on lactose); 0.2 mM (0.2 mL of 0.1M) pH 4.0 acetate buffer; Solvent - dichloromethane: dimethylformamide (90:10 v/v) at 40 °C.

3.3.2. Effect of substrate concentration

Effect of L-phenylalanine concentration on the synthesis of L-phenylalanyl-lactose using 90 mg CRL at a constant 0.5 mmol lactose and the effect of lactose concentration at a fixed 0.5 mmol L-phenylalanine concentration were studied (Fig. 3.5). When lactose concentration was varied, esterification decreased initially upto 3 equivalents of lactose, and thereafter increased to 71% (0.36 mmol) at 5 equivalents of lactose. But when L-phenylalanine was varied, no esterification was found after 2 equivalents and maximum yield of 61% (0.31 mmol) was obtained with 1:1 equivalent. In case of PPL catalyzed reactions, esterification decreased with increase in L-phenylalanine concentration. In this case also, a 1:1 equivalent gave a maximum yield of 60% (0.3 mmol).

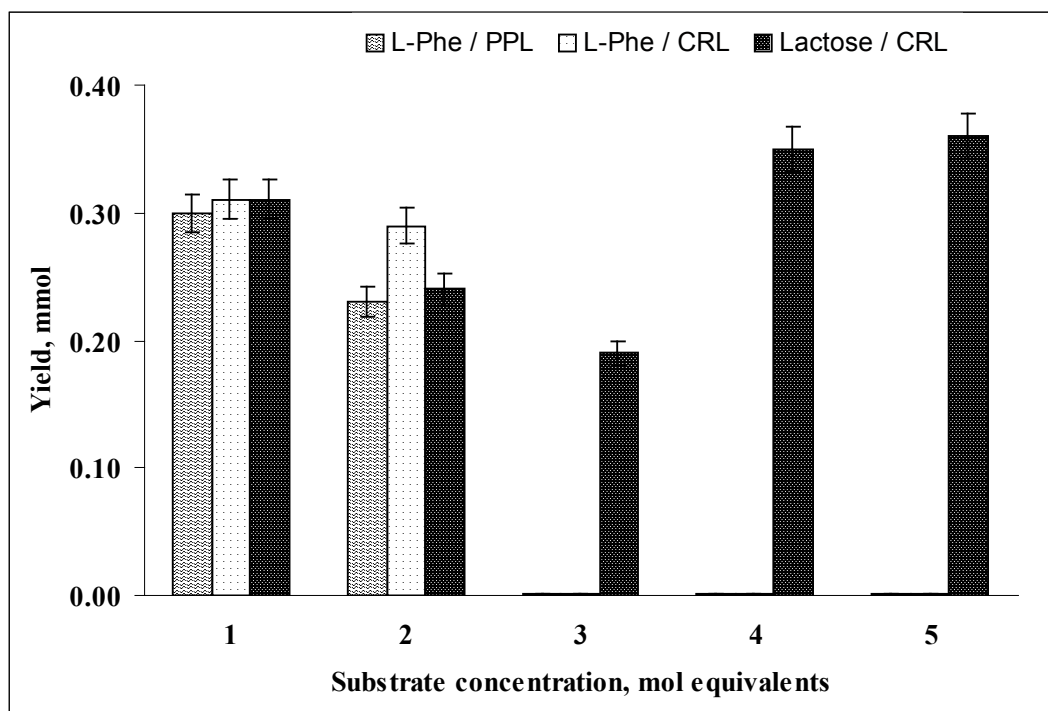


Fig 3.5. Effect of substrate concentration on synthesis of L-phenylalanyl-lactose. (▨) L-phenylalanine-0.5 – 2.5 mmol, lactose – 0.5 mmol, PPL-90 mg. (▩) L-phenylalanine-0.5 – 2.5 mmol, lactose – 0.5 mmol, CRL-90 mg. (■) lactose - 0.5 – 2.5 mmol, L-phenylalanine – 0.5 mmol, CRL-90 mg. Reaction conditions: Buffer – 0.2 mM (0.2 mL, 0.1 M) pH 4.0 acetate buffer, temperature - 40⁰C, incubation period - 72 h, Solvent - DMF and CH₂Cl₂ (10:90 v/v).

3.3.3. Effect of PPL and CRL concentration

Effect of PPL and CRL concentrations on L-phenylalanyl-lactose synthesis was studied by varying 10% to 50% (w/w based on lactose) of the enzymes. Reaction was carried out with 0.5 mmol lactose and 2.5 mmol L-phenylalanine in absence of buffer and in presence of 0.2 mM (0.2 mL of 0.1M) pH 4.0 acetate buffer in dichloromethane: DMF (90:10 v/v). In presence of buffer, maximum esterification of 10% (0.25 mmol) was observed with 50% PPL (w/w based on lactose) and no esterification was observed in the absence of buffer. In case of CRL, 50% (w/w based on lactose) enzyme gave a maximum yield of 34% (0.17 mmol) in the absence of buffer and 61% (0.31 mmol) in the presence of 0.2 mM (0.2 mL, 0.1M) pH 4.0 acetate buffer (Table 3.6).

Table 3.6. Effect of lipase concentrations on the synthesis of L-phenylalanyl-lactose

Enzyme concentration (w/w based on lactose)	Esterification ^a	Esterification ^b	Esterification ^b
	% (mmol) PPL 0.2 mM (0.2mL) pH 4.0	% (mmol) CRL	% (mmol) CRL 0.2 mM (0.2mL) pH 4.0
10%	01 (0.03)	21 (0.10)	12 (0.06)
20%	04 (0.10)	18 (0.09)	53 (0.27)
30%	06 (0.15)	24 (0.12)	47 (0.24)
40%	10 (0.24)	33 (0.16)	58 (0.29)
50%	10 (0.26)	34 (0.17)	61 (0.31)

^a Lactose – 0.5 mmol; L-phenylalanine – 2.5 mmol; incubation period - 72 h; solvent – CH₂Cl₂ : DMF (90:10 v/v) at 40 °C; ^b lactose and L-phenylalanine – 0.5 mmol each.

3.3.4. Effect of buffer salt

Conversion yields were enhanced thrice in the presence of buffer salts in CRL catalyzed synthesis of L-phenylalanyl-lactose. The effect buffer salts from pH 4.0 to 8.0 were studied by employing 0.2 mM buffer (0.2 mL of 0.1M pH 4.0-8.0) at 50% CRL.

Esterification decreased initially from pH 4.0 to 6.0 and increased between pH 7.0 and 8.0. Maximum esterification of 61% (0.31 mmol) was obtained in presence of pH 4.0 acetate buffers.

Effect of buffer salt concentration was studied using pH 4.0 acetate buffer (Table 3.7) in the concentration range 0.05 - 0.5 mM. Conversion yields increased from 40% (0.20 mmol) at 0.05 mM buffer salt to 61% (0.31 mmol) at 0.2 mM buffer salt and further increase in buffer salt to 0.5 mM concentration lowered the yield to 39% (0.19 mmol). Here also, a critical buffer concentration was found to be essential for esterification.

Table 3.7 Effect of buffer salts (pH and buffer volume) on the synthesis of L-phenylalanyl-lactose ^a

pH	Esterification ^b % (mmol)	Buffer volume (mL)	Esterification ^c % (mmol)
4.0	61 (0.31)	0.05	40 (0.20)
5.0	17 (0.08)	0.1	59 (0.29)
6.0	11 (0.06)	0.2	61(0.31)
7.0	31 (0.16)	0.3	53 (0.26)
8.0	60 (0.30)	0.4	53 (0.26)
-	-	0.5	39 (0.19)

^a Lactose and L-phenylalanine – 0.5 mmol each; incubation period - 72 h; enzyme – 50% w/w based on lactose; solvent - CH₂Cl₂ : DMF - (90:10 v/v) at 40 °C; ^b buffer – 0.2 mM (0.2 mL of 0.1M); ^c buffer - 0.1M of pH 4.0 acetate buffer.

3.4. Determination of Critical Micellar Concentration (CMC)

In order to evaluate the surfactant property of the amino acyl esters of carbohydrates, critical micellar concentration (CMC) values were determined by spectroscopic method (Beyaz *et al.* 2004) for L-phenylalanyl-D-glucose and L-phenylalanyl-lactose.

A 1.0 mL ester solution in the concentration range from 0 to 100 mM was prepared. Absorption at 254 nm was recorded for these solutions. Absorption values were plotted against concentrations of the ester. The concentration at which an abrupt change in the linearity of the plot observed was considered as the critical micellar concentration. Both L-phenylalanyl-D-glucose and L-phenylalanyl-lactose showed CMC of 3.25 mM (0.11%) and 9.5 mM (0.6%) respectively.

3.5. Discussion

The optimum conditions determined for these esterification reactions by studying the effect of variables like incubation period, enzyme and substrate concentration, pH and buffer concentration clearly explain the behaviour of the lipases. Most of the parameters show that esterification increases upto a certain point, and thereafter they remain as such or decrease a little. This complex esterification reaction is not controlled by kinetic factors or thermodynamic factors or water activity alone.

Use of lower enzyme concentrations did not result in thermodynamic yields. The thermodynamic binding equilibria regulate the concentrations of the bound and unbound substrates at different enzyme and substrate concentrations and thereby conversion as the reaction proceeds with time. At lesser enzyme concentrations, for a given amount of substrates (enzyme/substrate ratio low), rapid exchange between bound and unbound forms of both the substrates with the enzyme (on a weighted average based on binding constant values of both the substrates) leaves substantial number of unbound substrate

molecules at the start of the reaction and they decrease progressively as conversion takes place (Romero *et al.* 2003; Marty *et al.* 1992). This becomes more so, if one of them binds more firmly to the enzyme than the other (higher binding constant value) as the respective enzyme/substrate ratios keep changing (during the course of the reaction) unevenly till the conversion stops due to total predominant binding (inhibition). At intermediary enzyme concentrations, such a competitive binding results in a favorable proportions of bound and unbound substrates to effect quite a good conversion. At higher enzyme concentrations, most of the substrates would be in the bound form leading to inhibition and lesser conversion (higher enzyme/substrate ratios). Also, the esterification reaction requires larger amount of enzyme compared to hydrolysis. While this leads to lesser selectivity, they also give rise to varying bound and unbound substrate concentrations till the conversion ends. For a given amount of enzyme and substrate there is no increase in conversion beyond 72h to 120h. Longer incubation periods of especially lesser enzyme concentrations could also result in partial enzyme inactivation as shown in Fig. 3.4. However, not all the enzyme is inactivated before the end of the reaction.

Besides imparting 'pH memory', added water is essential for the integrity of the three-dimensional structure of the enzyme molecule and therefore its activity (Dordick 1989). Zaks and Klivanov (1988) reported that at low water activities, lower the solvent polarity, the higher the enzyme activity. Beyond the critical water concentration, esterification decreases because the size of the water layer formed around the enzyme retards the transfer of acyl donor to the active site of the enzyme (Humeau *et al.* 1998; Camacho-Paez *et al.* 2003) and also the water layer surrounding the enzymes makes enzyme to be more flexible by forming multiple H-bonds and interacting with organic solvent causing denaturation (Valiveti *et al.* 1991). Increase in buffer volume affected

this esterification reaction significantly. It could increase the water activity of the system in the initial stages by increasing the thickness of the microaqueous layer around the enzyme. Higher volumes of the buffer in the microaqueous layer could also cause slight inactivation of the enzyme due to increase in salt concentration beyond a critical point. Patridge *et al.* (2001) reported that when an enzyme is suspended in a low-water organic solvent, the counter ions are in closer contact with the opposite charges on the enzyme because of the lower dielectric constant of the medium. Thus, protonation of the ionizable groups on the enzyme could be controlled by the type and availability of these ions as well as hydrogen ions resulting in a 'pH memory'. The third factor is the increase in ionic strength, which could play a favourable role in esterification. Optimum pH for these reactions (pH 4.0 for RML and CRL and pH 6.0 for PPL) clearly indicates a slight unfavorable conformational change in the enzyme at about pH 4.0 to 6.0 leading to lesser conversion beyond pH 4.0 for RML or CRL and 6.0 for PPL.

The experimental setup employed in the present work is such that it maintained a low water activity ($a_w = 0.0054$) due to azeotropic distillation and recycling the solvent back into the reaction system after passing through a bed of desiccant (molecular sieves). Even the water of reaction formed could also be used to constitute the microaqueous layer around the enzyme and the excess water could be removed by azeotropic distillation. The same could occur even with the addition of added enzyme (with little water content) and buffer volume. The added carbohydrate molecule could also reduce the water content of the reaction mixture. Adachi *et al.* (2005) have reported that the hexose which is more hydrated decreased the water activity in the system and shifts the equilibrium towards synthesis. All these factors lead to maintenance of an equilibrium concentration of water around the enzyme all the time. Hence, thermodynamic binding equilibria interplayed by inactivation and inhibition along with maintenance of an

optimum water activity could be governing this reaction as reflected by the extent of conversion under different reaction conditions of added buffer, enzyme and substrate concentrations.

As carbohydrates contain several hydroxyl groups, several diastereomeric esters (mono, di, tri, tetra and penta) are possible for both the anomers of the carbohydrate molecule. For example in case of D-glucose 31 diastereomeric esters are possible for both the anomers. In case of L-phenylalanyl-D-glucose 6-*O*- was the major ester produced (24%) and in case of L-phenylalanyl-lactose only primary hydroxyl groups were esterified (Section 4.2.2.1 and 4.2.2.6). Hence, primary hydroxyl groups invariably formed esters in major proportions. The anomeric composition of D-glucose employed for the reaction was 40:60 (α : β) and the equal peak areas of anomeric H-1 chemical shift values observed at 4.24 and 4.0 ppm indicated that either both the anomers have reacted to equal extent (1:1) or D-glucose had undergone mutarotation.

Commercial crude PPL preparations contain variety of estero-/ lipo-lytic enzymes with low PPL concentrations (Birner-Grunberger *et al.* 2004, Manini *et al.* 2005), which could also perform facile esterification. Hence, a small amount of esters formed from esterases along with those of lipases in the present reaction cannot be ruled out. Since the reactions were carried out at a low temperature of 40° – 60 °C, the formation of peptide was less than 3%, even though unprotected L-phenylalanine was used for the reaction. NMR data (Section 4.2.2.1 and 4.2.2.6) clearly indicated that no Maillard reaction occurred. Under these reaction conditions, formation of Maillard reaction products are quite likely. For instance, Maillard and Pictet Spengler phenolic condensation products were reported in the reaction between phenolic amino acids and D-glucose in phosphate buffer at different pH from 5.0 to 9.0 at 90 °C (Manini *et al.* 2005). Similarly Maillard products from the reaction between D-glucose and N ^{α} -*t*-Boc-L-

lysine incubated with aminoguanidine in pH 7.4 phosphate buffer at 70 °C was also reported (Reihl *et al.* 2004). No such Maillard reaction type products were detected by mass as well as NMR in the present investigation. RML, PPL and CRL showed significant esterification (up to 98%) when unprotected L-phenylalanine, D-glucose and lactose were used. When N-acetyl-L-phenylalanine was used in the present work, both RML and PPL gave < 5% yield. Park *et al.* (1996) have reported that lipases from RML and PPL gave insignificant conversion with N-protected amino acids and only 6-O-t-Boc-L-phenylalanyl-D-glucose was formed when the reaction was carried out between t-Boc-L-phenylalanyl trifluoroester and D-glucose in pyridine using subtilisin. Maruyama *et al.* (2002) using a surfactant-subtilisin enzyme complex synthesized 6-O-N-acetyl-L-phenylalanyl-D-glucose with 68% conversion, whereas surfactant-lipase enzyme complex showed only 5-23% of esterification. Riva *et al.* (1988) have reported three monoesters (80% of 6-O-, 15% of 3-O- and 5% of 2-O- ester) in a 73% conversion yield when the reaction was carried out between N-acetyl-L-phenylalanyl chloroester and D-glucose in pyridine using subtilisin, a protease. Our present study has shown that comparable esterification yields to others could be achieved by employing PPL, RML and CRL instead of protease. Thus, our study clearly indicates that unprotected L-phenylalanine could be used for the esterification of carbohydrates.

3.6. Optimization of L-phenylalanyl-D-glucose synthesis using Response Surface Methodology (RSM).

Response surface methodology (RSM) is a useful statistical tool for industrial applications to optimize reaction conditions. It is widely employed in the lipase catalysed synthesis of esters (Liao *et al.* 2003; Guvene *et al.* 2003). Chang *et al.* (2003) used RSM to optimize the synthesis of hexyl butyrate using Lipozyme IM-77. Synthesis of kojic acid monolaurate using lipase from *Pseudomonas cepacia* was optimized using RSM (Chen *et al.* 2002).

In the present work *Rhizomucor miehei* lipase catalyzed preparation of L-phenylalanyl-D-glucose was optimized using RSM with unprotected L-phenylalanine and D-glucose in dichloromethane and DMF (90:10 v/v). A five variable parametric study was employed for the Central Composite Rotatable Design (CCRD) analysis (Montgomery 1991) with L-phenylalanine concentration in mmol, RML amount in mg, pH, incubation period in h and buffer concentration in mM. The experimental design included 32 experiments of five variables at five levels (-2, -1, 0, +1, +2). Table 3.8 shows the coded and actual levels of the variables employed in the design matrix.

Table 3.8 Coded values of the variables and their corresponding actual values used in the design of experiments

Variables	-2	-1	0	1	2
L-Phenylalanine in mmol	1	2	3	4	5
RML in mg	27	54	81	108	135
pH	4.0	5.0	6.0	7.0	8.0
Incubation period in h	24	48	72	96	120
Buffer concentration in mM	0.1	0.2	0.3	0.4	0.5

Actual set of experiments undertaken as per CCRD with coded values and the esterification yields obtained is given in Table 3.9. A second order polynomial equation was developed to study the effects of the variables on the esterification yields in terms of linear, quadratic and cross product terms. The equation is of the general form.

$$Y = A_0 + \sum_{i=1}^N A_i X_i + \sum_{i=1}^N A_{ii} X_i X_i + \sum_{i=1}^{N-1} \sum_{j=i+1}^N A_{ij} X_i X_j \dots\dots (1)$$

Where Y is the esterification yield (mmol), X_i is the variable, A_0 = constant term, A_i are the coefficients for the linear terms and A_{ii} are the coefficients for the quadratic terms and A_{ij} are the coefficients for the cross product terms and N is the number of variables.

The coefficients of the equation were determined by employing Microsoft Excel software, Version 5.0. Analysis of variance (ANOVA) for the final predictive equation was also carried out using Microsoft Excel software to test the significance and adequacy of the model (Table 3.10). The response surface equation was optimized for maximum yield in the range of process variables using Microsoft Excel Solver function.

The experimental data fitted the second order polynomial equation well as indicated by a R^2 value of 0.7 (Table 3.10). The final predictive equation is given by

$$Y = -3.13292 + 0.175788 * X_1 + 0.004961 * X_2 + 0.626492 * X_3 + 0.004151 * X_4 + 6.141212 * X_5 - 0.02203 * X_1 * X_1 - 2.2E-05 * X_2 * X_2 - 0.05053 * X_3 * X_3 - 4.3E-05 * X_4 * X_4 + 0.434091 * X_5 * X_5 + 0.001315 * X_1 * X_2 - 0.013 * X_1 * X_3 + 0.000115 * X_1 * X_4 + 0.0825 * X_1 * X_5 - 0.00052 * X_2 * X_3 + 4.75E-05 * X_2 * X_4 - 0.01787 * X_2 * X_5 + 0.002052 * X_3 * X_4 - 0.3475 * X_3 * X_5 - 0.04417 * X_4 * X_5$$

Y = conversion yield in mmol, X₁ = L-phenylalanine concentration (mmol), X₂ = RML concentration (mg), X₃ = Buffer pH, X₄ = incubation period (h), X₅ = Buffer concentration (mM).

Table 3.9 Experimental design with experimental and predicted yields of L-phenylalanyl-D-glucose based on the response surface equation

Expt. No	L-Phenylalanine	RML	pH	Incubation period	Buffer conc.	Yield Expt. mmol	Yield Pred. mmol
1	-1	-1	-1	-1	1	0.66	0.62
2	-1	-1	-1	1	-1	0.34	0.26
3	-1	-1	1	-1	-1	0.23	0.15
4	-1	-1	1	1	1	0.34	0.35
5	-1	1	-1	-1	-1	0.28	0.16
6	-1	1	-1	1	1	0.27	0.24
7	-1	1	1	-1	1	0.26	0.23
8	-1	1	1	1	-1	0.60	0.52
9	1	-1	-1	-1	-1	0.35	0.30
10	1	-1	-1	1	1	0.45	0.49
11	1	-1	1	-1	1	0.56	0.60
12	1	-1	1	1	-1	0.56	0.55
13	1	1	-1	-1	1	0.76	0.76
14	1	1	-1	1	-1	0.73	0.68
15	1	1	1	-1	-1	0.38	0.33
16	1	1	1	1	1	0.47	0.51
17	0	0	0	-2	0	0.27	0.37
18	0	0	0	2	0	0.45	0.48
19	0	0	-2	0	0	0.25	0.35
20	0	0	2	0	0	0.26	0.28
21	0	-2	0	0	0	0.41	0.44
22	0	2	0	0	0	0.38	0.47
23	-2	0	0	0	0	0.06	0.22
24	2	0	0	0	0	0.69	0.64
25	0	0	0	0	-2	0.27	0.47
26	0	0	0	0	2	0.76	0.69
27	0	0	0	0	0	0.42	0.52
28	0	0	0	0	0	0.63	0.52
29	0	0	0	0	0	0.67	0.52
30	0	0	0	0	0	0.32	0.52
31	0	0	0	0	0	0.81	0.52
32	0	0	0	0	0	0.40	0.52

Table 3.10 Analysis of variance of the response surface model along with coefficients of the response equation

Regression Statistics:					
Multiple R	0.84				
R Square	0.7				
Observations	32				
ANOVA:					
Source	Degrees of freedom	Sum of squares	Mean sum of squares	F ratio	P
Regression	20	0.7908	0.03954	1.28	0.347
Linear	5	0.1055	0.02109	0.68	0.647
Square	5	0.1124	0.02248	0.73	0.619
Interaction	10	0.3175	0.03175	1.02	0.481
Residual error	11	0.3409	0.03099	-	-
Lack of fit	6	0.1569	0.02615	0.17	0.658
Pure error	5	0.1839	0.03679	-	-
Total	31	-	-	-	-

Coefficients	Values of Coefficients	Standard Error	t-Stat
A ₀	-3.133	2.32853	-1.345
A ₁	0.176	0.40166	0.438
A ₂	0.005	0.40166	0.333
A ₃	0.626	0.47237	1.326
A ₄	0.004	0.01674	0.248
A ₅	6.141	4.01663	1.529
A ₁₁	-0.022	0.03250	-0.678
A ₂₂	-0.000	0.00004	-0.493
A ₃₃	-0.051	0.03250	-1.555
A ₄₄	0.000	0.00006	-0.770
A ₅₅	1.434	3.25020	0.441
A ₁₂	0.001	0.00163	0.807
A ₁₃	-0.013	0.04401	-0.295
A ₁₄	0.000	0.00183	0.062
A ₁₅	0.082	0.44008	0.187
A ₂₃	-0.001	0.00163	-0.318
A ₂₄	0.000	0.00007	0.699
A ₂₅	-0.018	0.0163	-1.096
A ₃₄	0.002	0.00183	1.119
A ₃₅	-0.348	0.44008	-0.790
A ₄₅	-0.044	0.01834	-2.409

An overall average absolute deviation (AAD) of 11.4% obtained showed good correlation between predicted and experimental yields. The conversion yield throughout has been expressed in mmol of L-phenylalanyl-D-glucose formed determined with respect to L-phenylalanine concentration from HPLC peak areas. All the experiments were carried out at a constant D-glucose concentration of 1 mmol. Also, the surface plots generated shows the effect of two variables with the other three variables maintained at 0 coded level conditions (Table 3.8).

Effect of L-phenylalanine concentration and RML concentration on the extent of esterification is shown in Fig. 3.6. At lower L-phenylalanine concentrations, the extent of esterification decreased with increase in RML concentrations. However, beyond 2 mmol of L-phenylalanine (two equivalents to D-glucose employed), the extent of esterification increased with increase in RML amounts from 27 mg to 135 mg. At less than 2 mmol of L-phenylalanine, increase in RML concentrations could result in total binding of D-glucose (present to the extent of 1 mmol) predominantly to the active site of RML compared to L-phenylalanine, due to competition in binding between L-phenylalanine and D-glucose, thus reducing the possibility of facile transfer of L-phenylalanyl group to D-glucose.

Rhizomucor miehei lipase concentration in conjunction with buffer concentration exhibited pronounced effect on the extent of esterification as shown in Fig. 3.7. Between 30 mg to 90 mg RML concentration, buffer concentration above 0.4 mM (0.4 mL, 0.1M buffer of pH 6.0) showed the highest conversion yield of 0.7 mmol. At buffer concentrations less than 0.35 mM (0.35 mL, 0.1M buffer of pH 6.0), less than 90 mg and more than 120 mg of RML concentration showed conversion yields less than 0.5 mmol. This clearly indicated that higher water activity (in the form of added buffer) could be

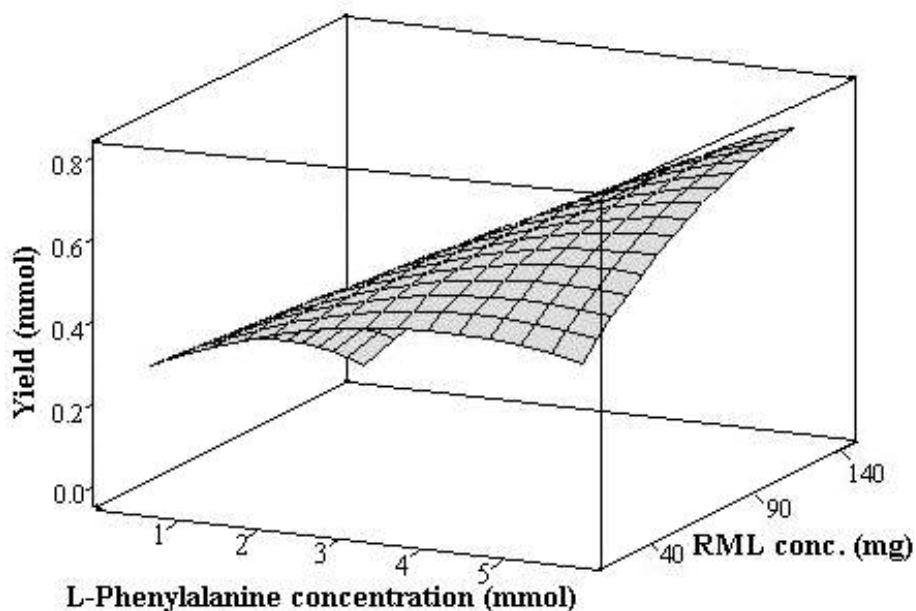


Fig. 3.6. Three-dimensional surface plot showing the effect of L-phenylalanine and RML concentration on the extent of esterification at 0.3 mM (0.3 ml of 0.1M) pH 6.0 buffer and 72h incubation period.

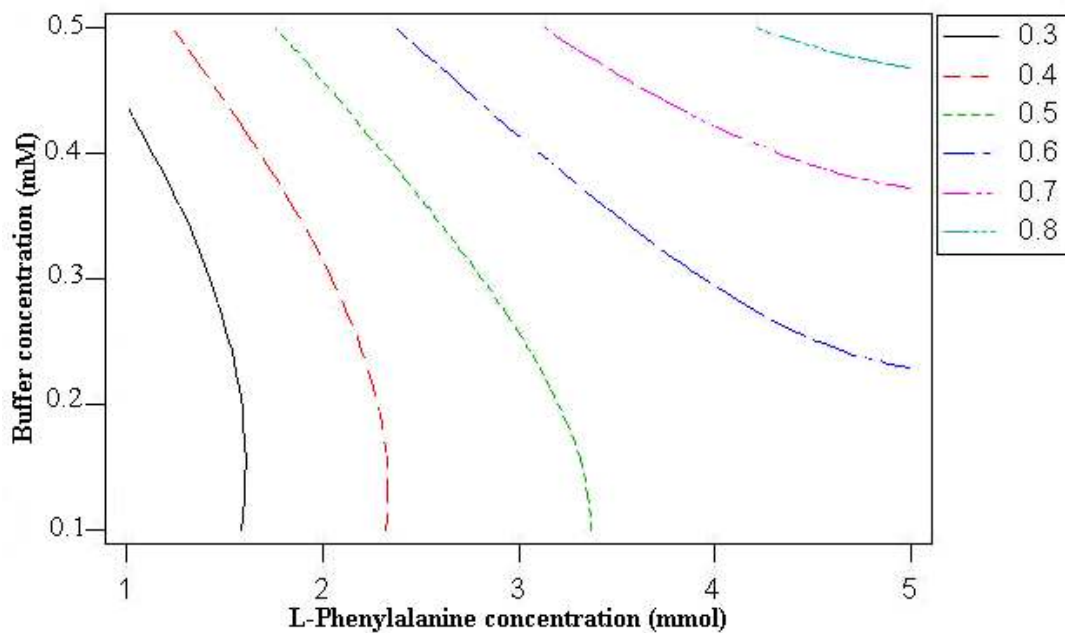


Fig. 3.7. Contour plot showing iso-esterification regions obtained due to the effect of RML and buffer concentration on the extent of esterification at 3.0 mmol L-phenylalanine, 72h incubation period and pH 6.0 buffer.

conducive to better activity of the enzyme leading to higher conversions. A critical amount of buffer has been found necessary for better esterification.

Effect of RML concentration and pH of the buffer employed on the extent of esterification (Fig. 3.8) indicated an optimum pH of 6.0 at all the RML concentrations. Although, increase in RML concentration showed only slight increase in ester conversion, an optimum concentration of 73.2 mg of RML was found to give the highest yield (0.55 mmol).

Figure 3.9 shows the effect of RML concentration and incubation period on the extent of esterification. The extent of esterification decreased with increase in RML concentration at incubation periods below 60 h. However, at incubation periods above 60h, esterification increased at all RML concentrations in the range of 27 mg to 135 mg. Effect of pH and incubation period also showed a similar behavior.

Effect of L-phenylalanine concentration and pH on the extent of esterification is shown in Fig. 3.10 in the form of a contour plot. The highest yield of 0.6 mmol was observed for a very narrow pH range of 4.5 to 6.5. At lower L-phenylalanine concentrations, lower iso-esterification (<0.6 mmol) regions were observed for a very broad pH range of 4.0 to 8.0. Increase in conversion yields thereafter resulted from a very narrow pH range around 6.0.

Effect of L-phenylalanine concentration and buffer concentration on the extent of esterification (Fig. 3.11) showed that lesser conversions below 0.5 mmol required lesser than 3.5 mmol L-phenylalanine concentration and a broad range of buffer concentration from 0.1 mM (0.1 mL, 0.1 M buffer of pH 6.0) to 0.5 mM (0.5 mL, 0.1M buffer of pH 6.0). However, between 3.5 mmol to 5.0 mmol of L-phenylalanine, buffer concentrations

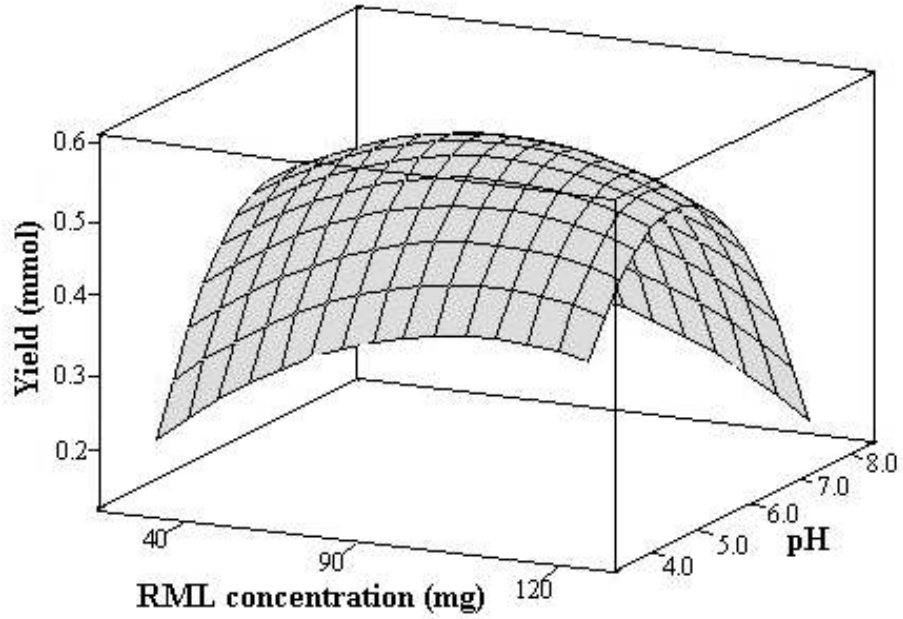


Fig. 3.8. Three-dimensional surface plot showing the effect of RML concentration and buffer pH on the extent of esterification at 3 mmol L-phenylalanine, 72h incubation period and 0.3 mM (0.3 ml of 0.1M) buffer concentration.

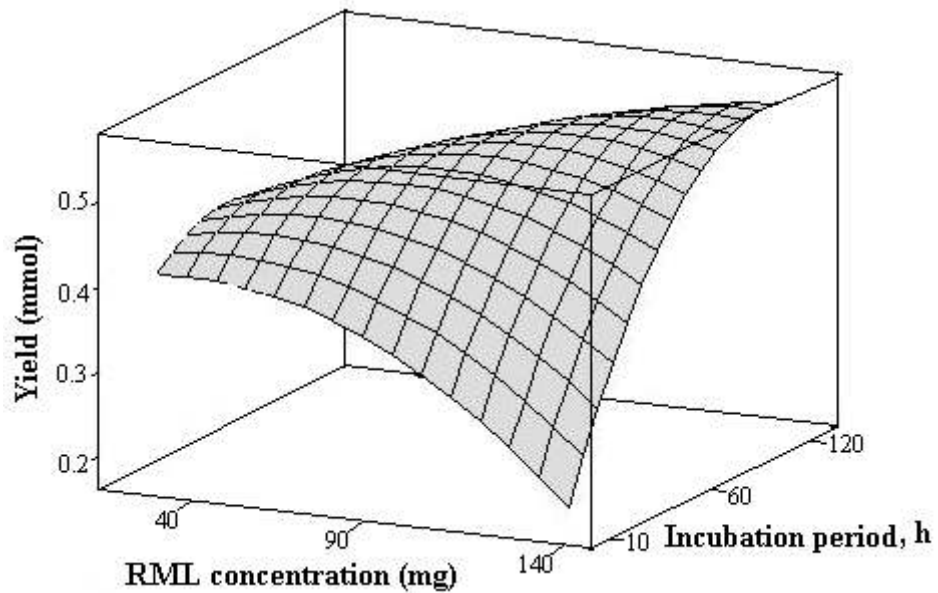


Fig. 3.9. Three-dimensional surface plot showing the effect of RML concentration and incubation period on the extent of esterification at 3 mmol L-phenylalanine and 0.3 mM (0.3 ml of 0.1M) pH 6.0 buffer.

above 0.25 mM (0.25mL, 0.1M buffer of pH 6.0) favoured higher conversion to 0.6 mmol and beyond (to 0.8 mmol).

RSM study clearly showed that an optimum buffer volume (concentration) in the form of a micro aqueous layer sheathing the enzyme and pH essential for facilitating the ionization states of the active site and charged amino acid residues on the surface (to maintain the active confirmation of the enzyme) are highly crucial for this esterification reaction. An optimum yield of 1.01 mmol was predicted from the optimized conditions of 3 mmol L-phenylalanine, 100 mg of RML, pH 4.8 acetate buffer, 24h incubation period and 0.5 mM buffer concentration. The experimental yield under such conditions was found to be 0.97 mmol. Validation experiments were also carried out at various random conditions predicted by the response plots. Table 3.11 shows results from validation experiments to be in good agreement with predicted yields.

Table 3.11. Validation of experimental data.

Expt. No.	L-Phe mmol	RML (mg)	pH	Incubation period (h)	Buffer conc. (mM)	Yield Predicted mmol	Yield^a Expt. mmol
1	3.0	50	6.0	72	0.45	0.69	0.64
2	3.0	110	6.0	72	0.30	0.58	0.65
3	3.0	81	5.0	72	0.45	0.65	0.74
4	4.5	81	6.0	72	0.50	0.82	1.07
5	3.0	80	6.0	60	0.30	0.50	0.55
6	4.0	81	6.0	70	0.30	0.60	0.66
7	3.0	100	4.8	24	0.5	1.01	0.97

^a Conversion yields were from HPLC. Experimental yields are an average from two experiments.

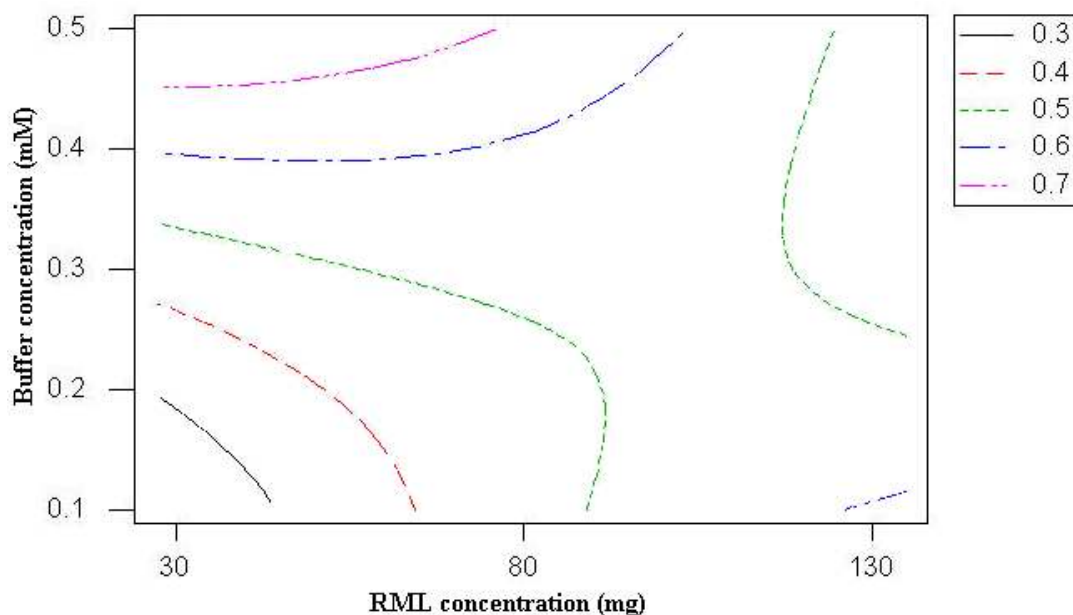


Fig. 3.10. Contour plot showing iso-esterification regions obtained due to the effect of L-phenylalanine concentration and buffer pH on the extent of esterification at 84 mg RML, 72h incubation period and 0.3 mM (0.3 ml of 0.1M) buffer concentration.

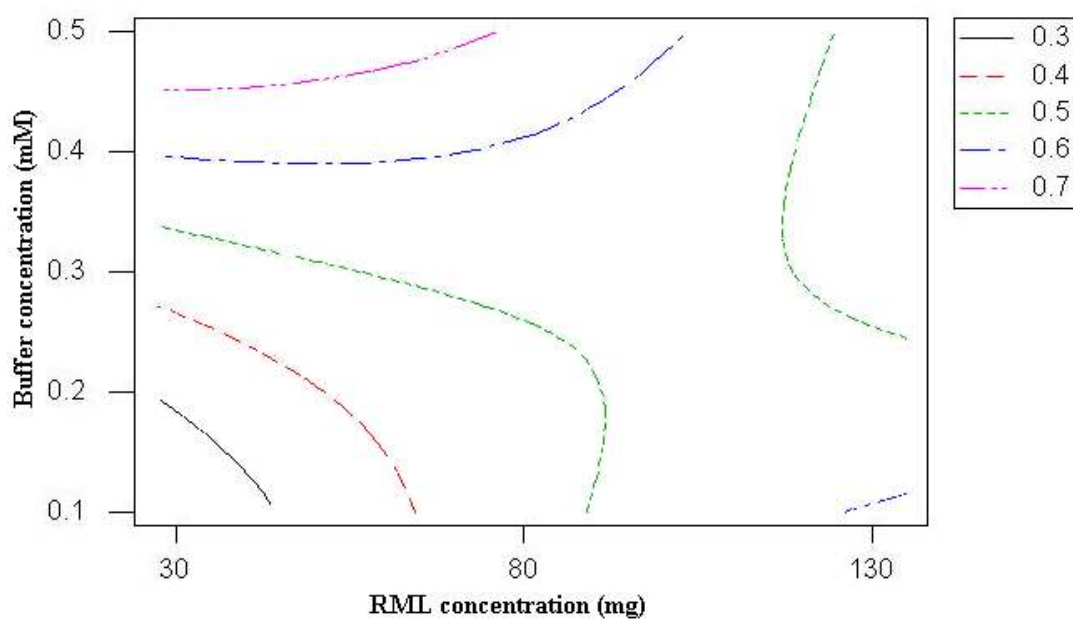


Fig. 3.11. Contour plot showing iso-esterification regions obtained due to the effect of L-phenylalanine concentration and buffer concentration on the extent of esterification at 84 mg RML, 72h incubation period and pH 6.0 buffer.

3.7. Experimental

3.7.1. Esterification procedure

L-Phenylalanyl-D-glucose and L-phenylalanyl-lactose were prepared in bench scale level. Reactants such as unprotected L-phenylalanine (0.001- 0.005 mol) and D-glucose (0.001 – 0.005 mol) or lactose (0.001 – 0.005 mol) were taken in a flat bottomed two necked flask along with 100 mL, CH₂Cl₂: DMF (90:10 v/v, 40 °C) or hexane: CHCl₃: DMF (45:45:10 v/v, 60 °C) in presence of 0.018- 0.225 g of lipases (10-50 % w/w carbohydrate employed) and refluxed for a period of 3 - 120 h. The condensed vapour of solvents, which formed an azeotrope with water was passed through a desiccant (molecular sieves of 4Å were used as desiccant) before being returned into the reaction mixture, thereby facilitating complete removal of water of reaction (Lohith and Divakar 2005). This experimental setup maintained a very low water activity of $a_w = 0.0054$ throughout the reaction period. The reaction mixture after distilling off the solvent was then added to 20 mL of water, stirred and filtered to remove the lipase. The filtrate was evaporated on a water bath to get unreacted carbohydrate, unreacted L-phenylalanine and the product esters which were then analyzed by HPLC. In reactions, which involved use of buffer salts, known volumes of 0.1 M buffer solutions at specified pH were added to the reaction mixture to impart 'pH memory' to the enzyme. Decimolar concentrations of CH₃COONa buffer for pH 4.0 and 5.0, Na₂HPO₄ for pH 6.0 and 7.0 and Na₂B₄O₇ .10 H₂O for pH 8.0 buffers were employed. The conversion yields were determined with respect to peak areas of the L-phenylalanine and that of the esters. The esters formed were separated by size exclusion chromatography using Sephadex G-10 and Bio Gel P-2 as column materials and eluted with water. The product esters separated were subjected to spectral characterization by UV, IR, mass, specific rotation and 2D-NMR (Sections 4.2.2.1 and 4.2.2.6). Although, the esters were separated from unreacted amino acids and carbohydrates by this procedure, the individual esters in the mixture of

esters formed could not be separated. This could be due to the similar polarity of the ester molecules. A partially purified lipase isolated from porcine pancreas was also employed for the preparation of L-phenylalanyl-D-glucose and L-phenylalanyl-lactose

3.7.2. High Performance Liquid Chromatography (HPLC)

A Shimadzu LC 10AT HPLC instrument connected to a μ -Bondapak aminopropyl column (10 μ m particle size, 3.9 x 300 mm length) was employed for analyzing the reaction mixture. Acetonitrile: water (80:20 v/v) as a mobile phase at a flow rate of 1 mL/min was used with Refractive Index detector. Also LiChrosorb RP-18 column (5 μ m particle size, 4.6 x 150 mm length) was employed with an UV detector at 254 nm using acetonitrile: water (20:80 v/v) as a mobile phase at a flow rate of 1 mL/min.

Chapter-4
***Candida rugosa* lipase catalysed syntheses**
of L-prolyl, L-phenylalanyl, L-tryptophanyl
and L-histidyl esters of carbohydrates

4.1. Introduction

Carbohydrates are information rich molecules, which are well suited for modification to new types of compounds with expected biological activity (Hurtley *et al.* 2001). Compared to fatty acid esters of carbohydrates, amino acid esters of carbohydrates can give added additional functionality in the side chain. Presence of hydroxyl as well as amine groups in the molecule help in the polycondensation reactions (Park *et al.* 1999). Recently Shiraki *et al.* (2004) reported that amino acid esters prevent thermal inactivation and aggregation of lysozyme. Hydrophobic amino acids, like L-phenylalanine, L-tyrosine and L-tryptophan with carbohydrate moiety may improve the water solubility (Maruyama *et al.* 2002), which is very much essential for bioavailability of amino acids.

Maruyama *et al.* (2002) employed different cyanomethyl esters of N-protected amino acids with D-glucose in the transesterification reaction using a protease surfactant-subtilisin complex. The yields were obtained in the 65-71% range and from ¹³C NMR only 6-O- ester formation was confirmed. Carbohydrates like D-glucose, D-galactose, D-mannose, D-fructose, lactose, sucrose and maltose gave good esterification with N-acetyl phenylalanine cyanomethyl ester (yields 54-68%), whereas α/β -methyl-glycosides showed very less yields (7-28%) with the amino acids under the same experimental conditions. Maruyama *et al.* (2002) also made an attempt to synthesize N-acetyl-phenylalanine esters of D-glucose in pyridine using lipase-surfactant complex (lipase from *Candida rugosa*, *Mucor javanicus*, *pseudomonas cepacia* and *pseudomonas fluorescens* were employed) with only 8-23% of yield (Maruyama *et al.* 2002). Jeon *et al.* (2001) prepared some amino acyl esters of sugar alcohols using Optimase M-440 as biocatalyst. Maximum yield of 93% N-t-Boc-L-methionine ester of D-sorbitol was obtained in pyridine and N-t-Boc-L-tyrosine ester of D-sorbitol showed very less yield of

8% under the same conditions (Jeon *et al.* 2001). Park *et al.* (1999) prepared different amino acyl (t-Boc derivatives of L-leucine, L-aspartic acid, L-lysine, L-phenylalanine, L-tyrosine and L-methionine) esters of sucrose using Optimase M-440 with the esterification yield of 9-60% and also reported that hydrophobic nature of the amino acids favored esterification over basic or acidic amino acids and there was not much variation in the yields with different carbohydrates employed in the reaction (Park *et al.* 1999).

4.2. Present work

Syntheses and characterization of L-prolyl, L-phenylalanyl, L-tryptophanyl and L-histidyl esters of carbohydrates

Using the same optimum conditions, which are employed for the L-phenylalanyl lactose synthesis, esterification was carried out between different amino acids (L-proline **1**, L-phenylalanine **2**, L-tryptophan **3** and L-histidine **4**) and carbohydrates (D-glucose **5**, D-galactose **6**, D-mannose **7**, D-fructose **8**, D-arabinose **9**, D-ribose **10**, lactose **11**, maltose **12**, sucrose **13**, D-mannitol **14**, D-sorbitol **15**) using *Candida rugosa* lipase (CRL) in presence of organic solvent. A 0.2 mM (0.2 mL) pH 4.0 acetate buffer was employed to the reaction mixture to impart the 'pH memory' to CRL. The reaction mixture containing the L-amino acid **1-4** (1 mmol), carbohydrate **5-15** (1 mmol), CRL (50% w/w based on respective carbohydrate) and the solvent were refluxed for a period of 72 h (experimental procedure is explained in Section 2.2.4). The esterification reaction described in this present work did not occur without the use of enzymes. Extent of esterification was analyzed by HPLC and esters were isolated by passing through Sephadex G-10 and Bio-Gel P2 eluted with water. The isolated esters were then subjected to characterization by UV, IR, Mass and 2D-NMR spectroscopy. Out of five amino acids employed for the reaction, L-tyrosine did not give esterification with any of

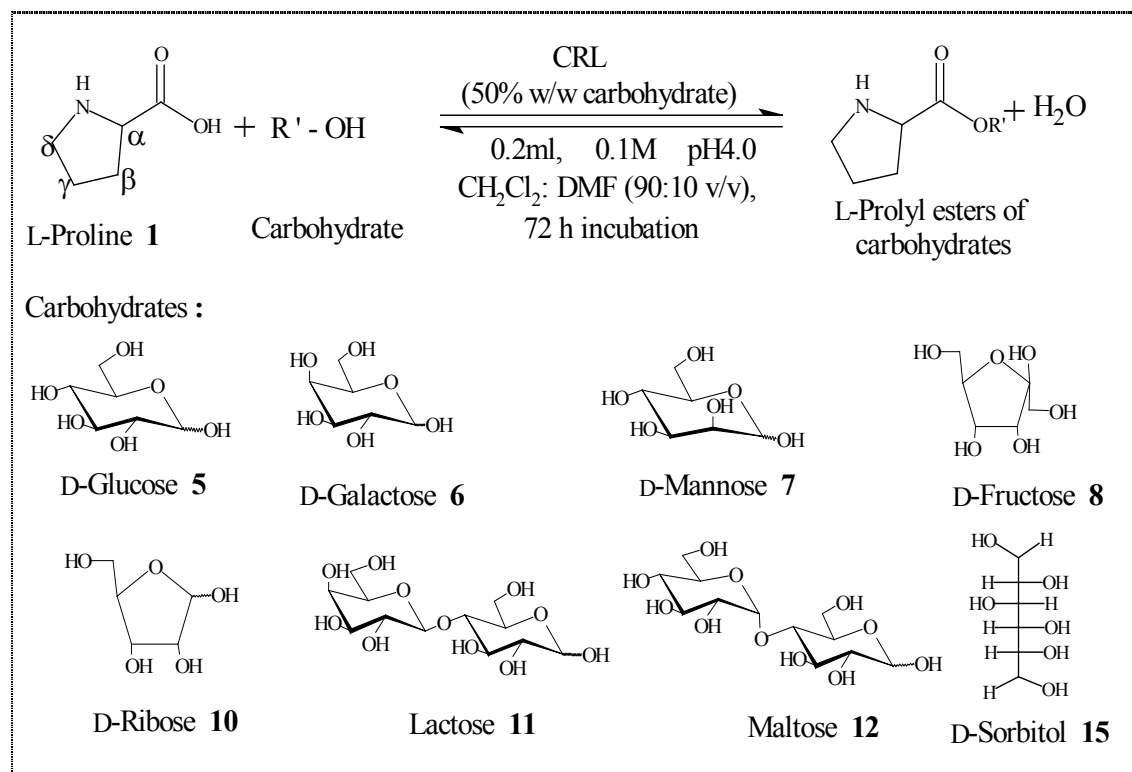
the carbohydrates. NMR assignments of amino acids and carbohydrates and though were esters were made according to literature reports (Suzuki *et al.* 1991; Rival *et al.* 1988; Park *et al.* 1996; 1999). Some of the assignment, especially ^{13}C signals mentioned in the section 4.2.1.1 – 4.2.1.8 for L-prolyl esters, 4.2.2.1 – 4.2.2.8 for L-phenylalanyl esters, 4.2.3.1 – 4.2.3.8 for L-tryptophanyl esters and 4.2.4.1 - 4.2.4.5 for L-histidyl esters are interchangeable. Only resolvable signals are shown. Non-reducing end carbohydrate signals in disaccharides are primed and aromatic signal numbers are subscripted. Since, the esters are surfactant molecules, they appear to aggregate in the solvent and usually give broad signals, thus, making it difficult to resolve the coupling constant values accurately. Mass data for the monoesters are shown. However, although NMR data clearly indicated the presence of *di-O*- esters, they were not detected in the mass spectra, which could be due to instantaneous decomposition. The percentage proportions of the individual esters formed were determined by considering the peak areas of the C6, C5 (in case of pentoses) of ^{13}C signals or cross peaks from 2D-NMR. Although column chromatography using Sephadex G-10, G-25 and Bio-gel P2 separated unreacted amino acids and carbohydrates from the esters, the individual esters could not be separated in many cases due to similar polarity of the ester molecules. However, NMR data from individual esters could be detected unequivocally.

4.2.1. L-Prolyl esters of carbohydrates

L-Proline is the only amino acid where the amine group is part of a five membered ring. L-Proline is highly hygroscopic in nature. L-Proline is one of the important active constituents in many of the peptide drugs. Proline derivatives like proline esters and its salts act as pharmaceutically active ingredients in tumor treatments (Zoser 2005).

Esterification of L-proline with carbohydrates was carried out using CRL under optimal conditions (Section 2.2.4, Scheme 4.1). The reaction mixtures consists of 1mmol

of L-proline and 1mmol of carbohydrates (D-glucose **5**, D-galactose **6**, D-mannose **7**, D-fructose **8**, D-arabinose **9**, D-ribose **10**, lactose **11**, maltose **12**, sucrose **13**, D-mannitol **14**, D-sorbitol **15**) along with 50% CRL (w/w based on respective carbohydrate) incubated in 100 mL of CH₂Cl₂ and DMF (v/v 90:10, 40 °C) containing 0.2 mM (0.2 mL of 0.1M) of pH 4.0 acetate buffer. The reaction mixture was analyzed by HPLC using C18 column using acetonitrile and water in the ratio of 20:80 (v/v) and detection was at 210 nm using UV detector (Fig. 4.1). The retention times and R_f values are shown in Table 4.1.



Scheme 4.1. *Candida rugosa* lipase catalysed syntheses of L-prolyl esters of carbohydrates

The isolated esters were subjected to UV, IR, MS and 2D- NMR characterization (Section 4.2.1.1 – 4.2.1.8). UV transitions for $\sigma \rightarrow \sigma^*$ in the range 200 nm – 219 nm for L-prolyl esters, compared to $\sigma \rightarrow \sigma^*$ transition for L-proline **1** at 194 nm indicated that **1** had undergone esterification. InfraRed spectral data showed that the ester carbonyl stretching frequency for the prepared esters were in the range 1604 – 1646 cm⁻¹ compared

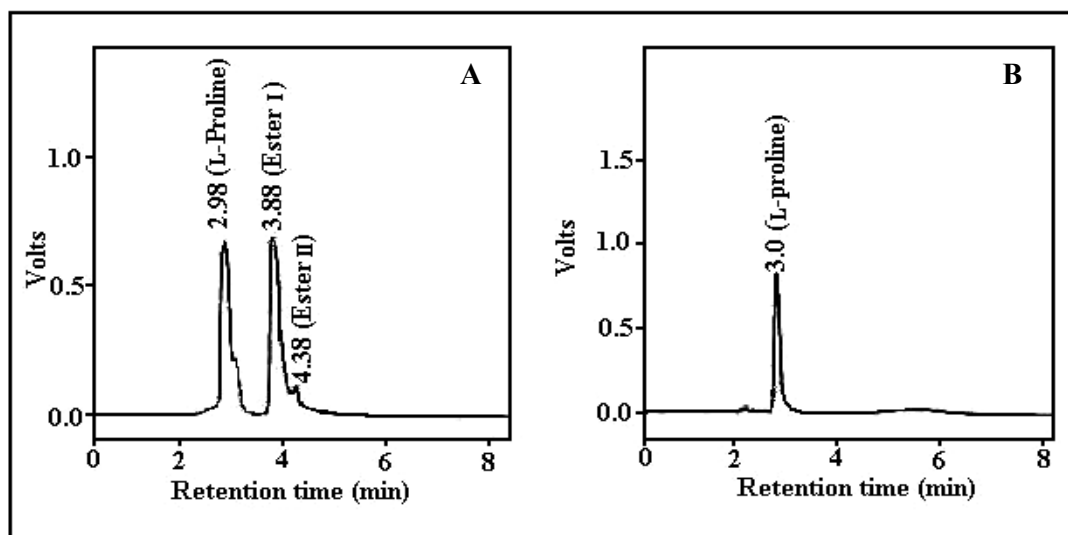


Fig. 4.1. HPLC chromatogram; (A) reaction mixture of L-proline and D-galactose esterification reaction catalysed by CRL. Column – C-18; mobile phase – acetonitrile: water (20:80 v/v); flow rate- 1 mL /min; detector – UV at 210nm; (B) standard chromatogram of L-proline; errors in yields are \pm 10-15%.

to 1658 cm⁻¹ observed for the carbonyl group of L-proline indicating that L-proline carboxylic group had been converted into its corresponding carbohydrate ester. Molecular ion peaks in mass spectrum further confirmed the formation of esters. Table 4.2 shows chemical shift values for free carbohydrates. Table 4.3 shows the ester yields from HPLC, types of esters formed and percentage proportions of the individual esters.

Table 4.1 Retention times and R_f values of L-prolyl esters of carbohydrates

Compound	Retention time (min)^a	R_f values^b
L-Proline	3.0	0.72
L-Prolyl-D-glucose	3.8	0.62
L-Prolyl-D-galactose	3.9 & 4.4 ^c	0.66
L-Prolyl-D-mannose	3.2 & 4.0 ^c	0.59
L-Prolyl-D-fructose	3.9	0.61
L-Prolyl-D-ribose	3.2 & 3.8 ^c	0.57
L-Prolyl-lactose	3.8	0.42
L-Prolyl-maltose	3.8	0.44
L-Prolyl-D-sorbitol	3.1 & 4.1 ^c	0.57

^a Conditions: column – C18; mobile phase –acetonitrile: water (20:80 v/v); flow rate– 1mL/min; detector– UV at 210 nm; ^b TLC - A 20 x 20 cm silica plate (mesh size 60 –120); mobile phase – butanol : acetic acid : water (70:20:10 v/v/v); peak identification – ninhydrin (amino acid); 1-naphthol (sugar);

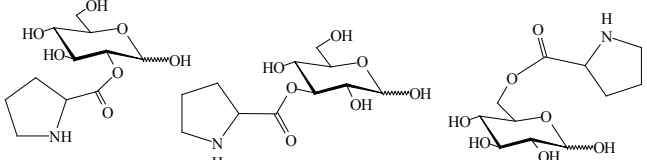
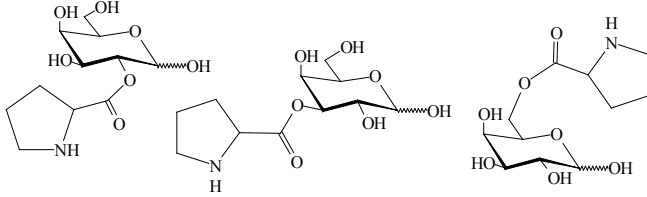
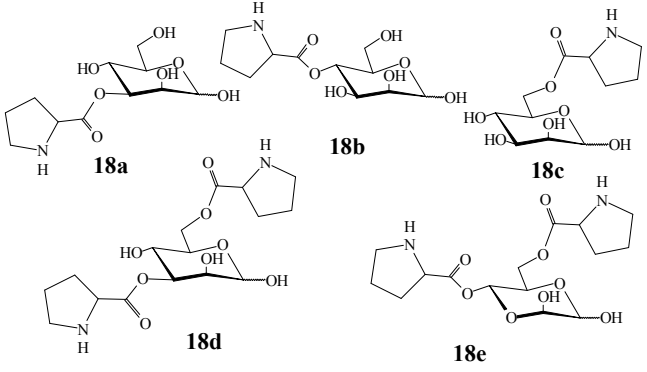
^c In case of few esters two ester peaks were detected.

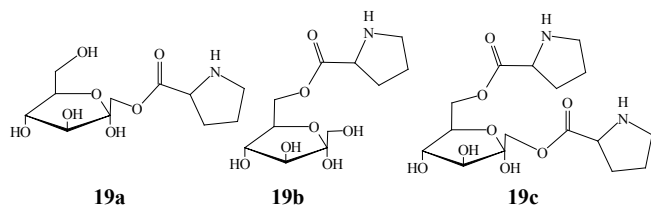
Table 4.2 NMR data of free carbohydrates

Carbohydrate	Chemical shift values in ppm (J Hz)																								
	¹ H ¹³ C		¹ H ¹³ C		¹ H ¹³ C		¹ H ¹³ C		¹ H ¹³ C		¹ H ¹³ C		¹ H ¹³ C												
	H-1	C1	H-2	C2	H-3	C3	H-4	C4	H-5	C5	H-6	C6	H-1'	C1'	H-2'	C2'	H-3'	C3'	H-4'	C4'	H-5'	C5'	H-6'	C6'	
D-Glucose	α	4.95	92.3	3.14	72.5	3.44	72.0	3.07	70.7	3.58	72.0	3.53	61.4												
	β	4.30	97.0	2.92	75.0	3.06	76.9	-	-	3.45	76.9	3.62	61.6												
D-Galactose	α	4.14	92.7	3.50	68.4	3.59	69.0	3.70	70.0	3.35	70.5	3.31	60.7												
	β	4.83	97.6	--		3.15	73.7	3.10	72.3	3.25	74.8	3.32	60.8												
D-Mannose	α	4.89	94.0	3.54	71.3	3.55	70.0	3.36	67.4	3.50	73.0	3.63	61.5												
	β	4.54	93.9	3.32	71.5	3.26	73.7	3.37	67.0	3.02	77.0	3.46	61.4												
D-Fructose	β	3.80	63.9	-	97.5	3.56	67.9	3.64	69.9	3.57	68.7	3.50	62.6												
D-Ribose	α	4.75	93.2	3.23	70.6	3.33	68.8	3.71	66.7	3.51	62.8														
	β	4.31	94.0	3.31	71.5	3.38	68.0	3.54	67.5	3.29	62.8														
D-Arabinose	α	4.92	92.3	4.32	-	4.6	-	4.08	-	3.73	60.4														
	β	4.33	96.2	3.65	69.1	4.02	68.9	3.37	67.1	3.64	60.7														
Lactose	α	4.90	91.9	3.70	69.8	3.54	71.4	3.27	80.8	3.55	72.1	3.64	60.5	4.19	103.7	3.30	70.7	3.18	73.2	3.62	68.2	2.93	75.4	3.52	60.9
	β	4.34	96.3	3.31	74.2	3.53	74.7	3.28	81.1	3.44	74.9	3.72	60.6												
Maltose	α	4.80	92.0	2.85	73.9	3.29	76.4	3.15	79.7	3.30	73.3	3.50	60.8	4.90	100.3	2.94	72.0	3.10	73.0	3.51	69.5	3.62	72.7	3.60	60.2
	β	4.20	96.9	3.10	74.3	3.31	76.0	3.19	79.4	3.38	76.4	3.34	60.9												
Sucrose Glc α Fru β														5.18	91.7	3.65	72.7	3.20	71.5	3.11	69.8	3.47	72.8	3.54	60.5
		3.41	62.0	-	103.9	3.78	77.1	3.88	74.1	3.41	82.4	3.55	62.0												
D-Sorbitol		3.41	62.5	3.54	73.6	3.68	68.9	3.39	72.2	3.48	71.4	3.56	63.3												
D-mannitol		3.40	63.7	3.47	71.2	3.54	69.6	3.54	69.6	3.47	71.2	3.61	63.7												

^a 40 mg of carbohydrate in 0.5 mL of DMSO-d₆ (Bock and Pedersen 1983; Bock *et al.* 1984)

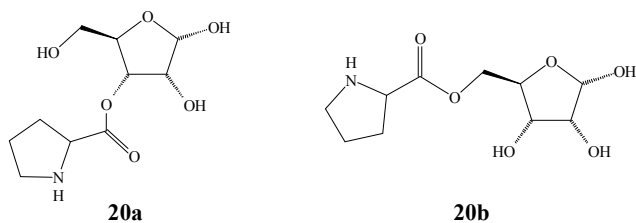
Table 4.3 Syntheses of L-prolyl esters of carbohydrates ^a

L-Prolyl esters of carbohydrates	Esterification yield (%)	Esters (% proportions ^b)
 <p>16a 16b 16c</p>	<p>60 (only mono esters)</p>	<p>16a: 2-<i>O</i>-L-prolyl- D-glucose (26) 16b: 3-<i>O</i>-L-prolyl-D-glucose (26) 16c: 6-<i>O</i>-L-prolyl-D-glucose (38)</p>
 <p>17a 17b 17c</p>	<p>52 (only mono esters)</p>	<p>17a: 2-<i>O</i>-L-prolyl-D-galactose (20) 17b: 3-<i>O</i>-L-prolyl-D- galactose (12) 17c: 6-<i>O</i>-L-prolyl-D-galactose (68)</p>
 <p>18a 18b 18c 18d 18e</p>	<p>62 (only mono esters)</p>	<p>18a: 3-<i>O</i>-L-prolyl-D-mannose (21) 18b: 4-<i>O</i>-L-prolyl-D-mannose (20) 18c: 6-<i>O</i>-L-prolyl-D-mannose (24) 18d: 3,6-<i>di-O</i>-L-prolyl-D-mannose (19) 18e: 4,6-<i>di-O</i>-L-prolyl-D-mannose (16)</p>



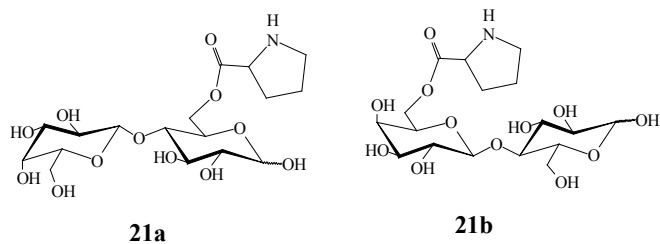
61
(mono esters-45,
diester-16)

19a: 1-*O*-L-prolyl-D-fructose (31)
19b: 6-*O*-L-prolyl-D-fructose (42)
19c: 1,6-*di-O*-L-prolyl-D-fructose (27)



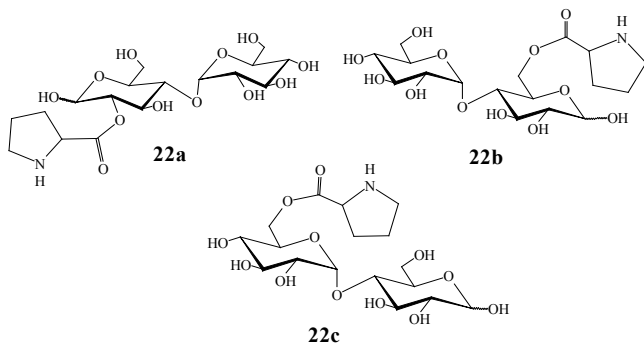
41
(only mono esters)

20a: 3-*O*-L-prolyl-D-ribose (35)
20b: 5-*O*-L-prolyl-D-ribose (65)



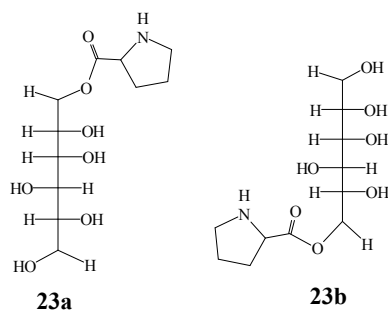
68
(only mono esters)

21a: 6-*O*-L-prolyl-lactose (58)
21b: 6'-*O*-L-prolyl-lactose (42)



66
(only mono esters)

22a: 2-*O*-L-prolyl-maltose (29)
22b: 6-*O*-L-prolyl-maltose (38)
22c: 6'-*O*-L-prolyl-maltose (33)



20
(only mono esters)

23a: 1-*O*-L-prolyl-D- sorbitol (73)
23b: 6-*O*-L-prolyl-D- sorbitol (27)

^a L-Proline – 1 mmol; carbohydrates – 1 mmol; CRL – 50% (w/w based on respective carbohydrate); buffer – 0.2mM (0.2mL) pH 4.0 acetate buffer; CH₂Cl₂: DMF (90: 10 v/v) at 40 °C; incubation period – 72 h; Conversion yields were from HPLC with respect to L-proline concentration; ^b The ester proportions were calculated from the area of respective ¹³C signals.

Spectral data for L-proline: Solid; mp- 258 °C; UV (H₂O, λ_{\max}): 194.0 nm ($\sigma \rightarrow \sigma^*$ $\epsilon_{194} = 339 \text{ M}^{-1}$); IR (KBr): 3280 cm⁻¹ (NH), 1658 cm⁻¹ (CO), 1322 cm⁻¹ (CN); $[\alpha]_{\text{D}}^{25} = -77.8^\circ$ (c 0.56, H₂O); 2D-HSQCT (DMSO-d₆): ¹H NMR δ_{ppm} (500.13 MHz): 3.78(αCH), 2.0(βCH_2), 1.79(γCH_2), 3.12(δCH_2); ¹³C NMR δ_{ppm} : 60.2(αCH), 29.0(βCH_2), 23.9(γCH_2), 45.1(δCH_2), 170.8(CO).

4.2.1.1. L-Prolyl-D-glucose 16a-c:

Solid; UV (H₂O, λ_{\max}): 200 nm ($\sigma \rightarrow \sigma^*$ $\epsilon_{200} = 1862 \text{ M}^{-1}$), 285 nm ($n \rightarrow \sigma^*$ $\epsilon_{285} = 512 \text{ M}^{-1}$); IR (KBr): 3261 cm⁻¹ (OH), 1631 cm⁻¹ (CO), 1384 cm⁻¹ (CN). $[\alpha]_{\text{D}}^{25} = -19.6^\circ$ (c 0.6, H₂O); MS (m/z) 302 [$\text{M}+2+\text{Na}$]⁺; RT: 3.8 min; R_f: 0.62.

2D-HSQCT (DMSO-d₆): **2-O-ester 16a:** ¹H NMR δ_{ppm} (500.13 MHz): 3.85(αCH), 2.84(βCH_2), 3.75(H-2 α), 3.63(H-2 β), 3.55(H-6a); ¹³C NMR δ_{ppm} (125 MHz): 58.0(αCH), 32.0(βCH_2), 75.0(C2 α), 80.0(C2 β), 61.5(C6 β).

3-O-ester 16b: ¹H NMR δ_{ppm} : 3.46(αCH), 2.84(βCH_2), 2.20(δCH_2), 3.84(H-3 α), 3.93(H-3 β), 3.46(H-6a); ¹³C NMR δ_{ppm} : 53.0(αCH), 32.0(βCH_2), 28.0(δCH_2), 98.5(C1 α), 82.4(C3 α), 84.0(C3 β), 61.0(C6 α).

6-O-ester 16c: ¹H NMR δ_{ppm} : 3.75(αCH), 2.85(βCH_2), 1.94(γCH_2), 3.15(δCH_2), 4.38(H-1 α), 4.20(H-1 β), 3.38(H-3 α), 4.20(H-4 α), 3.90(H-4 β), 3.82(H-6a); ¹³C NMR δ_{ppm} : 56.0(αCH), 35.0(βCH_2), 28.0(γCH_2), 46.0(δCH_2), 171.6(CO), 95.2(C1 α), 101.4(C1 β), 72.0(C3 α), 71.0(C4 α,β), 63.6(C6 β).

UV spectrum and 2D-HSQCT NMR spectrum for L-prolyl-D-glucose **16a-c** are shown in Figures 4.2 and 4.3 respectively.

4.2.1.2. L-Prolyl-D-galactose 17a-c:

Solid; UV (H₂O, λ_{\max}): 200 nm ($\sigma \rightarrow \sigma^*$ $\epsilon_{210} = 1950 \text{ M}^{-1}$), 285 nm ($n \rightarrow \sigma^*$ $\epsilon_{285} =$

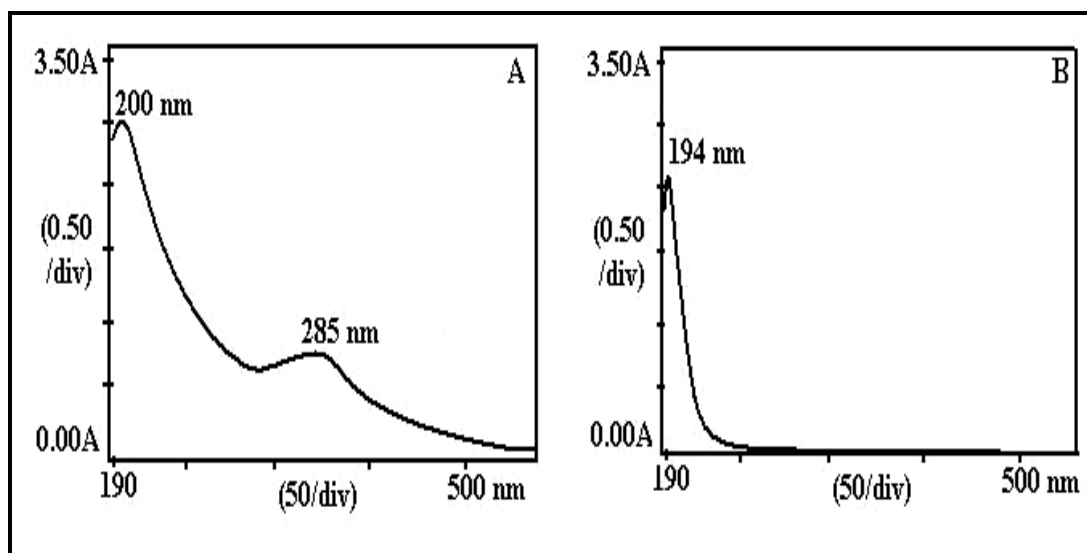


Fig. 4.2. UV spectra for L-prolyl-D-glucose of CRL catalysed reaction. (A) L-prolyl-D-glucose and (B) L-proline

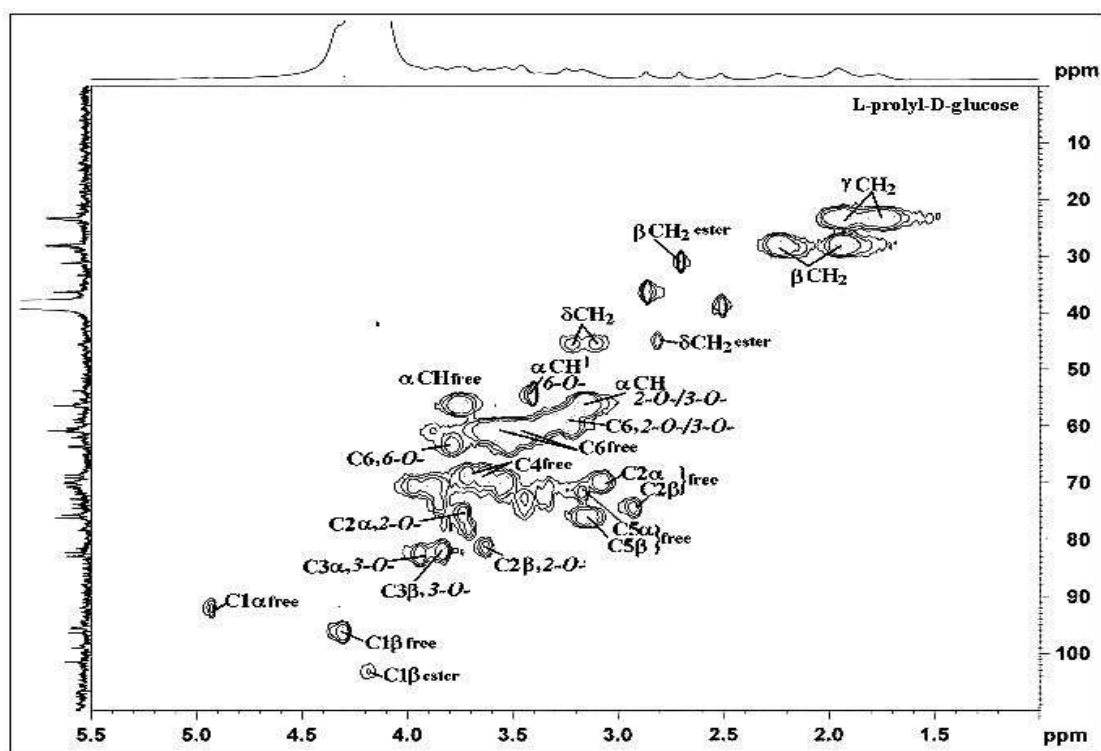


Fig. 4.3. Two-dimensional HSQCT NMR spectrum for L-prolyl-D-glucose **16a-c** reaction mixture

355 M⁻¹); IR (KBr): 3291 cm⁻¹ (OH), 1618 cm⁻¹ (CO), 1387 cm⁻¹ (CN); [α]_D²⁵ = -27.5° (*c* 0.4, H₂O); MS (*m/z*) 301[M+1+Na]⁺; RT: 3.9 and 4.4 min; R_f: 0.66.

2D-HSQCT (DMSO-d₆): **2-O-ester 17a**: ¹H NMR (δ_{ppm}): 2.82(α CH), 3.26(δ CH₂), 3.62(H-2 α), 3.30(H-2 β), 3.46 (H-6a); ¹³C NMR (δ_{ppm}): 60.2(α CH), 43.2(δ CH₂), 74.8 (C2 α), 75.3(C2 β), 60.8(C6 α).

3-O-ester 17b: ¹H NMR (δ_{ppm}): 2.99(α CH), 2.50(β CH₂), 1.74(γ CH₂), 3.20(δ CH₂), 3.91(H-3 α), 3.82(H-3 β), 3.32(H-6a); ¹³C NMR (δ_{ppm}): 60.1(α CH), 27.8(β CH₂), 44.5(δ CH₂), 97.2(C1 α), 79.8(C3 α), 81.0(C3 β), 61.0(C6 α).

6-O-ester 17c: ¹H NMR (δ_{ppm}): 2.88(α CH), 2.73(β CH₂), 1.88 (γ CH₂), 2.99 (δ CH₂), 4.20 (H-1 α), 3.38(H-3 α), 4.20(H-4 α), 3.90(H-4 β), 3.38(H-6a), 3.32(H-6b α); ¹³C NMR (δ_{ppm}): 60.4(α CH), 30.5(β CH₂), 21.0 (γ CH₂), 45.2(δ CH₂), 97.6(C1 α), 68.0(C2 α), 72.0(C3 α), 72.2(C4 α), 72.8(C5 α) 63.1(C6 α).

Two-dimensional HSQCT NMR spectrum for L-prolyl-D-galactose **17a-c** is shown in Fig. 4.4.

4.2.1.3. L-Prolyl-D-mannose 18a-e:

Solid; UV (H₂O, λ_{max}): 219 nm ($\sigma \rightarrow \sigma^*$ $\epsilon_{219} = 1288 \text{ M}^{-1}$), 278.0 nm ($n \rightarrow \sigma^*$ $\epsilon_{278} = 724 \text{ M}^{-1}$); IR (KBr): 3294 cm⁻¹ (OH), 1616 cm⁻¹ (CO) and 1411 cm⁻¹ (CN); [α]_D²⁵ = -31.4° (*c* 0.51, H₂O); MS (*m/z*) 302[M+2+Na]⁺; RT: 4.0 min; R_f: 0.59.

2D-HSQCT (DMSO-d₆): **3-O-ester 18a**: ¹H NMR (δ_{ppm}): 2.77(α CH), 2.06(β CH₂), 1.69(γ CH₂), 3.17(δ CH₂), 3.62(H-2 α), 3.54(H-2 β), 3.76(H-3 α), 3.88(H-3 β), 3.52(H-6a); ¹³C NMR (δ_{ppm}): 60.0(α CH), 29.0(β CH₂), 23.8(γ CH₂), 45.6(δ CH₂), 69.8(C2 α), 102.1(C1 β), 69.6(C2 β), 81.9(C3 α), 83.3(C3 β), 60.6(C6 α).

4-O-ester 18b: ^1H NMR (δ_{ppm}): 2.94(αCH), 1.89(βCH_2), 3.81(H-4 α), 3.72(H-4 β), 3.39(H-6a); ^{13}C NMR (δ_{ppm}): 59.8(αCH), 28.6(βCH_2), 74.6(C4 α), 75.4(C4 β), 60.4(C6 α).

6-O-ester 18c: ^1H NMR (δ_{ppm}): 3.05(αCH), 2.06 (βCH_2), 4.78(H-1 α), 4.10(H-1 β), 3.61(H-2 α), 3.54(H-3 α), 3.41(H-4 α), 3.37(H-5 α), 3.74(H-6a); ^{13}C NMR (δ_{ppm}): 59.7(αCH), 28.9(βCH_2), 97.2(C1 α), 100.9(C1 β), 69.3(C3 α), 69.1(C4 α,β), 63.2(C6 α).

3,6-di-O-ester 18d: ^1H NMR (δ_{ppm}): 3.54(H-3 α), 3.46(H-6a); ^{13}C NMR (δ_{ppm}): 81.5(C3 α), 62.8(C6 α); **4,6-di-O-ester 18e:** ^1H NMR (δ_{ppm}): 3.61(H-4 α), 3.38(H-6b); ^{13}C NMR (δ_{ppm}): 78.4(C3 α), 76.4 (C4 α), 79.0(C4 β), 63.0(C6 α).

Figure 4.5 shows two-dimensional HSQCT NMR spectrum for L-prolyl-D-mannose **18a-e**.

4.2.1.4. L-Prolyl-D-fructose 19a-c:

Solid; UV (H_2O , λ_{max}): 213 nm ($\sigma \rightarrow \sigma^*$ $\epsilon_{213} = 1479 \text{ M}^{-1}$), 280 nm ($n \rightarrow \sigma^*$ $\epsilon_{280} = 407 \text{ M}^{-1}$); IR (KBr): 3070 cm^{-1} (OH), 1604 cm^{-1} (CO), 1402 cm^{-1} (CN); $[\alpha]_{\text{D}}^{25} = -44.0^\circ$ (c 0.5, H_2O); MS (m/z): 300 $[\text{M}+\text{Na}]^+$; RT: 3.9min; R_f : 0.61.

2D-HSQCT (DMSO- d_6): **1-O-ester 19a:** ^1H NMR δ_{ppm} (500.13 MHz): 3.15(αCH), 2.72(βCH_2), 2.08(γCH_2), 3.12(δCH_2), 4.13(H-1a), 3.13(H-3 α), 3.40(H-3 β), 3.80(H-4 α), 3.62(H-4 β), 3.30(H-5 α), 3.93(H-5 β), 3.23(H-6a); ^{13}C NMR δ_{ppm} (125 MHz): 60.0(αCH), 31.0(βCH_2), 24.0(γCH_2), 48.2(δCH_2), 170.8(CO), 65.8 (C1 α), 104.2(C1 α), 71.4(C3 α), 82.1(C3 β), 69.9(C4 α), 78.2(C4 β), 74.0(C5 α), 82.9(C5 β), 63.7(C6 α).

6-O-ester 19b: ^1H NMR δ_{ppm} : 3.32(αCH), 3.33(δCH_2), 3.78(H-1a), 3.78(H-3 α), 3.29(H-3 β), 3.38(H-5 α), 4.12(H-5 β), 4.02(H-6a); ^{13}C NMR δ_{ppm} : 59.2(αCH), 49.3(δCH_2), 64.4(C1 α), 99.1(C2 α), 71.9(C3 α), 70.7(C4 α), 75.2(C5 α), 81.9(C5 β), 65.8(C6 α).

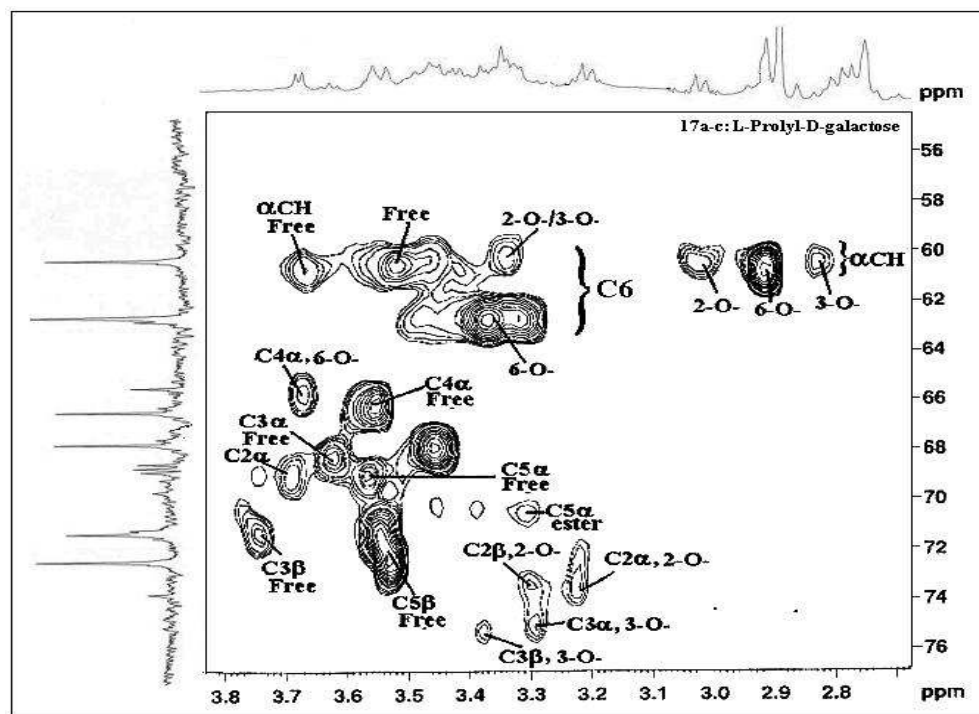


Fig. 4.4. Two-dimensional HSQCT NMR spectrum for L-prolyl-D-galactose **17a-c** reaction mixture

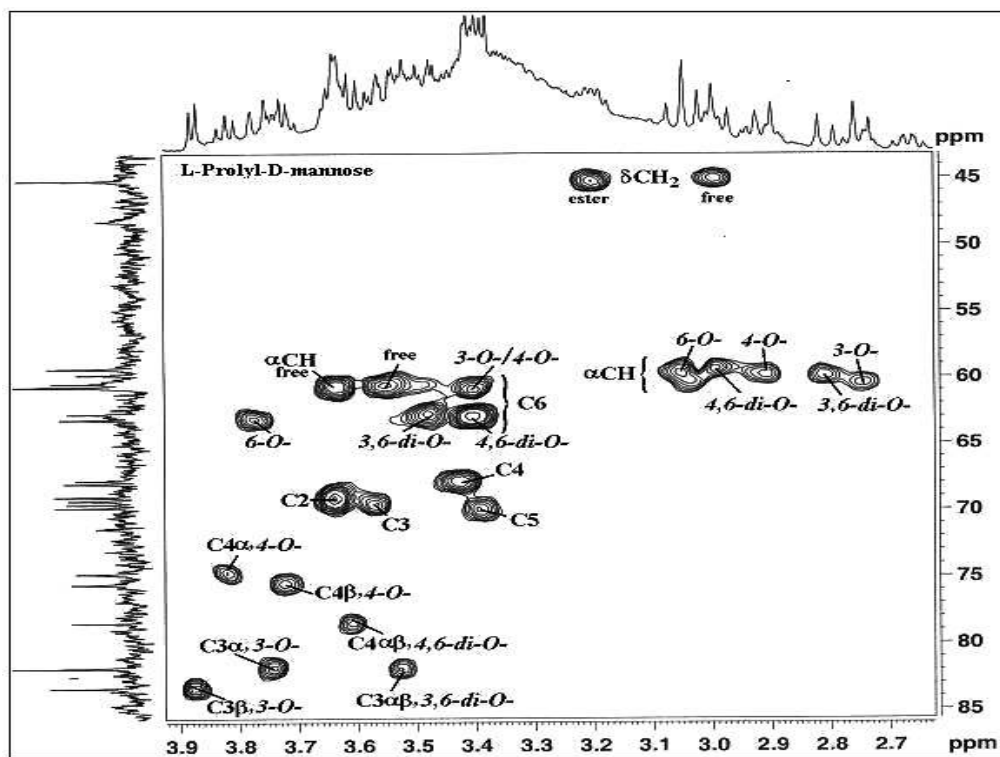


Fig. 4.5. Two-dimensional HSQCT NMR spectrum for L-prolyl-D-mannose **18a-e** reaction mixture

1,6-di-O-ester 19c: ^1H NMR δ_{ppm} : 2.91(αCH), 4.36(H-1a), 4.39(H-1b α), 3.42(H-3 α), 3.54(H-5 α), 4.27(H-6a), 4.31(H-6); ^{13}C NMR δ_{ppm} : 60.0(αCH), 66.5(C1 α), 102.0(C2 α), 70.1(C3 α), 75.6(C5 α), 66.2(C6 α).

Two-dimensional HSQCT NMR spectrum for L-prolyl-D-fructose **19a-c** is shown in Fig. 4.6.

4.2.1.4. L-Prolyl-D-ribose **20a and b**:

Solid; UV (H_2O , λ_{max}): 210 nm ($\sigma \rightarrow \sigma^*$ $\epsilon_{210} = 1820 \text{ M}^{-1}$), 280 nm ($n \rightarrow \sigma^*$ $\epsilon_{280} = 575 \text{ M}^{-1}$); IR (KBr): 3307 cm^{-1} (OH), 1621 cm^{-1} (CO), 1403 cm^{-1} (CN); $[\alpha]_{\text{D}}^{25} = -45.1^\circ$ (c 0.5, H_2O); MS (m/z) $272[\text{M}+\text{Na}]^+$; RT: 3.8 min; R_f : 0.57.

2D-HSQCT (DMSO- d_6): **3-O-ester 20a:** ^1H NMR δ_{ppm} (500.13 MHz): 3.52(αCH), 2.53(βCH_2), 1.78(γCH_2), 3.30(δCH_2), 4.20(H-1 α), 3.55(H-3 α), 3.45(H-4 α), 3.45(H-5a); ^{13}C NMR δ_{ppm} (125 MHz): 61.0(αCH), 34.5(βCH_2), 23.7(γCH_2), 54.0(δCH_2), 170.9(CO), 103.8(C1 α), 75.0(C3 α), 71.0(C4 β), 63.0(C5 α).

5-O-ester 19b: ^1H NMR δ_{ppm} : 3.62(αCH), 2.88(βCH_2), 1.90(γCH_2), 3.08(δCH_2), 3.32(H-2 α), 3.42(H-3 α), 3.45(H-4 α), 3.18(H-5a), 3.24(H-5b); ^{13}C NMR δ_{ppm} : 61.2(αCH), 35.8(βCH_2), 172.0(CO), 97.0(C1 α), 73.2(C2 α), 66.5(C3 α), 73.0(C4 α), 65.8(C5 α).

A typical UV spectrum, IR spectrum, mass spectrum and 2D-HSQCT NMR spectrum for L-prolyl-D-ribose **20a and b** are shown in Fig. 4.7, Fig. 4.8, Fig. 4.9 and Fig. 4.10 respectively.

4.2.1.6. L-Prolyl-lactose **21a and b**:

Solid; UV (H_2O , λ_{max}): 201 nm ($\sigma \rightarrow \sigma^*$ $\epsilon_{201-2239} \text{ M}^{-1}$), 278 nm ($n \rightarrow \sigma^*$ $\epsilon_{278} = 447 \text{ M}^{-1}$); IR (KBr): 3084 cm^{-1} (OH), 1609 cm^{-1} (CO), 1419 cm^{-1} (CN); $[\alpha]_{\text{D}}^{25} = -11.4^\circ$ (c 0.5, H_2O); MS (m/z) $462[\text{M}+\text{Na}]^+$; RT: 3.8 min; R_f : 0.42.

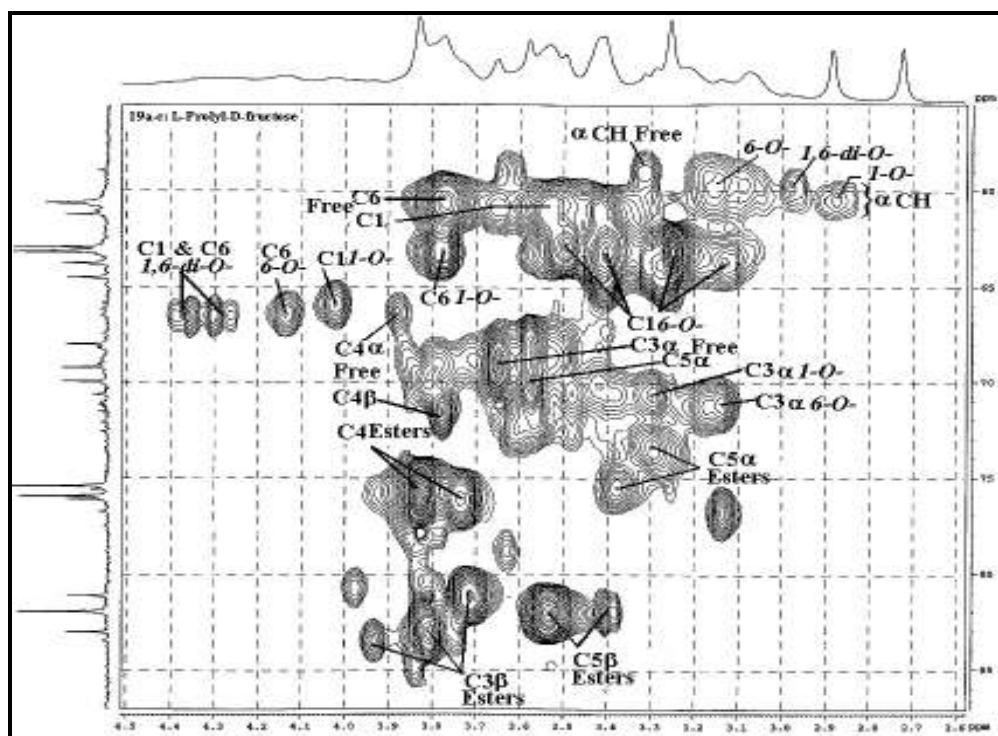


Fig. 4.6. Two-dimensional HSQC NMR spectrum for L-prolyl-D-fructose **19a-c** reaction mixture

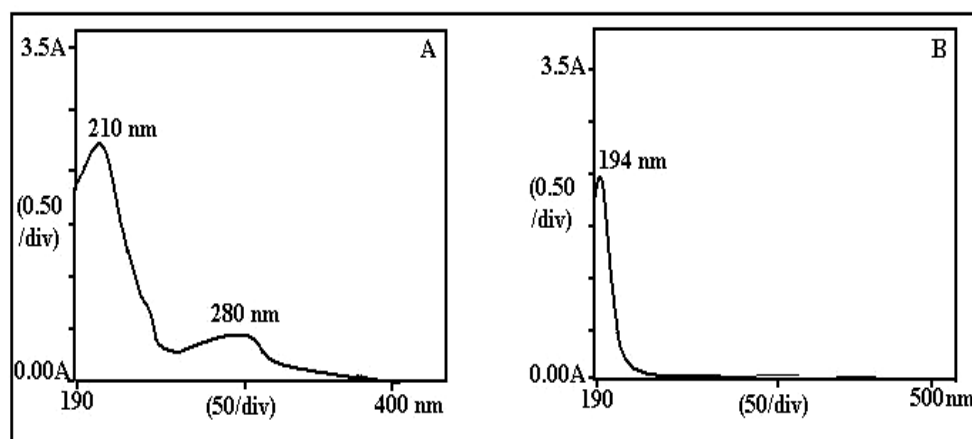


Fig. 4.7. UV spectra for L-prolyl-D-ribose of CRL catalysed reaction. (A) L-prolyl-D-ribose and (B) L-proline

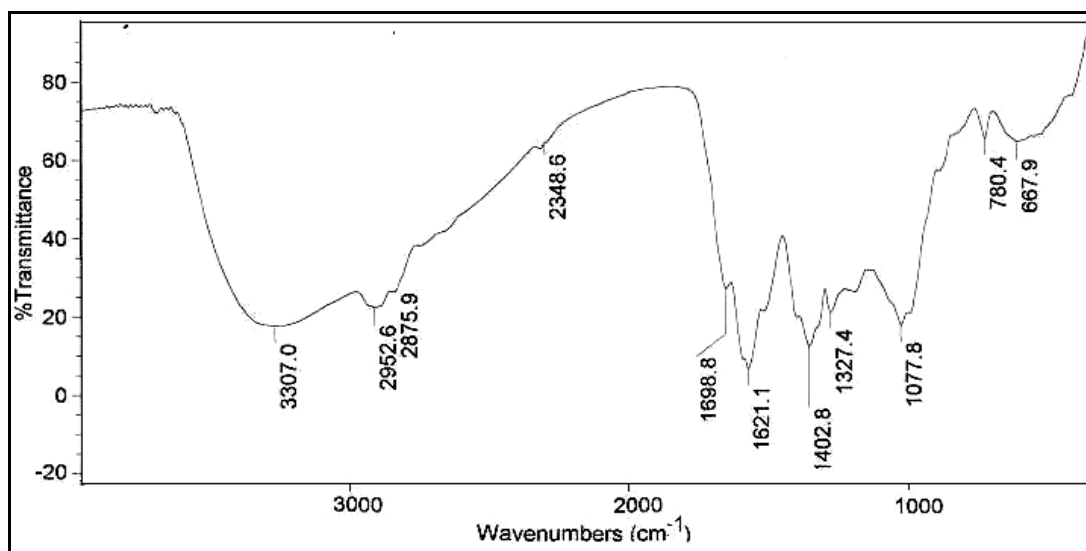


Fig. 4.8. A typical IR spectrum of L-prolyl-D-ribose of CRL catalysed reaction. A 2.0 mg of ester sample was prepared as KBr pellet.

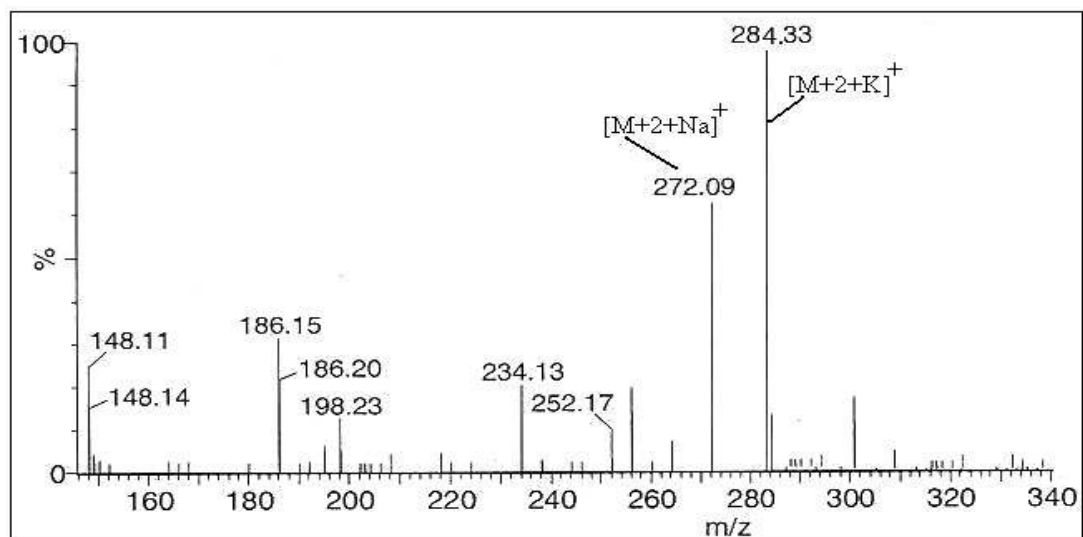


Fig. 4.9. A typical mass spectrum for L-prolyl-D-ribose.

2D-HSQCT (DMSO-d₆): **6-O-ester 21a**: ¹H NMR δ_{ppm} (500.13 MHz): 3.06(αCH), 2.72(βCH₂), 1.73 (γCH₂), 3.01(δCH₂), 4.12(H-1β), 3.29(H-2α), 3.36(H-3α), 4.10(H-4α), 3.84(H-5α), 3.76(H-5β), 3.85 (H-6a), 4.01(H-1'β), 3.24(H-2'), 3.33(H-3'), 3.41(H-4'), 3.36(H-5'), 3.44(H-6'); ¹³C NMR δ_{ppm} (125 MHz): 59.6(αCH), 30.4(βCH₂), 23.8(γCH₂), 44.5(δCH₂), 101.4(C1β), 70.6(C2α), 73.8(C3α), 81.6(C4α), 77.1(C5α), 64.8(C6), 102.9(C1'β), 70.0(C2'), 71.6(C3'), 68.2(C4'), 74.4(C5'), 60.5(C6').

6'-O-ester 21b: 2.86(αCH), 2.48(βCH₂), 3.99(H-4α), 3.78(H-5α), 3.75(H-6a), 3.27(H-2'), 3.58(H-4'), 3.38(H-5'), 3.45(H-6'); ¹³C NMR δ_{ppm} (125 MHz): 60.0(αCH), 33.2(βCH₂), 82.4(C4α), 77.3(C5α), 60.8(C6), 70.2(C2'), 68.9(C4'), 75.0(C5'), 62.8(C6').

Two-dimensional HSQCT NMR spectrum for L-prolyl-lactose **21a** and **b** is shown in Fig. 4.11.

4.2.1.7. L-Prolyl-maltose **22a-c**:

Solid; UV (H₂O, λ_{max}): 201 nm (σ→σ* ε₂₀₁ – 2399 M⁻¹), 280 nm (n→σ* ε₂₈₀ – 617 M⁻¹); IR (KBr): 3314 cm⁻¹ (OH), 1628 cm⁻¹ (CO), 1403 cm⁻¹ (CN); [α]_D²⁵ = +20.0° (c 1.9, H₂O); MS (*m/z*) 462[M+Na]⁺; RT: 3.8 min; R_f: 0.44.

2D-HSQCT (DMSO-d₆): **2-O-ester 22a**: ¹H NMR δ_{ppm} (500.13 MHz): 2.98(αCH), 2.61(βCH₂), 1.35(γCH₂), 2.60(δCH₂), 4.91(H-1β), 3.92(H-2α), 3.80(H-2β) 4.10(H-4β), 3.18(H-6a), 4.24(H-1'α), 3.61(H-4'), 3.19(H-6'); ¹³C NMR δ_{ppm} (125 MHz): 55.7(αCH), 30.9(βCH₂), 23.6(γCH₂), 45.5(δCH₂), 173.0(CO), 97.6(C1β), 77.7(C2α), 76.3(C2β), 80.8(C4β), 60.0(C6), 101.2(C1'α), 68.9(C3'), 62.7(C6').

6-O-ester 22b: ¹H NMR δ_{ppm}: 3.22(αCH), 2.88(βCH₂), 1.82(γCH₂), 3.58(δCH₂), 4.96(H-1β), 3.18(H-2β), 3.69(H-3α), 3.72(H-3β), 3.96(H-4α), 3.38(H-5α), 3.28(H-6a), 4.92(H-1'α), 3.39(H-3'), 3.73(H-4'), 3.49(H-6'); ¹³C NMR δ_{ppm}: 59.3(αCH), 35.8(βCH₂),

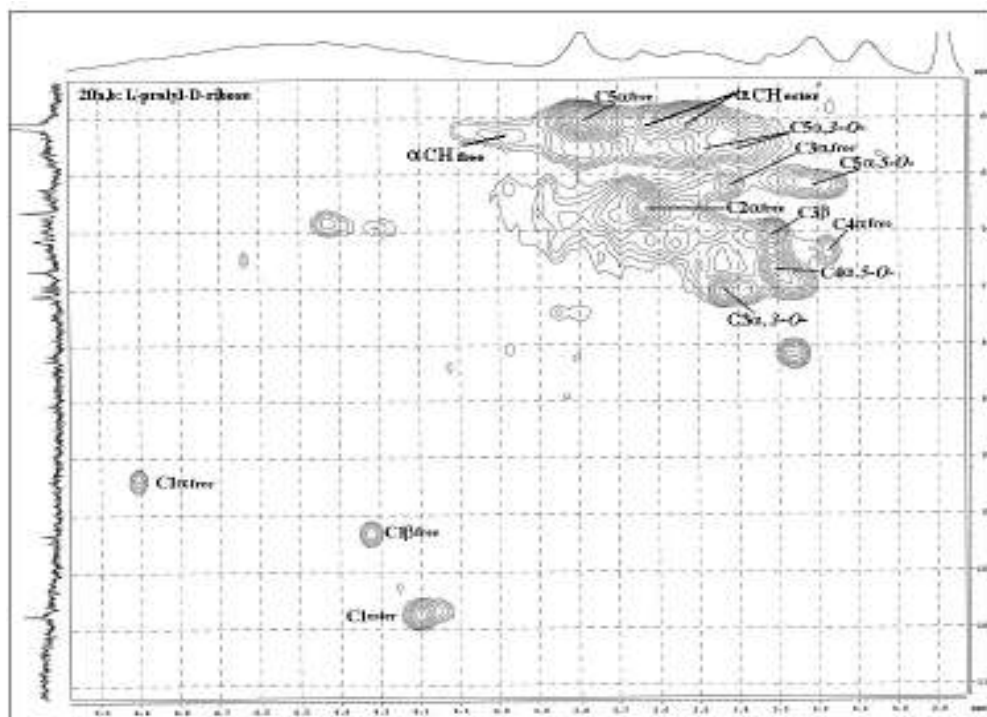


Fig. 4.10. Two-dimensional HSQCT NMR spectrum for L-prolyl-D-ribose **20a** and **b** reaction mixture

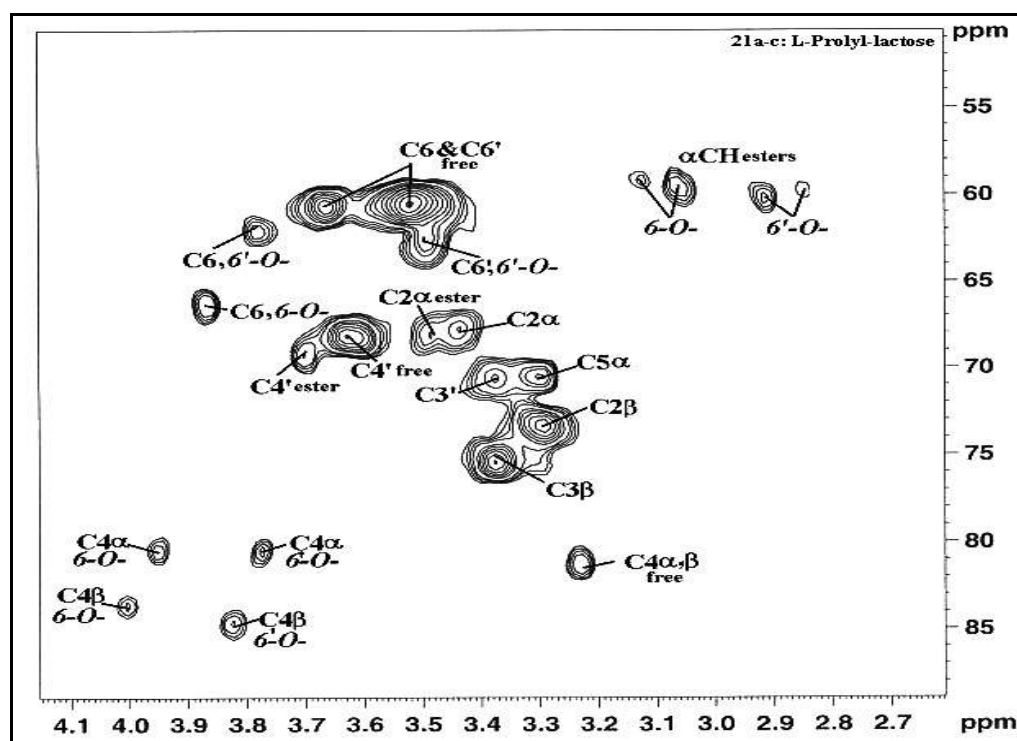


Fig. 4.11. Two-dimensional HSQCT NMR spectrum for L-prolyl-lactose **21a** and **b** reaction mixture

28.6(γ CH₂), 46.0(δ CH₂), 171.3(CO), 98.1(C1 β), 75.0(C2 β), 81.8(C3 α), 81.9(C3 β), 81.5(C4 β), 73.0(C5 β), 63.6(C6), 100.8(C1' α), 70.2(C3'), 68.7(C4'), 61.0(C6').

6'-O-ester 22c: ¹H NMR δ_{ppm} : 3.58(α CH), 2.52(β CH₂), 2.10(γ CH₂), 3.48(δ CH₂), 4.30(H-1 β), 3.08(H-2 β), 4.04(H-4 α), 3.60(H-6a), 4.15(H-1' α), 3.82(H-4'), 3.42(H-6'); ¹³C NMR δ_{ppm} : 58.3(α CH), 34.0(β CH₂), 28.3(γ CH₂), 46.0(δ CH₂), 172.6(CO), 96.8(C1 β), 70.0(C2 β), 81.0(C4 α), 61.3(C6), 102.8(C1' α), 69.2(C3'), 62.7(C6').

Figure 4.12 and Fig. 4.13 show respective mass and 2D-HSQCT NMR spectra for L-prolyl-maltose **22a-c**.

4.2.1.8. L-Prolyl-D-sorbitol **23a and b**:

Solid; UV (H₂O, λ_{max}): 214 nm ($\sigma \rightarrow \sigma^*$ $\epsilon_{214} = 1349 \text{ M}^{-1}$), 276 nm ($n \rightarrow \sigma^*$ $\epsilon_{276} = 246 \text{ M}^{-1}$); IR (KBr): 3353 cm⁻¹ (OH), 1646 cm⁻¹ (CO), 1399 cm⁻¹ (CN); $[\alpha]_{\text{D}}^{25} = -35.5^{\circ}$ (*c* 0.62, H₂O); MS (*m/z*) 304[M+2+Na]⁺; RT: 4.1 min; R_f: 0.57; 2D-HSQCT (DMSO-d₆): **1-O-ester 23a:** ¹H NMR δ_{ppm} (500.13 MHz): 3.58(α CH), 2.30(β CH₂), 1.92(γ CH₂), 3.58(δ CH₂), 3.70(H-1), 3.66(H-2), 3.55(H-3), 3.39(H-4), 3.56(H-5), 3.77(H-6); ¹³C NMR δ_{ppm} (125 MHz): 61.0(α CH), 29.8(β CH₂), 24.3(γ CH₂), 46.0(δ CH₂), 66.1(C1), 74.0(C2), 68.4(C3), 74.6(C4), 71.0(C5), 62.8(C6).

6-O-ester 23b: ¹H NMR δ_{ppm} : 3.23(α CH), 2.30(β CH₂), 1.92(γ CH₂), 3.59(δ CH₂), 3.68(H-1), 3.85(H-2), 3.66(H-3), 3.58(H-5), 3.89(H-6); ¹³C NMR δ_{ppm} : 59.4(α CH), 3.48(δ CH₂), 63.2(C1), 70.8(C3), 76.5(C5), 66.4(C6).

Figure 4.14 shows a typical IR spectrum and Fig. 4.15 shows a 2D-HSQCT NMR spectrum for L-prolyl-D-sorbitol **23a and b**.

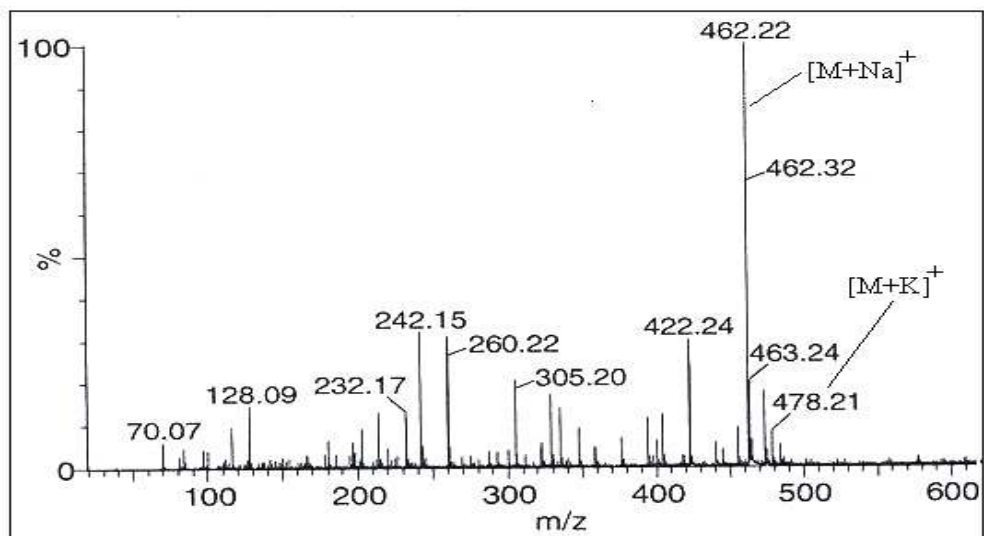


Fig. 4.12. A typical mass spectrum for L-prolyl-maltose.

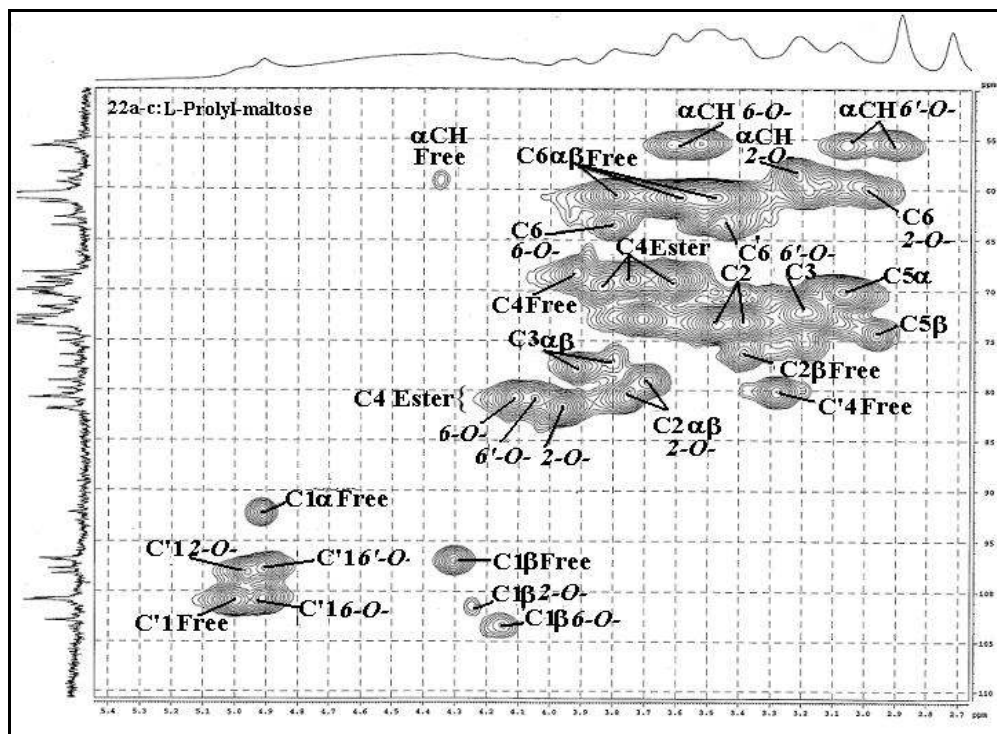


Fig. 4.13. Two-dimensional HSQCT NMR spectrum for L-prolyl-maltose **22a-c** reaction mixture

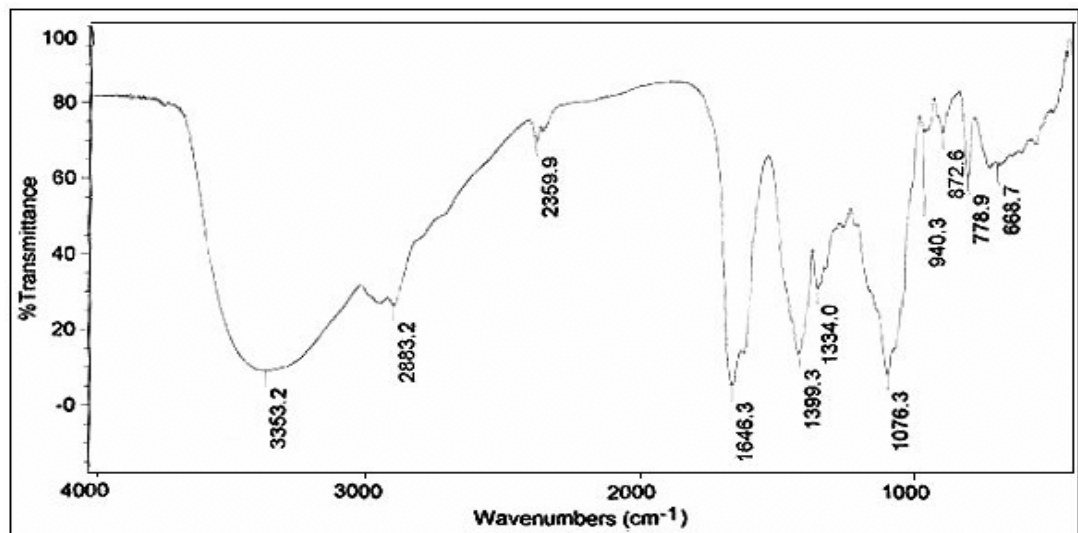


Fig. 4.14. A typical IR spectrum of L-prolyl-D-sorbitol of CRL catalysed reaction. A 2.0 mg of ester sample was prepared as KBr pellet.

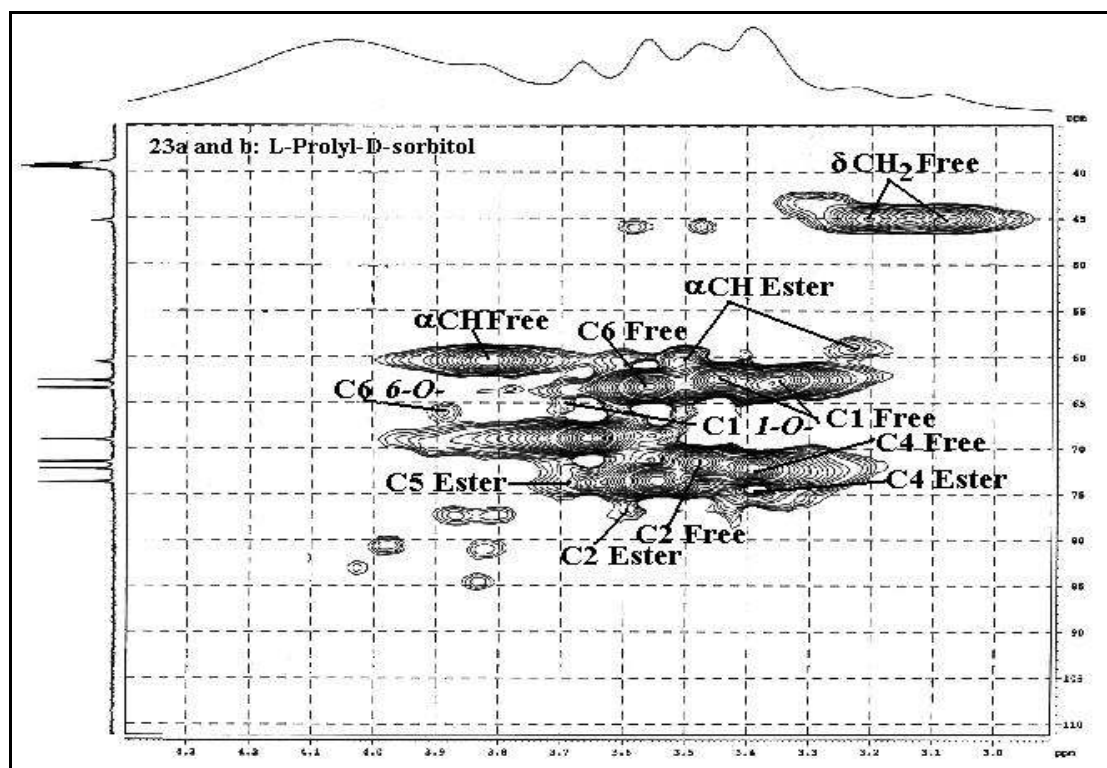
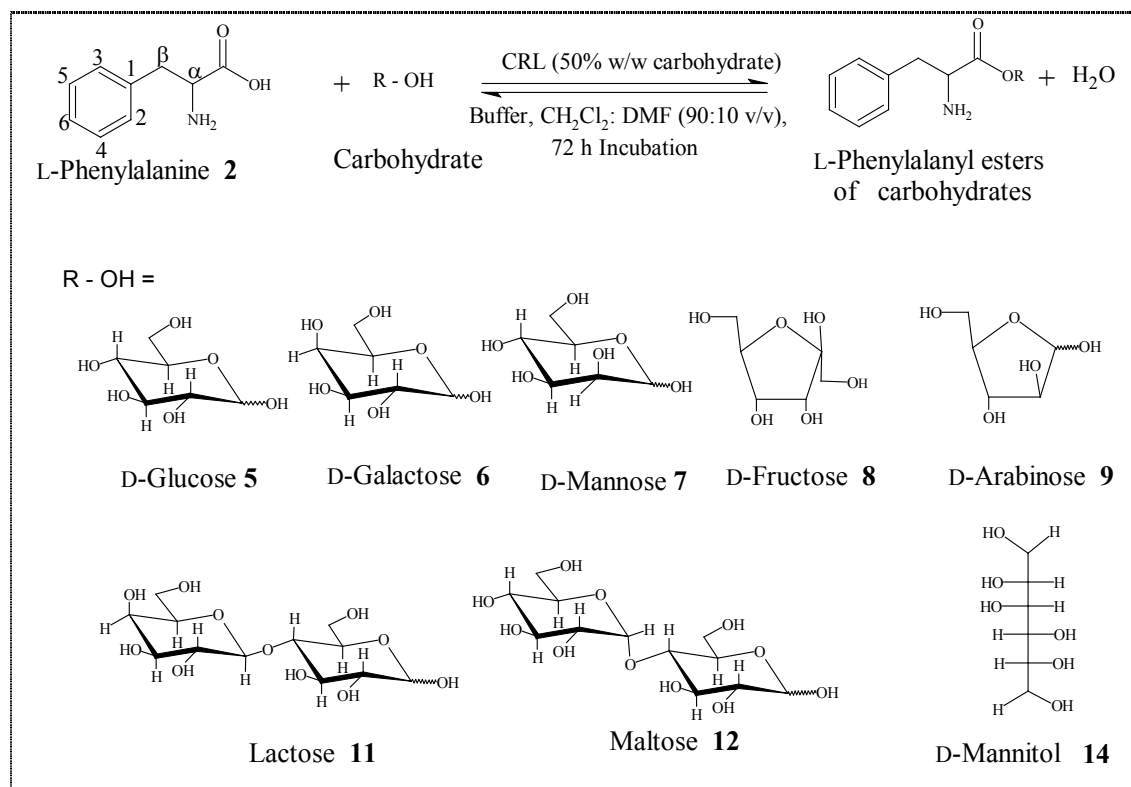


Fig. 4.15. Two-dimensional HSQCT NMR spectrum for L-prolyl-D-sorbitol 23a and b reaction mixture

4.2.2. L-Phenylalanyl esters of carbohydrates

L-Phenylalanine is one of the important, aromatic amino acid containing phenyl group as a side chain. The solubility in water is very less. Using optimum conditions, an attempt was made to prepare L-phenylalanyl esters of different carbohydrates (Scheme 4.2). The carbohydrates employed were aldohexoses (**5-7**), ketohexose (**8**), pentose (D-arabinose **9** and D-ribose **10**), disaccharides (**11-13**) and carbohydrate alcohol (**14, 15**). The reaction mixture consisting of 1 mmol L-phenylalanine, 1 mmol carbohydrate and 50% CRL (w/w of respective carbohydrate) in presence of 0.2mM (0.2 mL) pH 4.0 acetate buffer in CH₂Cl₂: DMF (90:10 v/v) was refluxed for a period of 72 h.



Scheme 4.2. CRL catalyzed syntheses of L-phenylalanyl esters of carbohydrates in anhydrous organic solvents

The HPLC retention times for L-phenylalanine and the corresponding carbohydrate esters are shown in Table 4.4. Ester formation was also monitored by TLC and spots were detected by spraying ninhydrin and 1-naphthol (for reducing sugar

detection) and the R_f values are shown in Table 4.4. The spectral data for the isolated esters were shown in Section 4.2.2.1 – 4.2.2.8. The shifts in transitions of $\sigma \rightarrow \sigma^*$ in the range 212 – 238 nm and $\pi \rightarrow \pi^*$ in the range 257 - 258 nm for the esters compared to $\sigma \rightarrow \sigma^*$ and $\pi \rightarrow \pi^*$ at 210 nm and 254 nm respectively for free L-phenylalanine indicated that L-phenylalanine had undergone esterification. Infra Red spectral data showed that the ester carbonyl stretching frequency for the prepared esters were in the range 1632 – 1771 cm^{-1} compared to 1628 cm^{-1} observed for free L-phenylalanine indicating that L-phenylalanine carboxylic group had been converted into its corresponding carbohydrate ester. Molecular ion peaks in mass spectrum further confirmed the formation of esters.

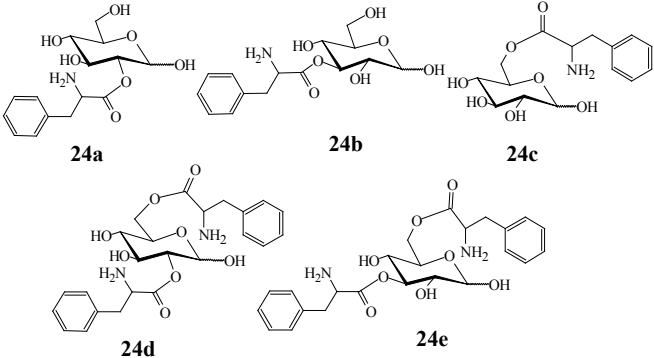
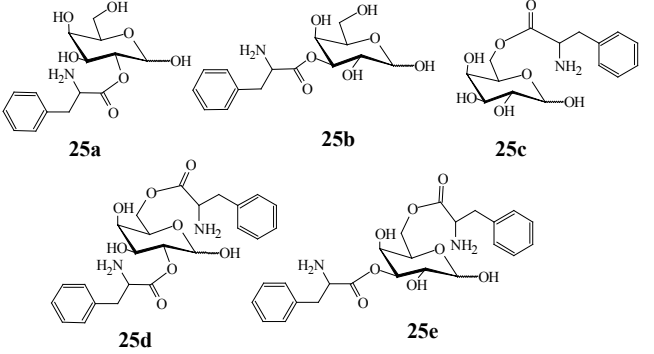
Table 4.4 Retention times and R_f values of L-phenylalanyl esters of carbohydrates

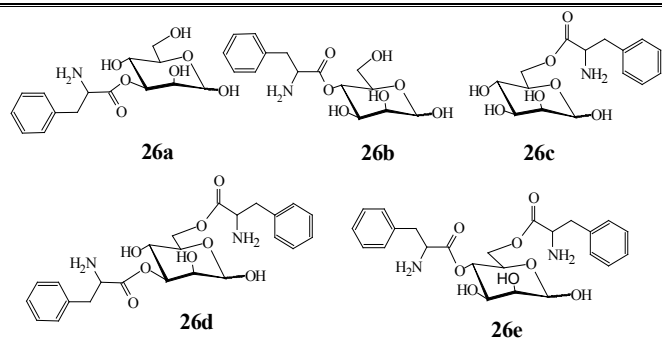
Compound	Retention time (min) ^a	R_f values ^b
L-Phenylalanine	2.2	0.58
L-Phenylalanyl-D-glucose	2.9 & 3.1 ^c	0.42
L-Phenylalanyl-D-galactose	3.3 & 3.8 ^c	0.44
L-Phenylalanyl-D-mannose	3.0 & 3.5 ^c	0.39
L-Phenylalanyl-D-fructose	3.4 & 4.1 ^c	0.45
L-Phenylalanyl-D-arabinose	4.6	0.47
L-Phenylalanyl-lactose	3.1	0.31
L-Phenylalanyl-maltose	4.5	0.36
L-Phenylalanyl-D-mannitol	2.9	0.52

^a Conditions: column – C18; mobile phase – acetonitrile : water (20:80 v/v); flow rate – 1mL /min; detector – UV at 254 nm; ^b A 20 x 20 cm silica plate (mesh size 60 –120); mobile phase – butanol : acetic acid : water (70:20:10 v/v/v); peak identification – ninhydrin (amine); 1-naphthol (sugar); ^c In case of few esters two ester peaks were detected.

Two-dimensional HSQCT NMR spectroscopy of the L-phenylalanyl esters of carbohydrates prepared by using CRL gave good information on the nature and proportion of esters formed. Table 4.5 shows the ester yields from HPLC, percentage proportions of individual esters determined from the peak areas of the ^{13}C C6 or C5 (in case of D-arabinose) signals or cross peaks from 2D-NMR. It was also confirmed from NMR that out of eleven carbohydrates employed for the reaction, eight were converted into esters with L-phenylalanine (D-glucose **5**, D-galactose **6**, D-mannose **7**, D-fructose **8**, D-arabinose **9**, lactose **11**, maltose **12** and D-mannitol **14**) and very less esterification (>5%) was observed with D-ribose **10**, sucrose **13** and D-sorbitol **15**.

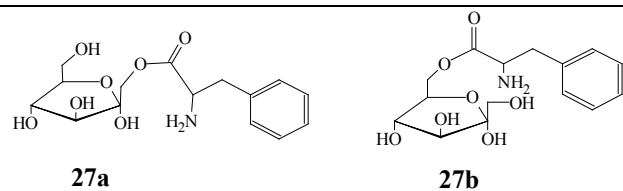
Table. 4.5 Syntheses of L-phenylalanyl esters of carbohydrates ^a

L-Phenylalanyl esters of carbohydrates	Esterification yield (%)	Esters (% proportions ^b)
 <p>24a 24b 24c</p> <p>24d 24e</p>	<p>79 (mono esters-53, diester-26)</p>	<p>24a: 2-<i>O</i>-L-phenylalanyl -D-glucose (19) 24b: 3-<i>O</i>-L-phenylalanyl -D-glucose (23) 24c: 6-<i>O</i>-L-phenylalanyl -D-glucose (25) 24d: 2,6-di-<i>O</i>-L-phenylalanyl-D-glucose(17) 24e: 3,6-di-<i>O</i>-L-phenylalanyl-D-glucose (16)</p>
 <p>25a 25b 25c</p> <p>25d 25e</p>	<p>45 (monoesters-33, diester-12)</p>	<p>25a: 2-<i>O</i>-L-phenylalanyl-D-galactose (19) 25b: 3-<i>O</i>-L-phenylalanyl-D-galactose (20) 25c: 6-<i>O</i>-L-phenylalanyl-D-galactose (32) 25d: 2,6-di-<i>O</i>-L-phenylalanyl-D-galactose (16) 25e: 3,6-di-<i>O</i>-L-phenylalanyl-D-galactose (13)</p>



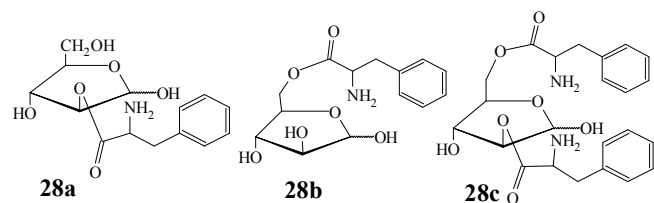
62
(mono esters-47,
diester-15)

26a: 3-*O*-L-phenylalanyl-D-mannose (19)
26b: 4-*O*-L-phenylalanyl-D-mannose (19)
26c: 6-*O*-L-phenylalanyl-D-mannose (38)
26d: 3,6-*di-O*-L-phenylalanyl-D-mannose (12)
26e: 4,6-*di-O*-L-phenylalanyl-D-mannose (12)



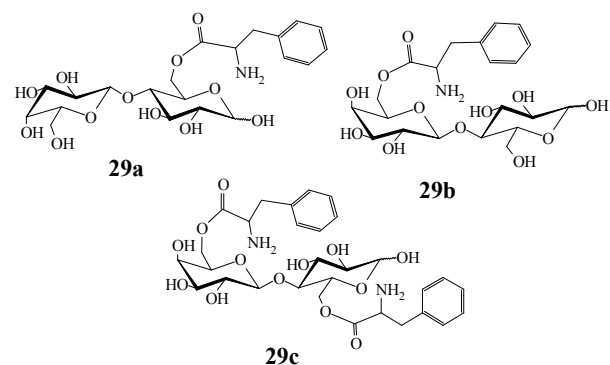
50
(only mono esters)

27a: 1-*O*-L-phenylalanyl-D-fructose (72)
27b: 6-*O*-L-phenylalanyl-D-fructose (28)



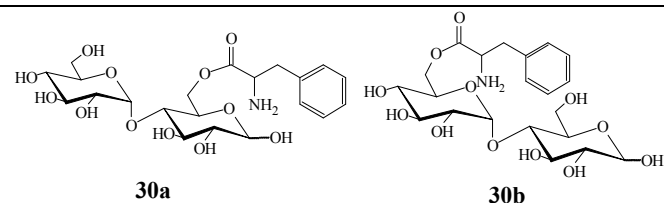
64
(mono esters-51,
diester-13)

28a: 2-*O*-L-phenylalanyl-D-arabinose (35)
28b: 5-*O*-L-phenylalanyl-D-arabinose (44)
28c: 2,5-*di-O*-L-phenylalanyl-D-arabinose (21)



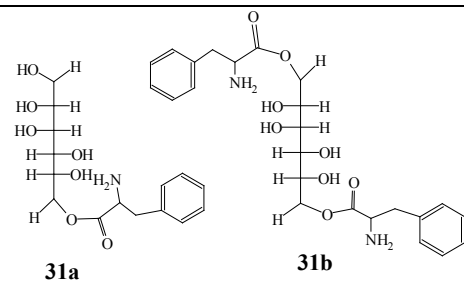
61
(mono esters-46,
diester-15)

29a: 6-*O*-L-phenylalanyl-lactose (42)
29b: 6'-*O*-L-phenylalanyl-lactose (34)
29c: 6,6'-*di-O*-L-phenylalanyl-lactose (24)



60
(only mono esters)

30a: 6-*O*-L-phenylalanyl-maltose (59)
30b: 6'-*O*-L-phenylalanyl-maltose(41)



43
(mono esters-29,
diester-16)

31a: 1-*O*-L-phenylalanyl -D-mannitol (62)
31b: 1,6-*di-O*-L-phenylalanyl-D-mannitol (38)

^a L-Phenylalanine – 1 mmol; carbohydrates – 1 mmol; CRL – 50% (w/w based on carbohydrate); buffer – 0.2 mM (0.2 mL of 0.1M) pH 4.0 acetate buffer; CH₂Cl₂: DMF (v/v 90: 10) at 40°C; Incubation period – 72 h; Conversion yields were from HPLC with respect to L-Phenylalanine concentration; ^b Percentage proportions of individual esters determined from the peak areas of the ¹³C C6, C5 (in case of pentoses) signals or from cross peaks of the 2D HSQC spectrum.

Spectral data for L-phenylalanine 2: Solid; mp- 174 °C; UV (H₂O, λ_{\max}): 210 nm ($\sigma \rightarrow \sigma^*$ $\epsilon_{210} - 240 \text{ M}^{-1}$), 254 nm ($\pi \rightarrow \pi^*$ $\epsilon_{254} - 120 \text{ M}^{-1}$); IR (KBr): 3418 cm⁻¹ (OH), 1628 cm⁻¹ (CO), 1515 cm⁻¹ (aromatic, -C=C-); $[\alpha]_{\text{D}}^{25} = -28.9^{\circ}$ (c 0.6 H₂O); 2D-HSQCT (DMSO-d₆): ¹H NMR δ_{ppm} (500.13 MHz): 4.01(α CH, J= 8.3, 4.8 Hz), 3.38(β CH_{2a}, J=6.8, 3.4 Hz), 3.18(β CH_{2b}, J=6.8, 3.4 Hz), Aromatic- 7.43(H₂, H₆), 7.52(H₃, H₅), 7.40(H₄); ¹³C NMR δ_{ppm} : 56.0(α CH), 37.0(β CH₂) Aromatic- 137.0(C₁), 129.3(C₂, C₆), 129.9(C₃, C₅), 129.4(C₄), 174.6(CO).

4.2.2.1. L-Phenylalanyl-D-glucose 24a-c:

Solid; UV (H₂O, λ_{\max}): 237 nm ($\sigma \rightarrow \sigma^*$ $\epsilon_{237} - 1318 \text{ M}^{-1}$), 257 nm ($\pi \rightarrow \pi^*$ $\epsilon_{257} - 1259 \text{ M}^{-1}$); 308 nm ($n \rightarrow \pi^*$ $\epsilon_{308} - 617 \text{ M}^{-1}$); IR (KBr): 3379 cm⁻¹ (OH), 1761 cm⁻¹ (CO), 1603 cm⁻¹ (aromatic, -C=C-); RT: 2.9 and 3.1 min; R_f: 0.42; $[\alpha]_{\text{D}}^{25} = -24.2^{\circ}$ (c 0.33 H₂O); MS (*m/z*) 350[M+Na]⁺.

2D-HSQCT (DMSO-d₆): **2-O-ester 24a:** ¹H NMR δ_{ppm} (500.13 MHz): 2.92(α CH), 2.51(β CH₂), 4.6(H-1 α), 3.79(H-2 α), 3.80(H-2 β), 3.4(H-6a); ¹³C NMR δ_{ppm} (125 MHz): 52.0(α CH), 35.8(β CH₂), Aromatic- 136.5(C₁), 96.3(C1 α), 172.0 (CO), 75.1(C2 α), 77.3(C2 β), 62.0(C6 α).

3-O-ester 24b: ¹H NMR δ_{ppm} : 3.01(α CH), 3.11(β CH_{2a}), 2.96(β CH_{2b}), 4.4(H-1 α), 3.61(H-2 α), 3.66(H-2 β), 3.82(H-3 α), 3.91(H-3 β), 3.40(H-6a); ¹³C NMR δ_{ppm} : 53.0(α CH), 36.8(β CH₂), Aromatic-136.4(C₁), 173.2 (CO), 97.3(C1 α), 83.4(C3 α), 83.9(C3 β), 61.9(C6 α).

6-O-ester 24c: ¹H NMR δ_{ppm} : 3.07(α CH), 3.18(β CH_{2a}), 3.06(β CH_{2b}), Aromatic- 7.18(H₂, H₆), 7.26(H₃, H₅), 7.16(H₄), 3.16(H-5 α), 3.78(H-6a), 3.66(H-6b); ¹³C NMR δ_{ppm} : 54.2(α CH), 36.7(β CH₂) Aromatic- 136.3(C₁), 128.9(C₂, C₆), 130.7(C₃, C₅), 130.3(C₄), 174.0(CO), 102.2(C1 α), 70.5(C5 α), 65.0(C6 α).

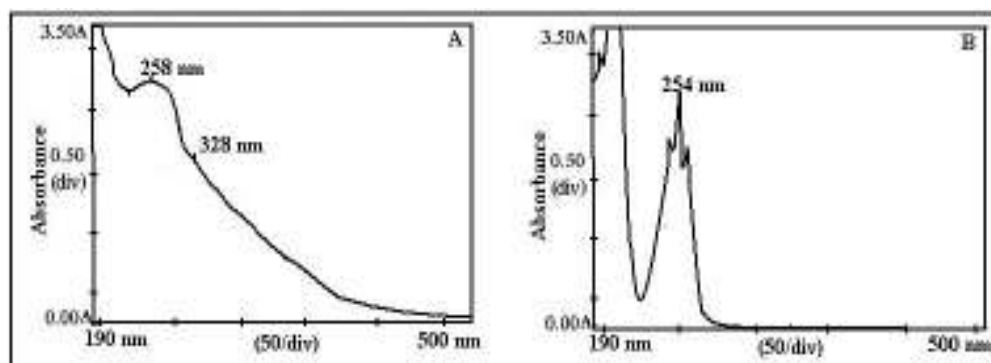


Fig. 4.16. UV spectra for (A) L-phenylalanyl-D-glucose, CRL catalysed reaction (B) L-phenylalanine; concentration – 2.6 mM.

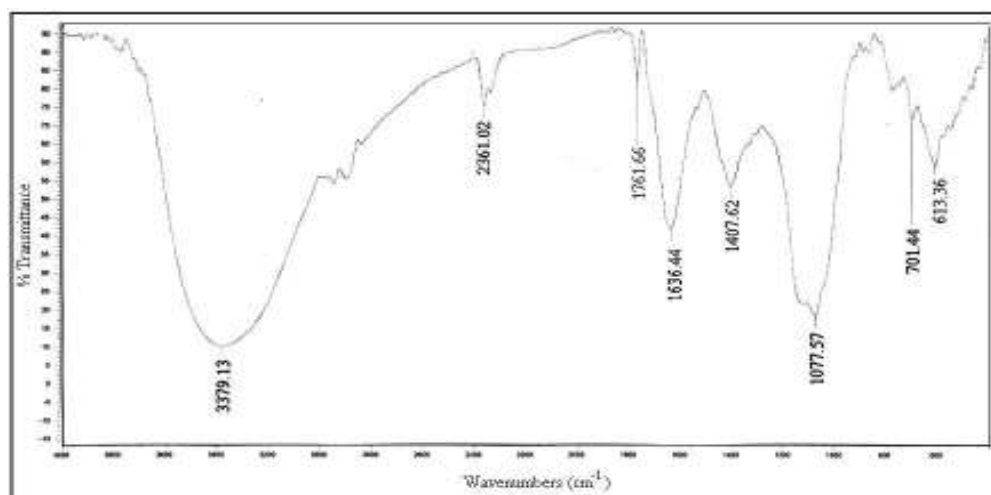


Fig. 4.17. A typical IR spectrum of L-phenylalanyl-D-glucose of CRL catalysed reaction. A 2.5 mg of ester sample was prepared as KBr pellet.

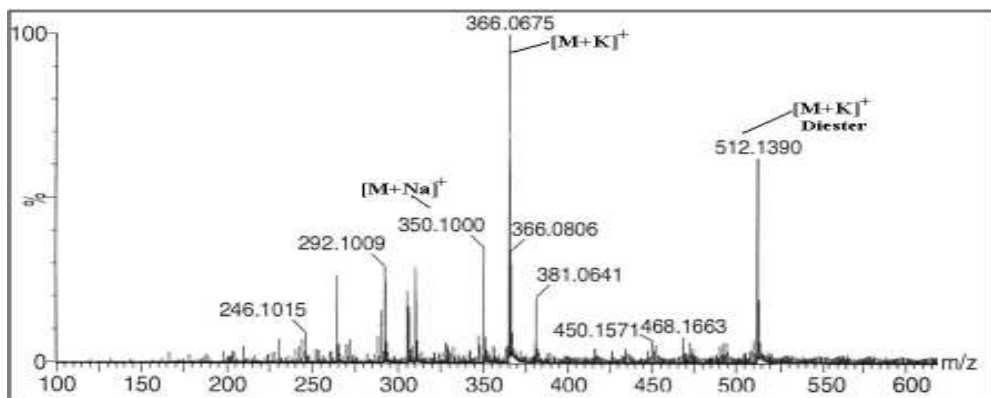


Fig. 4.18. A typical mass spectrum of L-phenylalanyl-D-glucose.

2,6-di-O- ester 24d: ^1H NMR δ_{ppm} : 3.67(H-2 α), 3.51(H-6 α), 3.61(H-6 α); ^{13}C NMR δ_{ppm} : 171.8 (CO), 77.0(C2 α), 79.0(C2 β), 62.1(C6 β).

3,6-di-O- ester 24e: ^1H NMR δ_{ppm} : 3.61(H-3 α), 3.66(H-3 β), 3.5(H-6 α); ^{13}C NMR δ_{ppm} : 172.2 (CO), 82.3(C3 α), 83.4(C3 β), 64.8(C6 α).

A Typical UV, IR, mass and 2D-HSQCT NMR spectra for L-phenylalanyl-D-glucose **24a-e** are shown in Fig. 4.16, Fig. 4.17, Fig. 4.18 and Fig. 4.19 respectively.

4.2.2.2. L-Phenylalanyl-D-galactose 25a-e:

Solid; UV (H_2O , λ_{max}): 222 nm ($\sigma \rightarrow \sigma^*$ $\epsilon_{222} - 871 \text{ M}^{-1}$), 257.5 nm ($\pi \rightarrow \pi^*$ $\epsilon_{257.5} - 437 \text{ M}^{-1}$); 299 nm ($n \rightarrow \pi^*$ $\epsilon_{299} - 331 \text{ M}^{-1}$); IR (KBr): 3186 cm^{-1} (OH), 1722 cm^{-1} (CO), 1636 cm^{-1} (aromatic, $-\text{C}=\text{C}-$); $[\alpha]_{\text{D}}^{25} = +31.1^{\circ}$ (c 0.45 H_2O); MS (m/z) diester - 512[M+K] $^{+}$;

^{13}C NMR δ_{ppm} (125 MHz, DMSO-d_6): **2-O- ester 25a:** 55.7(αCH), 36.7(βCH_2) Aromatic- 136.5(C $_1$), 127.4(C $_2$, C $_6$), 129.6(C $_3$, C $_5$), 129.1(C $_4$), 171.4(CO), 96.2(C1 α) 76.3(C2 α), 75.1(C2 β), 60.8(C6 α).

3-O- ester 25b: ^{13}C NMR δ_{ppm} : 97.2(C1 α), 82.4(C3 α), 81.5(C3 β), 61.0(C6 α).

6-O- ester 25c: ^{13}C NMR δ_{ppm} : 96.2(C1 α), 100.2 (C1 β), 70.6(C2 α), 75.2(C2 β), 72.2(C3 α), 73.1(C4 α), 63.0(C6 α).

2,6-di-O- ester 25d: ^{13}C NMR δ_{ppm} : 78.2 (C2 α), 77.7(C2 β), 63.1(C6 α).

3,6-di-O- ester 25e: ^{13}C NMR δ_{ppm} : 81.8(C3 α), 62.7 (C6 α).

Figure 4.20 shows a ^{13}C NMR spectrum for L-phenylalanyl-D-galactose **25a-e**.

4.2.2.3. L-Phenylalanyl-D-mannose 26a-e:

Solid; UV (H_2O , λ_{max}): 212 nm ($\sigma \rightarrow \sigma^*$ $\epsilon_{212} - 4786 \text{ M}^{-1}$), 257.5 nm ($\pi \rightarrow \pi^*$ $\epsilon_{257.5} - 1259 \text{ M}^{-1}$); 299 nm ($n \rightarrow \pi^*$ $\epsilon_{299} - 407 \text{ M}^{-1}$); IR (KBr): 3265 cm^{-1} (OH), 1699 cm^{-1} (CO),

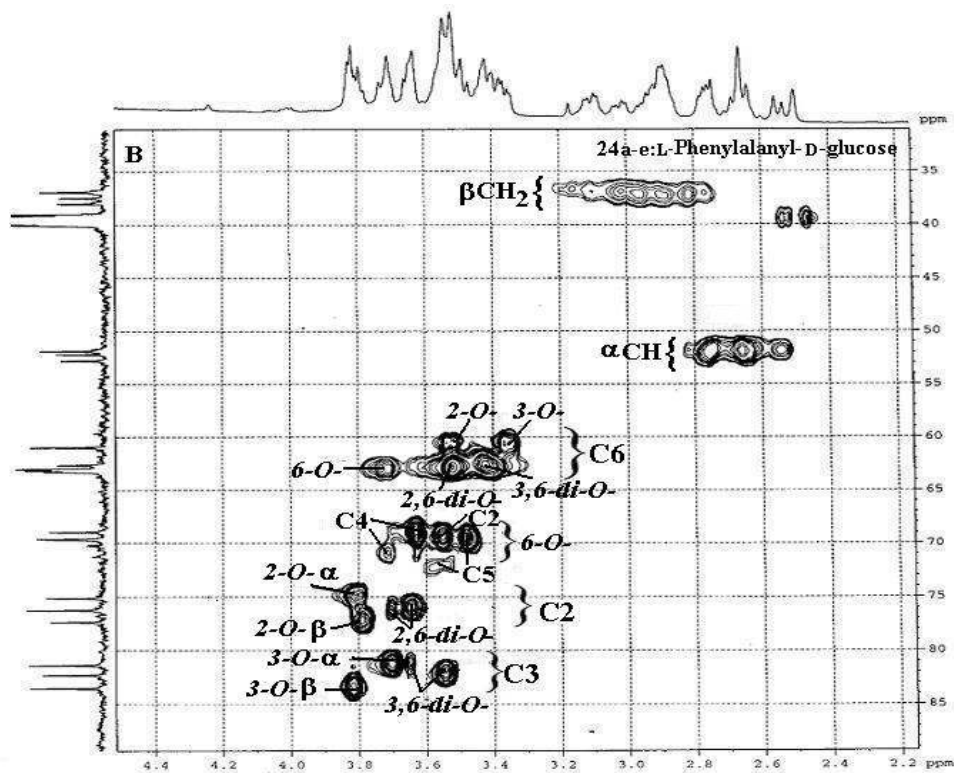
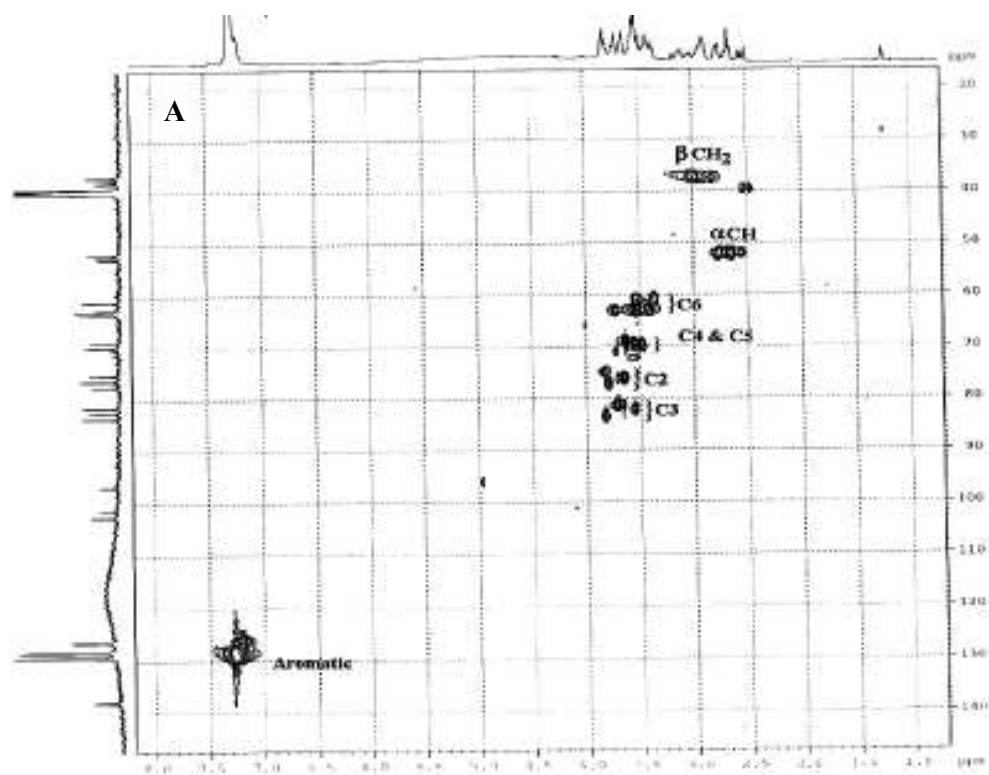


Fig. 4.19. Two-dimensional HSQCT NMR for L-phenylalanyl-D-glucose **24a-e** catalysed by RML. Isolated through HPLC using aminopropyl column eluted with acetonitrile: water (80:20 v/v). (A) Full spectrum (B) Expanded spectrum

1636 cm^{-1} (aromatic, $-\text{C}=\text{C}-$); $[\alpha]_{\text{D}}^{25} = +14.7^{\circ}$ (c 0.45 H_2O); MS (m/z) 350 $[\text{M}+\text{Na}]^+$; ^{13}C NMR δ_{ppm} (125 MHz, DMSO-d_6): **2-O-ester 26a**: 53.2(αCH), 38.4(βCH_2), Aromatic- 138.4(C_1), 101.6($\text{C1}\alpha$), 77.8($\text{C2}\alpha$), 75.6($\text{C2}\beta$) 60.8($\text{C6}\alpha$).

3-O-ester 26b: ^{13}C NMR δ_{ppm} : 52.6(αCH), 37.9(βCH_2), Aromatic- 138.1(C_1), 102.9($\text{C1}\alpha$), 84.0($\text{C3}\alpha$), 82.7($\text{C3}\beta$), 61.4($\text{C6}\alpha$).

6-O-ester 26c: ^{13}C NMR δ_{ppm} : 52.3(αCH), 37.4(βCH_2) Aromatic- 137.5(C_1), 126.9(C_2 , C_6), 129.8(C_3 , C_5), 128.6(C_4), 174.6(CO), 97.2($\text{C1}\alpha$), 76.7($\text{C2}\alpha$), 75.6($\text{C3}\alpha$), 70.1($\text{C4}\alpha$), 69.3($\text{C4}\beta$), 77.8($\text{C5}\beta$), 63.7($\text{C6}\alpha$).

2,6-di-O- ester 26d: ^{13}C NMR δ_{ppm} : Aromatic- 138.4(C_1), 76.3($\text{C2}\alpha$), 63.2($\text{C6}\alpha$).

3,6-di-O- ester 26e: ^{13}C NMR δ_{ppm} : 82.7($\text{C3}\alpha$), 63.5($\text{C6}\alpha$).

^{13}C NMR spectrum for L-phenylalanyl-D-mannose **26a-e** is shown in Fig. 4.21.

4.2.2.4. L-Phenylalanyl-D-fructose **27a** and **b**:

Solid; UV (H_2O , λ_{max}): 198 nm ($\sigma \rightarrow \sigma^*$ $\epsilon_{198} = 4467 \text{ M}^{-1}$), 257.5 nm ($\pi \rightarrow \pi^*$ $\epsilon_{257.5} = 776 \text{ M}^{-1}$); IR (KBr): 3380 cm^{-1} (OH), 1761 cm^{-1} (CO), 1636 cm^{-1} (aromatic, $-\text{C}=\text{C}-$); $[\alpha]_{\text{D}}^{25} = -14.3^{\circ}$ (c 0.45 H_2O); MS (m/z) 365 $[\text{M}-1+\text{K}]^+$; RT: 4.1 min; R_f : 0.45;

^{13}C NMR δ_{ppm} (125 MHz, DMSO-d_6): **1-O-ester 27a**: 55.1(αCH), 35.9(βCH_2), Aromatic- 138.4(C_1), 64.9($\text{C1}\alpha$), 102.4($\text{C2}\beta$), 76.2($\text{C4}\beta$), 69.6($\text{C5}\beta$), 63.9 ($\text{C6}\alpha$).

6-O-ester 27b: ^{13}C NMR δ_{ppm} : 55.2(αCH), 36.6(βCH_2), 63.4($\text{C1}\alpha$), 98.1($\text{C2}\beta$), 75.8($\text{C4}\beta$), 81.4($\text{C5}\beta$), 64.2($\text{C6}\beta$).

Figures 4.22 and 4.23 are spectra of IR and ^{13}C NMR for L-phenylalanyl-D-fructose **27a** and **b** respectively.

4.2.2.5. L-Phenylalanyl-D-arabinose **28a-c**:

Solid; UV (H_2O , λ_{max}): 215 nm ($\sigma \rightarrow \sigma^*$ $\epsilon_{215} = 2754 \text{ M}^{-1}$), 257.5 nm ($\pi \rightarrow \pi^*$ $\epsilon_{257.5}$

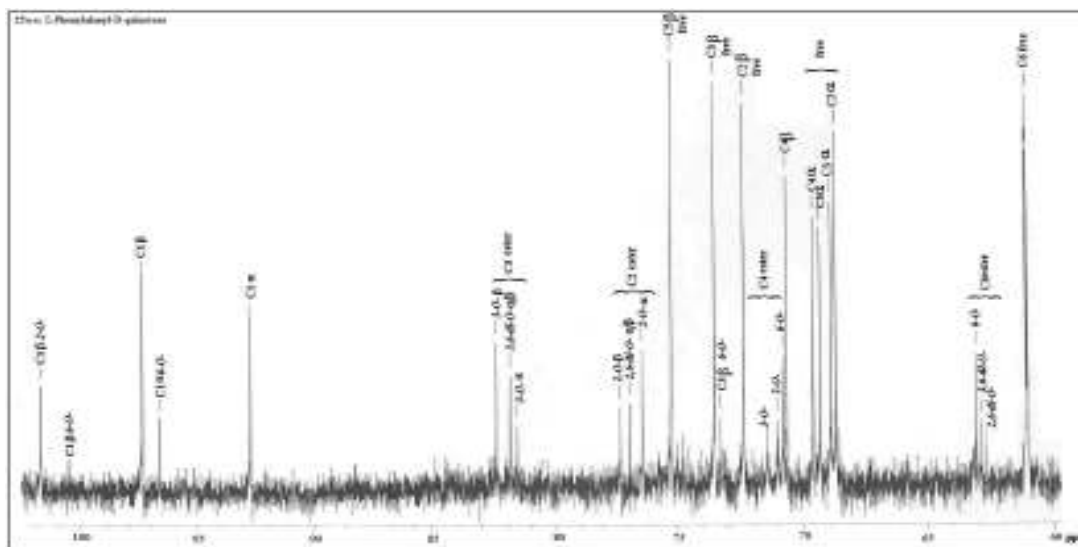


Fig. 4.20. ^{13}C NMR spectrum of CRL catalysed L-phenylalanyl-D-galactose **25a-e**

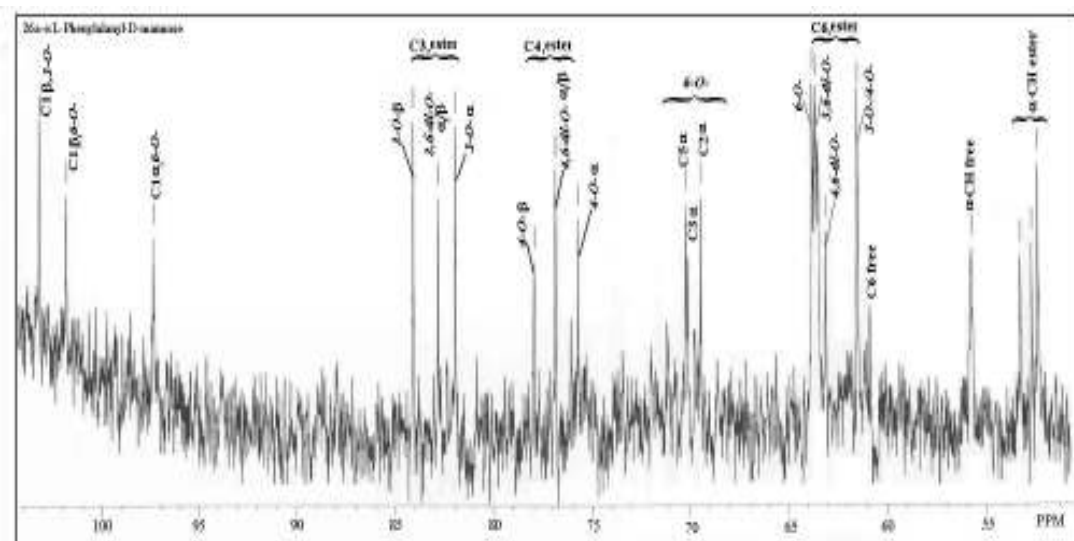


Fig. 4.21. ^{13}C NMR spectrum of CRL catalysed L-phenylalanyl-D-mannose **26a-e**.

– 891 M^{-1}); IR (KBr): 3352 cm^{-1} (OH), 1771 cm^{-1} (CO), 1624 cm^{-1} (aromatic, $-C=C-$); $[\alpha]_D^{25} = +12.0^\circ$ (c 1.0 H_2O); MS (m/z) 321[M+Na]⁺.

2D-HSQCT (DMSO- d_6): **2-O-ester 28a**: 1H NMR δ_{ppm} (500.13 MHz): 3.72(αCH), 2.70(βCH_{2a}), 2.85(βCH_{2b}), 7.40-7.10(Aromatic), 4.75(H-1 α), 4.25(H-1 β), 3.34(H-2 α), 3.33(H-2 β), 3.85(H-3 α), 3.28(H-4 α), 3.54(H-5a); ^{13}C NMR δ_{ppm} (125 MHz): 55.0(αCH), 31.3(βCH_2), 171.9(CO), Aromatic- 137.2(C₁), 128.1(C₂, C₆), 128.9(C₃, C₅), 129.1(C₄), 98.5(C1 α), 104.0(C1 β), 71.0(C2 α), 73.2(C2 β), 71.5(C3 α), 60.2(C5 α).

5-O-ester 28b: 1H NMR δ_{ppm} : 3.64(αCH), 2.95(βCH_{2a}), 3.25(βCH_{2b}), 4.92(H-1 α), 3.73(H-2 α), 3.66(H-2 β), 3.91(H-3 α), 3.35(H-4 α), 3.43(H-5a); ^{13}C NMR δ_{ppm} : 57.3(αCH), 36.2(βCH_2), 172.8(CO), Aromatic 137.4(C₁), 128.2(C₂, C₆), 131.1(C₃, C₅), 129.3(C₄), 93.0(C1 α), 69.2(C2 α), 70.2(C2 β), 67.2(C3 α), 64.2(C4 α), 63.3(C5 α).

2,5-di-O-ester 28c: 1H NMR δ_{ppm} : 3.74(αCH), 2.72(βCH_{2a}), 2.80(βCH_{2b}), 4.75(H-1 α), 4.25(H-1 β), 3.46(H-2 α), 3.40(H-2 β), 3.94(H-3 α), 3.51(H-5a); ^{13}C NMR δ_{ppm} : 57.0(αCH), 35.5(βCH_2), 170.2(CO), Aromatic 136.7(C₁), 98.5(C1 α), 75.4(C2 α), 75.2(C2 β), 63.1(C5 α).

Two-dimensional HSQCT NMR spectrum for L-phenylalanyl-D-arabinose **28a-c** is shown in Fig. 4.24.

4.2.2.6. L-Phenylalanyl-lactose **29a-c**:

Solid; UV (H_2O , λ_{max}): 214 nm ($\sigma \rightarrow \sigma^*$ $\epsilon_{214} = 6025 M^{-1}$), 257.5 nm ($\pi \rightarrow \pi^*$ $\epsilon_{257.5} = 562 M^{-1}$), 290 nm ($n \rightarrow \pi^*$ $\epsilon_{290} = 302 M^{-1}$); IR (KBr): 3378 cm^{-1} (OH), 1632 cm^{-1} (CO), 1556 cm^{-1} (aromatic, $-C=C-$); $[\alpha]_D^{25} = +31.3^\circ$ (c 0.16 H_2O); MS (m/z) 512[M+Na]⁺.

2D-HSQCT (DMSO- d_6): **6-O-ester 29a**: 1H NMR δ_{ppm} (500.13 MHz): 2.67(αCH), 2.89(βCH_2), Aromatic- 7.25(H₂, H₆), 7.28(H₃, H₅), 7.2(H₄), 4.32(H-1 α), 4.23(H-1 β), 3.36(H-2 α), 3.49(H-2 β), 3.32(H-3 α), 3.80(H-3 β), 3.56(H-4 α), 3.72(H-4 β), 3.90(H-5 α),

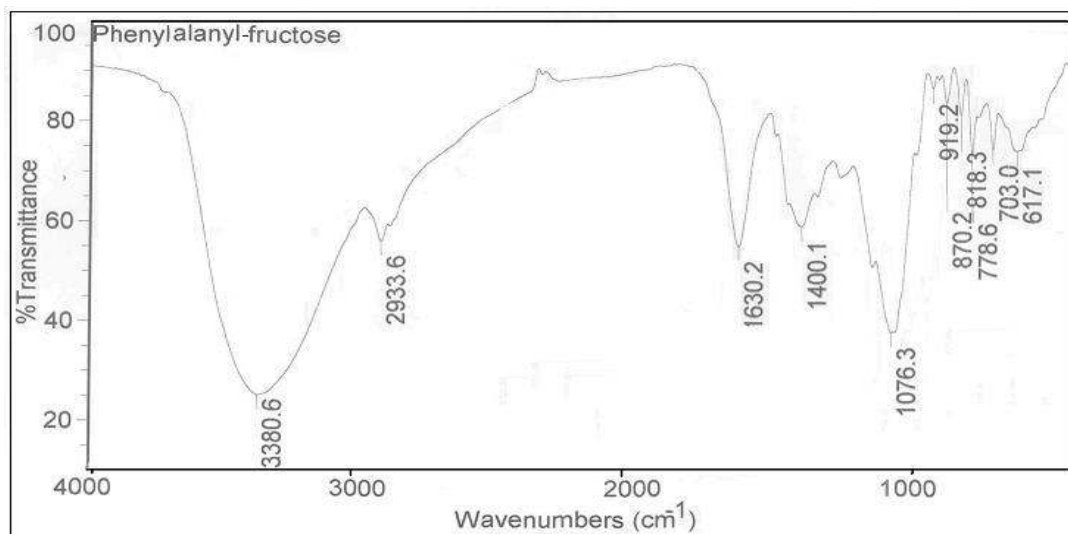


Fig. 4.22. A typical IR spectrum of L-phenylalanyl-D-fructose of CRL catalysed reaction. A 2.5 mg of ester sample was prepared as KBr pellet.

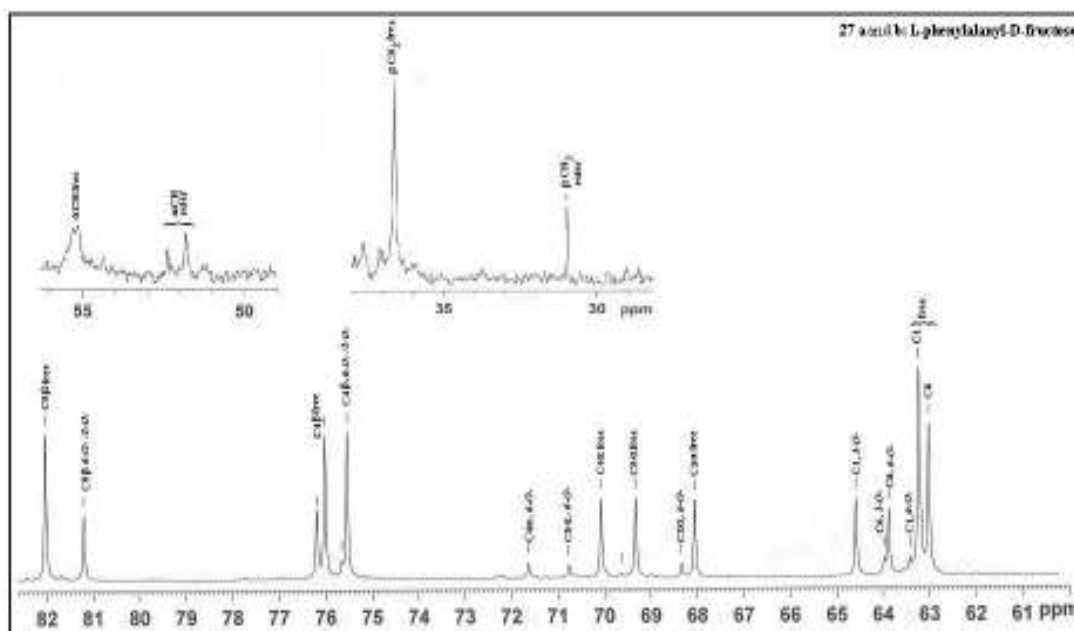


Fig. 4.23. ^{13}C NMR spectrum of CRL catalysed L-phenylalanyl-D-fructose **27a** and **b**. Inset –expanded portion for α -CH and β -CH₂ region.

3.47(H-6a), 4.16(H-1'β), 3.14(H-2'), 3.42(H-3'), 3.62(H-4'), 3.39(H-5'), 3.54(H-6'); ¹³C NMR δ_{ppm} (125 MHz): 51.9(αCH), 38.2(βCH₂) Aromatic- 138.0(C₁), 128.3(C₂, C₆), 129.1(C₃, C₅), 126.1(C₄), 172.5(CO), 96.6(C1α), 101.2(C1β), 70.5(C2α), 73.0(C2β), 74.0(C3β), 82.5(C4α), 83.3(C4β), 77.2(C5αβ), 62.1(C6β), 103.2(C1'β), 69.9(C2'), 71.6(C3'), 68.2(C4'), 74.4(C5'), 60.5(C6').

6'-O-ester 29b: ¹H NMR δ_{ppm}: 2.72(αCH), 3.00(βCH₂), 5.16(H-1α), 4.32(H-1β), 3.16(H-2α), 3.45(H-2β), 3.43(H-3α), 3.50(H-3β), 3.32(H-4α), 3.80(H-5α), 3.49(H-6a), 4.15(H-1'β), 3.36(H-2'), 3.89(H-4'), 3.89(H-5'), 3.45(H-6'); ¹³C NMR δ_{ppm}: 52.5(αCH), 37.1(βCH₂) Aromatic- 137.6(C₁), 92.0(C1α), 97.1(C1β), 69.7(C2α), 72.7(C2β), 72.1(C3α), 74.5(C3β), 79.9(C4α), 80.7(C4β), 76.0(C5α,β), 61.0(C6β), 104.0(C1'β), 69.3(C2'), 72.1(C3'), 66.3(C4'), 75.0(C5'), 63.1(C6').

6,6'-di-O-ester 29c: ¹H NMR δ_{ppm}: 2.55(αCH), 2.89(βCH₂), 4.32(H-1α), 3.23(H-2α), 3.68(H-2β), 3.33(H-3α), 4.02(H-4α), 4.01(H-5α,β), 3.45(H-6a), 4.21(H-1'β), 3.14(H-2'), 3.58(H-3'), 3.74(H-4'), 3.46(H-6'); ¹³C NMR δ_{ppm}: 51.7(αCH), 37.9(βCH₂) Aromatic- 137.8(C₁), 95.6(C1α), 101.9(C1β), 71.3(C2α), 73.2(C2β), 73.3(C3α), 74.7(C3β), 82.2(C4α), 84.2(C4β), 77.7(C5β), 62.4(C6β), 103.4(C1'β), 69.9(C2'), 72.4(C3'), 67.4(C4'), 74.7(C5'), 62.7(C6').

Figure 4.25 shows 2D-HSQCT NMR spectrum for L-phenylalanyl-lactose **29a-c**.

4.2.2.7. L-Phenylalanyl-maltose 30a and b:

Solid; UV (H₂O, λ_{max}): 215 nm (σ→σ* ε₂₁₄ – 1318 M⁻¹), 257.5 nm (π→π* ε_{257.5} – 525 M⁻¹); IR (KBr): 3405 cm⁻¹ (OH), 1649 cm⁻¹ (CO), 1582 cm⁻¹ (aromatic, –C=C–); [α]_D²⁵ = +72.7°(c 0.22 H₂O); MS (*m/z*) 527[M-1+K]⁺.

2D-HSQCT (DMSO-d₆): **6-O-ester 30a:** ¹³C NMR δ_{ppm} (125 MHz): Aromatic- 129.7(C₂ C₆), 129.8(C₃ C₅), 128.6(C₄), 97.2(C1α), 101.2(C1β), 75.0(C2α), 75.9(C3β), 80.2(C4α),

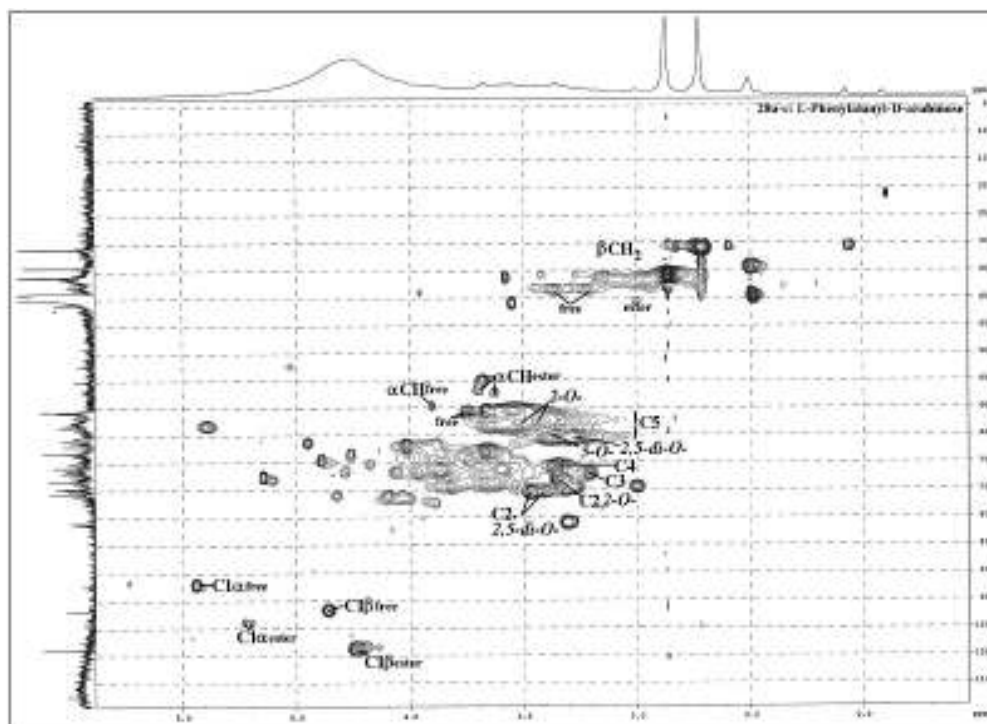


Fig. 4.24. Two-dimensional HSQCT NMR spectrum of CRL catalysed L-phenylalanyl-D- arabinose **28a-c**.

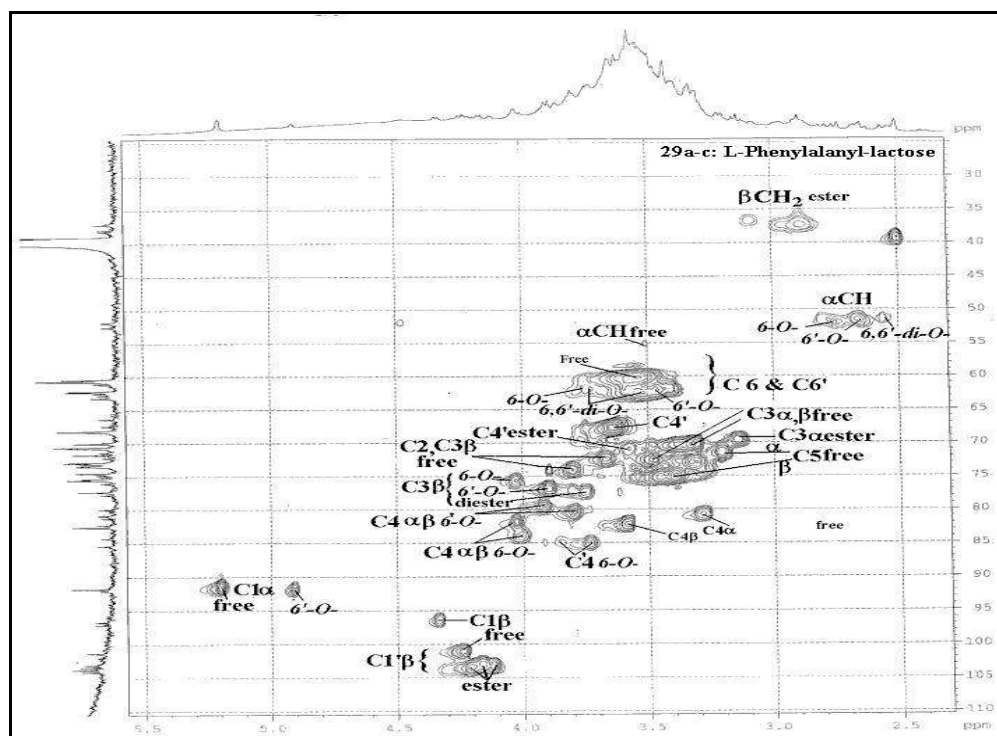


Fig. 4.25. Two-dimensional HSQCT NMR spectrum of CRL catalysed L-phenylalanyl-lactose **29a-c**.

83.3(C4 β), 63.3(C6 α), 104.2(C1' β), 73.0(C2'), 73.3(C3'), 70.3(C4'), 61.3(C6').

6'-O-ester 30b: ^{13}C NMR δ_{ppm} : 92.5(C1 β), 75.2(C2 α), 80.8(C4 α), 81.3(C4 β), 61.1(C6 α), 101.0(C1' β), 74.9(C2'), 75.2(C3'), 71.1(C4'), 63.5(C6').

A typical mass spectrum and ^{13}C NMR spectrum for L-phenylalanyl-maltose **30a** and **b** are shown in Figures 4.26 and 4.27 respectively.

4.2.2.8. L-Phenylalanyl-D-mannitol **31a** and **b**:

Solid; UV (H_2O , λ_{max}): 215 nm ($\sigma \rightarrow \sigma^*$ $\epsilon_{215} = 631\text{M}^{-1}$), 257.5 nm ($\pi \rightarrow \pi^*$ $\epsilon_{257.5} = 170\text{M}^{-1}$); IR (KBr): 3290 cm^{-1} (OH), 1637 cm^{-1} (CO), 1532 cm^{-1} (aromatic, $-\text{C}=\text{C}-$); $[\alpha]_{\text{D}}^{25} = +1.6^{\circ}$ (c 0.61 H_2O); 2D-HSQCT (DMSO- d_6): **I-O-ester 31a:** ^1H NMR δ_{ppm} (500.13 MHz): 3.48(αCH), 2.88(βCH_2), Aromatic- 7.26(H_2, H_6), 7.26(H_3, H_5), 7.18(H_4), 3.38(H-1), 3.46(H-2), 3.70(H-3), 3.84(H-4), 3.52(H-5), 3.36(H-6); ^{13}C NMR δ_{ppm} (125 MHz): 55.8(αCH), 37.1(βCH_2) Aromatic- 137.6(C_1), 131.2(C_2, C_6), 126.7(C_4), 171.0(CO), 66.0(C1/C6), 75.0(C2), 70.0(C3), 70.2(C4), 77.8(C5).

1,6-di-O-ester 31b: ^1H NMR δ_{ppm} : 3.39(αCH), 3.46(H-1), 3.45(H-2, H-6), 3.11(H-3, H-4), 3.46(H-6); ^{13}C NMR δ_{ppm} : 55.3(αCH), 66.8(C1), 77.0(C2, C5), 70.4(C3, C4), 66.8(C6).

Two dimensional HSQCT NMR spectrum for L-phenylalanyl-D-mannitol **31a** and **b** is shown in Fig. 4.28.

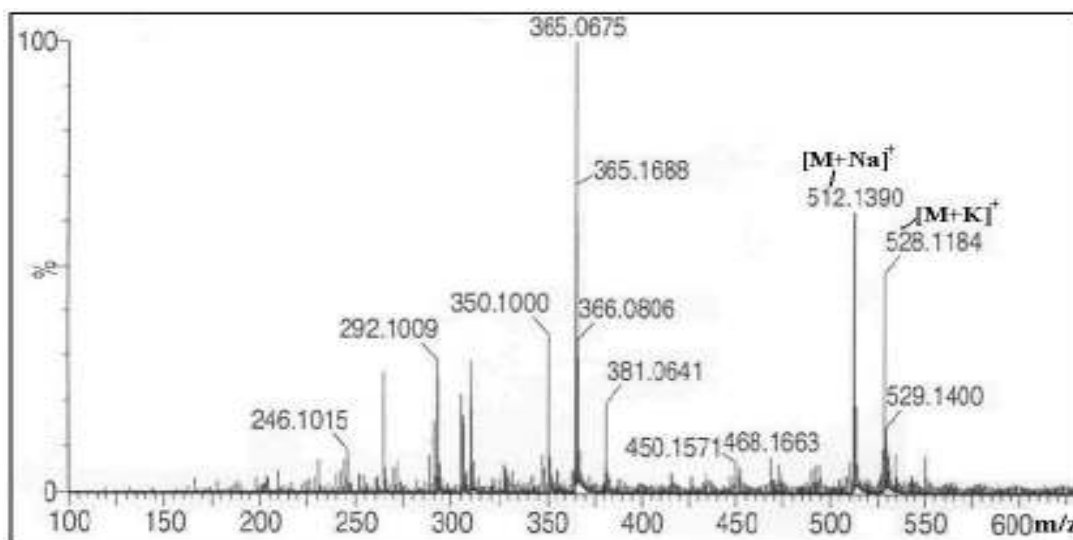


Fig. 4.26. A typical mass spectrum of L-phenylalanyl-maltose.

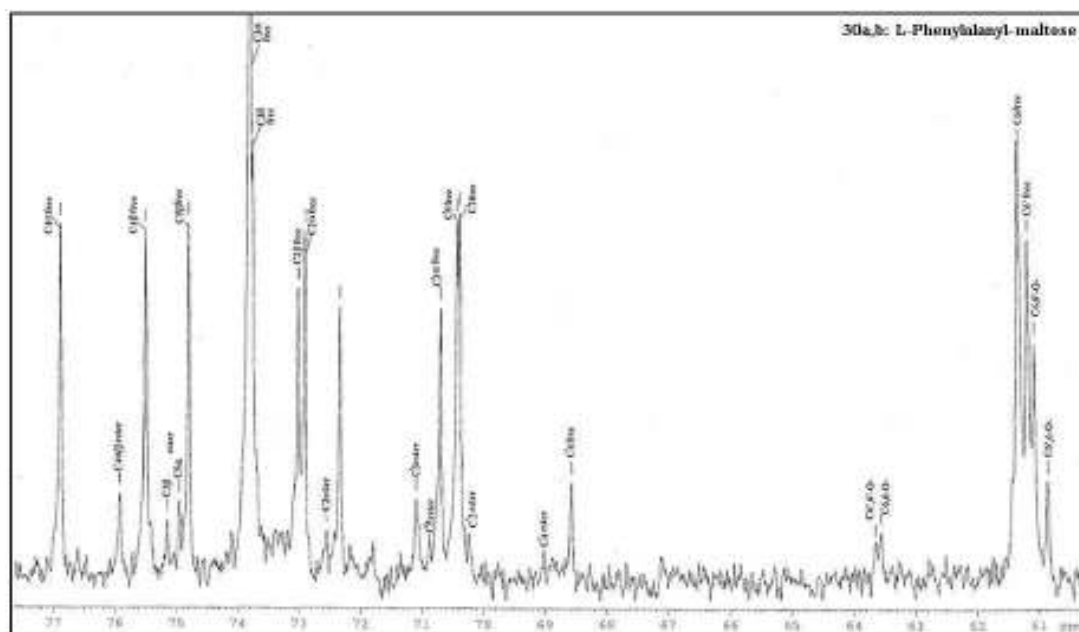


Fig. 4.27. ¹³C NMR spectrum of CRL catalysed L-phenylalanyl-maltose **30a** and **b**.

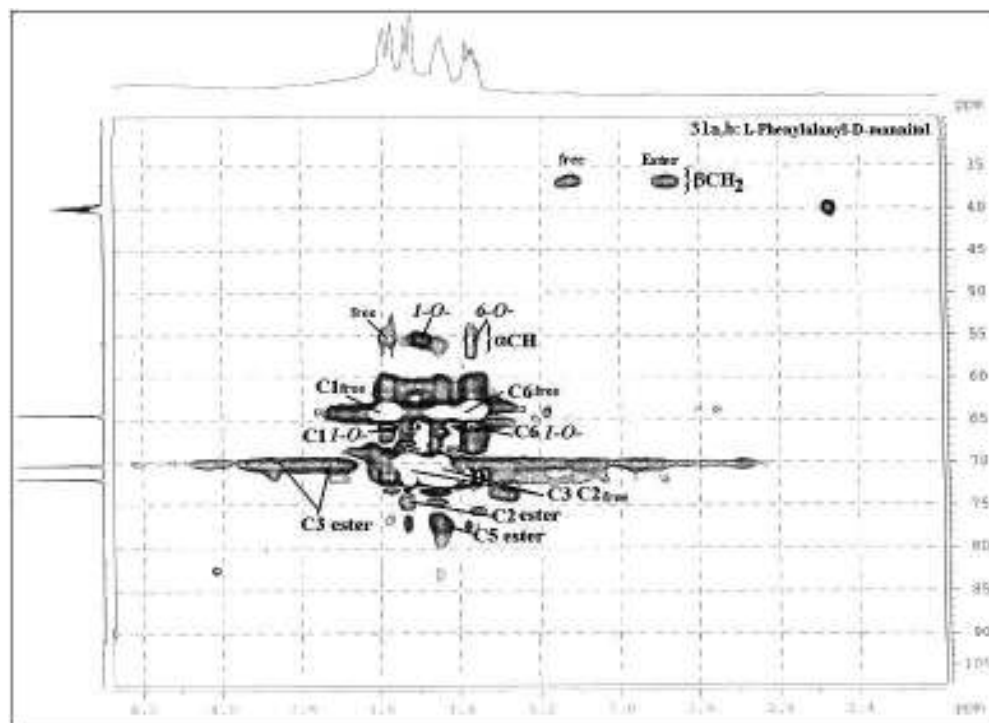
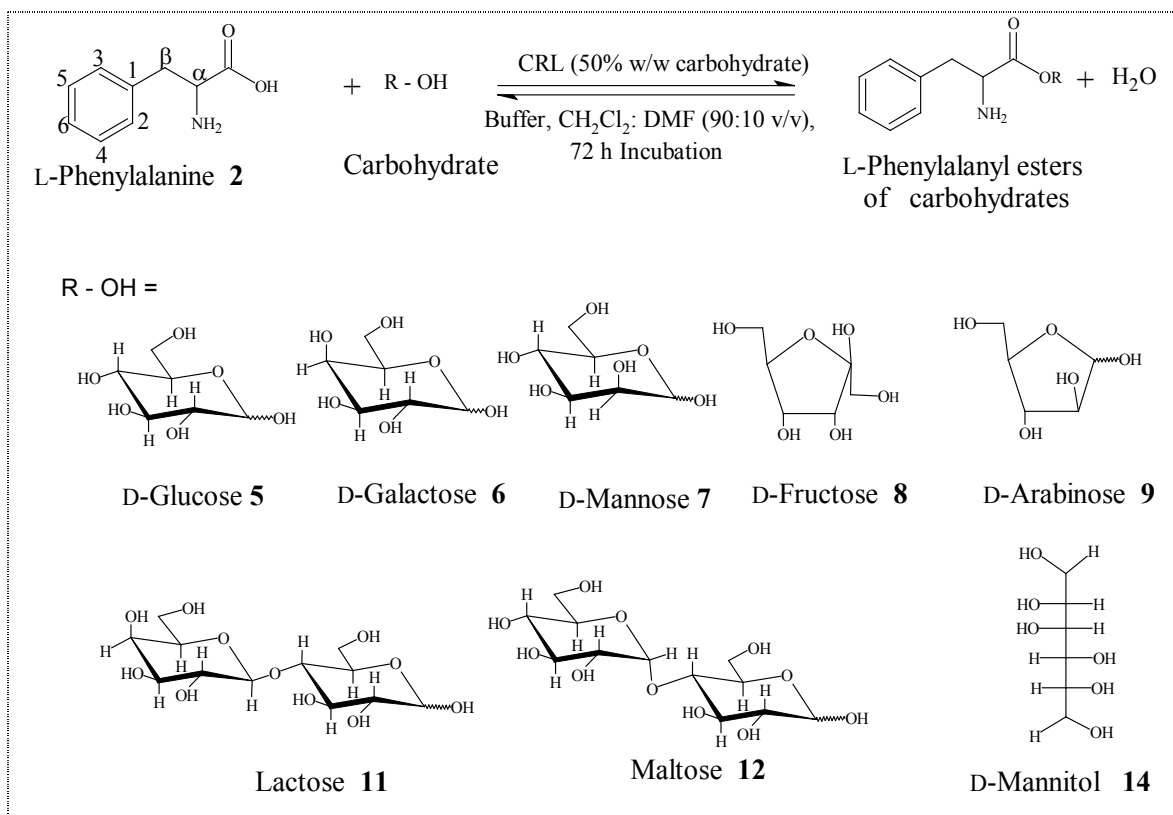


Fig. 4.28. Two-dimensional HSQCT NMR spectrum of L-phenylalanyl-D-mannitol **31a** and **b**.

4.2.3. L-Tryptophanyl esters of carbohydrates

L-Tryptophan is one of the important, aromatic amino acid with benzo pyrrole (indole) side chain. The solubility of L-tryptophan in water is 11.4g/L at 25 °C (Chapman and Halli 1982a). The esterification reaction was carried out between L-tryptophan and carbohydrates using CRL under optimum reaction conditions (Scheme 4.3). The reaction mixture consisting of equimolar (1mmol) concentration of L-tryptophan **3** and carbohydrates **5–15** and 50% CRL (w/w of respective carbohydrate) in presence of 0.2mM (0.2 mL) pH 4.0 acetate buffer in CH₂Cl₂: DMF (90:10 v/v) was refluxed for a period of 72h. Figure 4.29 shows a typical HPLC profile for L-tryptophanyl-maltose.



Scheme 4.3. CRL catalysed syntheses of L-tryptophanyl esters of carbohydrates

The HPLC retention times for the L-tryptophan and the corresponding carbohydrate esters are shown in Table 4.6. Ester formation was also monitored by TLC

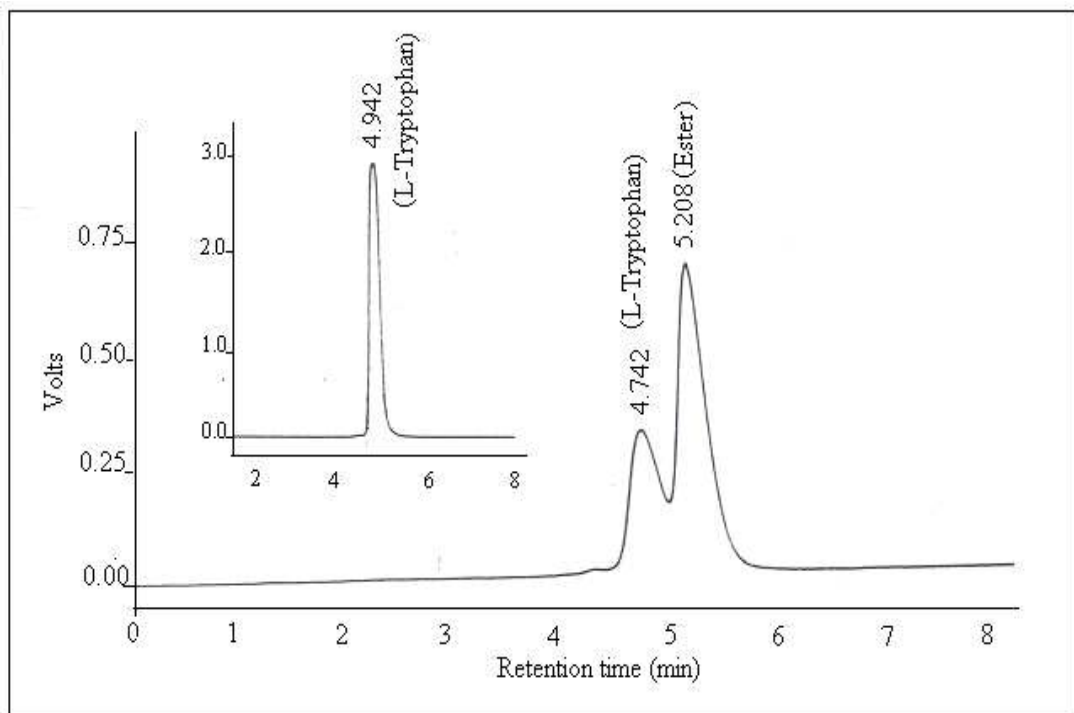


Fig. 4.29. HPLC chromatogram for reaction mixture of L-tryptophan and D-glucose esterification reaction catalysed by CRL. Column – C-18; mobile phase – acetonitrile: water (20:80 v/v); flow rate- 1 mL /min; detector – UV at 254nm; Inset - standard chromatogram of L-tryptophan; errors in yields are \pm 10-15%.

and spots were detected by spraying ninhydrin and 1-naphthol (for reducing sugar detection) and the R_f values are shown in Table 4.6.

Table 4.6 Retention times and R_f values of L-tryptophanyl esters of carbohydrates

Compound	Retention time (min) ^a	R_f values ^b
L-Tryptophan	4.9	0.62
L-Tryptophanyl-D-glucose	6.9	0.51
L-Tryptophanyl-D-galactose	6.2	0.46
L-Tryptophanyl-D-mannose	6.2	0.49
L-Tryptophanyl-D-fructose	7.1	0.42
L-Tryptophanyl-lactose	5.3	0.39
L-Tryptophanyl- maltose	5.2	0.42
L-Tryptophanyl-sucrose	5.8	0.41
L-Tryptophanyl-D-sorbitol	5.8	0.58

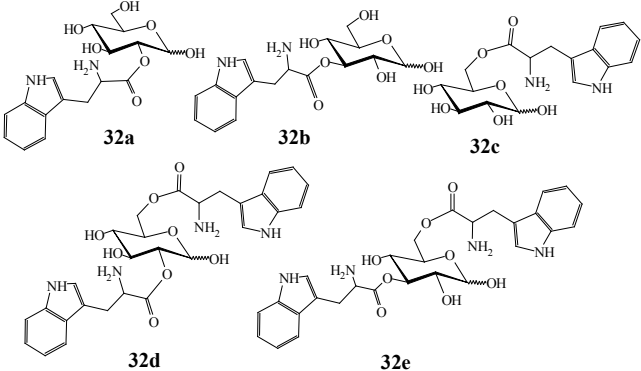
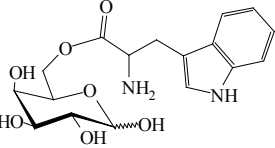
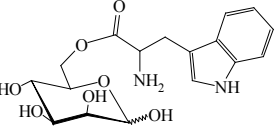
^a Conditions: column – C18; mobile phase –acetonitrile : water (20:80 v/v); flow rate – 1mL /min; detector – UV at 254 nm; ^b TLC - 20 x 20 cm silica plate (mesh size 60 –120); mobile phase – butanol : acetic acid : water (70:20:10 v/v/v); peak identification – ninhydrin (amino acid) and 1-naphthol (sugar).

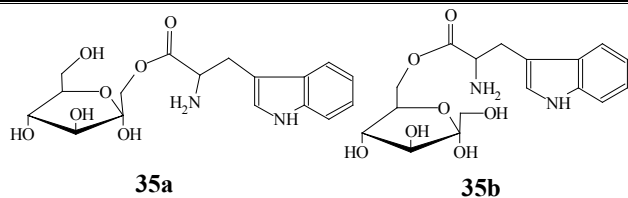
The spectral data of the isolated esters are shown in section 4.2.3.1. - 4.2.3.8.

The UV shifts for $\sigma \rightarrow \sigma^*$ transitions in the range 203 nm – 225 nm and $\pi \rightarrow \pi^*$ transitions in the range 269 nm – 279 nm for the L-tryptophanyl esters compared to $\sigma \rightarrow \sigma^*$ transitions at 201 nm and $\pi \rightarrow \pi^*$ at 262 nm for free L-tryptophan indicated that L-tryptophan had undergone esterification. InfraRed spectral data showed that the ester carbonyl stretching frequency for the prepared esters were in the range 1600 - 1649 cm^{-1} compared to 1667 cm^{-1} for L-tryptophan indicating that the L-tryptophan carboxylic group had been converted into its corresponding carbohydrate ester. Molecular ion peaks in mass spectrum further confirmed the formation of esters.

Two-dimensional HSQCT NMR spectroscopy of the L-tryptophanyl esters of carbohydrates prepared by using CRL gave good information on the nature and proportion of the esters formed. Multiplicities in the α CH of L-tryptophan indicated the esterification occurred at more than one hydroxyl group. Table 4.7 shows the ester yields from HPLC, percentage proportions of individual esters determined from the peak areas of the C5 (in case of pentoses) or C6 ^{13}C signals or from cross correlation peaks from 2D-NMR.

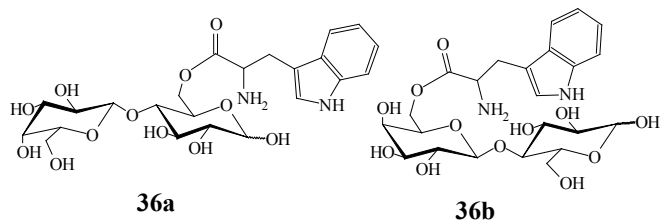
Table 4.7 Syntheses of L-tryptophanyl esters of carbohydrates ^a

L-Tryptophanyl esters of carbohydrates	Esterification yield (%)	Esters (% proportions ^b)
 <p>32a 32b 32c</p> <p>32d 32e</p>	<p>42 (mono esters-34, diester-8)</p>	<p>32a: 2-<i>O</i>-L-tryptophanyl -D-glucose (22) 32b: 3-<i>O</i>-L-tryptophanyl -D-glucose (21) 32c: 6-<i>O</i>-L-tryptophanyl-D-glucose (38) 32d: 2,6-<i>di-O</i>-L-tryptophanyl-D-glucose (10) 32e: 3,6-<i>di-O</i>-L-tryptophanyl-D-glucose (9)</p>
 <p>33</p>	<p>27 (only mono ester)</p>	<p>33: 6-<i>O</i>-L-tryptophanyl-D-galactose</p>
 <p>34</p>	<p>34 (only monoester)</p>	<p>34: 6-<i>O</i>- L-tryptophanyl-D-mannose</p>



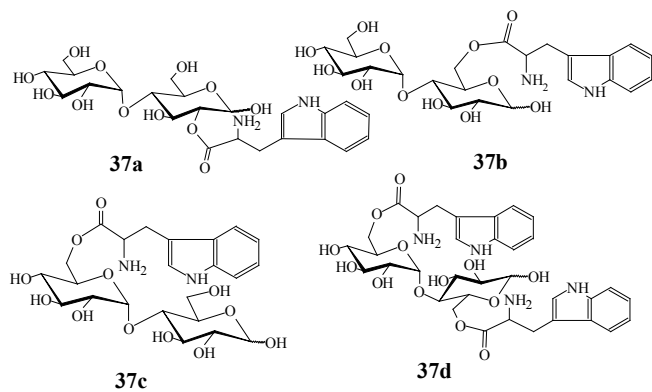
18
(only mono esters)

35a: *1-O-L*-tryptophanyl-D-fructose (55)
35b: *6-O-L*-tryptophanyl-D-fructose (45)



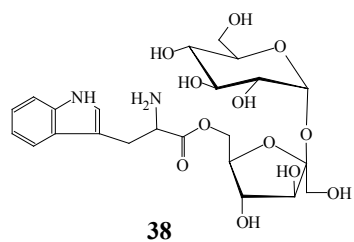
42
(only mono esters)

36a: *6-O-L*-tryptophanyl-lactose (64)
36b: *6'-O-L*-tryptophanyl-lactose (36)



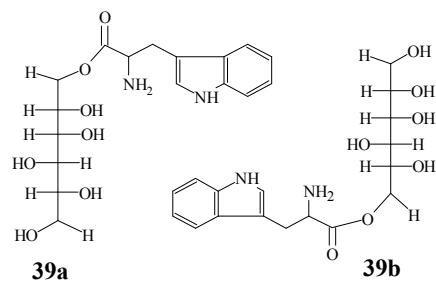
70
(mono esters-56,
diester-14)

37a: *2-O-L*-tryptophanyl-maltose (13)
37b: *6-O-L*-tryptophanyl-maltose (38)
37c: *6'-O-L*-tryptophanyl-maltose (29)
37d: *6,6'-di-O-L*-tryptophanyl-maltose (20)



7
(only monoester)

38: 6-*O*-L-tryptophanyl-sucrose



8
(only mono esters)

39a: 1-*O*-L-tryptophanyl-D-sorbitol (79)

39b: 6-*O*-L-tryptophanyl-D-sorbitol (21)

^a L-Tryptophan – 1 mmol; carbohydrates – 1 mmol; CRL – 50% (w/w based on respective carbohydrate); buffer – 0.2mM (0.2mL) pH 4.0 acetate buffer; CH₂Cl₂: DMF (90: 10 v/v) at 40 °C; incubation period – 72 h; Conversion yields were from HPLC with respect to L-tryptophan concentration; ^b The ester proportions were calculated from the area of respective ¹³C signals.

NMR data for L-tryptophan: Solid; mp- 215 °C; UV (H₂O, λ_{\max}): 201 nm ($\sigma \rightarrow \sigma^*$ $\epsilon_{201} = 956 \text{ M}^{-1}$), 262 nm ($\pi \rightarrow \pi^*$ $\epsilon_{262} = 191 \text{ M}^{-1}$); IR (KBr): 3218 cm⁻¹ (OH), 1667 cm⁻¹ (CO), 1567 cm⁻¹ (aromatic, -C=C-); $[\alpha]^{25}_{\text{D}} = -32.8^{\circ}$ (*c* 1.0 H₂O); 2D-HSQCT (DMSO-d₆): ¹H NMR δ_{ppm} (500.13 MHz): 3.60(αCH , *J*= 10.4, 4.2 Hz), 3.06($\beta\text{CH}_{2\text{a}}$, *J*=15.3, 6.8 Hz), 3.19($\beta\text{CH}_{2\text{b}}$, *J*=15.3, 6.8 Hz), Aromatic- 7.24(H₂), 7.36(H₅ *J*=7.5 Hz), 7.60(H₆ *J*=7.5 Hz), 7.0(H₇, *J*=14.0, 6.5 Hz), 7.07(H₈, *J*=14.0, 6.5 Hz); ¹³C NMR δ_{ppm} : 54.7(αCH), 27.0(βCH_2) Aromatic- 109.1(C₁), 124.3(C₂), 136.4(C₃), 127.3(C₄), 120.9(C₅), 111.4(C₆), 118.4(C₇, C₈), 171.5 (CO).

4.2.3.1. L-Tryptophanyl-D-glucose 32a-e:

Solid; UV (H₂O, λ_{\max}): 213 nm ($\sigma \rightarrow \sigma^*$ $\epsilon_{213} = 1479 \text{ M}^{-1}$), 276 nm ($\pi \rightarrow \pi^*$ $\epsilon_{276} = 389 \text{ M}^{-1}$), 315 nm ($n \rightarrow \pi^*$ $\epsilon_{315} = 117 \text{ M}^{-1}$); IR (KBr): 3523 cm⁻¹ (NH), 3336 cm⁻¹ (OH), 1633 cm⁻¹ (CO), 1524 (aromatic, -C=C-); $[\alpha]^{25}_{\text{D}} = -21.7^{\circ}$ (*c* H₂O 0.62); MS (*m/z*) 366[M]⁺; RT: 6.9 min; R_f: 0.51.

2D-HSQCT (DMSO-d₆): **2-O-ester 32a:** ¹H NMR δ_{ppm} (500.13 MHz): 2.92(αCH), 3.06(βCH_2), 6.96-7.59 (Aromatic), 4.60(H-1 α), 3.69(H-2 α), 3.72(H-2 β), 3.68(H-3 α), 3.54(H-6a); ¹³C NMR δ_{ppm} (125 MHz): 53.2(αCH), 35.0(βCH_2), Aromatic-109.4(C₁), 124.2(C₂), 136.0(C₄), 114.6(C₆), 120.8(C₇), 121.1(C₈), 100.8(C1 α), 75.9(C2 α), 76.2(C2 β) 72.9(C3 α), 62.8(C6 β).

3-O-ester 32b: ¹H NMR δ_{ppm} : 2.87(αCH), 2.84(βCH_2), 6.96-7.61(Aromatic), 3.82(H-2 α), 3.92(H-3 α), 3.59(H-3 β), 3.58(H-6a); ¹³C NMR δ_{ppm} : 52.3(αCH), 35.9(βCH_2), Aromatic-109.3(C₁), 124.3(C₂, C₃), 136.3(C₄), 121.0(C₅), 113.0(C₆), 116.5(C₇), 120.0(C₈), 100.1(C1 α), 101.8(C1 β), 74.2(C2 α), 71.2(C2 β), 82.0(C3 β), 62.5(C6 α).

6-O-ester 32c: ¹H NMR δ_{ppm} : 2.81(αCH), 2.70(βCH_2), 3.41(H-2 α), 3.51(H-2 β), 3.68(H-3 α), 3.52(H-4 α), 3.64(H-5 α), 3.70(H-5 β), 3.65(H-6a), ¹³C NMR δ_{ppm} : 51.5(αCH),

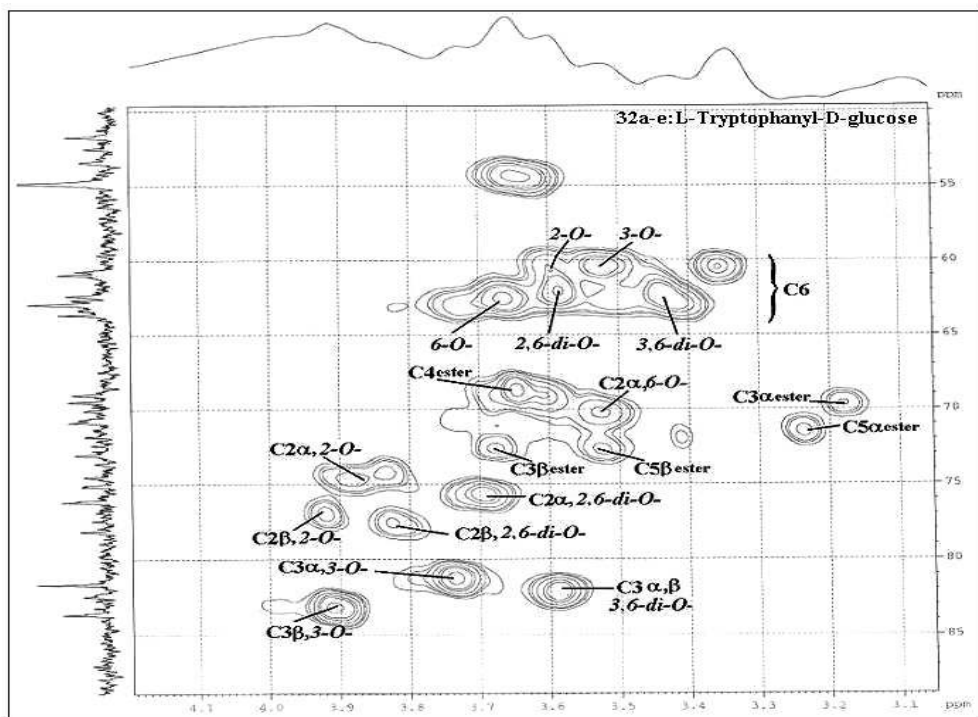


Fig. 4.30. Two-dimensional HSQCT NMR for L-tryptophanyl-D-glucose **32a-e** reaction mixture

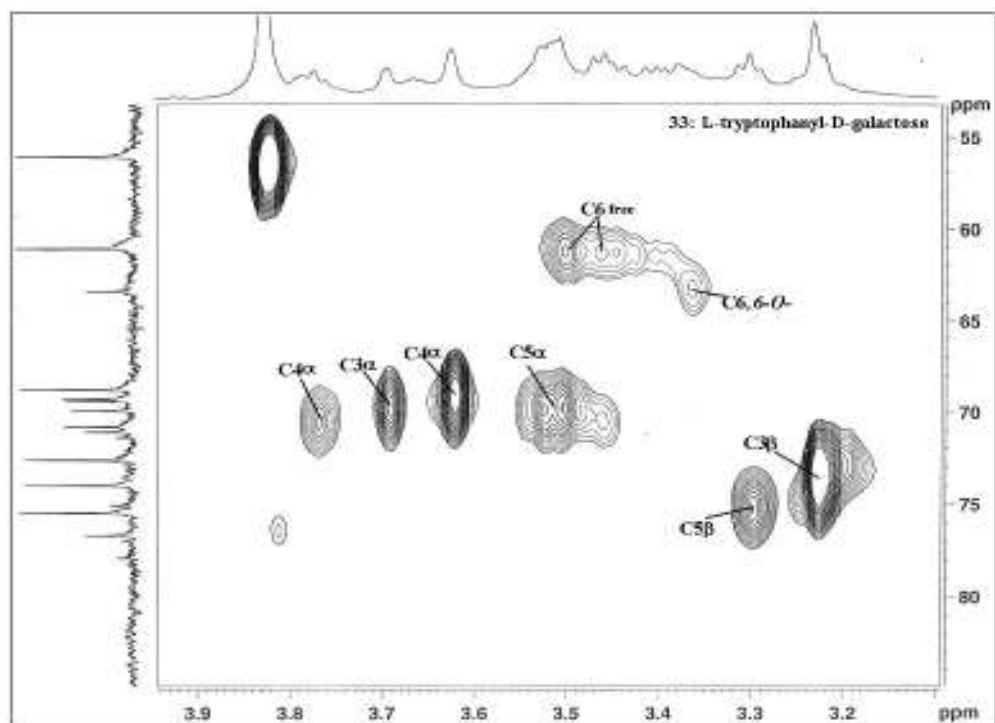


Fig. 4.31. Two-dimensional HSQCT NMR for L-tryptophanyl-D-galactose **33** reaction mixture

31.0(βCH_2), 172.0(CO), 96.9(C1 α), 101.9(C1 β), 71.8(C2 α), 69.5(C2 β), 72.6(C3 α), 69.6(C4 α), 68.9(C5 α), 70.2(C5 β), 63.0(C6 β).

2,6-di-O-ester 32d: ^1H NMR δ_{ppm} : 2.78(βCH_2), 3.92(H-2 α), 3.82(H-2 β), 3.54(H-6a). ^{13}C NMR δ_{ppm} : 31.0(βCH_2), 77.0(C2 α), 77.3(C2 β), 63.2(C6 α).

3,6-di-O-ester 32e: ^1H NMR δ_{ppm} : 2.82(αCH), 2.61(βCH_2), 3.74(H-3 α), 3.44(H-6a); ^{13}C NMR δ_{ppm} : 51.8(αCH), 31.0(βCH_2), 81.2(C3 α), 63.9(C6 α).

Two-dimensional HSQCT NMR spectrum for L-tryptophanyl-D-glucose **32a-e** is shown in Fig. 4.30.

4.2.3.2. L-Tryptophanyl-D-galactose 33:

Solid; mp - 119 °C; UV (H_2O , λ_{max}): 225 nm ($\sigma \rightarrow \sigma^*$ $\epsilon_{225} = 4677 \text{ M}^{-1}$), 278 nm ($\pi \rightarrow \pi^*$ $\epsilon_{278} = 3715 \text{ M}^{-1}$); 302 nm ($n \rightarrow \pi^*$ $\epsilon_{302} = 118 \text{ M}^{-1}$); IR (KBr): 3190 cm^{-1} (NH), 3002 cm^{-1} (OH), 1615 cm^{-1} (CO), 1454 cm^{-1} (aromatic, $-\text{C}=\text{C}-$); $[\alpha]_{\text{D}}^{25} = -22.2^\circ$ (c 1.08 H_2O); MS (m/z) 389 $[\text{M}+\text{Na}]^+$; RT: 6.2 min; R_f : 0.46.

2D-HSQCT (DMSO- d_6): **6-O-ester 33:** ^1H NMR δ_{ppm} : 3.08(αCH), Aromatic- 6.92(H₂), 7.30(H₅), 7.33(H₆), 7.23(H₇, H₈), 4.82(H-1 α), 4.14(H-1 β), 3.61(H-2 α), 3.68(H-3 α), 3.22(H-3 β), 3.77(H-4 α), 3.47(H-5 α), 3.37(H-6b); ^{13}C NMR δ_{ppm} : 52.8(αCH), 24.0(βCH_2), Aromatic - 124.8(C₂), 133.8(C₄), 171.6(CO), 95.8(C1 α), 102.2(C1 β), 68.5(C2 α), 69.6(C3 α), 73.4(C3 β), 70.8(C4 α), 70.6(C5 α), 75.0(C5 β), 63.2(C6 α).

Figure 4.31 shows 2D-HSQCT NMR spectrum for L-tryptophanyl-D-galactose **33**.

4.2.3.3. L-Tryptophanyl-D-mannose 34:

Solid; mp - 132 °C; UV (H_2O , λ_{max}): 203 nm ($\sigma \rightarrow \sigma^*$ $\epsilon_{225} = 4786 \text{ M}^{-1}$), 276 nm ($\pi \rightarrow \pi^*$ $\epsilon_{276} = 1548 \text{ M}^{-1}$), 307 nm ($n \rightarrow \pi^*$ $\epsilon_{307} = 977 \text{ M}^{-1}$); IR (KBr): 3444 cm^{-1} (OH), 1600 cm^{-1} (CO), 1431 cm^{-1} (aromatic, $-\text{C}=\text{C}-$); $[\alpha]_{\text{D}}^{25} = -14.9^\circ$ (c 0.82 H_2O); MS (m/z)

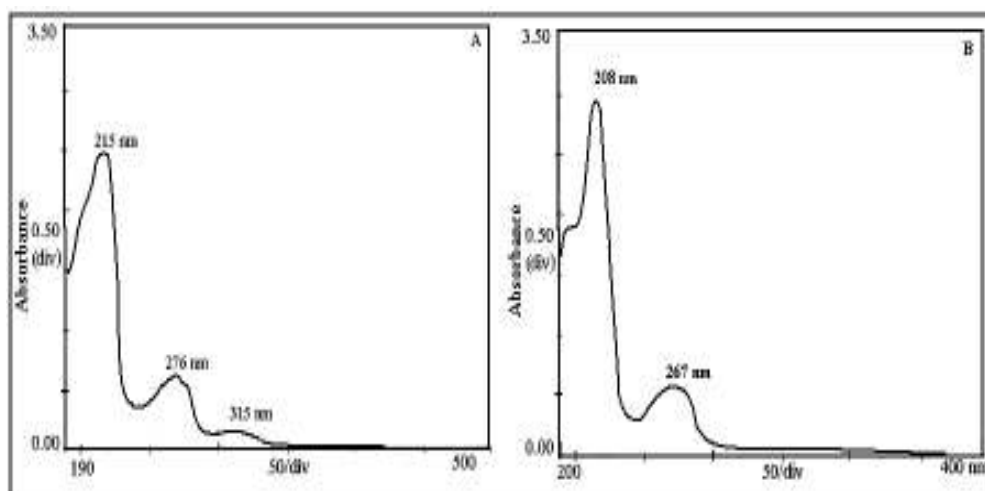


Fig. 4.32. UV spectra for L-tryptophanyl-D-mannose of CRL catalysed reaction. (A) L-tryptophanyl-D-mannose and (B) L-tryptophan

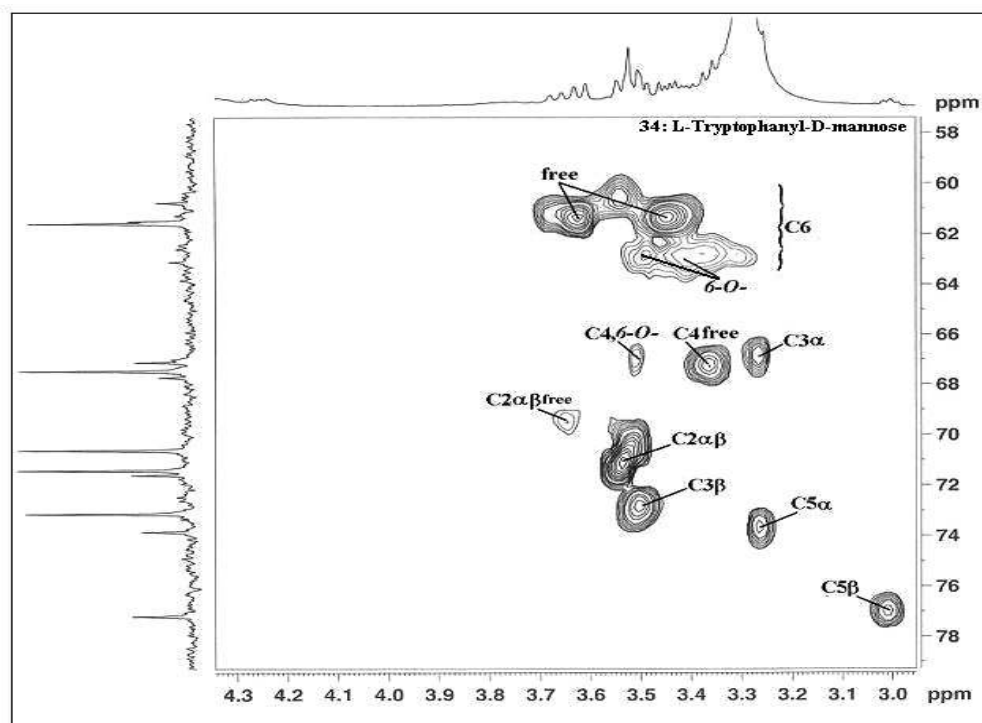


Fig. 4.33. Two-dimensional HSQCT NMR for L-tryptophanyl-D-mannose **34** reaction mixture

365[M-1]⁺; RT: 6.2 min; R_f: 0.49.

2D-HSQCT (DMSO-d₆): **6-O-ester 34**: ¹H NMR δ_{ppm}: 2.98(αCH), 2.15(βCH₂), Aromatic- 7.19(H₂), 7.04(H₅), 7.63(H₆), 7.03(H₇, H₈), 4.86(H-1α), 4.54(H-1β), 3.52(H-2α), 3.61(H-3α), 3.50(H-3β), 3.47(H-4β), 3.24(H-5α), 3.02(H-5β), 3.40(H-6a), 3.49(H-6b); ¹³C NMR δ_{ppm}: 52.8 (αCH), 24.0(βCH₂), 124.8(C₂), 133.8(C₄), 171.6(CO), 94.8(C1α), 95.4(C1β), 71.2(C2α), 69.5(C3α), 73.0(C3β), 66.8(C4α), 73.6(C5α), 77.0(C5β), 63.8(C6α).

Figures 4.32 and 4.33 show UV and 2D-HSQCT NMR spectra for L-tryptophanyl-D-mannose **34** respectively.

4.2.3.4. L-Tryptophanyl-D-fructose **35a** and **b**:

Solid; UV (H₂O, λ_{max}): 212 nm (σ→σ* ε₂₁₂ - 5495 M⁻¹), 269 nm (π→π* ε₂₆₉ - 1862 M⁻¹); 308 nm (n→π* ε₃₀₈ - 1175 M⁻¹); IR (KBr): 3373 cm⁻¹ (OH), 1624 cm⁻¹ (CO), 1399 cm⁻¹ (CN), 1457 cm⁻¹ (aromatic, -C=C-); [α]_D²⁵ = -10.8° (c 0.74 H₂O); MS (m/z) 365 [M-1]⁺; RT: 7.1 min; R_f: 0.42.

2D-HSQCT (DMSO-d₆): **1-O-ester 35a**: ¹H NMR δ_{ppm} (500.13 MHz): 3.44(αCH), 2.59(βCH₂), Aromatic - 7.1(H₂), 8.18(H₃), 7.32(H₇), 7.74(H₈), 4.32(H-1), 3.78(H-3α), 3.48(H-4α), 3.42(H-6a); ¹³C NMR δ_{ppm} (125 MHz): 58.2(αCH), 30.2(βCH₂), Aromatic- 109.5(C₁), 124.0(C₂), 122.0(C₃), 111.5(C₆), 120.6(C₇), 119.0(C₈), 66.2(C1α), 104.2(C2α), 71.6(C3α), 70.6(C4α), 63.1(C6α).

6-O-ester 35b: ¹H NMR δ_{ppm}: 3.32(αCH), 2.50(βCH₂), 3.27(H-1α), 4.38(H-6a); ¹³C NMR δ_{ppm}: 59.0(αCH), 29.8(βCH₂), 63.9(C1α), 102.0(C2α), 72.5(C4α), 65.4(C6α).

UV, IR, mass and 2D-HSQCT NMR spectra for L-tryptophanyl-D-fructose **35a** and **b** are shown in Fig. 4.34, Fig. 4.35, Fig. 4.36 and Fig. 4.37 respectively.

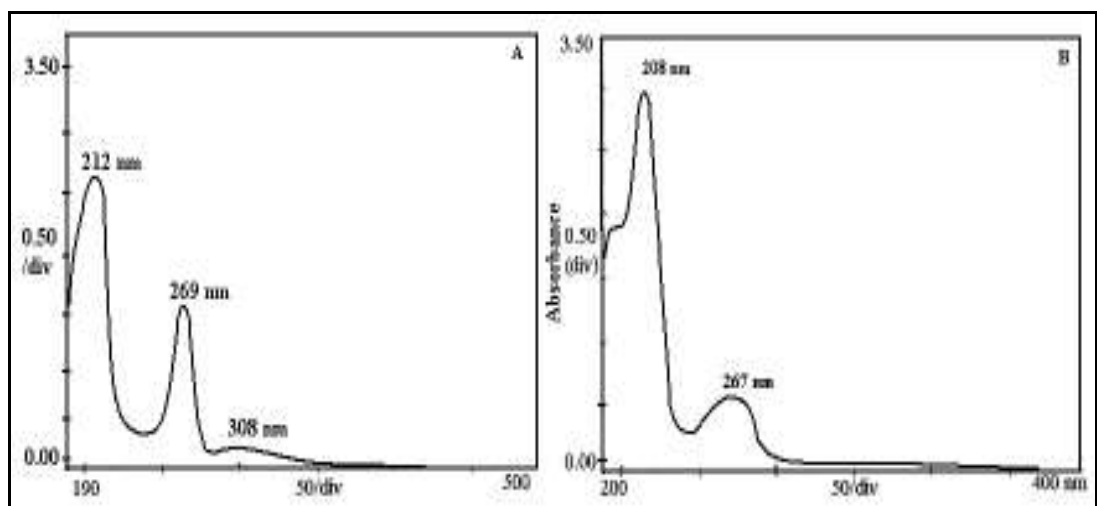


Fig. 4.34. UV spectrum for L-tryptophanyl-D-fructose of CRL catalysed reaction. (A) L-tryptophanyl-D-glucose and (B) L-tryptophan.

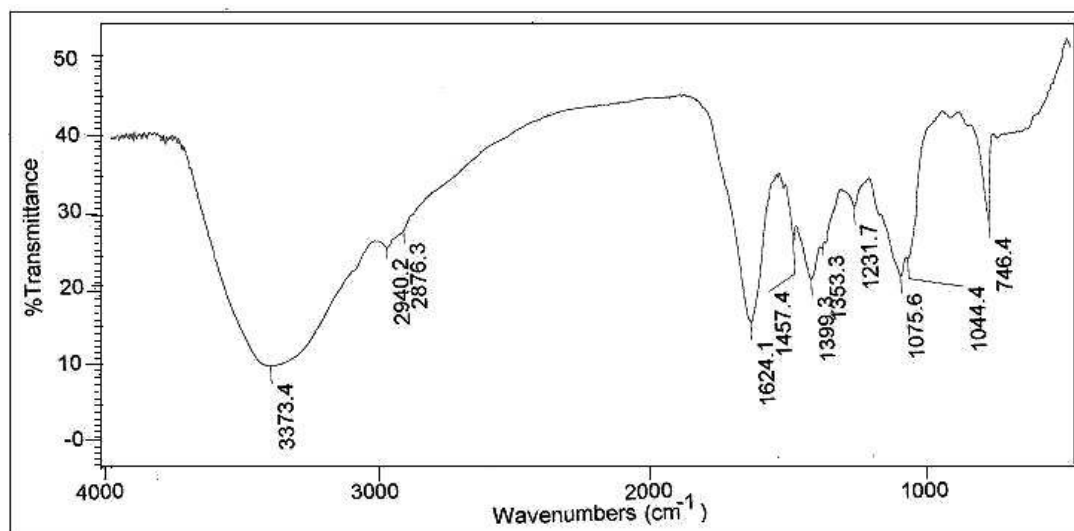


Fig. 4.35. A typical IR spectrum of L-tryptophanyl-D-fructose of CRL catalysed reaction. A 2.5 mg of ester sample was prepared as KBr pellet.

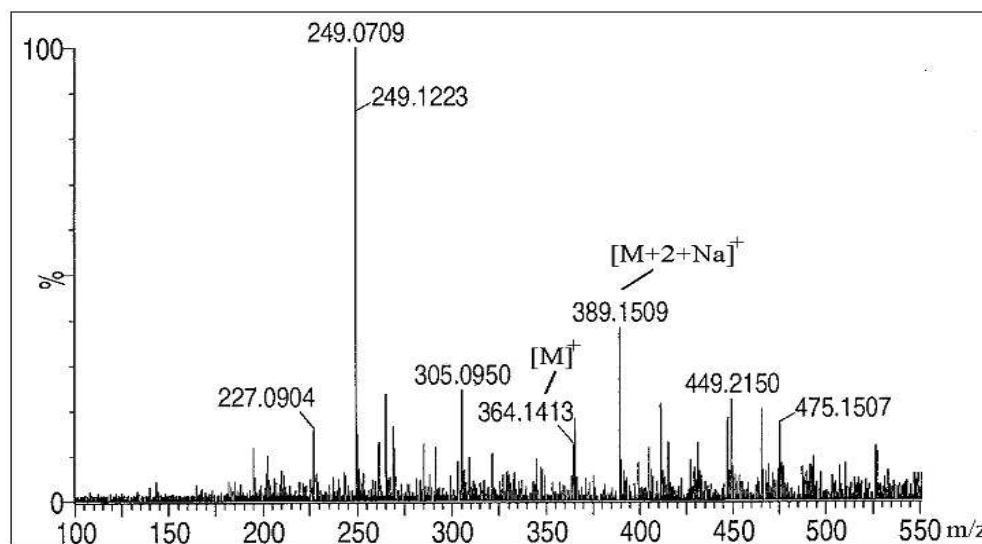


Fig. 4.36. A typical mass spectrum of L-tryptophanyl-D-fructose.

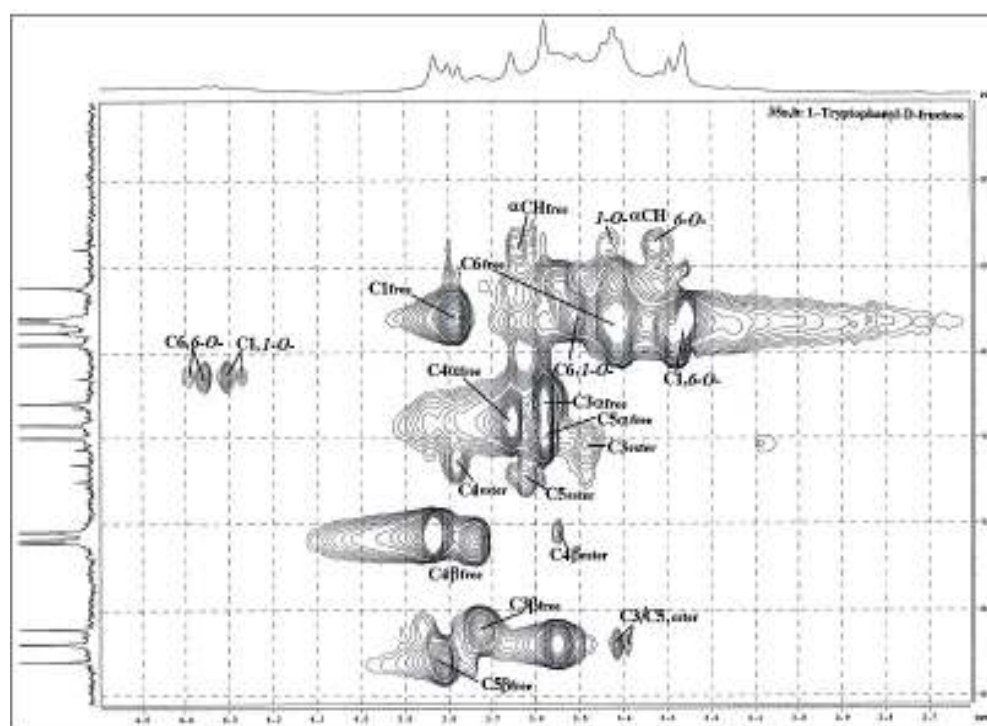


Fig. 4.37. Two-dimensional HSQC NMR for L-tryptophanyl-D-fructose **35a** and **b** reaction mixture

4.2.3.5. L-Tryptophanyl-lactose **36a** and **b**:

Solid; UV (H₂O, λ_{\max}): 220 nm ($\sigma \rightarrow \sigma^*$ $\epsilon_{220} = 1738 \text{ M}^{-1}$), 278 nm ($\pi \rightarrow \pi^*$ $\epsilon_{278} = 1380 \text{ M}^{-1}$); IR (KBr): 3352 cm⁻¹ (OH), 1635 cm⁻¹ (CO), 1341 cm⁻¹ (NH), 1423 cm⁻¹ (arom, -C=C-); $[\alpha]_{\text{D}}^{25} = +23.0^{\circ}$ (c 1.0 H₂O); MS (m/z) 551[M+Na]⁺; RT: 5.3 min; R_f: 0.39. 2D-HSQCT (DMSO-d₆): **6-O-ester 36a**: ¹H NMR δ_{ppm} : 2.84(α CH), 3.04(β CH₂), Aromatic-7.16(H₂), 7.08(H₅), 7.62(H₆), 7.01(H₇, H₈), 4.89(H-1 α), 4.18(H-1 β), 3.28(H-2 α), 3.26(H-2 β), 3.53(H-3 α), 3.38(H-3 β), 3.74(H-4 α), 3.81(H-4 β), 3.17(H-5 α), 3.65(H-6a), 4.11(H-1' β), 3.28(H-3'), 3.65(H-5'), 3.33(H-6'); ¹³C NMR δ_{ppm} : 51.8(α CH), 26.4(β CH₂), Aromatic-109.8(C₁), 124.4(C₂), 127.2(C₃), 136.6(C₄), 121.6(C₅), 111.9(C₆), 118.9(C₇), 118.4(C₈), 170.8(CO), 94.8(C1 α), 96.8(C1 β), 70.8(C2 α), 75.2(C2 β), 71.7(C3 α), 75.8(C3 β), 81.6(C4 α), 72.0(C5 α), 74.7(C5 β), 63.2(C6 β), 101.3(C1' β), 74.2(C3'), 70.1(C4'), 60.7(C6').

6'-O-ester 36b: ¹H NMR δ_{ppm} : 2.81(α CH), 2.98(β CH₂), 3.87(H-4 α), 3.72(H-6a), 4.03(H-1' β), 3.27(H-3'), 3.82(H-4'), 3.43(H-6'); ¹³C NMR δ_{ppm} : 53.4(α CH), 26.8(β CH₂) Aromatic-109.3(C₁), 136.4(C₃), 170.9(CO), 80.2(C4 α), 60.8(C6 β), 103.5(C1' β), 73.1(C3'), 68.7(C4'), 63.2(C6').

Two-dimensional HSQCT NMR spectrum for L-tryptophanyl-lactose **36a** and **b** is shown in Fig. 4.38.

4.2.3.6. L-Tryptophanyl-maltose **37a-d**:

Solid; UV (H₂O, λ_{\max}): 223 nm ($\sigma \rightarrow \sigma^*$ $\epsilon_{223} = 6607 \text{ M}^{-1}$), 279 nm ($\pi \rightarrow \pi^*$ $\epsilon_{279} = 4169 \text{ M}^{-1}$); IR (KBr): 3286 cm⁻¹ (OH), 1606 cm⁻¹ (CO), 1353 cm⁻¹ (CN), 1485 cm⁻¹ (arom, -C=C-); $[\alpha]_{\text{D}}^{25} = +27.1^{\circ}$ (c 1.0 H₂O); MS (m/z) 551[M+Na]⁺; RT: 5.2 min; R_f: 0.42. 2D-HSQCT (DMSO-d₆): **2-O-ester 37a**: ¹H NMR δ_{ppm} : 2.82(α CH), 2.59(β CH₂), 4.88(H-1 α), 4.60(H-1 β), 3.65(H-2 α), 3.75(H-2 β), 3.74(H-3 α), 3.78(H-3 β), 3.31(H-6a),

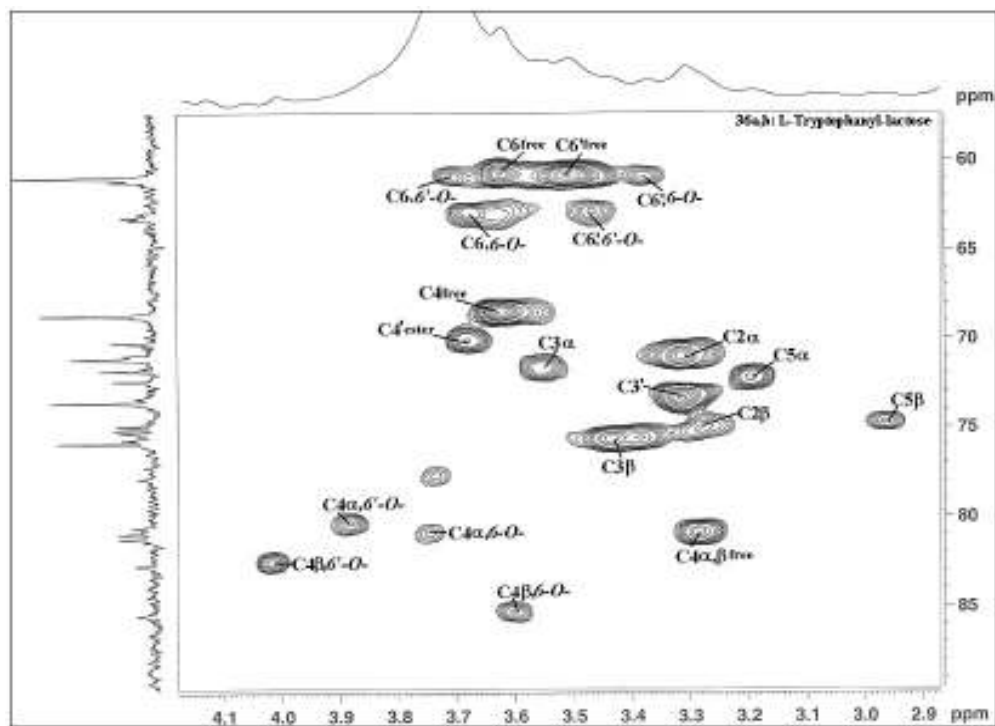


Fig. 4.38. Two-dimensional HSQCT NMR for L-tryptophanyl-lactose **36a** and **b** reaction mixture

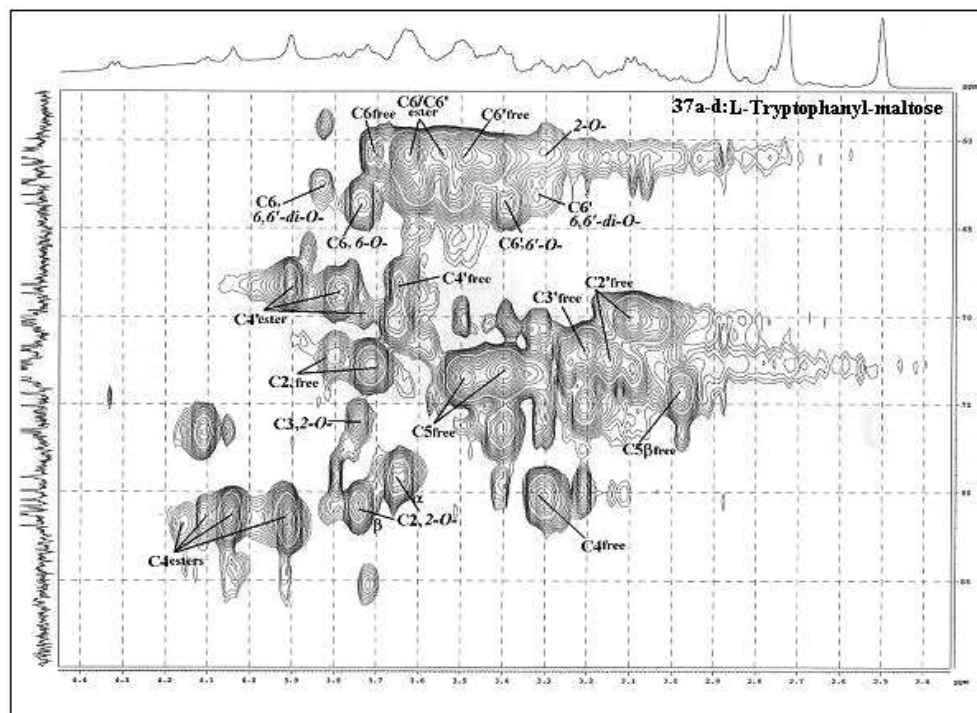


Fig. 4.39. Two-dimensional HSQCT NMR for L-tryptophanyl-maltose **37a-d** reaction mixture

4.20(H-1' α), 3.31(H-6'); ^{13}C NMR δ_{ppm} : 54.6(αCH), 30.6(βCH_2) Aromatic- 109.9(C_1), 171.2(CO), 97.3($\text{C}1\alpha$), 99.8($\text{C}1\beta$), 79.2($\text{C}2\alpha$), 81.3($\text{C}2\beta$), 76.0($\text{C}3\alpha$), 79.1($\text{C}3\beta$), 101.2($\text{C}1'\alpha$), 69.9($\text{C}4'$), 60.5($\text{C}6'$).

6-O-ester 37b: ^1H NMR δ_{ppm} : 2.87(αCH), 2.72(βCH_2), 4.82(H-1 α), 4.9(H-1 β), 3.21(H-3 α), 3.92(H-4 α), 4.05(H-4 β), 3.40(H-5 α), 3.35(H-5 β), 3.74(H-6a), 4.22(H-1' α), 3.74(H-4'), 3.31(H-6'); ^{13}C NMR δ_{ppm} : 51.2(αCH), 30.8(βCH_2), Aromatic-109.0(C_1), 124.0(C_2), 127.3(C_3), 136.3(C_4), 120.8(C_5), 111.8(C_6), 118.4(C_7), 118.5(C_8), 171.2(CO), 96.5($\text{C}1\alpha$), 100.5($\text{C}1\beta$), 75.0($\text{C}3\alpha$), 81.2($\text{C}4\alpha$), 81.4($\text{C}4\beta$), 70.5($\text{C}5\alpha$), 70.8($\text{C}5\beta$), 63.6($\text{C}6\alpha$), 101.2($\text{C}1'\alpha$), 69.9($\text{C}4'$), 60.8($\text{C}6'$).

6'-O-ester 37c: ^1H NMR δ_{ppm} : 2.76(αCH), 2.88(βCH_2), 7.12 - 7.35(Aromatic), 5.22(H-1 α), 4.64(H-1 β), 3.24(H-3 α), 3.92(H-4 α), 4.05(H-4 β), 3.62(H-6a), 4.20(H-1' α), 2.98(H-2'), 3.09(H-3'), 3.90(H-4'), 3.30(H-6'); ^{13}C NMR δ_{ppm} : 51.9(αCH), 36.0(βCH_2) Aromatic-109.5(C_1), 123.8(C_2), 136.2(C_4), 121.0(C_5), 172.9(CO), 90.9($\text{C}1\alpha$), 96.8($\text{C}1\beta$), 61.2($\text{C}6\alpha$), 103.8($\text{C}1'\alpha$), 74.1($\text{C}2'$), 73.2($\text{C}3'$), 68.8 ($\text{C}4'$), 63.6($\text{C}6'$).

6,6'-di-O-ester 37d: ^1H NMR δ_{ppm} : 2.68(αCH), 2.73(βCH_2), 4.92(H-1 α), 5.2(H-1 β), 4.10(H-4 α), 3.83(H-6a), 4.08(H-1' α), 3.79(H-3'), 3.32(H-6'); ^{13}C NMR δ_{ppm} : 53.1(αCH), 35.2(βCH_2), Aromatic-109.8(C_1), 123.6(C_2), 136.1(C_5), 172.0(CO), 99.0($\text{C}1\alpha$), 100.7($\text{C}1\beta$), 81.9($\text{C}4\alpha$), 82.0($\text{C}4\beta$), 62.9($\text{C}6\alpha$), 103.4($\text{C}1'\alpha$), 69.0 ($\text{C}4'$), 62.8($\text{C}6'$).

Figure 4.39 shows two-dimensional HSQCT NMR spectrum for L-tryptophanyl-maltose **37a-d**.

4.2.3.7. L-Tryptophanyl-sucrose **38**:

Solid; mp - 122 $^\circ\text{C}$; UV (H_2O , λ_{max}): 218 nm ($\sigma \rightarrow \sigma^*$ $\epsilon_{218} - 490 \text{ M}^{-1}$), 272 nm ($\pi \rightarrow \pi^*$ $\epsilon_{272} - 120 \text{ M}^{-1}$); IR (KBr): 3356 cm^{-1} (OH), 1649 cm^{-1} (CO), 1371 cm^{-1} (CN), 1499 cm^{-1} (arom, -C=C-); $[\alpha]_{\text{D}}^{25} = +32.4^\circ$ (c 0.72 H_2O); MS (m/z) 551[M+Na] $^+$; RT: 5.8min; R_f : 0.41.

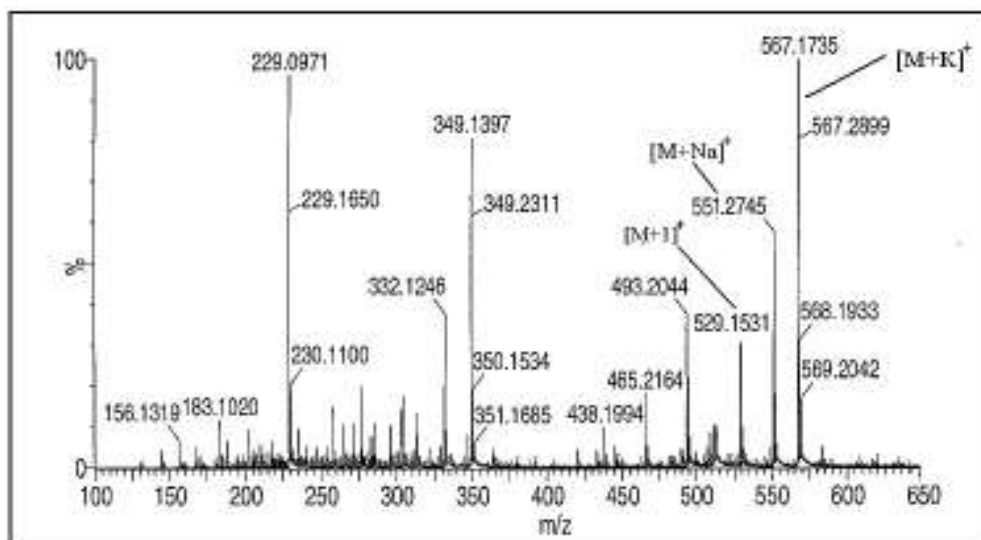


Fig. 4.40. A typical mass spectrum of L-tryptophanyl-sucrose.

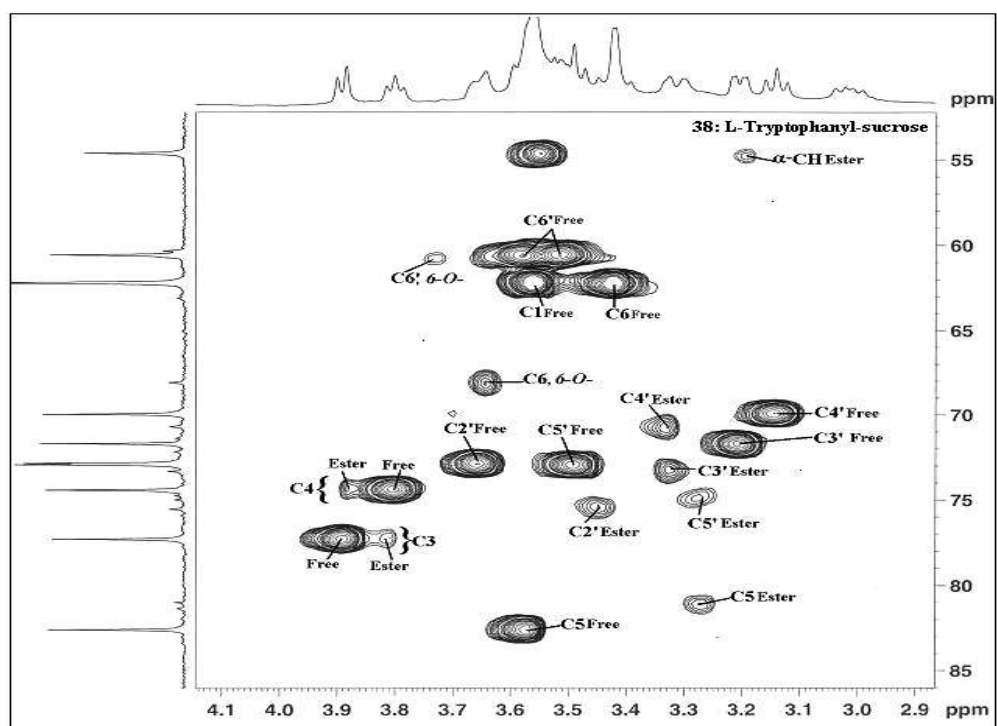


Fig. 4.41. Two-dimensional HSQCT NMR for L-tryptophanyl-sucrose **38** reaction mixture

2D-HSQCT (DMSO-d₆): **6-O-ester 38**: ¹H NMR δ_{ppm}: 3.14(αCH), 2.45(βCH₂), Aromatic-7.22(H₂), 7.08(H₅), 6.94(H₆), 7.18(H₇), 7.08(H₈), 3.53(H-1α), 3.81(H-3α), 3.87(H-4α), 3.28(H-5α), 3.65(H-6a), 4.12(H-1'α), 3.45(H-2'), 3.26(H-3'), 3.30(H-4'), 3.32(H-5'), 3.74(H-6'); ¹³C NMR δ_{ppm}: 54.8(αCH), 28.2(βCH₂), Aromatic-109.1(C₁), 124.9(C₂), 128.0(C₃, C₄), 122.2(C₅), 119.2(C₆), 118.8(C₇), 118.7(C₈), 170.9(CO), 63.1(C1α), 103.8(C2α), 77.2(C3α), 74.0(C4α), 81.0(C5α), 66.8(C6α), 96.7(C1'α), 75.2(C2'), 74.8(C3'), 70.8(C4'), 73.2(C5'), 61.0(C6').

A typical mass spectrum and 2D-HSQCT NMR spectrum for L-tryptophanyl-sucrose **38** is shown in Figures 4.40 and 4.41 respectively.

4.2.3.8. L-Tryptophanyl-D-sorbitol **39a** and **b**:

Solid; UV (H₂O, λ_{max}): 215 nm (σ→σ* ε₂₁₅ = 2884 M⁻¹), 276 nm (π→π* ε₂₇₆ = 1445 M⁻¹); IR (KBr): 3475 cm⁻¹ (OH), 1631 cm⁻¹ (CO), 1386 cm⁻¹ (CN), 1591 cm⁻¹ (arom, -C=C-); [α]_D²⁵ = -6.5° (c 0.31 H₂O); MS (m/z) 387[M+Na]⁺; RT: 3.8 min; R_f: 0.58.

2D-HSQCT (DMSO-d₆): **1-O-ester 39a**: ¹H NMR δ_{ppm} (500.13 MHz): 3.06(αCH), 3.18(βCH_{2a}), 3.04(βCH_{2b}), Aromatic - 7.13(H₂), 7.34(H₅), 7.54(H₆), 7.04(H₇), 7.13(H₈), 3.58(H-1), 3.71(H-2), 3.58(H-3), 3.43(H-4), 3.58(H-5), 3.70(H-6); ¹³C NMR δ_{ppm} (125 MHz): 54.8(αCH), 27.5(βCH₂), Aromatic-109.0 (C₁), 123.5(C₂, C₃), 136.4(C₄), 120.8(C₅), 124.3(C₆), 118.4(C₇), 120.0(C₈), 66.4(C1), 75.2(C2), 69.2(C3), 73.0(C4), 71.5(C5), 64.2(C6).

6-O-ester 39b: ¹H NMR δ_{ppm}: 3.08(αCH), 3.35(βCH₂), 3.45(H-1), 3.42(H-2), 3.58(H-3), 3.46(H-4), 3.48(H-5), 3.70(H-6); ¹³C NMR δ_{ppm}: 54.7(αCH), 27.2(βCH₂), 64.5(C1), 74.0(C2), 69.0(C3), 74.2(C5), 66.0(C6).

A typical IR spectrum and 2D-HSQCT NMR spectrum for L-tryptophanyl-D-sorbitol **39a** and **b** are shown in Figures 4.42 and 4.43 respectively.

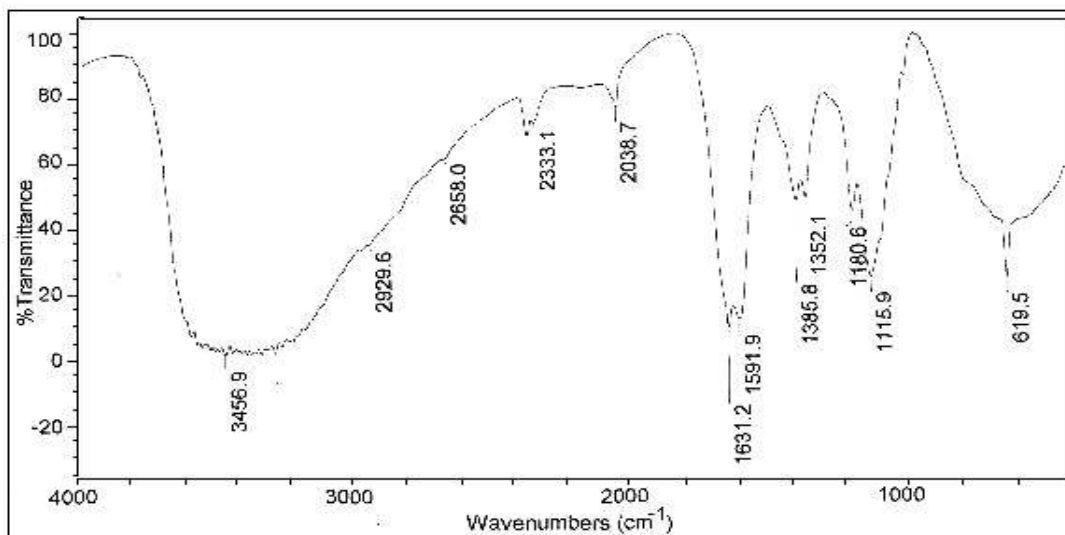


Fig. 4.42. A typical IR spectrum of L-tryptophanyl-D-sorbitol of CRL catalysed reaction. A 2.0 mg of ester sample was prepared as KBr pellet.

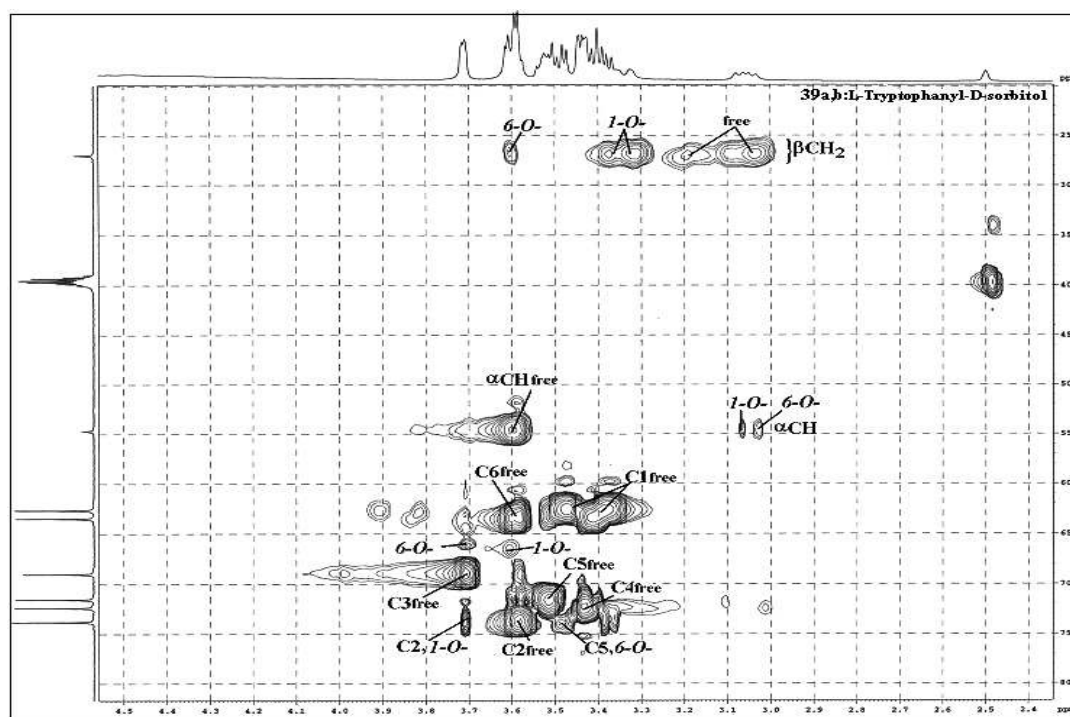
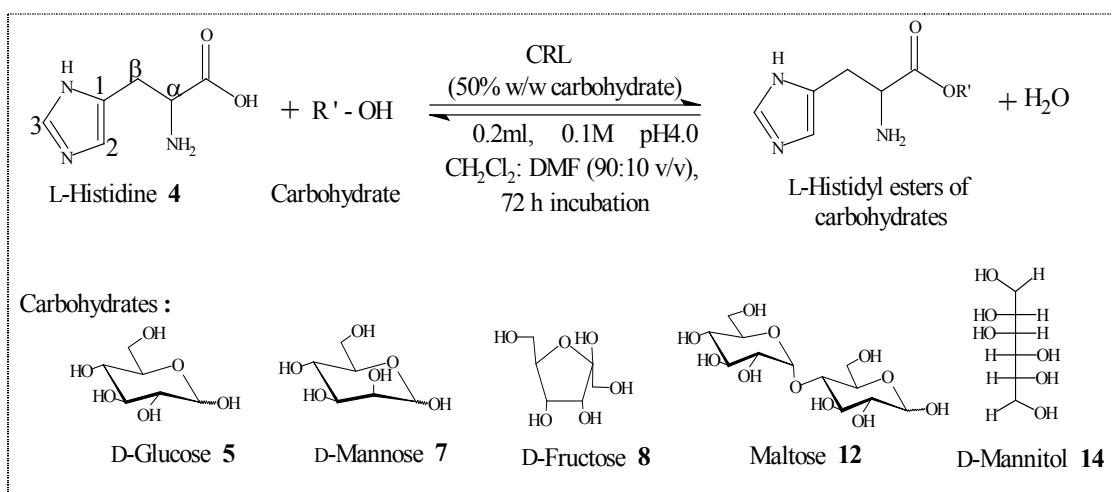


Fig. 4.43. Two-dimensional HSQCT NMR for L-tryptophanyl-D-sorbitol **39a** and **b** reaction mixture

4.2.4. L-Histidyl esters of carbohydrates

L-Histidine is a basic amino acid and the solubility in water is 41.9g/L at 25 °C (Chapman and Halli 1982b).. Esterification of L-histidine with carbohydrates was carried out using CRL under optimal reaction conditions of 1 mmol each of L-histidine and carbohydrates with 50% (w/w based on respective carbohydrate) CRL and 0.2 mM (0.2 mL) pH 4.0 acetate buffer and incubated for 72h (Scheme 4.4). Figure 4.44 shows a typical HPLC profile for L-histidyl-maltose. The HPLC retention time and R_f values are shown in Table 4.8.



Scheme 4.4. CRL catalysed syntheses of L-histidyl esters of carbohydrates

Spectral data for L-histidyl esters of carbohydrates are shown in Section 4.2.4.1 – 4.2.4.8. The shifts in UV transitions for $\sigma \rightarrow \sigma^*$ in the range 210 – 215 nm and $\pi \rightarrow \pi^*$ in the range 264 – 267 nm for the esters compared to $\sigma \rightarrow \sigma^*$ and $\pi \rightarrow \pi^*$ at 204 nm and 251 nm respectively for free L-histidine indicated that L-histidine had undergone esterification. InfraRed spectral data showed that the ester carbonyl stretching frequency for the prepared esters were in the range 1605 - 1720 cm^{-1} compared to 1634 cm^{-1} observed for the carbonyl group of L-histidine indicating that L-histidine carboxylic group had been converted into its corresponding carbohydrate ester. Molecular ion peaks

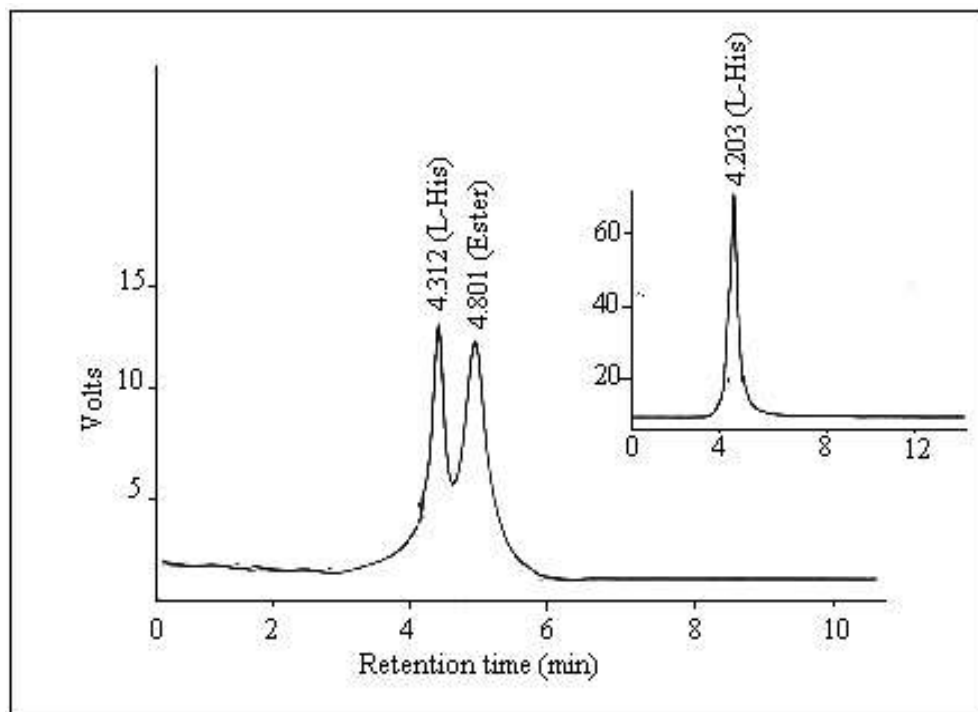


Fig. 4.44. HPLC chromatogram for reaction mixture of L-histidine and maltose esterification reaction catalysed by CRL. Column – C-18; mobile phase – acetonitrile: water (20:80 v/v); flow rate- 1 mL /min; detector – UV at 254 nm; Inset - standard chromatogram of L- histidine; errors in yields are \pm 10-15%.

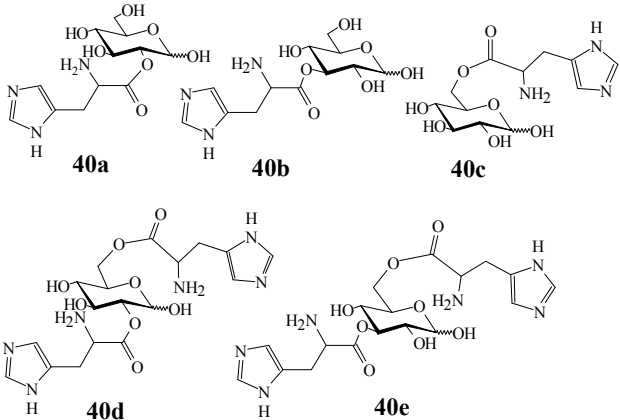
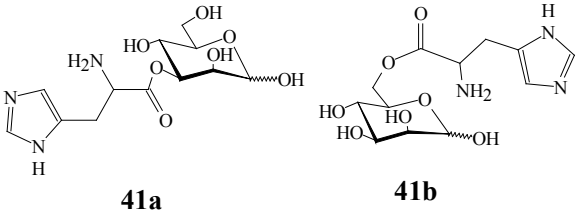
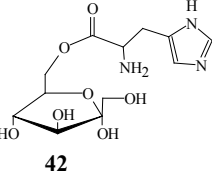
in mass spectrum further confirmed the formation of esters. The percentage proportions of the individual esters formed were determined by taking the peak areas of the C6 or C5 (in case of pentoses) of ^{13}C signals or cross peaks from 2D-NMR. Table 4.9 shows the ester yields from HPLC, types of esters formed and percentage portions of the individual esters.

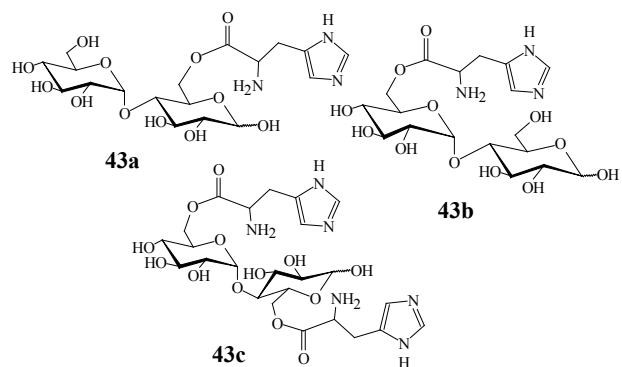
Table 4.8 Retention times and R_f values of L-histidyl esters of carbohydrates

Compound	Retention time (min) ^a	R_f values ^b
L-Histidine	4.2	0.56
L-Histidyl-D-glucose	4.7	0.43
L-Histidyl-D-mannose	4.7	0.41
L-Histidyl-D-fructose	4.8	0.38
L-Histidyl-maltose	4.8	0.32
L-Histidyl-D-mannitol	4.8	0.43

^a Conditions: column – C18; mobile phase – acetonitrile : water (20:80 v/v); flow rate – 1 mL /min; detector – UV at 254 nm; ^b TLC - 20 x 20 cm silica plate (mesh size 60 –120); mobile phase – butanol : acetic acid : water (70:20:10 v/v/v); peak identification – ninhydrin (amino acid) and 1-naphthol (sugar).

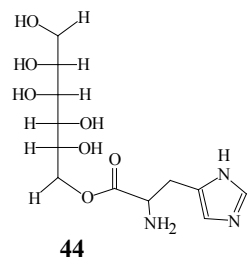
Table 4.9 Syntheses of L-histidyl esters of carbohydrates^a

L-Histidyl esters of carbohydrates	Esterification yield (%)	Esters (% proportions ^b)
 <p>40a 40b 40c</p> <p>40d 40e</p>	<p>32 (mono esters-25, diester-7)</p>	<p>40a: 2-<i>O</i>-L-histidyl-D-glucose (25) 40b: 3-<i>O</i>-L-histidyl-D-glucose (24) 40c: 6-<i>O</i>-L-histidyl-D-glucose (28) 40d: 2,6-<i>di-O</i>-L-histidyl-D-glucose (12) 40e: 3,6-<i>di-O</i>-L-histidyl-D-glucose (11)</p>
 <p>41a 41b</p>	<p>72 (only mono esters)</p>	<p>41a: 3-<i>O</i>-L-histidyl-D-mannose (28) 41b: 6-<i>O</i>-L-histidyl-D-mannose (72)</p>
 <p>42</p>	<p>58 (only monoester)</p>	<p>42: 6-<i>O</i>-L-histidyl-D-fructose</p>



58
(mono esters-42,
diester-16)

43a: 6-*O*-L-histidyl-maltose (38)
43b: 6'-*O*-L-histidyl-maltose (34)
43c: 6,6'-*di-O*-L-histidyl-maltose (28)



62
(only monoester)

44: 1-*O*-L-histidyl-D-mannitol

^a L-Histidine – 1 mmol; carbohydrates – 1 mmol; CRL – 50% (w/w based on respective carbohydrate); buffer – 0.2mM (0.2ml) pH 4.0 acetate buffer; dichloromethane: DMF (90: 10 v/v) at 40 °C; incubation period – 72 h; Conversion yields were from HPLC with respect to L-histidine concentration; ^b The ester proportions were calculated from the area of respective ¹³C signals.

Spectral data for L-histidine 4: Solid; mp- 277 °C; UV (H₂O, λ_{\max}): 204 nm ($\sigma \rightarrow \sigma^*$ $\epsilon_{204} - 660 \text{ M}^{-1}$), 251 nm ($\pi \rightarrow \pi^*$ $\epsilon_{251} - 123 \text{ M}^{-1}$); IR (KBr): 3015 cm⁻¹ (NH), 1634 cm⁻¹ (CO), 1343 cm⁻¹ (CN), 1587 cm⁻¹ (aromatic, -C=C-); $[\alpha]_{\text{D}}^{25} = -39.7^{\circ}$ (c 0.59 H₂O); RT: 4.2 min; R_f: 0.56; 2D-HSQCT (DMSO-d₆): ¹H NMR δ_{ppm} (500.13 MHz): 3.62(α CH, J= 8.2, 4.1 Hz), 3.15(β CH_{2a}, J=12.0, 6.0 Hz), 3.17(β CH_{2b}, J=12.0, 6.0 Hz), Aromatic- 6.87(H₂), 7.68(H₃); ¹³C NMR δ_{ppm} : 54.1(α CH), 27.1(β CH₂), Aromatic-115.0(C₁), 128.4(C₂), 139.2(C₃), 170.4 (CO).

4.2.4.1. L-Histidyl-D-glucose 40a-e:

Solid; UV (H₂O, λ_{\max}): 210 nm ($\sigma \rightarrow \sigma^*$ $\epsilon_{210} - 1072 \text{ M}^{-1}$), 264 nm ($\pi \rightarrow \pi^*$ $\epsilon_{264} - 933 \text{ M}^{-1}$); IR (KBr, cm⁻¹): 3126 (OH), 1720 (CO), 1343 (NH), 1588 (aromatic, -C=C-); $[\alpha]_{\text{D}}^{25} = -33.3^{\circ}$ (c 1.0 H₂O); MS (*m/z*) 318[M+1]⁺; RT: 4.7 min; R_f: 0.43.

2D-HSQCT (DMSO-d₆): **2-O-ester 40a:** ¹H NMR δ_{ppm} (500.13 MHz): 3.08(α CH), 2.70(β CH₂), Aromatic-6.93(H₂), 7.69(H₃), 4.78(H-1 α), 3.86(H-2 α), 3.76(H-2 β), 3.19(H-3 α), 3.12(H-3 β), 3.62(H-4 α), 3.58(H-6a); ¹³C NMR δ_{ppm} (125 MHz): 52.0(α CH), 30.8(β CH₂), Aromatic-115.6(C₁), 134.2(C₂), 134.8(C₃), 171.5(CO), 96.2(C1 α), 75.0(C2 α), 76.7(C2 β), 70.0(C3 α), 80.0(C3 β), 69.3(C4 α), 62.2(C6 α).

3-O-ester 40b: ¹H NMR δ_{ppm} : 3.00(α CH), 2.82(β CH₂), Aromatic- 6.93(H₂), 7.71(H₃), 4.75(H-1 α), 3.60(H-2 α), 3.32(H-2 β), 3.77(H-3 α), 3.93(H-3 β), 3.67(H-4 α), 3.42(H-6a); ¹³C NMR δ_{ppm} : 52.8(α CH), 27.7(β CH₂), Aromatic-116.2(C₁), 134.4(C₂), 134.8(C₃), 171.0(CO), 95.5(C1 α), 72.2(C2 α), 74.9(C2 β), 81.7(C3 α), 83.2(C3 β), 68.9(C4 α), 61.3(C6 α).

6-O-ester 40c: ¹H NMR δ_{ppm} : 2.84(α CH), 3.06(β CH₂), Aromatic - 6.93(H₂), 7.72(H₃), 4.72(H-1 α), 3.59(H-2 α), 3.12(H-3 α), 3.80(H-4 α), 2.90(H-5 α), 3.80(H-6a); ¹³C NMR δ_{ppm} : 51.2(α CH), 26.8(β CH₂) Aromatic- 115.6(C₁), 134.4(C₂), 134.9(C₃), 170.3(CO),

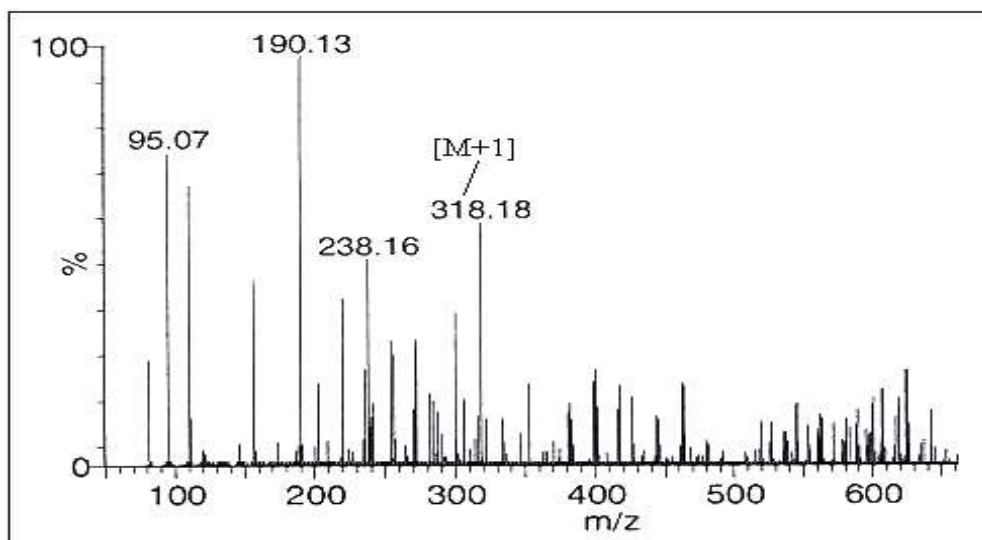


Fig. 4.45. A typical mass spectrum of L-histidyl-D-glucose.

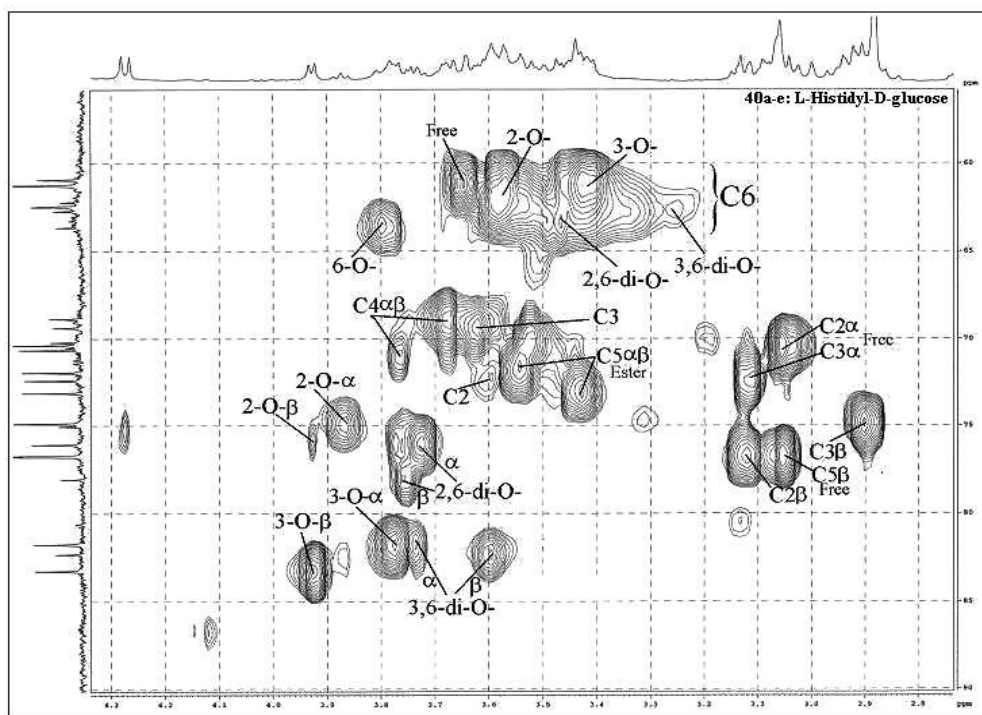


Fig. 4.46. Two-dimensional HSQCT NMR for L-histidyl-D-glucose **40a-e** reaction mixture

95.0(C1 α), 100.2 (C1 β), 72.5(C2 α), 73.1(C3 α), 70.6(C4 α), 75.0(C5 α), 63.6(C6 β).

2,6-di-O-ester 40d: ^1H NMR δ_{ppm} 2.90(αCH), 2.78(βCH_2), 3.73(H-2 α), 3.75(H-2 β), 3.47(H-6b); ^{13}C NMR δ_{ppm} : 52.5(αCH), 30.8(βCH_2), 102.1(C1 β), 76.7(C2 α), 78.0(C2 β), 70.5(C4 α), 62.7(C6 β).

3,6-di-O-ester 40e: ^1H NMR δ_{ppm} : 2.80(βCH_2), 3.73(H-3 α), 3.60(H-3 β), 3.26(H-6b); ^{13}C NMR δ_{ppm} : 30.0(βCH_2), 81.7(C3 α), 82.3(C3 β), 70.2(C4 α), 62.4(C6 β).

A typical mass spectrum and 2D-HSQCT NMR spectrum for L-histidyl-D-glucose **40a-e** are shown in Figures 4.45 and 4.46 respectively.

4.2.4.2. L-Histidyl-D-mannose **41a** and **b**:

Solid; UV (H_2O , λ_{max}): 215 nm ($\sigma \rightarrow \sigma^*$ $\epsilon_{210} - 1413 \text{ M}^{-1}$), 267 nm ($\pi \rightarrow \pi^*$ $\epsilon_{267} - 427 \text{ M}^{-1}$), 321 nm ($n \rightarrow \pi^*$ $\epsilon_{321} - 275 \text{ M}^{-1}$); IR (KBr): 3284 cm^{-1} (OH), 1663 cm^{-1} (CO), 1384 cm^{-1} (CN), 1569 cm^{-1} (aromatic, $-\text{C}=\text{C}-$); $[\alpha]_{\text{D}}^{25} = -15.8^{\circ}$ (c 0.2 H_2O); MS (m/z) 318 $[\text{M}+1]^+$; RT: 4.7 min; R_f : 0.41.

2D-HSQCT (DMSO- d_6): **3-O-ester 41a:** ^1H NMR δ_{ppm} : 3.25(αCH), 1.62(βCH_2), Aromatic- 7.12(H₂), 7.82(H₃), 4.68(H-1 α), 3.62(H-2 α), 3.60(H-3 α), 3.72(H-4 α), 3.54(H-5 α), 3.66 (H-5 β), 3.51(H-6a); ^{13}C NMR δ_{ppm} : 44.8(αCH), 28.4(βCH_2), Aromatic-117.0(C₁), 133.1(C₂), 133.8(C₃), 170.8(CO), 98.2(C1 α), 69.8(C2 α), 79.6(C3 α), 69.2(C4 α), 61.8(C6 β).

6-O-ester 41b: ^1H NMR δ_{ppm} : 3.04(αCH), 2.09(βCH_2), 3.52(H-5 α), 3.49(H-5 β), 3.25(H-6b); ^{13}C NMR δ_{ppm} : 46.2(αCH), 29.8(βCH_2), 170.6(CO), 70.1(C5 α), 78.5(C5 β), 65.2(C6 β).

Two-dimensional HSQCT NMR spectrum for L-histidyl-D-mannose **41a** and **b** is shown in Fig. 4.47.

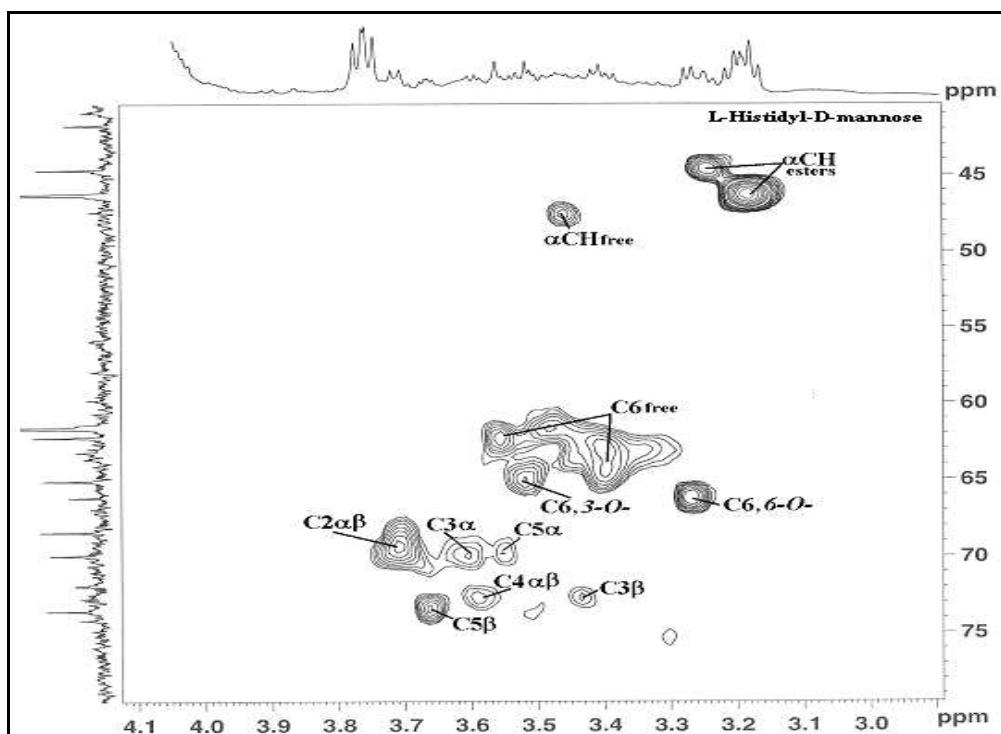


Fig. 4.47. Two-dimensional HSQCT NMR for L-histidyl-D-mannose **41a** and **b** reaction mixture

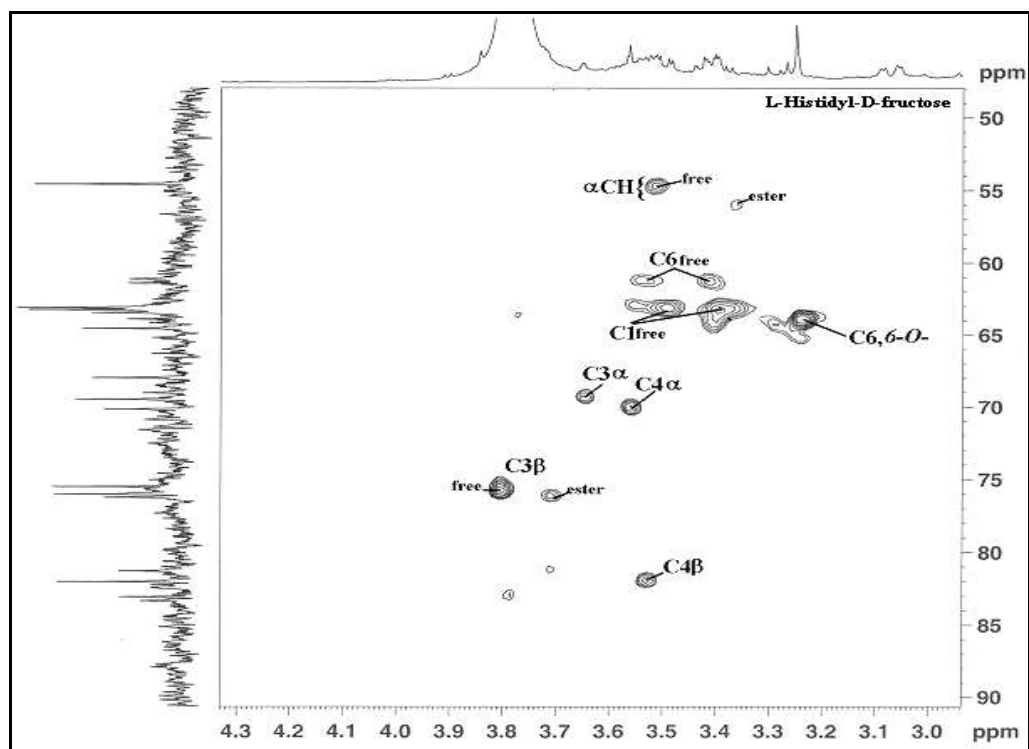


Fig. 4.48. Two-dimensional HSQCT NMR for L-histidyl-D-fructose **42** reaction mixture

4.2.4.3. L-Histidyl-D-fructose **42**:

Solid; mp - 123 °C; UV (H₂O, λ_{\max}): 210 nm ($\sigma \rightarrow \sigma^*$ $\epsilon_{210} - 617 \text{ M}^{-1}$), 267 nm ($\pi \rightarrow \pi^*$ $\epsilon_{267} - 240 \text{ M}^{-1}$), 321 nm ($n \rightarrow \pi^*$ $\epsilon_{321} - 170 \text{ M}^{-1}$); IR (KBr): 3136 cm⁻¹ (OH), 1605 cm⁻¹ (CO), 1393 cm⁻¹ (CN), 1592 cm⁻¹ (aromatic, -C=C-); $[\alpha]_{\text{D}}^{25} = -20.0^\circ$ (*c* 0.6 H₂O); MS (*m/z*) 340[M+Na]⁺; RT: 4.8 min; R_f: 0.38.

2D-HSQCT NMR: **6-O-ester 42**: ¹H NMR δ_{ppm} (500.13 MHz): 3.45(α CH), 3.21(β CH₂), aromatic - 6.85 (H₂), 7.42 (H₃), 3.67(H-3 α), 3.52(H-4 α), 3.24(H-6b); ¹³C NMR δ_{ppm} (125 MHz): aromatic-116.5(C₁), 134.2(C₂), 124.5(C₃), 170.5 (CO), 62.8(C1 α), 102.1(C2 α), 69.2(C3 α), 70.0 (C4 α) 70.6(C4 α), 64.2(C6 α).

Two-dimensional HSQCT NMR spectrum for L-histidyl-D-fructose **42** is shown in Fig. 4.48.

4.2.4.4. L-Histidyl-maltose **43a-c**:

Solid; UV (H₂O, λ_{\max}): 210 nm ($\sigma \rightarrow \sigma^*$ $\epsilon_{210} - 2399 \text{ M}^{-1}$), 267 nm ($\pi \rightarrow \pi^*$ $\epsilon_{267} - 1072 \text{ M}^{-1}$), 324 nm ($n \rightarrow \pi^*$ $\epsilon_{324} - 186 \text{ M}^{-1}$); IR (KBr): 3337 cm⁻¹ (OH), 1654 cm⁻¹ (CO), 1399 cm⁻¹ (CN); $[\alpha]_{\text{D}}^{25} = -20.5^\circ$ (*c* 0.4 H₂O); MS (*m/z*) 480[M+1]⁺; RT: 4.8 min; R_f: 0.32.

2D-HSQCT NMR: **6-O-ester 43a**: ¹H NMR δ_{ppm} : 2.90(α CH), 3.06(β CH), Aromatic- 6.92(H₂), 7.62(H₃), 4.74(H-1 α), 3.63(H-2 α), 3.64(H-3 α), 3.68(H-3 α), 3.66(H-4 α), 3.92(H-6a), 4.20(H-1' α), 3.12(H-4'), 3.80(H-6'); ¹³C NMR δ_{ppm} : 51.2(α CH), 27.3(β CH₂), Aromatic- 114.6(C₁), 135.0(C₂), 134.7(C₃), 171.2(CO), 92.8(C1 α), 79.8(C2 α), 75.8(C3 α), 78.8(C4 α), 64.8(C6 α), 97.2(C1' α), 67.8(C4'), 61.8(C6').

6'-O-ester 43b: ¹H NMR δ_{ppm} : 2.88(α CH), 2.78(β CH₂), 3.28(H-3 α), 4.06(H-4 α), 3.42(H-5 α), 3.51(H-6a), 4.92(H-1' α), 3.14(H-4'), 3.64(H-6'); ¹³C NMR δ_{ppm} :

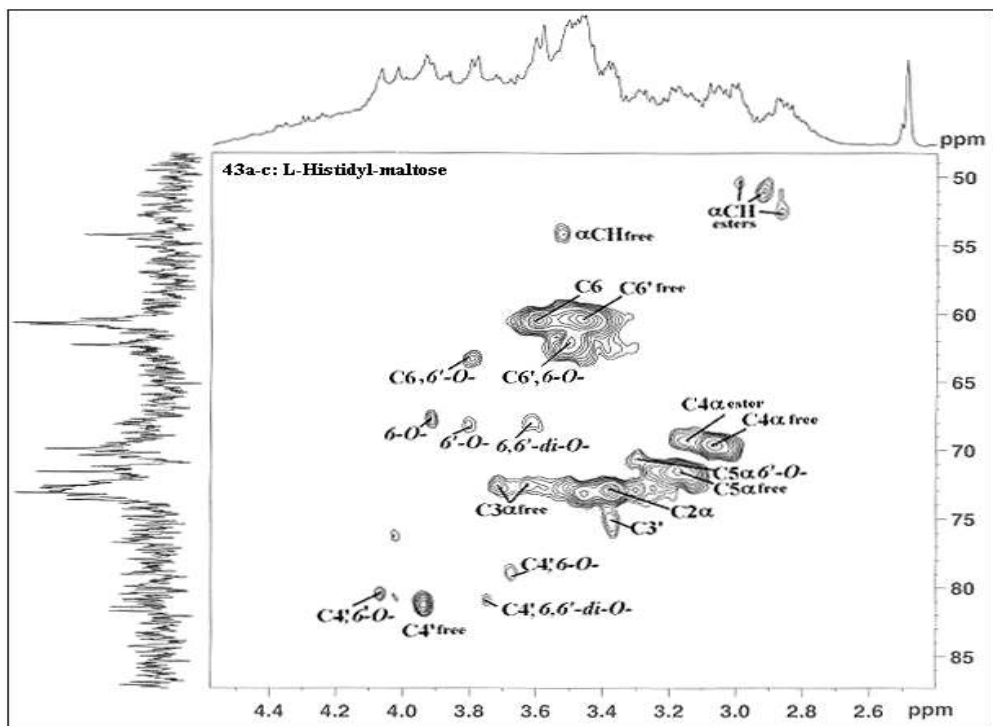


Fig. 4.49. Two-dimensional HSQC NMR for L-histidyl-maltose **43a-c** reaction mixture

52.0(α CH), 27.8(β CH₂), 75.8(C3 α), 80.4(C4 β), 71.2(C5 α), 61.5(C6 α), 100.4(C1' α), 67.9(C4'), 65.4(C6').

6,6'-di-O-ester 43c: ¹H NMR δ_{ppm} : 2.92(α CH), 4.98(H-1 α), 3.78(H-4 α), 3.72(H-6a), 3.70(H-6'); ¹³C NMR δ_{ppm} : 50.0(α CH), 100.6(C1 α), 80.6(C4 α), 65.3(C6 α), 68.9 (C4'), 65.1(C6').

Two-dimensional HSQCT NMR spectrum for L-histidyl-maltose **43a-c** is shown in Fig. 4.49.

4.2.4.5. L-Histidyl-D-mannitol 44:

Solid; mp - 182 °C; UV (H₂O, λ_{max}): 210 nm ($\sigma \rightarrow \sigma^*$ $\epsilon_{210} = 3802 \text{ M}^{-1}$), 267 nm ($\pi \rightarrow \pi^*$ $\epsilon_{267} = 1349 \text{ M}^{-1}$), 324 nm ($n \rightarrow \pi^*$ $\epsilon_{324} = 776 \text{ M}^{-1}$); IR (KBr): 3344 cm⁻¹ (OH), 1631 cm⁻¹ (CO), 1319 cm⁻¹ (CN), 1511 cm⁻¹ (aromatic); $[\alpha]_{\text{D}}^{25} = +17.4^{\circ}$ (*c* 0.23 H₂O); RT: 4.8 min; R_f: 0.43.

2D-HSQCT NMR: **1-O-ester 44:** ¹H NMR δ_{ppm} (500.13 MHz): 3.46 (α CH), 3.32(β CH₂), aromatic - 7.38(H₃), 3.44(H-1), 3.39(H-2), 3.47(H-3), 3.54(H-4), 3.57(H-5), 3.38(H-6); ¹³C NMR δ_{ppm} (125 MHz): 54.3(α CH), aromatic- 128.2(C₂), 123.4(C₃), 63.8(C1, C6), 71.4(C2, C5), 69.8(C3, C4).

UV, IR, mass and 2D-HSQCT NMR spectra for L-histidyl-D-mannitol **44** are shown in Figures 4.50, 4.51, 4.52 and 4.53 respectively

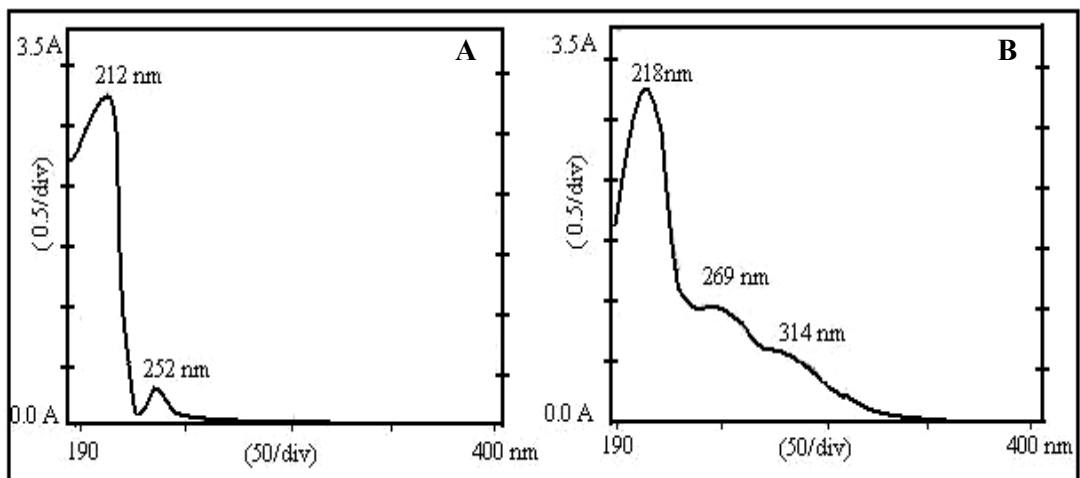


Fig. 4.50. UV spectrum for L-histidyl-D-mannitol of CRL catalysed reaction. (A) L-histidine. (B) L-histidyl-D-mannitol.

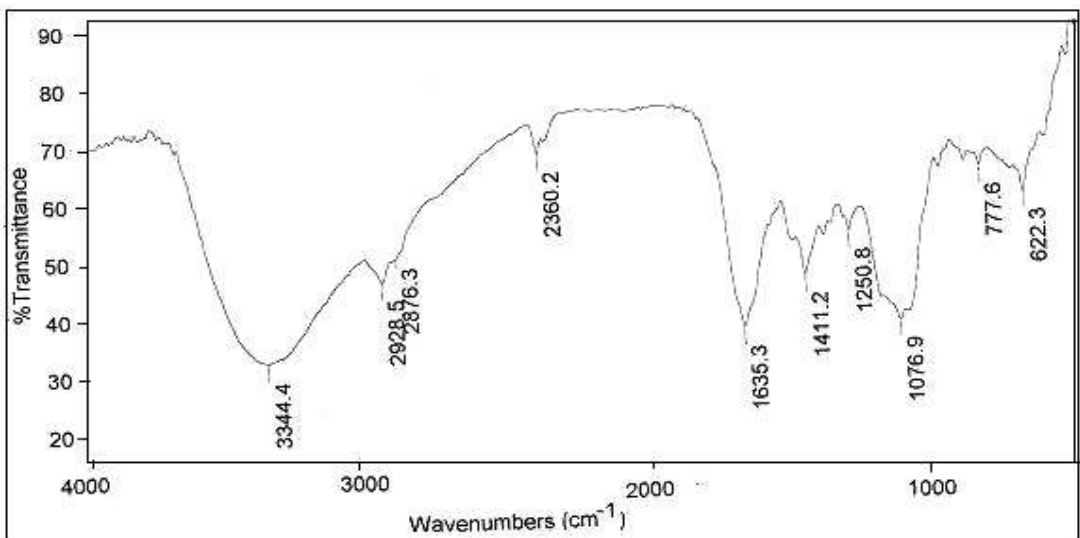


Fig. 4.51. A typical IR spectrum of L-histidyl-D-mannitol of CRL catalysed reaction. A 2.0 mg of ester sample was prepared as KBr pellet.

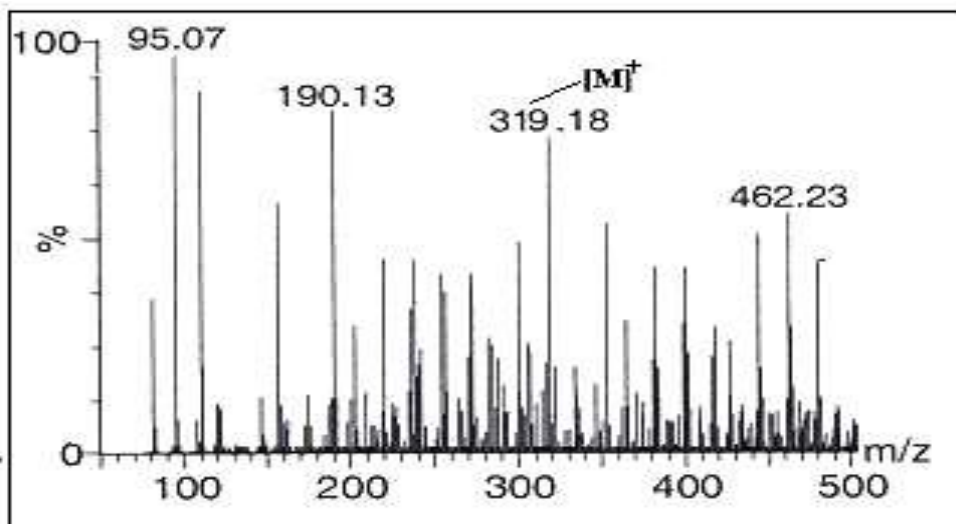


Fig. 4.52. A typical mass spectrum for L-histidyl-D-mannitol

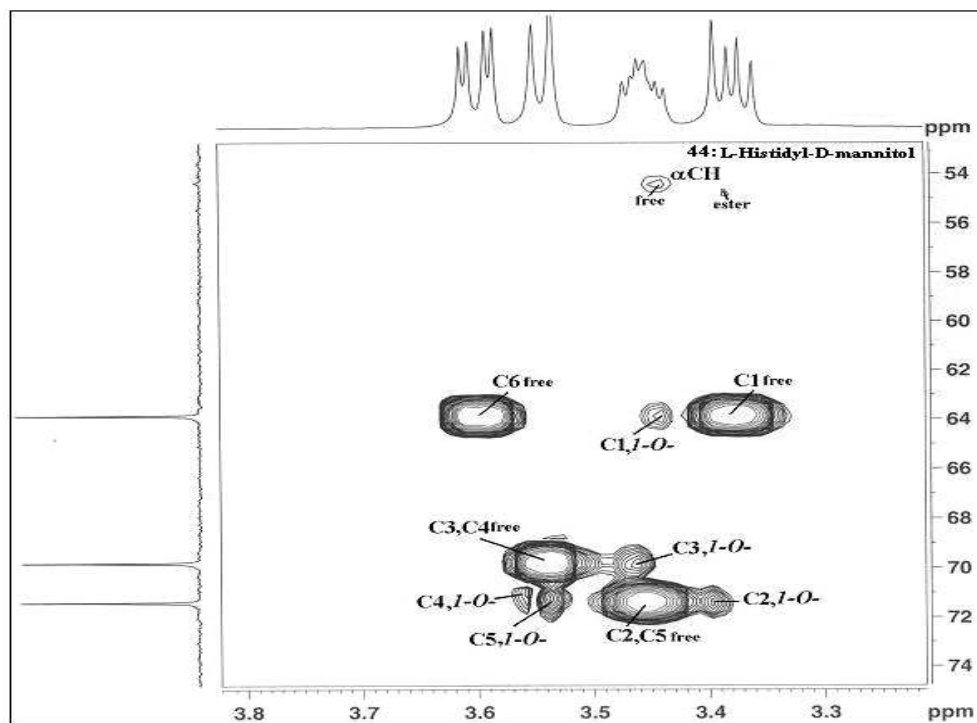


Fig. 4.53. Two-dimensional HSQC NMR for L-histidyl-D-mannitol 44 reaction mixture

4.3. NMR characterization of spectral data for L-prolyl, L-phenylalanyl, L-tryptophanyl and L-histidyl esters of carbohydrates

Two-dimensional HSQCT NMR spectroscopy of all the four amino acyl esters of carbohydrates gave good information on the nature and proportion of the esters formed (Table 4.10). Two-dimensional HSQCT NMR data showed that upfield chemical shift values for α -CH, β -CH₂, heterocyclic or aromatic protons from L-prolyl, L-phenylalanyl, L-tryptophanyl and L-histidyl units indicated that the respective amino acids reacted with the carbohydrates and multiple cross peaks indicated that the reaction occurred at more than one hydroxyl group of the carbohydrate molecules employed.

4.3.1. L-Prolyl esters of carbohydrates 16-23:

The downfield chemical shift values for C1 α at 65.8 ppm and the corresponding proton cross peak at 4.13 ppm in case of **19a** and C1 at 66.1 ppm (¹H at 3.70 ppm) in case of **23a** indicated that *1-O-* esters of D-fructose **8** and D-sorbitol **15** are formed respectively. C2 α in the range 74.8 - 77.7 ppm (¹H at 3.62 - 3.92 ppm) and C2 β in the range 75.3 - 80.0 ppm (¹H at 3.30 - 3.60 ppm) respectively indicated that *2-O-* esters **16a**, **17a** and **22a** are formed with D-glucose **5**, D-galactose **6** and maltose **12** respectively. C3 α and C3 β in the range 75.0 - 84.0 ppm (¹H at 3.55 - 3.93 ppm) confirmed that *3-O-* esters **16b**, **17b**, **18a** and **20a** are formed with **5**, **6**, D-mannose **7** and D-ribose **10** respectively. *4-O-* ester **18b** from **7** was confirmed by C4 α and C4 β at 74.6 and 75.4 ppm (¹H at 3.81 and 3.72 ppm) respectively and *5-O-* ester **20b** from D-ribose **10** was confirmed by C5 α at 65.8 ppm (¹H at 3.20 ppm). C6 in the range 63.1 - 66.4 ppm (¹H at 3.28 - 4.02 ppm) confirmed that L-proline **1** formed *6-O-* esters **16c**, **17c**, **18c**, **19b**, **21a**, **22b** and **23b** with **5**, **6**, **7**, D-fructose **8**, lactose **11**, **12** and D-sorbitol **15** respectively. With lactose **11** and maltose **12**, C6' (non-reducing end) chemical shift values at 62.8 and 63.6 ppm (¹H at 3.45 and 3.28 ppm) respectively indicated that the primary hydroxyl

groups are esterified leading to 6'-*O*- esters **21b** and **22c** respectively. D-Mannose **7** showed 3,6-*di-O*- ester **18d** formation by the cross peaks for C3 α at 81.5 ppm (^1H at 3.54 ppm) and C6 at 62.8 ppm (^1H at 3.46 ppm) and 4,6-*di-O*- ester **18e** formation by the cross peaks for C4 α at 76.4 ppm (^1H at 3.61 ppm), C4 β at 79.0 ppm (^1H at 3.61 ppm) and C6 at 63.0 ppm (^1H at 3.38 ppm). D-Fructose **8** showed 1,6-*di-O*- ester **19c** through cross peaks for C1 α at 66.5 ppm and C6 at 66.2 ppm (^1H at 4.37 and 4.28 ppm respectively).

4.3.2. L-Phenylalanyl esters of carbohydrates 24-31:

Formation of 1-*O*- esters, **27a** and **31a** respectively, are characterized by the downfield chemical shift values for C1 α of **8** at 64.9 ppm and C1 of D-mannitol **14** at 66.0 ppm (^1H at 3.38 ppm). C2 α in the range 70.3 - 77.3 ppm (^1H at 3.33 - 3.88 ppm) confirmed that 2-*O*- esters **24a**, **25a** and **28a** are formed in case of **5**, **6** and **9** respectively. C3 α and C3 β in the range 81.5 - 84.0 ppm indicated formation of 3-*O*- esters **24b**, **25b**, and **26a** respectively with **5**, **6**, and **7**. C4 α and C4 β at 77.8 and 75.6 ppm respectively for **26b** from **7** indicated 4-*O*- ester and C5 α at 63.3 ppm (^1H at 3.43 ppm) for **28b** from **9** indicated the formation of 5-*O*- ester. C6 in the range 63.1 - 65.0 ppm indicated that 6-*O*- esters **24c**, **25c**, **26c**, **27b**, **29a**, and **30a** are formed in case of **5**, **6**, **7**, **8**, **11** and **12** respectively. 6'-*O*- esters formation were deduced from C6' (non-reducing end) signals in **29b** at 63.1 ppm (^1H at 3.45 ppm) from **11** and 63.5 ppm for **30b** from **12**. Diverse diesters formation were detected clearly by NMR. The set of cross peaks for C1 and C6 centered at 66.8 ppm (^1H at 3.46 ppm) indicated 1,6-*di-O*- ester **31b** is formed with **14**. Similarly 2,5-*di-O*- ester **28c** from **9** was confirmed by C2 α and C2 β at 75.4 and 75.2 ppm (^1H at 3.46 and 3.40 ppm) respectively and C5 α at 63.1 ppm (^1H at 3.51 ppm). Formation of 2,6-*di-O*- esters **24d** from **5** was confirmed through C2 α at 77.0 ppm (^1H at

3.67 ppm) and C6 at 62.1 ppm (^1H at 3.61 ppm) and **25d** from **6** was confirmed through C2 α at 77.2 ppm and C6 at 63.1 ppm (^1H at 3.61 ppm). 3,6-*di-O*- esters **24e**, **25e** and **26d** formation from **5**, **6** and **7** respectively were confirmed by C3 α and C3 β in the range 81.8 - 84.0 ppm and C6 in the range 62.7 – 64.8 ppm. Similarly, 4,6-*di-O*- ester **26e** from **7** was confirmed by C4 α at 76.3 ppm and C6 at 63.2 ppm. Lactose **11** showed 6,6'-*di-O*- ester **29c** formation by the cross peaks for C6 (reducing end) at 62.4 ppm (^1H at 3.45 ppm) and C6' (non reducing end) at 62.7 ppm (^1H at 3.46 ppm).

4.3.3. L-Tryptophanyl esters of carbohydrates 32-39:

Among the aldohexoses only D-glucose gave five L-tryptophanyl-D-glucose esters **32a-e**. Downfield chemical shift values for C1 at 66.2 and 66.4 ppm (^1H at 4.32 and 3.58 ppm) indicated 1-*O*- esters **35a** and **39a** formation from **8** and **15** respectively. C2 α and C2 β in the range 75.9 - 81.3 ppm (^1H at 3.65 - 3.75 ppm) showed 2-*O*- esters **32a** and **37a** from **5** and **12** respectively. C3 α,β centered at 82.0 ppm (H3 α at 3.92 ppm and H3 β 3.59 ppm) confirmed formation of 3-*O*- ester **32b** from **5**. C6 in the range 63.0 - 66.8 ppm (^1H at 3.42 - 4.38 ppm) indicated that 6-*O*- esters **32c**, **33**, **34**, **35b**, **36a**, **37b**, **38** and **39b** are formed from carbohydrates **5**, **6**, **7**, **8**, **11**, **12**, **13** and **15** respectively. 6'-*O*- ester **37c** from **11** was confirmed by the cross peak for C6' at 63.6 ppm (^1H at 3.30 ppm). From **5**, diesters 2,6-*di-O*- **32d** was confirmed by C2 α and C2 β at 77.0 and 77.3 ppm (^1H at 3.92 and 3.82 ppm) respectively and C6 at 63.2 ppm and 3,6-*di-O*- **32e** was confirmed by C3 α at 81.2 ppm (^1H at 3.74 ppm) with C6 at 63.9 ppm (^1H at 3.44 ppm). Diester 6,6'-*di-O*- **37d** from **12** was confirmed by the cross peaks for C6 at 62.9 ppm (^1H at 3.83 ppm) and C6' at 62.8 ppm (^1H at 3.32 ppm).

4.3.4. L-Histidyl esters of carbohydrates 40-44:

Five C6 signals in L-histidyl-D-glucose **40a-e** clearly indicated the formation of five different esters. In case of D-mannitol **14**, *1-O-* ester **44** formation is confirmed by the downfield chemical shift value for C1 at 63.8 ppm (^1H at 3.44 ppm). C2 α and C2 β at 75.0 and 76.7 ppm (^1H at 3.86 and 3.76 ppm) respectively indicated that *2-O-* ester **40a** is formed from **5**. C3 α and C3 β in the range 79.6 - 83.2 ppm (^1H at 3.60 - 3.93 ppm) for **40b** and **41a** indicated that *3-O-* esters are formed from the respective carbohydrate molecules **5** and **7**. C6 in the range 63.6 - 65.2 ppm (^1H - 3.25 - 3.92 ppm) indicated that *6-O-* esters **40c**, **41b**, **42** and **43a** are formed from **5**, **7**, **8** and **12** respectively. From **12**, C6' (non-reducing end) at 65.4 ppm (^1H at 3.64 ppm) indicated the formation of *6'-O-* ester **43b**. From **5**, formation of *2,6-di-O-* ester **40d** was confirmed by C2 α and C2 β at 76.7 and 78.0 ppm (^1H at 3.73 and 3.75 ppm) respectively and C6 at 62.7 ppm (^1H at 3.47 ppm) and *3,6-di-O-* **40e** was confirmed by C3 α and C3 β at 81.7 and 82.3 ppm (^1H at 3.73 and 3.60 ppm) respectively. From **12**, *6,6'-di-O-* ester **43c** formation was confirmed through the cross peaks for C6 at 65.1 ppm (^1H at 3.70 ppm) and C6' at 65.3 ppm (^1H at 3.72 ppm).

4.4. Discussion

Aldohexoses, aldopentoses, ketose, carbohydrate alcohols and disaccharides contain several hydroxyl groups, which can give lot of diastereomeric esters (mono, di, tri, tetra and penta) from both the anomers in some cases and several such esters from the other carbohydrate molecules as well. Since the reactions were carried out at a low temperature of 40 °C, the formation of peptides were less than 3%, even though unprotected L-amino acids were employed for the reaction. Maillard and Pictet Spengler phenolic condensation products are also possible in such reactions (Manini et al. 2005). However, no such products were observed in the present work as, such reactions require high

temperature of the order of 90 °C. Mass as well as NMR also detected no Maillard products in the present investigation.

Candida rugosa lipase showed broad substrate specificity towards amino acids as well as carbohydrates (Table 4.10). The present work describes preparation of 29 L-amino acyl esters of carbohydrates of which 19 esters have not been reported before. Unreported esters are L-prolyl-D-glucose **16a-c**, L-prolyl-D-galactose **17a-c**, L-prolyl-D-mannose **18a-e**, L-prolyl-D-ribose **19a** and **b**, L-prolyl-D-fructose **20a-c**, L-prolyl-lactose **21a** and **b**, L-prolyl-maltose **22a-c**, L-prolyl-D-sorbitol **23a** and **b**, L-phenylalanyl-D-arabinose **28a-c**, L-tryptophanyl-D-mannose **33**, L-tryptophanyl-D-galactose **34**, L-tryptophanyl-D-fructose **35a** and **b**, L-tryptophanyl-lactose **36a** and **b**, L-tryptophanyl-maltose **37a-d**, L-histidyl-D-glucose **40a-e**, L-histidyl-D-mannose **41a** and **b**, L-histidyl-D-fructose **42**, L-histidyl-maltose **43a-c** and L-histidyl-D-mannitol **44**. D-Glucose **5**, D-mannose **7**, D-fructose **8** and maltose **12** have reacted with all the four amino acids **1-4**. D-Glucose gave five diastereomeric esters with L-phenylalanine **24a-e**, L-tryptophan **32a-e** and L-histidine **40a-e**, the only exception being L-proline where only three monoesters **16a-c** are formed. Aldohexoses (D-glucose, D-mannose and D-galactose), ketose (D-fructose) and the disaccharides (lactose and maltose) showed better conversions with all the four amino acids. Least conversions were observed for carbohydrate alcohols and sucrose esters. Among the four amino acids investigated, L-tryptophan showed lesser conversion (7-70%) to esters compared to the other three amino acids (20-79%). L-Tryptophan could not form stable acyl enzyme complex due to its bulkiness and its transfer to the carbohydrate moiety could also be sterically difficult. L-Prolyl as well as L-phenylalanyl esters showed better conversion (20-79%) followed by L-histidyl esters (32-72%, Table 4.10). L-Histidine reacted only with D-glucose, D-mannose, D-fructose, maltose and D-mannitol. L-Histidine could be a less efficient acyl

Table 4.10. Percentage yields and proportions of L-prolyl, L-phenylalanyl, L-tryptophanyl and L-histidyl esters of carbohydrates from CRL catalysed reactions ^a

Carbohydrate	L-Prolyl		L-Phenylalanyl		L-Tryptophanyl		L-Histidyl	
	Yield ^a	% Proportions	Yield ^a	% Proportions	Yield ^a	% Proportions	Yield ^a	% Proportions
D-glucose	62	16a: 2-O- Ester (26) 16b: 3-O- Ester (26) 16c: 6-O- Ester (48)	79	24a: 2-O- Ester (19) 24b: 3-O- Ester (23) 24c: 6-O- Ester (25) 24d: 2,6-di-O- Ester (17) 24e: 3,6-di-O- Ester (16)	42	32a: 2-O- Ester (22) 32b: 3-O- Ester (21) 32c: 6-O- Ester (38) 32d: 2,6-di-O- Ester (10) 32e: 3,6-di-O- Ester (9)	32	40a: 2-O- Ester (25) 40b: 3-O- Ester (24) 40c: 6-O- Ester (28) 40d: 2,6-di-O- Ester (12) 40e: 3,6-di-O- Ester (11)
D-galactose	52	17a: 2-O- Ester (20) 17b: 3-O- Ester (12) 17c: 6-O- Ester (68)	45	25a: 2-O- Ester (19) 25b: 3-O- Ester (20) 25c: 6-O- Ester (32) 25d: 2,6-di-O- Ester (16) 25e: 3,6-di-O- Ester (13)	27	33: 6-O- Ester	44	--
D-mannose	40	18a: 3-O- Ester (21) 18b: 4-O- Ester (20) 18c: 6-O- Ester (24) 18d: 3,6-di-O- Ester (19) 18e: 4,6-di-O- Ester (16)	62	26a: 3-O- Ester (18) 26b: 4-O- Ester (18) 26c: 6-O- Ester (39) 26d: 3,6-di-O- Ester (13) 26e: 4,6-di-O- Ester (12)	34	34: 6-O- Ester	72	41a: 3-O- Ester (28) 41b: 6-O- Ester (72)
D-fructose	61	19c: 1-O- Ester (31) 19b: 6-O- Ester (42) 19c: 1,6-di-O- Ester (27)	50	27a: 1-O- Ester (28) 27b: 6-O- Ester (72)	18	35a: 1-O- Ester (45) 35b: 6-O- Ester (55)	58	42: 6-O- Ester
D-arabinose	--	--	64	28a: 2-O- Ester (35) 28b: 5-O- Ester (44) 28c: 2,5-di-O-Ester (21)	--	--	--	--
D-ribose	41	20a: 3-O- Ester (35) 20b: 5-O- Ester (65)	--	--	--	--	--	--
lactose	68	21a: 2-O- Ester (27) 21b: 6-O- Ester (38) 21c: 6'-O- Ester (35)	61	29a: 6-O- Ester (42) 29b: 6'-O- Ester (31) 29c: 6,6'-di-O- Ester (27)	42	36a: 6-O- Ester (64) 36b: 6'-O- Ester (36)	--	--
maltose	66	22a: 2-O- Ester (29) 22b: 6-O- Ester (38) 22c: 6'-O- Ester (33)	60	30a: 6-O- Ester (59) 30b: 6'-O- Ester (41)	70	37a: 2-O- Ester (13) 37b: 6-O- Ester (38) 37c: 6'-O-Ester (29) 37d: 6,6'-di-O- Ester (20)	58	43a: 6-O- Ester (40) 43b: 6'-O-Ester (32) 43c: 6,6'-di-O Ester (28)
sucrose	--	--	--	--	7	38: 6-O- Ester	--	--
D-sorbitol	20	23a: 1-O- Ester (73) 23b: 6-O- Ester (27)	--	--	8	39a: 1-O- Ester (79) 39b: 6-O- Ester (21)	8	--
D-mannitol	--	--	43	31a: 1-O- Ester (62) 31b: 1,6-di-O-Ester (38)	--	--	62	44: 1-O- Ester

^a Confirmation of esters and their percentage proportions were determined by 2D-HSQC NMR. Conversion yields are an average from two experiments. ^b Yields from HPLC. Errors in yield measurements will be \pm 10%.

donor compared to the other amino acids. This could be due to the extra hydrogen bonding potentialities of the imidazolium hydrogens of histidine compared to the other amino acids studied.

D-Arabinose, D-mannitol and sucrose in case of L-proline, D-ribose, sucrose and D-sorbitol in case of L-phenylalanine, D-arabinose, D-ribose and D-mannitol in case of L-tryptophan did not undergo any reaction. L-tryptophanyl-D-galactose 33, L-tryptophanyl-D-mannose 34, L-tryptophanyl-sucrose 38, L-histidyl-D-fructose 42 and L-histidyl-D-mannitol 44 formed only 6-*O*- ester. D-Ribose reacted only with L-proline 20a and b and D-arabinose only with L-phenylalanine 28a-c. Both L-tryptophan and L-histidine did not react with D-ribose and D-arabinose.

Nature of the products clearly indicated that primary hydroxyl groups of the carbohydrates (*1-O*-, *5-O*-, *6-O*-, *6'-O*- and *6,6'-di-O*-) esterified predominantly over secondary hydroxyl groups (*2-O*-, *3-O*- and *4-O*-). Among the secondary hydroxyl groups, *4-O*- ester was formed only in case of D-mannose. Carbohydrates containing axial hydroxyl groups in axial position like C2 in D-mannose and D-ribose and C4 in D-galactose, have not reacted indicating that esterification with axial secondary hydroxyl groups are difficult, especially with bulky amino acyl groups.

Generally, the anomeric hydroxyl groups of carbohydrate molecules did not react because of rapid glycosidic ring opening and closing process. Loss of specificity could be due to use of larger amount of enzymes (about 50% w/w of carbohydrate), which gave a large number of esters.

Carbohydrates like D-arabinose, D-ribose, sucrose, D-sorbitol and D-mannitol reacted selectively depending on the amino acid indicating that they may not be good nucleophiles. This could be due to the steric factor involved like smaller size in case D-ribose and D-arabinose, more hydrogen bonding propensity in case of sugar alcohols and

steric hindrance in case of sucrose. The ease and the firmness with which the carbohydrate molecule binds to the active site of CRL could be the deciding factor. In case of aldopentoses (D-arabinose and D-ribose), NMR spectrum clearly indicated degradation and/or ring opening during the reaction. In case of L-phenylalanyl-D-arabinose, opening of the five membered ring during esterification was noticed by a large number of signals in the 4.0 – 5.0 ppm (^1H) and 65 - 75 ppm (^{13}C) region which could be due to excess strain on the ring due to introduction of bulky amino acid groups to D-arabinose -OH groups. Thus, this study has shown that amino acyl esters of carbohydrates using bulky aromatic and cyclic amino acid molecules could be prepared enzymatically with ease and good selectivity

4.5. Experimental

4.5.1. Esterification procedure

Esterification was carried out in a flat bottom two necked flask by reacting 0.001 mol unprotected L-amino acid (L-proline **1**, L-phenylalanine **2**, L-tryptophan **3** and L-histidine **4**) and 0.001 mol of carbohydrate (D-glucose **5**, D-galactose **6**, D-mannose **7**, D-fructose **8**, D-arabinose **9**, D-ribose **10**, lactose **11**, maltose **12**, sucrose **13**, D-sorbitol **14**, D-mannitol **15**) along with 100 mL CH₂Cl₂: DMF (90:10 v/v, 40 °C) in presence of 0.75 - 0.180 g of lipases (50% w/w carbohydrate employed) under reflux for a period of three days. *Candida rugosa* lipase (CRL) in presence of 0.2 mM (0.2 mL) pH 4.0 acetate buffer to impart 'pH memory' to the enzyme was employed. The condensed vapour of solvents which formed an azeotrope with water was passed through a desiccant (molecular sieves of 4Å were used as desiccant) before being returned into the reaction mixture, thereby facilitating complete removal of water of reaction (Lohith and Divakar 2005). This set up maintained a very low water activity of $a_w = 0.0054$ throughout the reaction period. After completion of the reaction, the solvent was distilled off and 20- 30 mL of warm water was added, stirred and filtered to remove the lipase. The filtrate was evaporated to get a mixture of the unreacted carbohydrate, unreacted L-amino acids and the product esters, which were then analyzed by HPLC. The conversion yields were determined with respect to peak areas of the L-amino acid and that of the esters. The esters formed were separated by size exclusion chromatography using Sephadex G-10, G-25 and Bio Gel P-2 as column materials and eluted with water. Although, the esters were separated from unreacted amino acids and carbohydrates by this procedure, the individual esters in the mixture of esters formed could not be separated. This could be due to the similar polarity of the ester molecules. The product esters separated were subjected to spectral characterization by UV, IR, mass, specific rotation and 2D-NMR.

4.5.2. High Performance Liquid Chromatography

A Shimadzu LC 10AT HPLC connected to LiChrosorb RP-18 column (5 μ m particle size, 4.6 x 150 mm length) with acetonitrile and water in the ratio 20: 80 (v/v) as a mobile phase at a flow rate of 1 mL/ min was employed using an UV detector at 254 nm in case of L-tryptophan and L-histidine reactions and 210 nm in case of L-proline reactions.

4.5.3. Spectral characterization

A Shimadzu UV – 1601 spectrophotometer was used for recording UV spectra of the isolated esters in water at 0.2 - 1.0 mM concentrations. A Nicolet 5700 FTIR instrument was used for recording the IR spectra with a 2.0 - 3.0 mg of ester sample as KBr pellet. Specific rotation of the isolated esters were measured at 25 $^{\circ}$ C using Perkin-Elmer 243 polarimeter with a 0.2 – 1.2 % solution of the esters in water. Mass spectra of the isolated esters were recorded using a Q-TOF Waters Ultima instrument (No.Q-Tof GAA 082, Waters corporation, Manchester, UK) fitted with an electron spray ionization (ESI) source.

4.5.4. Nuclear Magnetic Resonance Spectroscopy

4.5.4.1. ^1H NMR

A Bruker DRX-500 MHz spectrometer operating at 500.13 MHz was used to record ^1H NMR. A 40 mg of sample was dissolved in 0.5 mL of DMSO- d_6 solvent. About 50-200 scans were accumulated with a recycle period of 2-3 seconds to obtain good spectra. The spectra were recorded at 35 $^{\circ}$ C with TMS as internal standard for measuring the chemical shift values to within ± 0.001 ppm. A region from 0 –10 ppm was scanned for all the samples.

4.5.4.2. ^{13}C NMR

A Bruker DRX-500 MHz spectrometer operating at 125 MHz was used to record ^{13}C NMR. A region from 0-200 ppm region was scanned and about 500 – 6000 scans were accumulated for each spectrum to get good spectrum. TMS was taken as an internal standard. Samples were dissolved in 0.5 mL of DMSO- d_6 and recorded at 35 °C.

4.5.4.3. Two-dimensional HSQCT

Two dimensional Heteronuclear Multiple Quantum Coherence Transfer spectra (2-D HMQCT) and Heteronuclear Single Quantum Coherence Transfer spectra (2-D HSQCT) were recorded at 500 MHz on a Bruker DRX-500 MHz spectrometer (500.13 MHz for ^1H and 125 MHz ^{13}C). Chemical shift values were expressed in ppm relative to internal tetramethylsilane standard. About 40mg of the sample dissolved in DMSO- d_6 was used for recording the spectra.

Chapter-5
Competitive inhibition by substrates in
Rhizomucor miehei* and *Candida rugosa
lipases catalyzed esterification of
D-glucose with L-phenylalanine

5.1. Introduction

In recent years, lipases (EC 3.1.1.3) have been successfully used in organic solvents for the synthesis of esters. Lipase is a single-domain molecule belonging to the family of α/β hydrolase proteins (Derewenda *et al.* 1992; Grochulski *et al.* 1993). Most of the lipases reported contain Ser-His-Asp/Glu catalytic triads in their active site (Grochulski *et al.* 1993) with exceptions like esterases from *Streptomyces scabies* which contain only Ser 14 and His 283 (Wei *et al.* 1995). Many reports available on lipase catalysed reactions in organic solvents deal with reaction kinetics of esterification (Yadav and Trivedi 2003; Kiran and Divakar 2002; Janssen *et al.* 1999; Lortie *et al.* 1993), racemization (Duan *et al.* 1997) and hydrolysis (Van-Tol *et al.* 1995). In some esterification reactions, lipases follow Ping-Pong Bi-Bi mechanism (Zhang *et al.* 2005; Zaidi *et al.* 2002; Yadav and Lathi 2004). Chulalaksananukul *et al.* (1990) first proposed that kinetics of *Rhizomucor miehei* lipase catalyzed esterification of ethyl oleate followed Ping Pong Bi Bi mechanism. This mechanism involves binding of acid and alcohol in successive steps releasing water and the product ester again in succession. The kinetic investigation of RML catalysed synthesis of isoamyl acetate followed Ping-Pong Bi-Bi mechanism with competitive inhibition by the substrates and product forming dead end inhibitor complexes (Rizzi *et al.* 1992). Bousquet-Dubouch *et al.* (2001) reported a competitive inhibition in CRL catalyzed alcoholysis of methylpropionate, in which water was also found to be a competitive inhibitor with a higher inhibition constant than *n*-propanol. Kinetic behaviour of CRL in the esterification of long chain fatty acids and alcohols (Zaidi *et al.* 2002) and tetrahydrofurfuryl alcohol with butyric acid (Yadav and Devi 2004) showed that both the reactions followed Ping-Pong Bi-Bi mechanism with competitive inhibition by both the substrates

In the present work, comparative kinetic investigations were carried out involving lipases from *Rhizomucor miehei* and *Candida rugosa* on the esterification reaction between L-phenylalanine and D-glucose to form L-phenylalanyl-D-glucose. The results from these investigations are described below.

5.2. Present work

For each concentration of D-glucose and L-phenylalanine, individual experiments in duplicate (30 x 2 lipases) were performed for incubation periods of 3h, 6h, 12h, 24h and 36h. Initial velocities (v) were determined from the initial slope values of the plots from amounts of esters (conversion yields, M) formed versus incubation periods (h). R^2 values obtained from least square analysis for the initial velocities in both the cases were found to be 0.85-0.95.

Typical rate plots for RML and CRL catalysed reactions is shown in Fig. 5.1. In case of RML catalysed reactions, initial velocities (v) were found to be in the range 35×10^{-6} to 245×10^{-6} M/h.mg protein and CRL catalysed experiments showed initial velocities in the range 40×10^{-6} to 325×10^{-6} M/h.mg protein. At initial periods of incubation, the reaction is relatively fast due to shift in equilibrium towards the esterification direction and slows down at longer incubation periods beyond 24 h resulting from a stable steady-state equilibrium. Effect of external mass transfer phenomenon - internal and external diffusion (Marty *et al.* 1992; Yadav and Devi 2004), if any, in case of RML and CRL enzymes employed in this reaction were not tested in this present work.

5.2.1. *Rhizomucor miehei* lipase catalysis

Double reciprocal plots were constructed and the reciprocal plot patterns for the two substrates in RML catalysed reactions are almost symmetrical (Figures 5.2 and 5.3). The double reciprocal plots shown in the present work were constructed from all the

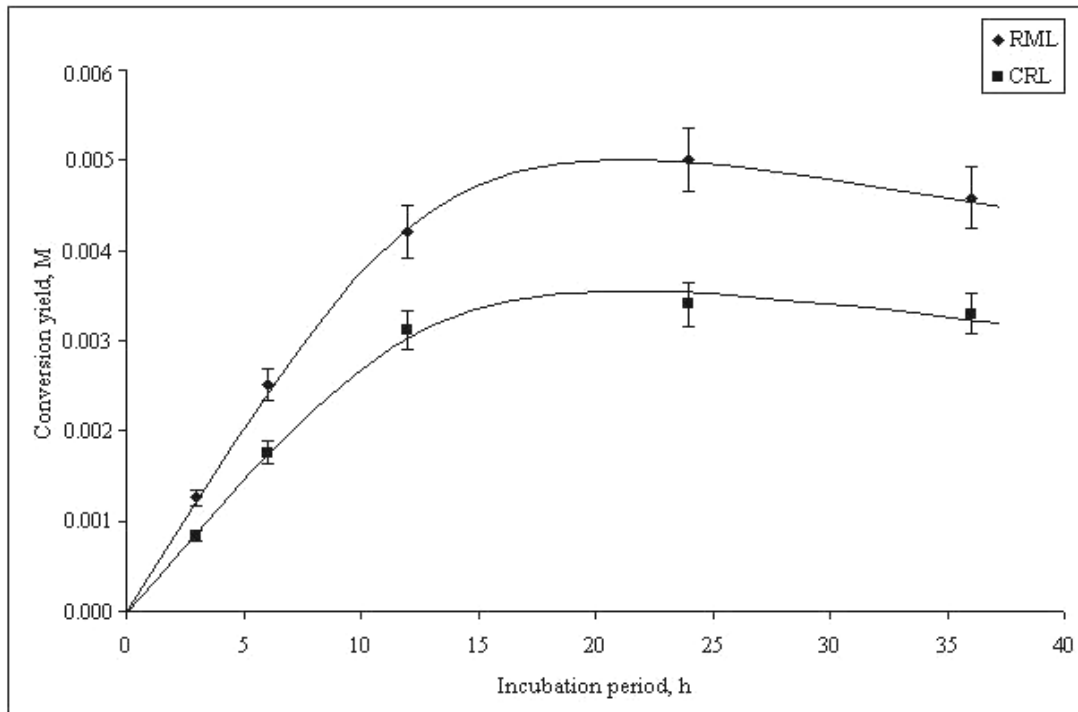


Fig. 5.1 Initial rate (v) plots - conversion yields versus incubation period: (—◆— RML and —■— CRL). Reaction conditions are: CH₂Cl₂: dimethylformamide (90:10 v/v), RML/CRL – 90mg. L-phenylalanine – 0.015 M, D-glucose – 0.01 M, 0.2 ml, 0.1 M, pH 4.0 acetate buffer.

experimentally determined initial rate values and few initial rate values determined from the curve-fitting procedure. Figure 5.2 shows $1/v$ versus $1/[D\text{-glucose}]$ plots, exhibiting series of curves obtained for different fixed level concentrations of L-phenylalanine at varying D-glucose concentrations. Slight increase in rates are observed at lower D-glucose concentrations and at higher concentrations of D-glucose, the rates reduce drastically. Figure 5.3 shows $1/v$ versus $1/[L\text{-phenylalanine}]$ plots, exhibiting series of curves obtained for different fixed level concentrations of D-glucose at varying L-phenylalanine concentrations. Here also, slight increase in rates are observed at lower L-phenylalanine concentrations and at higher concentrations of L-phenylalanine, the rates reduce drastically. When either substrate is varied at different fixed levels of the other, the plots curve up as they approach the $1/v$ – axis. As the concentration of the fixed substrate increases, the minimum points moves closer to the $1/v$ -axis as the fixed substrate overcomes the inhibition by varied substrate and the slope of the reciprocal plot increases as the fixed substrate introduces its own inhibitory effect. Figures 5.4 and 5.6 show the replots of slopes from Figures 5.2 and 5.3 respectively.

The plots in Figures 5.2 and 5.3 showed that the kinetics could be best described by (Segel 1993) Ping-Pong Bi-Bi model with competitive double substrate inhibition leading to dead-end inhibition by EB (RML-D-glucose complex) and FA (L-phenylalanyl-RML-L-phenylalanine complex) complexes (Scheme 5.1).

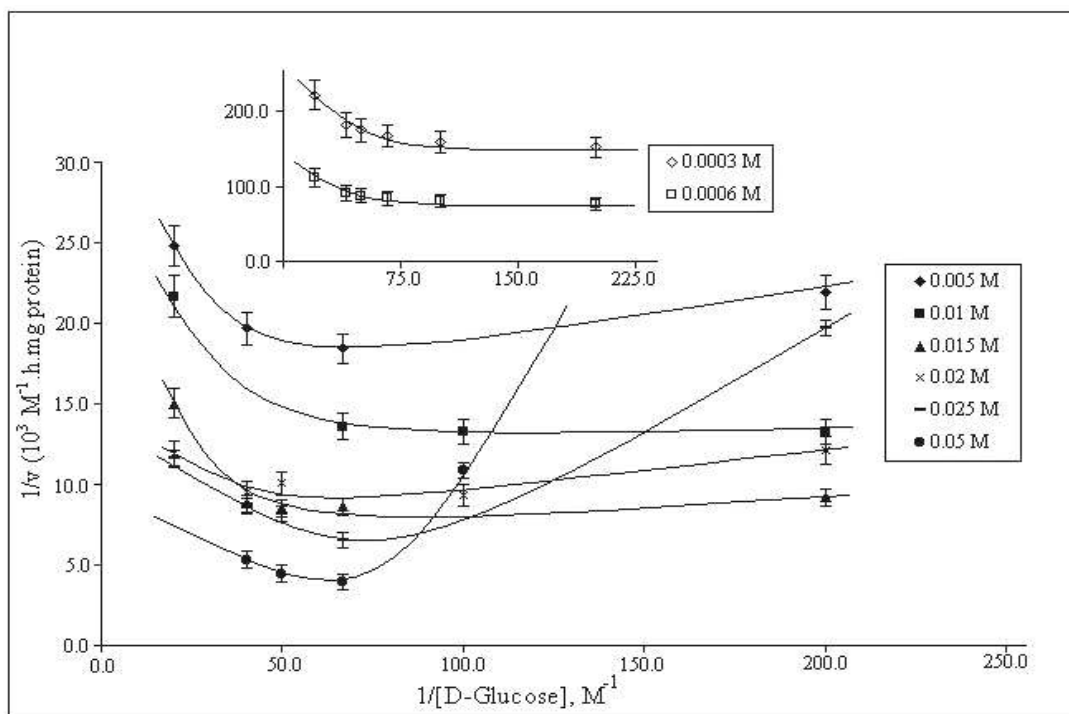


Fig. 5.2 Double reciprocal plots for RML catalysed L-phenylalanyl-D-glucose reaction: $1/v$ versus $1/[D\text{-glucose}]$, series of curves showing the effect of varying D-glucose concentrations at different fixed concentrations of L-phenylalanine in the range 0.005 M to 0.05 M. Inset shows plots obtained from the computer simulation procedure for L-phenylalanine at 0.0003 M and 0.0006 M concentrations.

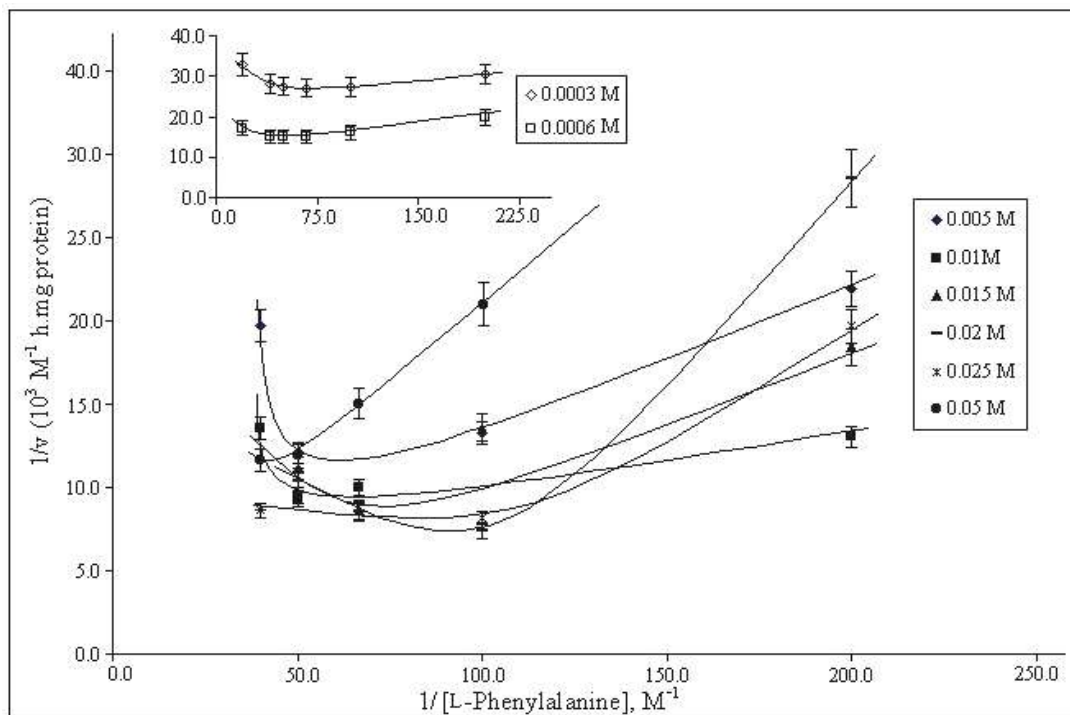
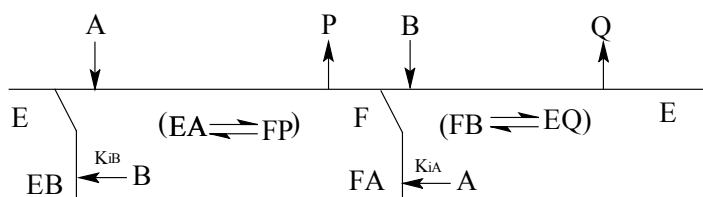


Fig. 5.3 Double reciprocal plots for RML catalysed L-phenylalanyl-D-glucose reaction: $1/v$ versus $1/[L\text{-phenylalanine}]$, series of curves showing effect of varying L-phenylalanine concentrations at different fixed concentrations of D-glucose in the 0.005 M to 0.05 M range. Inset shown for 0.0003 M and 0.0006 M concentrations of D-glucose are from the computer simulation procedure.



A = L-phenylalanine, P = H₂O, B = D-glucose, E = Lipase -*Rhizomucor miehei* lipase, F = L-phenylalanyl-RML complex, EA = RML-L-phenylalanine complex, FP = L-phenylalanyl-RML-water complex, EB = RML-D-glucose complex, FA = L-phenylalanyl-RML-L-phenylalanine complex, K_{iB} = dissociation constant of RML-D-glucose complex, K_{iA} = dissociation constant of RML-L-phenylalanine complex, FB = L-phenylalanyl-RML-D-glucose complex, EQ = RML-L-phenylalanyl-D-glucose complex, Q = L-phenylalanyl-D-glucose.

Scheme 5.1. Ping-Pong Bi-Bi mechanism of RML catalysed synthesis of L-phenylalanyl-D-glucose showing inhibition by both D-glucose and L-phenylalanine.

This model could be described by the following rate equation.

$$\frac{v}{V_{\max}} = \frac{[A][B]}{K_{mA}[B] \left(1 + \frac{[B]}{K_{iB}}\right) + K_{mB}[A] \left(1 + \frac{[A]}{K_{iA}}\right) + [A][B]} \dots\dots\dots(1)$$

Where, v = initial rate, V_{max} = maximum velocity, A = L-phenylalanine concentration, B = D-glucose concentration, K_{mA} = Michelis-Menten constant for L-phenylalanine, K_{mB} = Michelis-Menten constant for D-glucose. K_{iB} = dissociation constant of the RML-D-glucose complex, K_{iA} = dissociation constant of the RML-L-phenylalanine complex. Since the initial rates are in M/h.mg of the protein, V_{max} is expressed as k_{cat} as k_{cat} = V_{max}/enzyme concentration.

The five important kinetic parameters K_{i D-glucose}, K_{i L-phenylalanine}, K_{m L-phenylalanine}, K_{m D-glucose} and k_{cat} were evaluated graphically. Intercept of the positive slopes of Fig. 5.2 on

the Y- axis, especially, at the higher concentrations of L-phenylalanine employed, gave $1/k_{cat}$ (Table 5.1). From Fig. 5.4, slope = $K_m \text{ L-phenylalanine} / (k_{cat} K_{iB})$, Y intercept = $K_m \text{ L-phenylalanine} / k_{cat}$ and X intercept = $-K_{iB}$. From Fig. 5.5 slope = $K_m \text{ D-glucose} / (k_{cat} K_{iA})$, Y intercept = $K_m \text{ D-glucose} / k_{cat}$ and X intercept = $-K_{iA}$, where K_{iA} and K_{iB} represents dissociation constant for RML-L-phenylalanine and RML-D-glucose complexes respectively.

Table 5.1 Apparent values of kinetic parameters for RML catalysed synthesis of L-phenylalanyl-D-glucose.

Name of the Compound		k_{cat} mM/h.mg protein	K_{mA} mM	K_{mB} mM	K_{iA} mM	K_{iB} mM
L-Phenylalanyl	a	0.13 ± 0.002	3.13 ± 0.33	2.13 ± 0.2	6.0 ± 0.58	9.0 ± 0.86
-D-glucose	b	2.24 ± 0.23	95.6 ± 9.7	80.0 ± 8.5	90.0 ± 9.2	13.6 ± 1.42

A = L-phenylalanine, B = D-glucose, ^a graphical method, ^b computer simulated values.

As a confirmatory approach, the values of the five important kinetic parameters, K_{mA} , K_{mB} , k_{cat} , K_{iA} and K_{iB} were also estimated through a curve-fitting procedure by using eq.1. The range of values tested for these parameters and the constraints employed for the iteration procedure are: $k_{cat \text{ D-glucose}} < 10 \text{ mM/h.mg}$, $K_{i \text{ D-glucose}} > K_m \text{ D-glucose}$, $K_m \text{ D-glucose} < K_m \text{ L-phenylalanine}$, and $K_m \text{ L-phenylalanine} < 90 \text{ mM}$. The iteration procedure involved determination of initial velocities (v_{pred}) by incrementing the above mentioned five kinetic parameters in eq. 1 from their lowest approximations (bound by the above mentioned constraints) and subjecting the v_{pred} (obtained for all the concentrations of D-glucose and L-phenylalanine) to non-linear optimization, by minimizing the sum of squares of deviations between v_{pred} and v_{exptl} . The set of five kinetic parameters which resulted in minimum sum of squares of deviation between v_{pred} and v_{exptl} were considered the best set (Table 5.1). Table 5.2 shows the comparison between experimental and predictive

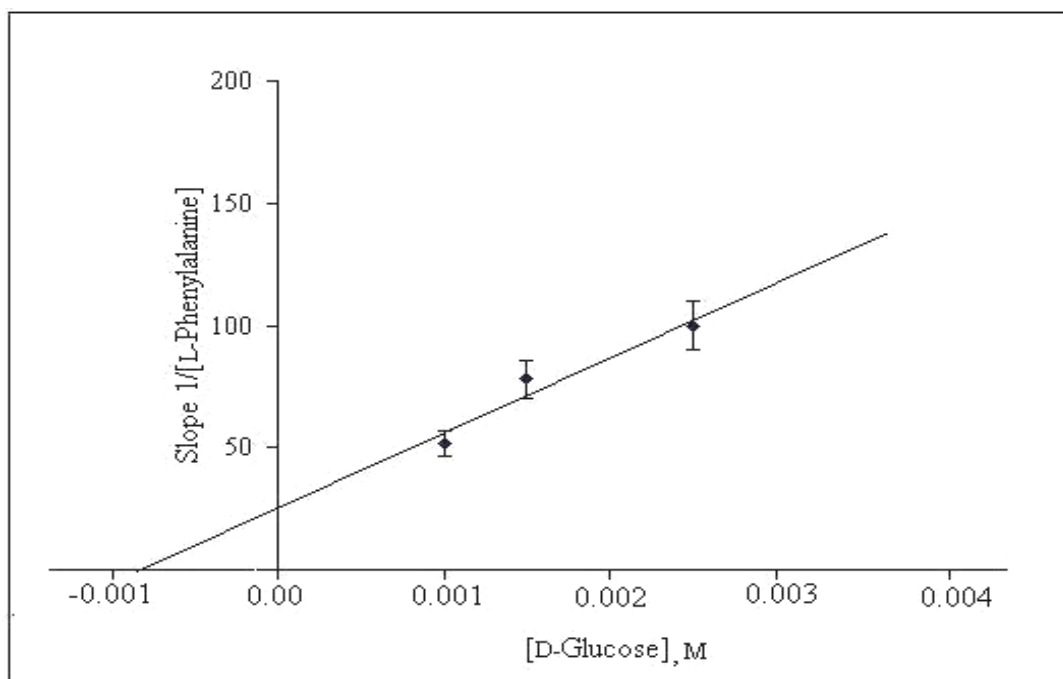


Fig. 5.4 Replot of slopes of $1/[\text{L-phenylalanine}]$ versus $[\text{D-glucose}]$ from Fig. 5.3. from RML catalysed reaction.

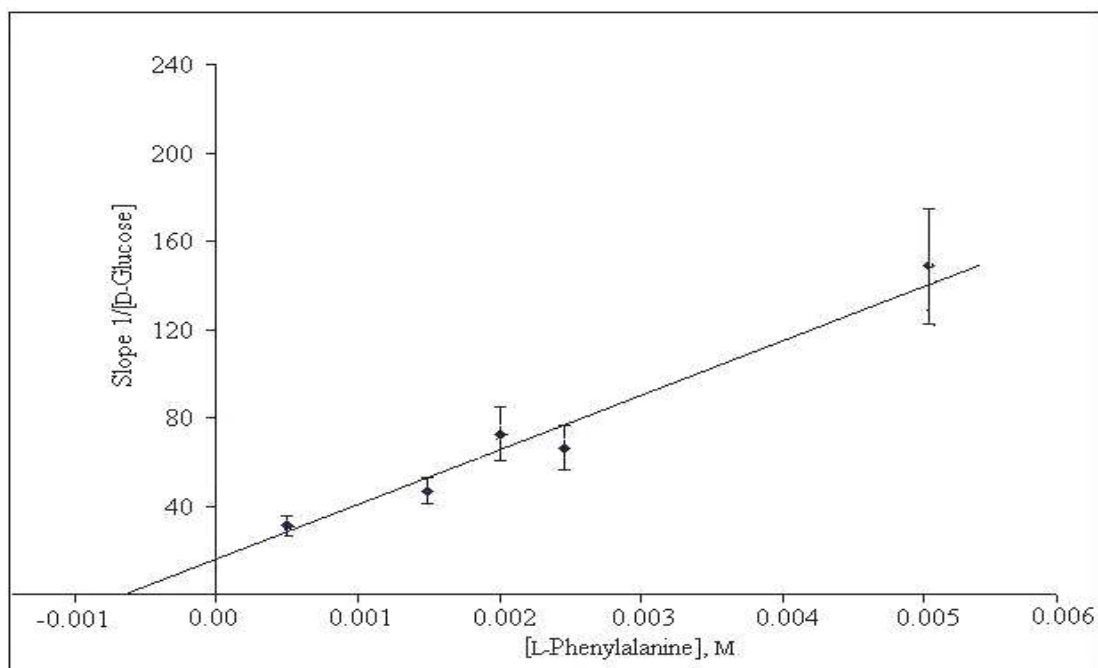


Fig. 5.5 Replot of slopes of $1/[\text{D-glucose}]$ versus $[\text{L-phenylalanine}]$ from Fig. 5.2 from RML catalysed reaction.

initial rate values obtained under different reaction conditions. Computer simulated v_{pred} values showed a R^2 value of 0.65.

Table 5.2 Experimental and predicted initial rate values for the synthesis of L-phenylalanyl-D-glucose by RML

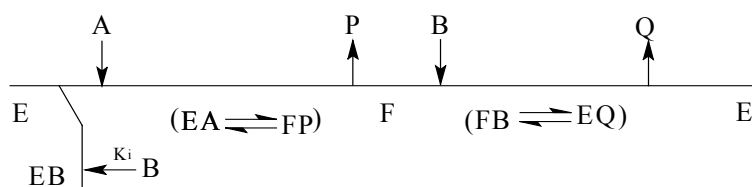
L-Phenylalanine conc. (M)	D-Glucose conc. (M)	K_{cat} -experimental ^a 10^{-6} M/h. mg protein	K_{cat} -predictive ^b 10^{-6} M/h. mg protein
0.005	0.005	46	51
0.005	0.01	79	53
0.005	0.015	54	48
0.005	0.02	35	43
0.005	0.025	50	38
0.005	0.050	40	24
0.01	0.005	75	70
0.01	0.01	75	84
0.01	0.015	74	83
0.01	0.02	135	77
0.01	0.025	123	71
0.01	0.050	46	47
0.015	0.005	109	79
0.015	0.01	100	705
0.015	0.015	116	709
0.015	0.02	117	105
0.015	0.025	113	98
0.015	0.050	67	69
0.02	0.005	83	83
0.02	0.01	107	117
0.02	0.015	89	127
0.02	0.02	96	126
0.02	0.025	105	121
0.02	0.050	84	89
0.025	0.005	51	84
0.025	0.01	74	125
0.025	0.015	153	141
0.025	0.02	123	144
0.025	0.025	116	140
0.025	0.050	86	107
0.05	0.01	92	133
0.05	0.015	245	168
0.05	0.02	224	187
0.05	0.025	186	196

^a Graphical method, ^b Curve fitted values, Average absolute deviation in initial velocities – 21.7% .

5.2.2. *Candida rugosa* lipase catalysis

Double reciprocal plots constructed for the CRL catalysed reaction showed that Figures 5.6 and 5.7 are not similar unlike those of the RML catalysed reaction. Figure 5.6 represents $1/v$ versus $1/[D\text{-glucose}]$ and Fig. 5.7 represents $1/v$ versus $1/[L\text{-phenylalanine}]$. Figure 5.8 shows the replot of slopes from Fig. 5.7. Figure 5.6 shows series of curves obtained for different fixed levels concentrations of L-phenylalanine at varying D-glucose concentrations where slight increase in rates are observed at lower D-glucose concentrations and at higher concentrations of D-glucose, the rates reduce drastically. Figure 5.7 shows series of parallel lines for different fixed lower D-glucose concentrations at various L-phenylalanine concentrations, and this changes to lines with different slopes at higher D-glucose concentrations.

Here also, the plots in Figures 5.6 and 5.7 showed that the kinetics could be best described by (Segel 1993) Ping-Pong Bi-Bi model (Scheme 5.2), however, with a difference that only one substrate (D-glucose) functions as a competitive inhibitor forming dead-end CRL-D-glucose complex.



A = L-phenylalanine, P = H₂O, B = D-glucose, E = Lipase - *Candida rugosa* lipase, F = L-phenylalanyl-CRL complex, EA = CRL-L-phenylalanine complex, FP = L-phenylalanyl-lipase-water complex, EB = CRL-D-glucose complex, K_i = dissociation constant of CRL-D-glucose complex, FB = L-phenylalanyl-CRL-D-glucose complex, EQ = CRL-L-phenylalanyl-D-glucose complex, Q = L-phenylalanyl-D-glucose.

Scheme 5.2. Ping-Pong Bi-Bi mechanism of CRL catalysed synthesis of L-phenylalanyl-D-glucose showing inhibition by D-glucose.

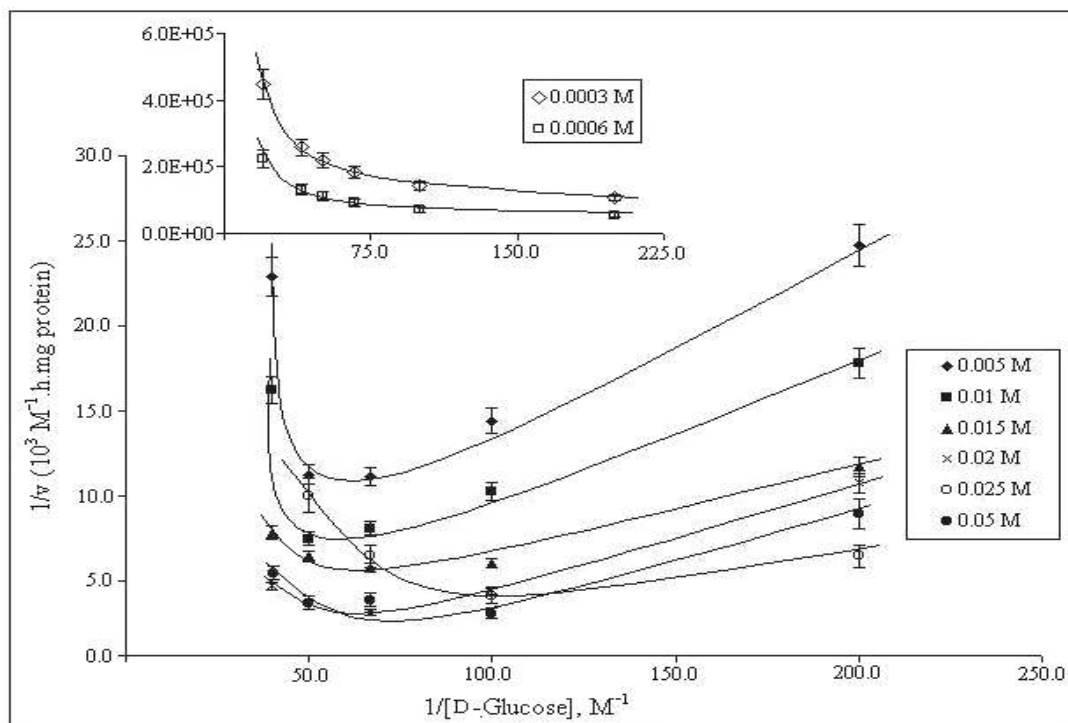


Fig. 5.6. Double reciprocal plots for CRL catalysed L-phenylalanyl-D-glucose reaction: $1/v$ versus $1/[D\text{-glucose}]$, series of curves showing the effect of varying D-glucose concentrations at different fixed concentrations of L-phenylalanine in the 0.005 M to 0.05 M concentration range. Inset shown for 0.0003 M and 0.0006 M concentrations of L-phenylalanine are from the computer simulation procedure.

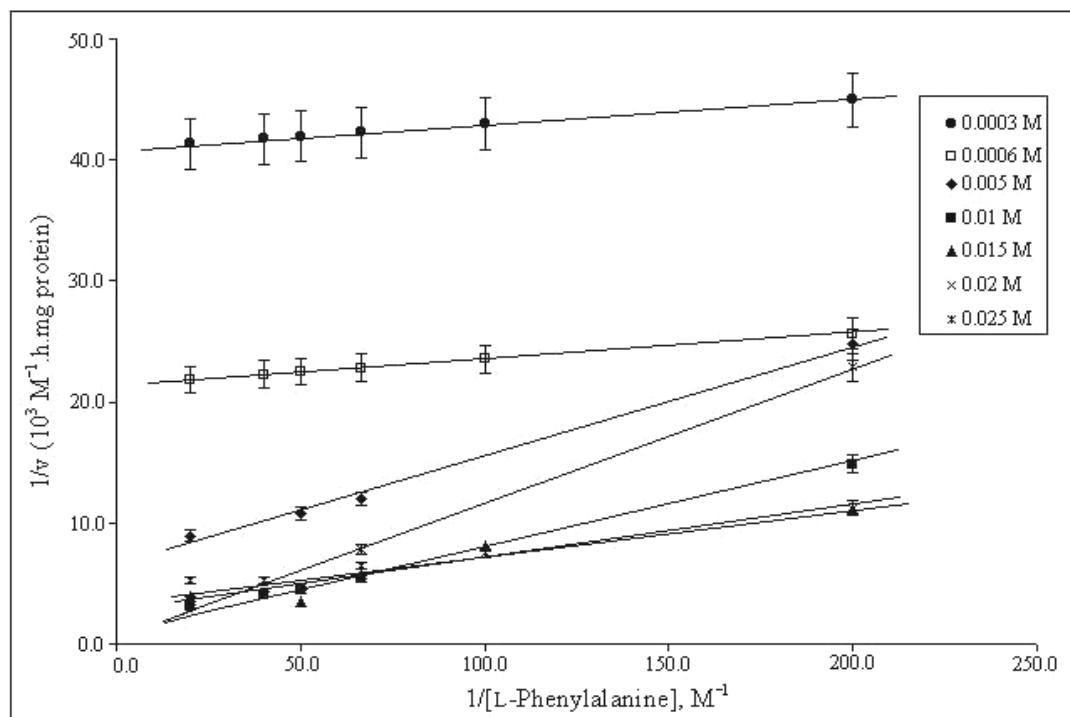


Fig. 5.7 Double reciprocal plots for CRL catalysed L-phenylalanyl-D-glucose reaction: $1/v$ versus $1/[L\text{-phenylalanine}]$, series of plots showing effect of varying L-phenylalanine concentrations at different fixed concentrations of D-glucose in the 0.005 M to 0.025 M concentration range and the plots for 0.0003 M and 0.0006 M concentrations of D-glucose are from the computer simulation procedure.

This model could be described by the following rate equation.

$$\frac{v}{V_{\max}} = \frac{[A][B]}{K_{mA}[B] \left(1 + \frac{[B]}{K_i}\right) + K_{mB}[A] + [A][B]} \dots\dots\dots(2)$$

where, v = initial rate, V_{max} = maximum velocity, A = L-phenylalanine concentrations, B = D-glucose concentrations, K_{mA} = Michelis-Menten constant for L-phenylalanine, K_i = dissociation constant of the CRL-inhibitor (D-glucose) complex, K_{mB} = Michelis-Menten constant for D-glucose.

The four important kinetic parameters K_i D-glucose, K_m L-phenylalanine, K_m D-glucose and k_{cat} were evaluated graphically. Intercept of the positive slopes of Fig. 5.6 on the Y- axis, especially, at the higher concentration of L-phenylalanine, gave 1/ k_{cat} (Table 5.3). From Fig. 5.8, slope = K_m L-phenylalanine / (k_{cat} K_i), Y intercept = K_m L-phenylalanine/k_{cat} and X intercept = -K_i where K_i represents dissociation constant for the CRL-D-glucose complex. K_m D-glucose was obtained from equation 3 by rearranging equation 2,

$$K_{mB} = \frac{k_{cat}[B]}{v} - \frac{K_{mA}[B]}{[A]} - \frac{K_{mA}[B]^2}{[A]K_i} - [B] \dots\dots\dots(3)$$

where, K_{mB} = Michelis-Menten constant for D-glucose.

Table 5.3 Apparent values of kinetic parameters for CRL catalysed synthesis of L-phenylalanyl-D-glucose

Name of the Compound	k _{cat} mM/h.mg protein	K _{mA} MM	K _{mB} mM	K _{iB} mM	
L-Phenylalanyl-D-glucose	a	0.40 ± 0.005	5.6 ± 0.58	6.48 ± 0.69	7.0 ± 0.73
	b	0.51 ± 0.06	10.0 ± 0.98	6.0 ± 0.64	8.5 ± 0.81

A = L-phenylalanine, B = D-glucose, ^a graphical method, ^b computer simulated values.

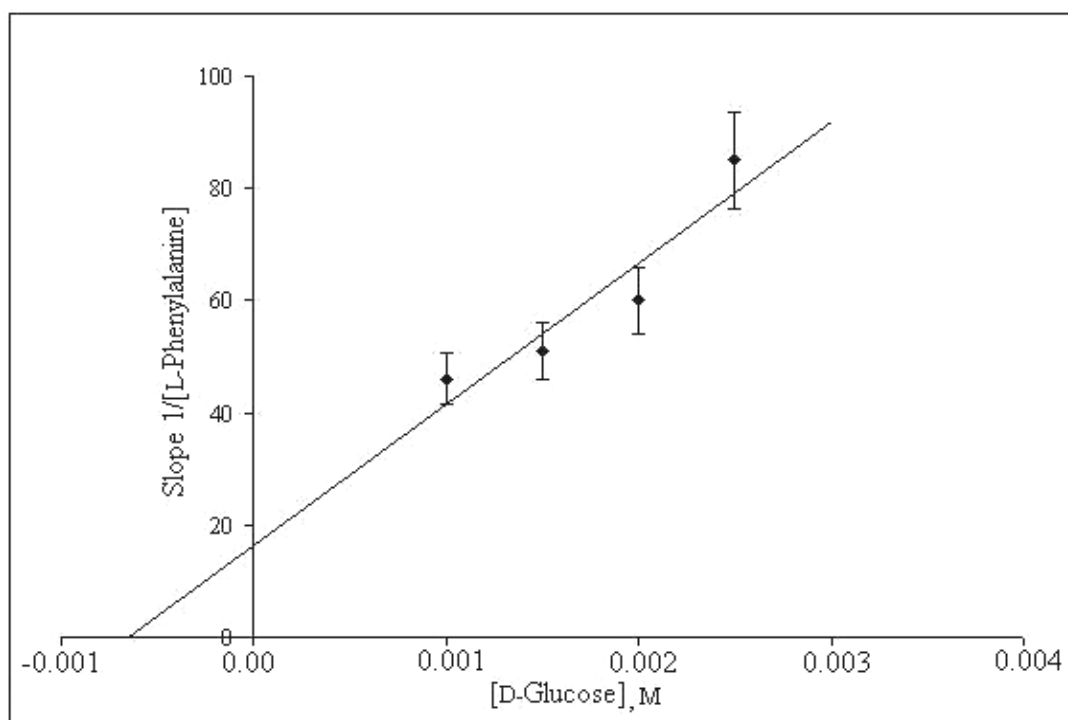


Fig. 5.8 Replot of slopes of $1/[\text{L-phenylalanine}]$ versus $[\text{D-glucose}]$ from Fig. 5.7 from CRL catalysed reaction.

Table 5.4 Experimental and predicted initial rate values for the synthesis of L-phenylalanyl-D-glucose by CRL

L-Phenylalanine Conc. (M)	D-Glucose conc. (M)	K_{cat} -experimental ^a 10 ⁻⁶ M/h. mg protein	K_{cat} -predictive ^b 10 ⁻⁶ M/h. mg protein
0.005	0.005	40	96
0.005	0.01	67	86
0.005	0.015	90	74
0.005	0.02	89	64
0.005	0.025	44	56
0.01	0.005	56	136
0.01	0.01	92	136
0.01	0.015	123	123
0.01	0.02	133	110
0.01	0.025	62	99
0.015	0.005	85	158
0.015	0.01	187	168
0.015	0.015	173	158
0.015	0.02	155	145
0.015	0.025	128	133
0.02	0.005	93	171
0.02	0.01	224	191
0.02	0.015	317	185
0.02	0.02	100	173
0.02	0.025	213	160
0.025	0.005	155	181
0.025	0.01	243	208
0.025	0.015	155	205
0.025	0.02	100	195
0.025	0.025	191	182
0.05	0.005	256	204
0.05	0.01	325	252
0.05	0.015	258	263
0.05	0.02	269	261
0.05	0.025	291	253

^a Graphical method, ^b Curve fitted values, Average absolute deviation in initial velocities – 26.3%.

Here also, a curve-fitting procedure was carried out using eq. 2 to estimate k_{cat} , K_i , K_{mA} , and K_{mB} , to confirm that the kinetics of CRL catalysed L-phenylalanyl-D-glucose reactions followed the above mentioned model. The range of values tested and the constraints employed are : $k_{cat \text{ D-glucose}} < 1 \text{ mM/h.mg}$, $K_i \text{ D-glucose} > K_m \text{ D-glucose}$, $K_m \text{ D-glucose} < K_m \text{ L-phenylalanine}$, and $K_m \text{ L-phenylalanine} < 10 \text{ mM}$. Here also, the iteration procedure was the same as that employed for the RML catalysed reaction. Table 5.3 lists graphical as well as the computer simulated values for comparison. Table 5.4 shows the comparison

between experimental and predictive initial rate values obtained under different reaction conditions. Computer simulated v_{pred} values showed a R^2 of value 0.63.

In case of CRL, at increasing fixed concentrations of L-phenylalanine (Fig. 5.6), the rate increases at lower concentrations of D-glucose. At higher concentrations of D-glucose corresponding to minimum $1/v$, the rate decreases, the plots tend to become closer to $1/v$ axis. Figure 5.7 (CRL) also reflect the same behaviour, where at lower concentrations of D-glucose, the plots appear parallel probably so for as $K_i > K_{\text{mB}}$. However at higher fixed concentrations of D-glucose, the slopes vary drastically. Thus the kinetic data clearly shows the inhibitory nature of D-glucose in this reaction.

5.3. Discussion

5.3.1. *Rhizomucor miehei* lipase

This kinetic data clearly shows the inhibitory nature of both D-glucose and L-phenylalanine towards RML. Competition between L-phenylalanine and D-glucose for the active site (binding site) of RML could result in predominant binding of either substrates at their higher concentrations leading to the formation of the dead-end complexes (RML-D-glucose/L-phenylalanine). K_{mA} (95.6 ± 9.7 mM) is slightly higher than K_{mB} (80.0 ± 8.5 mM, Table 5.1), which shows that both the substrates possess almost equal propensity for the reaction ($K_{\text{mA}}/K_{\text{mB}} = 1.19$). The dissociation constant values, $K_{\text{i L-phenylalanine}}$ (90.0 ± 9.2 mM) $>$ $K_{\text{i D-glucose}}$ (13.6 ± 1.42 mM), indicate that D-glucose is more inhibitory than L-phenylalanine.

Both RML and CRL contain such amino acid residues in their active site capable of forming hydrogen bonds. The catalytic triad in RML consists of Ser 144, His 257 and Asp 203 (Brady *et al.* 1990). D-Glucose possesses five hydroxyl groups capable of forming hydrogen bonds with polar side chains of amino acid residues. Ser-144 hydroxyl and Asp 203 carboxyl groups of RML are good candidates for exhibiting H-bonding

interactions. Meanwhile, the hydrophobic amino acids in the active site of RML could also facilitate the stabilization of L-phenylalanyl-RML complex through hydrophobic interactions. Hence, between D-glucose and L-phenylalanine, stabilization of D-glucose through H-bonding interactions could result in better inhibition than stabilization of L-phenylalanine through hydrophobic interaction at their respective higher concentrations.

5.3.2. *Candida rugosa* lipase

In case of CRL Competition between L-phenylalanine and D-glucose for the active site of CRL could result in predominant binding of D-glucose at higher concentrations, displacing L-phenylalanine, leading to the formation of the dead-end lipase-D-glucose complex. Here also, K_{mA} (10.0 ± 0.98 mM) is slightly higher (Table 5.3) than K_{mB} (6.0 ± 0.64 mM, $K_{mA}/K_{mB} = 1.67$). The respective kinetic parameter values (K_{mA} and K_{mB}) are higher for RML compared to CRL indicating that RML can give better conversions than CRL.

The crystal structure of CRL reveals that Ser-209, Glu-341 and His-449 are the catalytic triads (Grochulski *et al.* 1994; 1993). The active site polar residues, Ser-209 and Glu-341 could play an important role in efficient H-bonding interactions with D-glucose (Grochulski *et al.* 1993). Between D-glucose and L-phenylalanine the former possesses more H-bonding functions than the amino or carboxyl groups of L-phenylalanine in CRL leading to inhibition by D-glucose. Zaidi *et al.* (2002) reported that interaction between enzyme and alcohol through hydrogen bonding could result in blocking of the nucleophilic site of the enzyme engaged in the acylation process, leading to inhibition.

Hence, this kinetic reports has clearly brought out the inhibition of RML by both D-glucose and L-phenylalanine and CRL by D-glucose with far reaching biochemical implications.

5.4. Experimental

5.4.1. Kinetic experiments

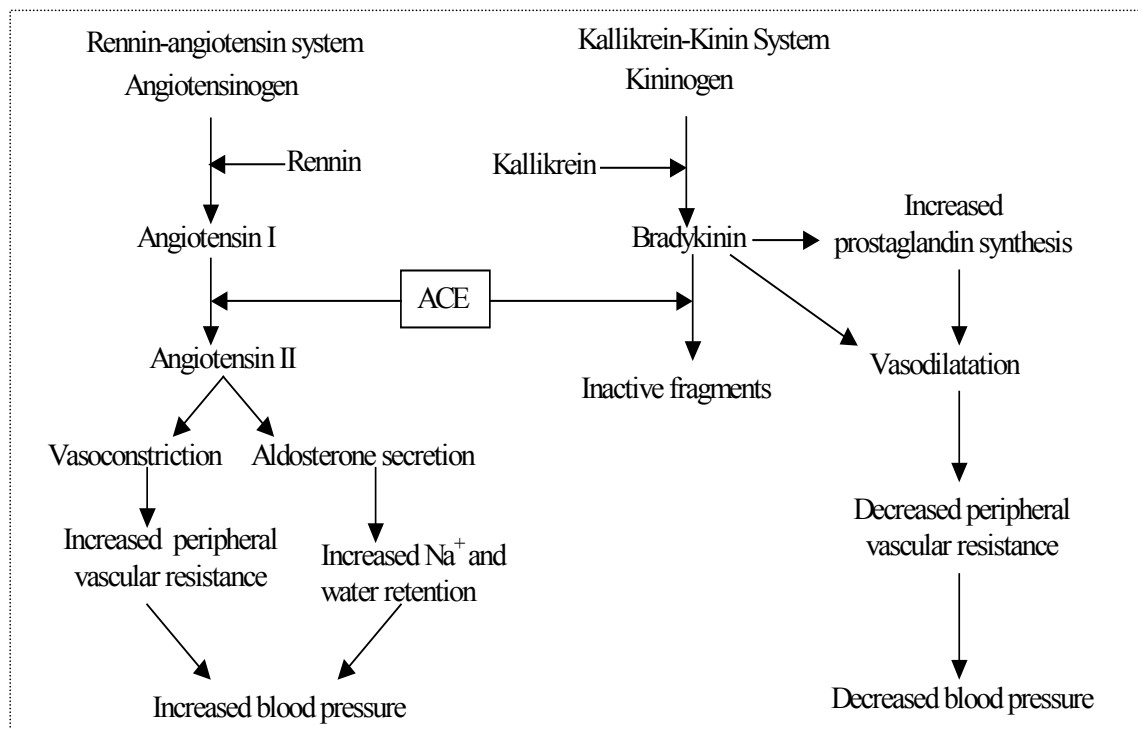
Kinetic experiments were conducted by refluxing L-phenylalanine and D-glucose along with 90 mg RML/CRL in 100 mL of dichloromethane and dimethylformamide (90:10 v/v) solvent mixture containing 0.2 ml 0.1M pH 4.0 acetate buffer (Vijayakumar *et al.* 2004; Lohith and Divakar 2005) at 40 °C. Unprotected and unactivated L-phenylalanine and D-glucose were employed. Experiments were conducted with both the enzymes by maintaining the concentration of one of the substrate constant (range 0.005 M to 0.05 M) and varying the concentration of the other (range 0.005 M to 0.05 M) and *vice versa*. Product workout involved distilling off the solvent, heating to denature the enzyme, stirring and filtering off the lipase. The filtrate was then evaporated to obtain a residue containing L-phenylalanine, D-glucose and the ester. The residue was subjected to HPLC analysis using a C-18 column (LiChrosorb 100 Å, 5 µm 25cm x 4.6mm) with 80: 20 v/v water: acetonitrile as mobile phase at a flow rate of 1 ml/min and monitoring by UV detector at 254 nm. Retention times of L-phenylalanine and L-phenylalanyl-D-glucose were found to be 2.2 min and 3.1 min respectively. Conversion yields were determined from peak areas of L-phenylalanyl-D-glucose and that of the L-phenylalanine in the reaction mixture and expressed as molar concentration of L-phenylalanyl-D-glucose formed. Error in measurement of yields will be in the order $\pm 10\%$. The esters formed were separated by size exclusion chromatography using Sephadex G-10 column and eluted with water and subjected to spectral characterization by UV, IR and 2D-Heteronuclear Single Quantum Coherence Transfer (HSQCT) NMR. The complete spectral characterization of L-phenylalanyl-D-glucose is shown in Section 4.2.2.1.

Chapter-6

**Angiotensin Converting Enzyme inhibition
activity of L-prolyl, L-phenylalanyl,
L-tryptophanyl and L-histidyl
esters of carbohydrates**

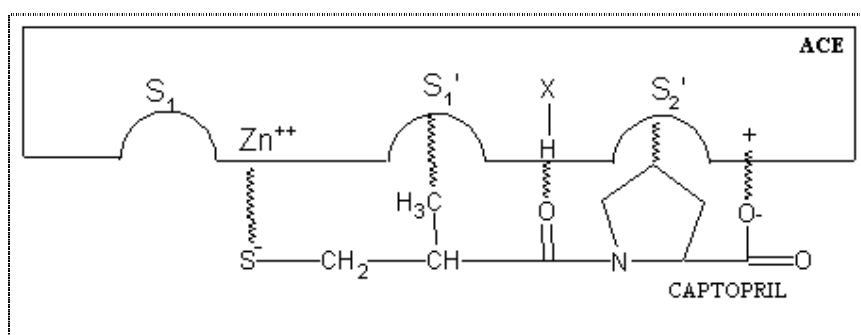
6.1. Introduction

Angiotensin Converting Enzyme (dipeptidyl carboxypeptidase, EC 3.4.15.1) is a zinc containing nonspecific dipeptidyl carboxypeptidase widely distributed in mammalian tissues (Li *et al.* 2004). Angiotensin-converting enzyme (ACE) regulates the blood pressure by modulating renin-angiotensin system (Vermeirssen *et al.* 2002). This enzyme increases the blood pressure by converting the decapeptide angiotensin I into the potent vaso-constricting octapeptide, angiotensin II. Angiotensin II brings about several central effects, all leading to a further increase in blood pressure (Scheme 6.1). ACE is a multifunctional enzyme that also catalyses the degradation of bradykinin (blood pressure-lowering nanopeptide) and therefore inhibition of ACE results in an overall antihypertensive effect (Li *et al.* 2004; Johnston 1992).

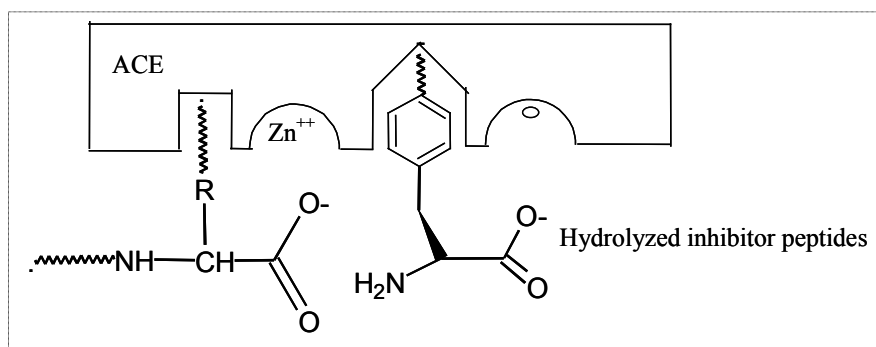


Scheme 6.1 Role of angiotensin converting enzyme (ACE) in blood pressure regulation (Li *et al.* 2004)

Synthetic drugs available for ACE inhibition exhibit significant side effects. Captopril is a successful synthetic anti-hypertensive drug and a large number of synthetic molecules like enalapril, perindopril, ceranopril, ramipril, quinapril, and fosinopril, also show ACE inhibitory activities (Hyuncheol *et al.* 2003; Dae-Gill *et al.* 2003; Chong-Qian *et al.* 2004). The mechanism of ACE inhibition by captopril is shown in Scheme 6.2 (De- Lima 1999). The hypothetical representation of inhibitors (hydrolysed products of peptides) binding to the ACE is shown in Scheme 6.3 and also reported that proline at carboxyl terminus of the inhibitor was found to be the most potent inhibitor (De-Lima 1999).



Scheme 6.2. Schematic representation of ACE inhibition by captopril to the active sites (De-Lima 1999)



Scheme 6.3. Schematic representation of ACE active sites and binding of inhibitors (De-Lima 1999)

Some naturally occurring 'biologically active peptides' also act as ACE inhibitors. Deloffre *et al.* (2004) reported that a neuro-peptide from leach brain showed ACE inhibition with an IC₅₀ value of 19.8 μM. The N-terminal dipeptide (Tyr-Leu) of β-lactorphin was found to be the most potent inhibitor (Mullally *et al.* 1996). Many peptide inhibitors are derived from different food proteins like Asp-Leu-Pro and Asp-Gly from soy protein hydrolysis (Wu and Ding 2002) and Gly-Pro-Leu and Gly-Pro-Val from bovine skin gelatin hydrolysis (Kim *et al.* 2001). Cooke *et al.* (2003) prepared 4-substituted phenylalanyl esters of alkyl or benzyl derivatives, which exhibited ACE inhibitory activity.

Amino acyl esters of carbohydrates find wide variety of applications in food and pharmaceutical industries. Amino acyl esters have not been shown so far to exhibit ACE inhibition activity. Since most of the ACE inhibitory drugs are peptides, it was envisaged that the amino acyl esters of carbohydrates also could possess ACE inhibition activities as they contain amino acyl groups as part of their structure. Hence, this chapter deals with detection of ACE inhibition activities for some enzymatically synthesized L-prolyl **1**, L-phenylalanyl **2**, L-tryptophanyl **3** and L-histidyl **4** esters of carbohydrates using lipases in organic media.

6.2. Present work

Some selective synthesized esters (each one from aldohexoses, ketose, pentose, disaccharide and carbohydrate alcohol esters of L-proline **1**, L-phenylalanine **2**, L-tryptophan **3** and L-histidine **4**) were tested for the inhibitory activities of ACE isolated from pig lung (Section 6.4.1). Thus amino acyl esters - L-prolyl **1**, L-phenylalanyl **2**, L-tryptophanyl **3** and L-histidyl **4** esters of D-glucose **5**, D-galactose **6**, D-fructose **8**, D-ribose **10**, lactose **11** and D-mannitol **15** were subjected to ACE inhibition activities studies. The enzymatic reactions were carried out under optimized conditions worked out

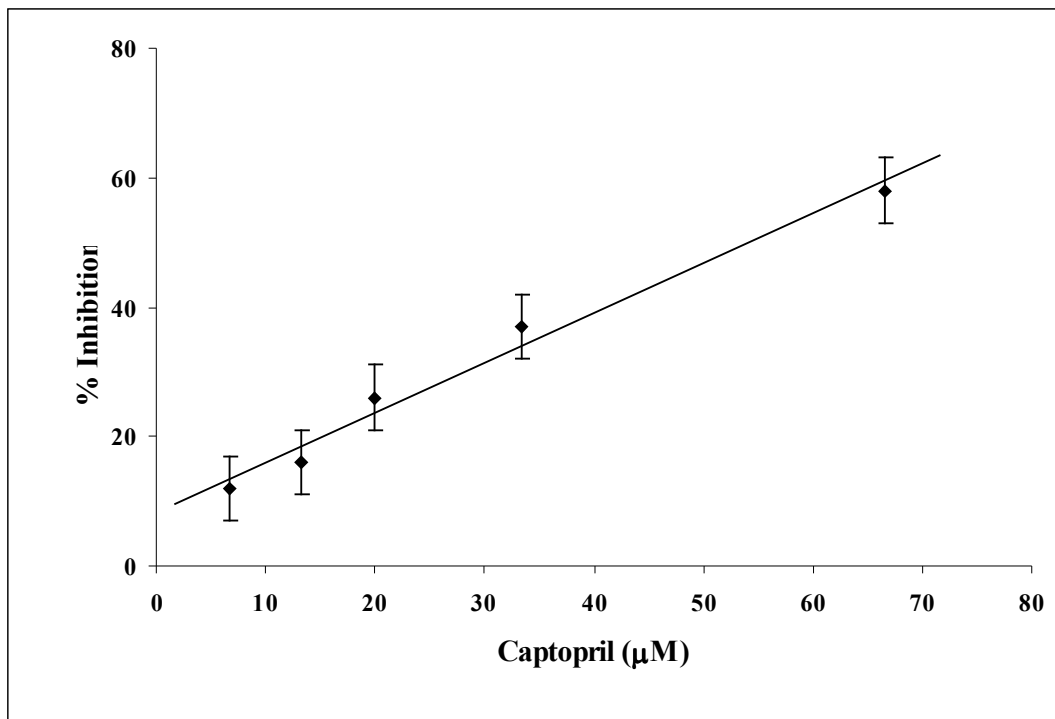


Fig. 6.1. A typical ACE inhibition plot for captopril, concentration range – 6.7 –66.7 µM Substrate – 0.1 mL hippuryl-histidyl-leucine (5 mM), Buffer – 100 mM phosphate buffer pH 8.3 containing 300 mM NaCl, Incubation period –30 min, temperature-37 °C. IC₅₀ value - 0.060 ± 0.006 mM

for these reactions (Section 6.4.2). ACE inhibition activity of the above mentioned amino acyl esters of carbohydrates were carried out by the Cushman and Cheung method (1971). Since hippuryl-L-histidyl-L-leucine (HHL) mimics the carboxyl dipeptide of angiotensin I, it has been routinely used as the substrate for screening ACE inhibitors.

Underivatized L-amino acids and carbohydrates were also tested for ACE inhibition as such as controls and they did not show any ACE inhibitory activities. Only esters showed activities. Isolated ACE inhibitor tested for lipase and protease activity (Table 6.1) showed a small extent of protease activity (13.3%) compared to ACE activity but no lipase activity. In presence of amino acyl esters prepared, the isolated ACE showed 8.9% protease activity (Table 6.1) compared to the ACE activity. This confirmed that the ACE inhibition observed in the presence of amino acyl esters prepared is more due to ACE inhibition rather than protease inhibition.

Table 6.1 Protease inhibition assay for D-glucose ester ^a

System	Protease activity Unit min⁻¹mg⁻¹ enzyme protein ^b	Percentage of protease activity with respect to ACE activity ^c
ACE- 0.5 ml + 0.5 ml of 0.6% hemoglobin + 0.5 ml Buffer	0.0436	13.3
Ester - 0.5 ml ester + ACE -0.5 ml + 0.5 ml of 0.6% hemoglobin	0.0267	8.9

^a Conditions: ACE – 0.5 ml (0.5mg), All the solutions were prepared in 0.1 M pH 7.5 Tris-HCl, incubation period – 30 min, temperature – 37°C, 0.5 ml of 10% trichloro acetic acid added to arrest the reaction; Blank performed without enzyme and ester; Absorbance measured at 440 nm; ester – 0.5 ml of 0.8 mM; ^bAverage absorbance values from three individual experiments; ^c Percentage protease activity with respect to an ACE activity of 0.327 μmol/min.mg protein.

Figure 6.1 shows a typical ACE inhibition plot for captopril which showed an IC₅₀ value of 0.060 ± 0.006 mM. Typical ACE inhibition plots for all the tested esters, such as L-prolyl esters (Fig. 6.2), L-phenylalanyl esters (Fig. 6.3), L-tryptophanyl esters

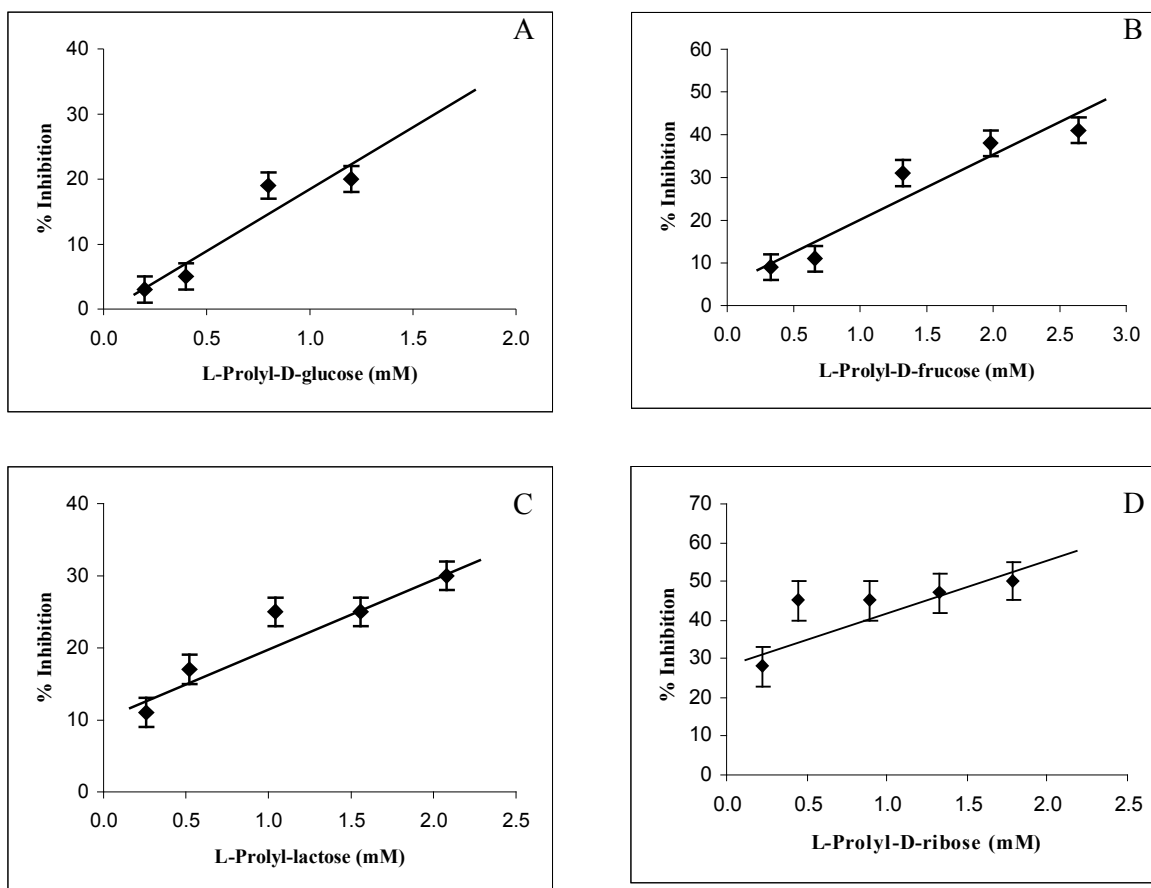


Fig. 6.2. ACE inhibition plots for L-prolyl esters of carbohydrates (A) L-prolyl-D-glucose **16a-e**, concentration range–0.2–1.6 mM, substrate – 0.1 mL HHL (5 mM), Buffer – 100 mM phosphate buffer pH 8.3 containing 300 mM NaCl, Incubation period –30 min, Temperature–37 °C. (B) L-prolyl-D-fructose **19a-c**, concentration range – 0.33 –2.64 mM, (C) L- prolyl-lactose **21a** and **b**, concentration range – 0.2 –1.6 mM, (D) L-prolyl-D-ribose **20a-c**, Concentration range 0.2 –1.8 mM

(Fig. 6.4) and L-histidyl esters (Fig. 6.5) are shown. Table 6.2 shows the compounds tested, their conversion yields from the respective enzymatic reactions, proportions and nature of the esters formed and ACE inhibitory activities for these compounds.

Table 6.2. IC₅₀ values for ACE inhibition by amino acyl esters of carbohydrates ^a

Amino acyl ester of carbohydrates	Conversion Yield (%) ^b	Products (% Proportion) ^c	IC ₅₀ value (mM) ^d
L-Prolyl-D-glucose	62	16a: 2- <i>O</i> -L-prolyl-D-glucose (26) 16b: 3- <i>O</i> -L-prolyl-D-glucose (26) 16c: 6- <i>O</i> -L-prolyl-D-glucose (48)	1.7±0.17
L-Prolyl-D-fructose	61	19a: 1- <i>O</i> -L-prolyl-D-fructose (31) 19b: 6- <i>O</i> -L-prolyl-D-fructose (42) 19c: 1,6- <i>di-O</i> -L-prolyl-D-fructose (27)	4.4±0.43
L-Prolyl-D-ribose	41	20a: 3- <i>O</i> -L-prolyl-D-ribose (35) 20b: 5- <i>O</i> -L-prolyl-D-ribose (65)	2.0±0.19
L-Prolyl-lactose	68	21a: 6- <i>O</i> -L-prolyl-lactose (58) 21b: 6'- <i>O</i> -L-prolyl-lactose (42)	1.6±0.15
L-Phenylalanyl-D-glucose	79	24a: 2- <i>O</i> -L-phenylalanyl-D-glucose (19) 24b: 3- <i>O</i> -L-phenylalanyl-D-glucose (23) 24c: 6- <i>O</i> -L-phenylalanyl-D-glucose (25) 24d: 2,6- <i>di-O</i> -L-phenylalanyl-D-glucose (17) 24e: 3,6- <i>di-O</i> -L-phenylalanyl-D-glucose (16)	1.0±0.09
L-Phenylalanyl-D-galactose	45	25a: 2- <i>O</i> -L-phenylalanyl-D-galactose (32) 25b: 3- <i>O</i> -L-phenylalanyl-D-galactose (20) 25c: 6- <i>O</i> -L-phenylalanyl-D-galactose (19) 25d: 2,6- <i>di-O</i> -L-phenylalanyl-D-galactose (16) 25e: 3,6- <i>di-O</i> -L-phenylalanyl-D-galactose (13)	4.6±0.45
L-Phenylalanyl-D-fructose	50	27a: 1- <i>O</i> -L-phenylalanyl-D-fructose (72) 27b: 6- <i>O</i> -L-phenylalanyl-D-fructose (28)	13.6±1.35
L-Phenylalanyl-lactose	61	29a: 6- <i>O</i> -L-phenylalanyl-lactose (42) 29b: 6'- <i>O</i> -L-phenylalanyl-lactose (31) 29c: 6,6'- <i>di-O</i> -L-phenylalanyl-lactose (27)	7.8±0.77
L-Phenylalanyl-D-mannitol	43	31a: 1- <i>O</i> -L-phenylalanyl-D-mannitol (62) 31b: 1,6- <i>di-O</i> -L-phenylalanyl-D-mannitol (38)	2.6±0.25

L-Tryptophanyl -D-glucose	42	32a: 2- <i>O</i> -L-tryptophanyl-D-glucose (22) 32b: 3- <i>O</i> -L-tryptophanyl-D-glucose (21) 32c: 6- <i>O</i> -L-tryptophanyl-D-glucose (38) 32d: 2,6- <i>di-O</i> -L-tryptophanyl-D-glucose (10) 32e: 3,6- <i>di-O</i> -L-tryptophanyl-D-glucose (9)	7.4±0.73
L-Tryptophanyl -D-fructose	18	35a: 1- <i>O</i> -L-tryptophanyl-D-fructose (45) 35b: 6- <i>O</i> -L-tryptophanyl-D-fructose (55)	0.9±0.09
L-Histidyl-D- glucose	42	40a: 2- <i>O</i> -L-histidyl-D-glucose (25) 40b: 3- <i>O</i> -L-histidyl-D-glucose (24) 40c: 6- <i>O</i> -L-histidyl-D-glucose (28) 40d: 2,6- <i>di-O</i> -L-histidyl-D-glucose (12) 40e: 3,6- <i>di-O</i> -L-histidyl-D-glucose (11)	3.5±0.34
L-Histidyl-D- fructose	58	42: 6-<i>O</i>-L-histidyl-D-fructose	0.9±0.09
L-Histidyl-D- mannitol	8	44: 1- <i>O</i> -L-histidyl-D-mannitol	1.7±0.16

^a Respective amino acids and carbohydrates as controls showed no ACE inhibition activity; ^b Conversion yields were from HPLC with ± 10-15% errors in HPLC yield measurements; ^c Product proportions determined from ¹³C, 2D HSQCT NMR C6 peak areas (C5 cross peaks in case of ribose) or their cross peaks; ^d IC₅₀ values compared to that of captopril 0.060 ± 0.006 mM determined by Cushman and Cheung method.

The compounds were characterised by two-dimensional Heteronuclear Single Quantum Coherence Transfer (2D-HSQCT) NMR spectra recorded for the samples (Chapter 4). From NMR it was confirmed that mono and di esters, in different proportions were detected (Table 6.2). In some cases like L-prolyl-D-glucose **16a-c**, L-prolyl-D-ribose **20a** and **b**, L-prolyl-lactose **21a** and **b**, L-phenylalanyl-D-fructose **27a** and **b**, L-tryptophanyl-D-fructose **35a** and **b**, L-histidyl-D-fructose **42** and L-histidyl-D-mannitol **44** only monoesters were found to be formed. A 1-*O*- is formed in case of L-prolyl-D-fructose **19a-c**, L-phenylalanyl-D-fructose **27a** and **b**, L-phenylalanyl-D-mannitol **31a** and **b**, L-tryptophanyl-D-fructose **35a** and **b**, and L-histidyl-D-mannitol **44** and 2-*O*- and 3-*O*- monoesters are found to be formed in case of L-prolyl-D-glucose **16b** and **c**, L-prolyl-D-ribose **19b**, L-phenylalanyl-D-glucose **24b** and **c**, L-phenylalanyl-D-galactose **25b** and **c**, L-tryptophanyl-D-glucose **32b** and **c** and L-histidyl-D-glucose **40a**

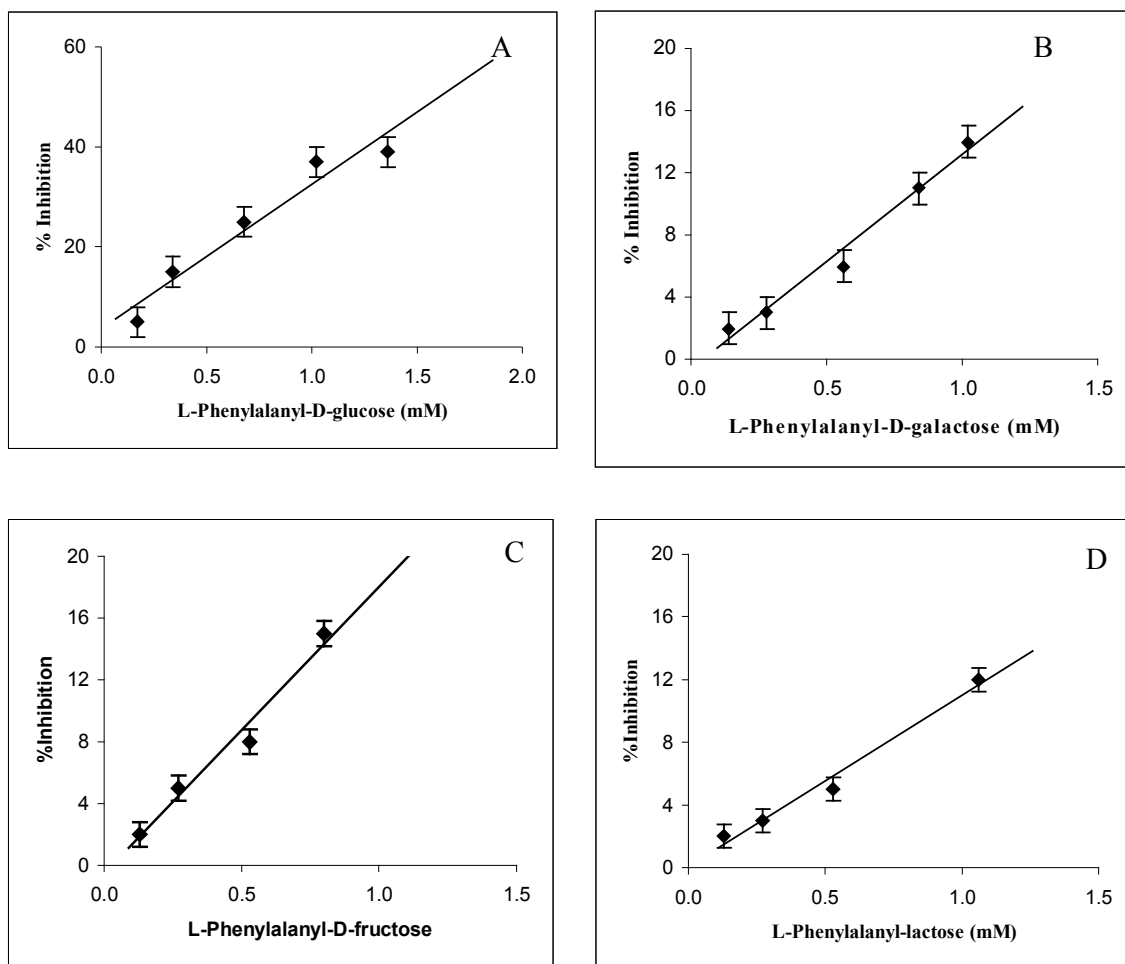


Fig. 6.3. ACE inhibition plots for L-phenylalanyl esters of carbohydrates, (A) L-phenylalanyl-D-glucose **24a-e**, concentration range – 0.17 –1.36 mM, substrate – 0.1 mL hippuryl-histidyl-leucine (5 mM), Buffer – 100 mM phosphate buffer pH 8.3 containing 300 mM NaCl, Incubation period –30 min, Temperature-37 °C, (B) L-phenylalanyl-D-galactose **25a-e**, concentration range – 0.14 -1.02 mM. (C) L-phenylalanyl-D-fructose **27a** and **b**, concentration range – 0.13 -1.36 mM. (D) L-phenylalanyl-lactose **29a** and **c**, concentration range – 0.13 -1.06 mM.

and **b**. All the esters invariable showed formation of *6-O*- monoester except L-prolyl-D-ribose **19a-c** where C5 the primary hydroxyl group reacted to formation of *5-O*- ester **19a**. Diesters such as *1,6-di-O*-, *2,6-di-O*-, *3,5-di-O*-, and *6,6'-di-O*- were found to be formed in case of L-prolyl-D-fructose **20c**, L-phenylalanyl-D-glucose **24c** and **d**, L-phenylalanyl-D-galactose **25d** and **c**, L-phenylalanyl-lactose **29c**, L-phenylalanyl-D-mannitol **31b**, L-tryptophanyl-D-glucose **32d** and **e** and L-histidyl-D-glucose **40d** and **e**. It was not possible to separate the individual esters from their reaction mixtures even by separating them by chromatography on Sephadex G-10 or Bio-gel P2. Thus the activities described are for the mixtures of these mono and diesters.

6.3. Discussion

IC₅₀ values ≤ 1.0 mM were obtained for L-phenylalanyl-D-glucose **24a-e** (1.0 ± 0.09 mM), L-tryptophanyl-D-fructose **35a** and **b** (0.9 ± 0.09 mM) and L-histidyl-D-fructose **42** (0.9 ± 0.09 mM). Among amino acyl esters tested for ACE inhibition activity, L-phenylalanyl-D-glucose **24a-e** (1.0 ± 0.09 mM), L-tryptophanyl-D-fructose **35a** and **b** (0.9 ± 0.09 mM) and L-histidyl-D-fructose **42** (0.9 ± 0.09 mM) were found to exhibit the best inhibitory activity. Among the carbohydrates employed, D-fructose **8** and D-mannitol **15** esters showed better ACE inhibition (Table 6.2) than the other carbohydrate esters. L-Prolyl esters (**16a-c**, **19a-c**, **20a** and **b** and **21a** and **b**) containing prolyl unit, an active unit of captopril, showed IC₅₀ values in the 1.4 - 4.4 mM concentrations range (Table 6.2). Although amino acyl esters were separated from the reaction mixture by column chromatography, it was difficult to separate the individual esters. Hence, the actual potency of the individual esters could not be unequivocally established in the present work.

The present work for the first time has shown the ACE inhibitory potency of the above mentioned esters prepared enzymatically. Since milder reaction conditions were

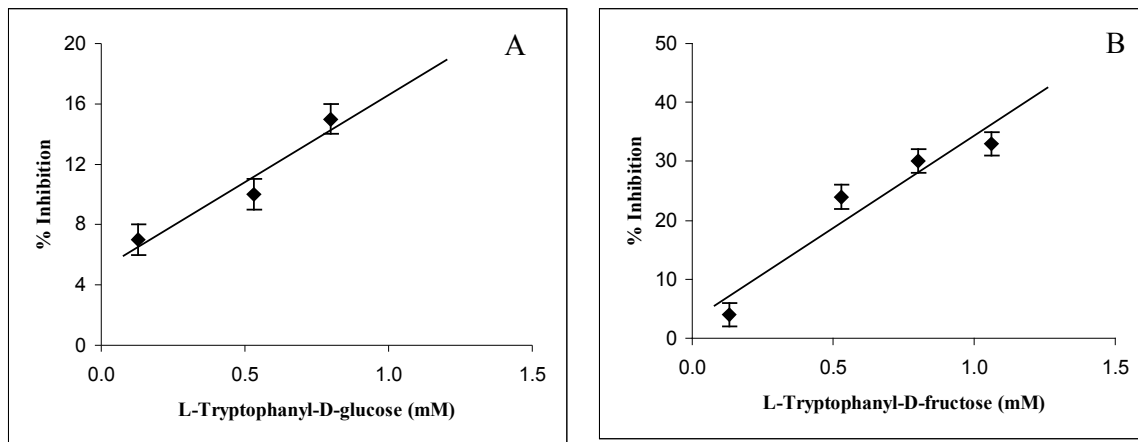


Fig. 6.4. ACE inhibition plots for L-tryptophanyl esters of carbohydrates (A) L-tryptophanyl-D-glucose **32a-e**, concentration range – 0.13–1.06 mM, substrate – 0.1 mL hippuryl-histidyl-leucine (5 mM), Buffer – 100 mM phosphate buffer pH 8.3 containing 300 mM NaCl, Incubation period –30 min, Temperature-37 °C. (B) L-tryptophanyl-D-fructose **35a** and **b**, concentration range – 0.13 –1.06 mM, concentration range – 0.2 –1.2 mM.

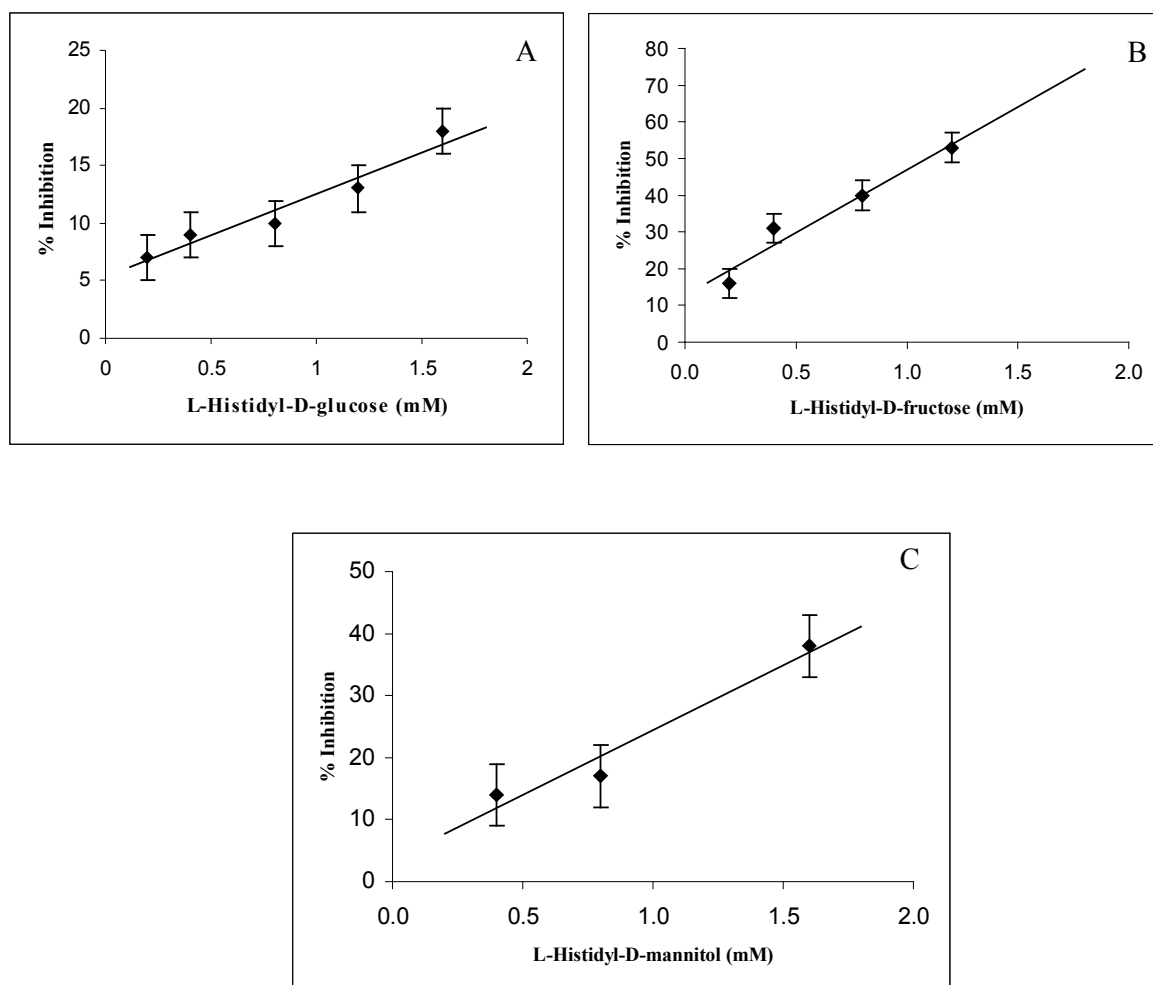


Fig. 6.5. ACE inhibition plots for L-histidyl esters of carbohydrates (A) L- histidyl-D-glucose **40a-e**, concentration range – 0.2–1.6 mM, substrate – 0.1 mL hippuryl-histidyl-leucine (5 mM), Buffer – 100 mM phosphate buffer pH 8.3 containing 300 mM NaCl, Incubation period –30 min, Temperature-37 °C. (B) L-histidyl-D-fructose **42**, concentration range – 0.2 –1.6 mM, (C) L- histidyl-D-mannitol **44**, concentration range – 0.2 –1.6 mM.

employed, the products formation did not suffer due to side reactions. Captopril is N-[(S)-3-mercapto-2-methylpropionyl]-L-proline containing prolyl unit as essential for ACE inhibition (De-Lima 1999). Although, the prolyl esters of D-glucose, D-fructose, D-ribose, lactose and D-mannitol were prepared and tested, mere presence of a prolyl unit does not give rise to a high level of ACE inhibition. However, the esters tested in the present work, clearly possess groups like pyrrolidine ring and aromatic groups, which can be accommodated in the hydrophobic S₁ and S₂ subsites of Angiotensin I converting enzyme (Michaud *et al.* 1997, De-Lima 1999). The free amino group in the amino acid esters can also serve as good ligands for Zn²⁺ in the ACE active site. Carbohydrates in esters could also bind to the hydrophobic and/or hydrophilic subsites S₁ and S₂ of Angiotensin I converting enzyme, as they possess both hydrophobic and hydrophilic groups in their structure. Thus the results indicate that amino acyl esters of carbohydrates bind to these enzymes and hence hold promise as potential inhibitors for the ACE.

6.4. Experimental

6.4.1. Extraction of ACE from pig lung

ACE was extracted from pig lung (Section 2.2.15) using the method described by Andujar-Sanchez *et al.* (2003). A 100 g of pig lung was minced and homogenized using a blender with 10 mM HEPES buffer pH 7.0 containing 0.4M NaCl at a volume ratio of 5:1 (v/w of pig lung) at 4 °C. The homogenate was centrifuged at 9000 g for 60 min. The supernatant was discarded and the precipitate was washed twice with 200 mL of 10 mM HEPES buffer pH 7.0 containing 0.4M NaCl. The final precipitate was resuspended in 200 mL of 10 mM HEPES buffer pH 7.0 containing, 0.4M NaCl, 10 µM ZnCl₂, 0.5%(w/v) Triton X100 and stirred over night at 4 °C. The solution was centrifuged to remove the pellets. The supernatant was dialyzed against water and later lyophilized. The protein content of ACE determined by Lowry's method was found to be 8.3%.

6.4.2. Esterification Procedure

A general procedure employed for the esterification reaction is as follows. Esterification was carried out in a flat bottom two necked flask by reacting 0.001- 0.008 mol unprotected L-amino acid (L-proline, L-phenylalanine, L-tryptophan and L- histidine) and 0.001 – 0.002 mol of carbohydrate (D-glucose, D-galactose, D-fructose, D-ribose, lactose and D-mannitol) along with 100 mL CH₂Cl₂: DMF (90:10 v/v, 40 °C) or hexane: CHCl₃: DMF (45:45:10 v/v, 61 °C) in presence of 0.60 - 0.180 g of lipases (40 to 50% w/w carbohydrate employed) under reflux for a period of three days. *Candida rugosa* lipase (CRL) in presence of 0.2 mM (0.2 mL) pH 4.0 acetate buffer was employed. The condensed vapour of solvents which formed an azeotrope with water was passed through a desiccant before being returned into the reaction mixture, thereby facilitating complete removal of water of reaction (Lohith and Divakar 2005). This set up maintained a very low water activity of $a_w = 0.0054$ throughout the reaction period. After completion of the reaction, the solvent was distilled off 20- 30 mL of warm water was added, stirred and filtered to remove the lipase. The filtrate was evaporated to get a mixture of the unreacted carbohydrate, unreacted L-amino acids and the product esters, which were then analyzed by HPLC. A Shimadzu LC10AT HPLC connected to LiChrosorb RP-18 column (5 µm particle size, 4.6 x 150 mm length) with acetonitrile: water (20:80 v/v) as a mobile phase at a flow rate of 1mL/min was employed using an UV detector at 210nm in case of L-prolyl esters and at 254nm in case of L-phenylalanyl, L-tryptophanyl and L-histidyl esters of carbohydrates. The conversion yields were determined with respect to peak areas of the L-amino acid and that of the esters. The esters formed were separated by size exclusion chromatography using Sephadex G-10 and Bio Gel P-2 as column materials and eluted with water. The product esters separated were subjected to spectral characterization by UV, IR, mass, specific rotation and 2D-NMR.

6.4.3. Angiotensin Converting Enzyme (ACE) inhibition assay

ACE inhibition assay for the esters prepared were performed by the Cushman and Cheung method (Cushman and Cheung 1971). Aliquots of ester solutions in the concentration range 0.12 to 1.60 mM (0.1 mL to 0.8 mL of 2.0 mM stock solution) were taken and to this 0.1 mL of ACE solution (0.1% in 0.1 M phosphate buffer, pH 8.3 containing 300 mM NaCl) was added. To this solution, 0.1 mL of 5.0 mM hippuryl-L-histidyl-L-leucine (HHL) was also added and the total volume made upto 1.25 mL by adding phosphate buffer (0.95 mL to 0.25 mL of 0.1 M pH 8.3 containing 300 mM NaCl). The solution was incubated on a Heto-Holten shaking water bath for 30 min at 37 °C. Blanks were performed without the enzyme by taking only the ester solution (0.1 to 0.8 mL) along with 0.1 mL of 5.0 mM HHL. The total volume was made upto to 1.25 mL by adding same buffer (1.05 mL to 0.35 mL). The reaction was terminated by adding 0.25 mL of 1M HCl. Hippuric acid formed in the reaction was extracted with 1.5 mL of ethyl acetate. One ml of the ethyl acetate layer was evaporated to dryness and treated with equal amount of distilled water and absorbance was measured at 228 nm for hippuric acid. The hippuric acid formed in 1.5 mL of ethyl acetate was determined from a calibration plot prepared by using a standard hippuric acid in 1 mL of distilled water in the concentration range 0-400 nmol and measuring its absorbance at 228 nm. Specific activity was expressed as mM of hippuric acid formed per min per mg of enzyme protein.

$$\text{Specific activity} = \frac{A_{\text{ts}} - A_{\text{blank}}}{T \times S \times E}$$

A_{ts} = absorbance of test solution, A_{blank} = absorbance of blank solution, T = incubation period in min, S = slope value of the calibration plot (1.006×10^{-2} Abs units/nmol of hippuric acid), E = amount of the enzyme in mg protein. Percentage inhibition was

expressed as the ratio of the specific activity of ACE in the presence of the inhibitor to that in the absence of the inhibitor, the latter being considered as 100%. IC₅₀ value was expressed as the concentration of the inhibitor required for 50% reduction in ACE specific activity. Molecular weights of the esters employed in the calculations are weighted averages of molecular weights of esters detected by NMR spectroscopy.

A Shimadzu UV-1601 spectrophotometer was employed for the measurement of absorbance readings at 228nm.

Conclusions

The important findings of the present investigation are:

1. The esterification potentialities of lipases from *Rhizomucor miehei* (RML), *Candida rugosa* (CRL) and porcine pancreas (PPL) were explored in detail for the syntheses of L-prolyl **1**, L-phenylalanyl **2**, L-tryptophanyl **3** and L-histidyl **4** esters of carbohydrates (D-glucose **5**, D-galactose **6**, D-mannose **7**, D-fructose **8**, D-arabinose **9**, D-ribose **10**, lactose **11**, maltose **12**, sucrose **13**, D-sorbitol **14**, D-mannitol **15**) using unprotected and unactivated amino acids and carbohydrates.
2. About 29 L-amino acyl esters of carbohydrates (**16a-c - 44**) have been synthesized in the present work and about 19 esters are reported for the first time. The new esters reported are: L-prolyl-D-glucose **16a-c**, L-prolyl-D-galactose **17a-c**, L-prolyl-D-mannose **18a-e**, L-prolyl-D-ribose **19a** and **b**, L-prolyl-D-fructose **20a-c**, L-prolyl-lactose **21a** and **b**, L-prolyl-maltose **22a-c**, L-prolyl-D-sorbitol **23a** and **b**, L-phenylalanyl-D-arabinose **28a-c**, L-tryptophanyl-D-mannose **33**, L-tryptophanyl-D-galactose **34**, L-tryptophanyl-D-fructose **35a** and **b**, L-tryptophanyl-lactose **36a** and **b**, L-tryptophanyl-maltose **37a-d**, L-histidyl-D-glucose **40a-e**, L-histidyl-D-mannose **41a** and **b**, L-histidyl-D-fructose **42**, L-histidyl-maltose **43a-c** and L-histidyl-D-mannitol **44**.
3. Lipase catalyzed esterification reactions of L-phenylalanyl-D-glucose **24a-e** and L-phenylalanyl-lactose **29a-c** were optimized in terms of incubation period, solvents, lipase concentrations, substrate concentrations, buffer pH and its concentrations and lipase reusability.
4. An experimental set-up for these esterification reactions has been developed which maintains a very low water activity ($a_w = 0.005$). The set-up involves refluxing an

appropriate amount of L-amino acid and carbohydrate in presence of buffer salts and lipases in the specified low boiling solvent mixture. The condensed vapors of the solvent was passed through a desiccant before being returned into the reaction mixture, which facilitates complete removal of water of reaction. This set-up uses larger concentrations of substrates and lesser amounts of the enzymes and results in higher conversions.

5. NMR spectral characterization confirmed that only monoesters (*1-O-*, *2-O-*, *3-O-*, *4-O-*, *5-O-*, *6-O-* and *6'-O-*) and in most of the cases few diesters (*1,6-di-O-*, *2,5-di-O-*, *2,6-di-O-*, *3,6-di-O-*, *4,6'-di-O-* and *6,6'-di-O-*) were found to be formed in this esterification reaction. Primary hydroxyl groups of mono and disaccharides were found to be invariably esterified (*1-O-*, *5-O-*, *6-O-*, *6'-O-* and *6,6'-di-O-*). Out of secondary hydroxyl groups *2-O-*, *3-O-* and *4-O-* were found to be esterified to different extents depending on the L-amino acids, lipase and the carbohydrate employed. NMR spectroscopy also indicated that both α and β anomers reacted in case of D-glucose **5**, D-galactose **6**, D-mannose **7**, D-arabinose **9**, D-ribose **10**, lactose **11** and maltose **12**. Among the carbohydrates, only D-mannose formed *4-O-* ester. The anomeric hydroxyl groups did not react.
6. Certain carbohydrates containing axial hydroxyl groups like, C2 position in D-mannose **7** and D-ribose **10** and C4 position in D-galactose **6** have not reacted indicating that esterification with axial secondary hydroxyl group is difficult to achieve, especially with bulky acyl donor amino acids. Carbohydrates like D-arabinose **9**, D-ribose **10**, sucrose **13**, D-sorbitol **14** and D-mannitol **15** reacted selectively indicating that they are not very good acyl acceptors. This could be due

to smaller size of the carbohydrate molecule in case of D-arabinose **9** and D-ribose **10** resulting in firm binding, more hydrogen bonding propensity in case of the linear carbohydrate molecules, D-sorbitol **14** and D-mannitol **15** and steric hindrance in case of sucrose **13**.

7. Loss of stereoselectivity could be due to use of larger amount of the enzymes employed.
8. In the present esterification no maillard reaction product was found to be formed. Although underivatised amino acids were employed, less than 3% peptide formation had been detected and that too in few cases only.
9. Response surface methodological study was carried out to optimize the RML catalysed esterification reaction of L-phenylalanyl-D-glucose **24a-e**. Five important variables like L-phenylalanine concentration, RML concentration, buffer pH, buffer concentration and incubation period in h were considered. Predictive equation developed and the surface and contour plots generated brought out the salient features of this esterification reaction.
10. Kinetic studies of the esterification reaction between L-phenylalanine **2** and D-glucose **5** catalysed by RML and CRL showed that kinetics followed Ping-Pong Bi-Bi mechanism with competitive substrate inhibition by one or two substrates leading to dead end lipase substrate complex formation. This kinetic study showed competitive substrate inhibition by both L-phenylalanine and D-glucose in case of RML and only by D-glucose in case of CRL.
11. Among 14 amino acyl esters of carbohydrates tested for Angiotensin Converting Enzyme inhibition activity, a few like, L-phenylalanyl-D-glucose **24a-e** (1.0 ± 0.09

mM), L-tryptophanyl-D-fructose **35a** and **b** (0.9 ± 0.09 mM) and L-histidyl-D-fructose **42** (0.9 ± 0.09 mM) were found to exhibit the best ACE inhibition activities.

Summary

Enzymatic synthesis is advantageous compared to chemical synthesis in many ways. Very few reports are available on the synthesis of amino acyl esters of carbohydrates, which involves mainly proteases, protected and activated amino acids and carbohydrates (Maruyama *et al.* 2002; Park *et al.* 1996; 1999; Riva *et al.* 1988). However, there are practically no reports on the synthesis of amino acyl esters of carbohydrates using unprotected and unactivated amino acids and carbohydrates with lipases as catalysts. The present work describes lipases catalysed synthesis of amino acyl esters of few carbohydrates using unprotected and unactivated amino acids and carbohydrates. Amino acyl esters of carbohydrates possess wide variety of applications in food and pharmaceutical industries as sweeteners, surfactants, microcapsules in pharmaceutical preparation, anti viral nucleoside amino acids, antitumor agents and intermediates in the synthesis of biologically active peptides (Krik 1992; Zaks and Dodds 1997). Use of lipases in non-polar solvents for the synthesis of amino acyl esters of carbohydrates offers many advantages like milder conditions, low temperature, stereo and regio selectivity, easy work out procedures, improved product yields, less byproducts and no colouring of products (Klibanov 1986).

Chapter **ONE** deals with literature survey on mainly lipase catalysed esterification reactions. Applications of lipase catalysis in different food and pharmaceutical industries are discussed. Factors affecting esterification reaction like nature of substrates, nature of solvents, thermal stability of lipases, water activity and immobilization are discussed. Different strategies in lipase catalysis, like esterification using reverse micelles, supercritical carbon dioxide and micro oven assisted reactions are presented. Kinetics of lipase catalysis and optimization of reaction parameters using

response surface methodology are also described. The chapter ends with a brief description on the scope of the present investigation.

Chapter **TWO** deals with materials and methods. Chemicals employed and their sources are listed. Methods of preparation of L-amino acyl esters of carbohydrates and the other related appropriate aspects of the same are discussed in detail.

Chapter **THREE** describes results from investigations on the synthesis of L-phenylalanyl-D-glucose **24a-e** and L-phenylalanyl-lactose **29a-c** using lipases from *Rhizomucor miehei* (RML), porcine pancreas (PPL) and *Candida rugosa* (CRL). Enzymatic esterification between L-phenylalanine **2** with D-glucose **5** and lactose **11** using RML, PPL and CRL were investigated in terms of incubation period, solvent, enzyme concentrations, substrate concentrations, buffer salts (pH and concentration) and enzyme reusability. Under the experimental conditions employed, all the three lipases exhibited good esterification potentialities. Among the various solvents mixtures employed for the synthesis of L-phenylalanyl-D-glucose **24a-e**, CH₂Cl₂ and DMF (90:10 v/v) was found to be the best. Both PPL and RML showed maximum conversion yields of L-phenylalanyl-D-glucose **24a-e** (98% and 76% of respectively) at 40% (w/w D-glucose) of enzyme employed and CRL showed a maximum conversion of 64% of L-phenylalanyl-lactose **29a-c** at 50% (w/w lactose) enzyme concentration. In presence of buffer salts, conversion yields enhanced by 10% in case of RML and PPL whereas in case of CRL more than 30% esterification enhancement was observed. At higher equivalents of substrates, decrease in conversion yields observed could be due to inhibition at higher concentrations of L-phenylalanine **2**, D-glucose **5** and lactose **11**. In the synthesis of L-phenylalanyl-D-glucose **24a-e** RML could be reused upto four cycles where as PPL could used only upto two cycles.

Reaction conditions for *Rhizomucor miehei* lipase (RML) catalysed synthesis of L-phenylalanyl-D-glucose **24a-e** using unprotected L-phenylalanine **2** and D-glucose **5** were optimized using Response Surface Methodology (RSM). A Central Composite Rotatable Design (CCRD) was employed involving 32 experiments of five variables (L-phenylalanine concentration in mmol, amount of RML in mg, pH, incubation period in h and buffer concentration in mM) at five levels. A second order polynomial equation was developed in terms of linear, quadratic and cross product terms to study the effects of variables on esterification yields. Surface and contour plots obtained, explained the esterification behaviour clearly. An optimum predicted yield of 1.01 mmol for L-phenylalanyl-D-glucose at 3 mmol L-phenylalanine, 100 mg of RML, 24h incubation period, 0.5 mM (0.5 mL of 0.1M buffer), pH 4.8 acetate buffer was found to agree with 0.97 mmol obtained under these experimental conditions. Validation experiments carried out under random conditions also exhibited good correspondence between predicted and experimental yields.

Chapter **FOUR** describes the syntheses and characterization of L-prolyl **1**, L-phenylalanyl **2**, L-tryptophanyl **3** and L-histidyl **4** esters of carbohydrates (D-glucose **5**, D-galactose **6**, D-mannose **7**, D-fructose **8**, D-arabinose **9**, D-ribose **10**, lactose **11**, maltose **12**, sucrose **13**, D-mannitol **14**, D-sorbitol **15**). Esterification was carried out using lipase from *Candida rugosa* (50% w/w carbohydrate) in 100 mL of CH₂Cl₂ and DMF (90 : 10 v/v, 40 °C) containing 0.2 mL of 0.1M (corresponds to 0.2 mM in 100 mL solvent) pH 4.0 acetate buffer for 72 h incubation. *Candida rugosa* lipase (CRL) showed broad substrate specificity towards amino acids as well as carbohydrates.

Esterification yields were obtained in the range of 7-79%. About 29 L-prolyl (**16 a-c** – **23a** and **b**), L-phenylalanyl (**24a-e**– **31a** and **b**), L-tryptophanyl (**32a-e** – **39a** and **b**) and

L-histidyl (**40a-e – 44**) esters of carbohydrates were prepared, of which 19 esters have not been reported before. These are: L-prolyl-D-glucose **16a-c**, L-prolyl-D-galactose **17a-c**, L-prolyl-D-mannose **18a-e**, L-prolyl-D-ribose **19a** and **b**, L-prolyl-D-fructose **20a-c**, L-prolyl-lactose **21a** and **b**, L-prolyl-maltose **22a-c**, L-prolyl-D-sorbitol **23a** and **b**, L-phenylalanyl-D-arabinose **28a-c**, L-tryptophanyl-D-mannose **33**, L-tryptophanyl-D-galactose **34**, L-tryptophanyl-D-fructose **35a** and **b**, L-tryptophanyl-lactose **36a** and **b**, L-tryptophanyl-maltose **37a-d**, L-histidyl-D-glucose **40a-e**, L-histidyl-D-mannose **41a** and **b**, L-histidyl-D-fructose **42**, L-histidyl-maltose **43a-c** and L-histidyl-D-mannitol **44**. Aldohexoses (**5-7**), ketose (**8**) and disaccharides (**11** and **12**) showed better conversions with all the four L-amino acids **1-4**. L-Tryptophan **3** showed lesser conversion (7-70%) to esters compared to the other three amino acids (20-79%). L-Tryptophanyl-D-galactose **33**, L-tryptophanyl-D-mannose **34**, L-tryptophanyl-sucrose **38**, L-histidyl-D-fructose **42** and L-histidyl-D-mannose **44** formed only one ester. D-Glucose gave five diastereomeric esters with L-phenylalanine **24a-e**, L-tryptophan **32a-e** and L-histidine **40a-e** and the only exception being L-proline where only three monoesters **16a-c** are formed. Characterization of the isolated product esters (**16a-c – 44**) using UV, IR, mass and NMR spectroscopy were carried out. Molecular ion peaks in mass spectrum further confirmed the formation of esters. Two-dimensional HSQCT NMR spectroscopy of the product esters (**16a-c – 44**) gave good information on the nature and proportion of the esters formed. Nature of the products clearly indicated that primary hydroxyl groups of the carbohydrates (*1-O-*, *5-O-*, *6-O-*, *6'-O-* and *6,6'-di-O-*) esterified predominantly over secondary hydroxyl groups (*2-O-*, *3-O-* and *4-O-*). Anomeric region in NMR clearly indicated that both α and β anomers reacted in case of D-glucose **5**, D-galactose **6**, D-mannose **7**, D-arabinose **9**, D-ribose **10**, lactose **11** and maltose **12**.

Chapter **FIVE** describes kinetic study of the esterification reaction between D-glucose **5** and L-phenylalanine **2** catalyzed by lipases from *Rhizomucor miehei* (RML) and *Candida rugosa* (CRL). Detailed investigation showed that both RML and CRL followed Ping-Pong Bi-Bi mechanism with two distinct types of competitive inhibitions. Graphical double reciprocal plots and computer simulative studies showed that competitive double substrates inhibition at higher concentrations leading to dead-end inhibition in case of RML by both L-phenylalanine and D-glucose and in case of CRL, only by D-glucose at higher concentrations leading to dead end lipase-D-glucose complex. An attempt to obtain the best fit of these kinetic models through curve fitting yielded in good approximation, the values of important kinetic parameters, RML: $k_{cat} = 2.24 \pm 0.23$ mM/h.mg protein, K_m L-phenylalanine = 95.6 ± 9.7 mM, K_m D-glucose = 80.0 ± 8.5 mM, K_i L-phenylalanine = 90.0 ± 9.2 mM, K_i D-glucose = 13.6 ± 1.42 mM; CRL: $k_{cat} = 0.51 \pm 0.06$ mM/h.mg protein, K_m L-phenylalanine = 10.0 ± 0.98 mM, K_m D-glucose = 6.0 ± 0.64 mM, K_i D-glucose = 8.5 ± 0.81 mM.

Chapter **SIX** describes potentiality of L-prolyl-D-glucose **16a-c**, L-prolyl-D-fructose **19a-c**, L-prolyl-D-ribose **20a** and **b**, L-prolyl-lactose **21a** and **b**, L-phenylalanyl-D-glucose **24a-e**, L-phenylalanyl-D-galactose **26a-e**, L-phenylalanyl-D-fructose **27a** and **b**, L-phenylalanyl-lactose **29a-c**, L-phenylalanyl-D-mannitol **31a** and **b**, L-tryptophanyl -D-glucose **32a-e**, L-tryptophanyl -D-fructose **35a** and **b**, L-histidyl-D-glucose **40a-e**, L-histidyl-D-fructose **42** and L-histidyl-D-mannitol **44** as inhibitors towards Angiotensin Converting Enzyme (ACE) activity. Amino acyl esters of carbohydrates tested for ACE inhibition activity showed IC_{50} values for ACE inhibition in the 0.9 mM to 13.6 mM range. L-phenylalanyl-D-glucose **24a-e** (IC_{50} : 1.0 ± 0.09 mM), L-tryptophanyl-D-fructose

35a and **b** (IC_{50} : 0.9 ± 0.09 mM) and L-histidyl-D-fructose **42** (IC_{50} : 0.9 ± 0.09 mM) showed the best ACE inhibitory activities.

The present investigation has thus demonstrated the potentiality of RML, PPL and CRL to syntheses biologically and nutritionally active amino acyl esters of carbohydrates (**16a-c** – **44**) using unprotected and unactivated L-amino acids and carbohydrates.

Bibilography

- Adachi, S., Kobayashi, T. (2005). Synthesis of esters by immobilized lipase catalyzed condensation reaction of sugars and fatty acids in water-miscible organic solvent. **J. Biosci. Bioeng.** 99(2), 87-94.
- Adlerhorst, K., Björking, F., Godtfredsen, S.E., Kirk, O. (1990). Enzyme catalyzed preparation of 6-O-acylglucopyranosides. **Synthesis** 1, 112-115.
- Aires-Barros, M.R., Cabral, J.M.S., Willson, R.C., Hamel, J.F.P., Cooney, C.L. (1989) Esterification coupled extraction of organic acids. Partition enhancement and underlying reaction and distribution equilibria. **Biotechnol. Bioeng.** 34, 909-915.
- Akoh, C.C., Copper, C., Nwosu, C.V. (1992). Lipase G-catalysed synthesis of monoglycerides in organic solvent and analysis by HPLC. **J. Am. Oil Chem. Soc.** 69, 257-260.
- Alhir, S., Markajis, S., Chandan, R. (1990). Lipase of *Penicillium caseicolum*. **J. Agri. Food Chem.** 38, 598-601.
- Andujar-Sanchez, M., Camara-Artigas, A., Jara-Perez V. (2003). Purification of angiotensin I converting enzyme from pig lung using concanavalin-A sepharose chromatography. **J Chromatogr B. Analyt Technol Biomed Life Sci.** 783(1), 247-52.
- Athawale, V., Manjrekar, N., Athawale, M. (2002). Lipase-catalyzed synthesis of geranyl methacrylate by transesterification: study of reaction parameters. **Tetrahedron Lett.** 43, 4797-4800.
- Belarbi, E.H., Molina, E., Chisti, Y. (2000). A process for high yield and scaleable recovery of high purity eicosapentaenoic acid esters from microalgae and fish oil. **Enzyme Microb. Technol.** 26, 516-529.
- Berger, R.G. (1995). In: Aroma Biotechnology. Springer. Berlin Heidelberg. NY, USA. pp-92-105.
- Bevinakatti, H., Banerjee, A. (1988). Lipase catalysis: factors governing transesterification. **Biotechnol. Lett.** 10(6), 397-398.
- Beyaz, A., Oh, W.S., Reddy, P. (2004) Synthesis and CMC studies of 1-methyl-3-(pentafluorophenyl)imidazolium quaternary salts. **Colloids and Surfaces B: Biointerfaces.** 15, 71-74.
- Birner-Grünberger, R., Scholze H., Faber K., Hermetter, A. (2004). Identification of various lipolytic enzymes in crude porcine pancreatic lipase preparations using covalent fluorescent. **Biotechnol. Bioeng.** 85, 147-154.
- Blanco, R.M., Guisan, J., Halling, P.J. (1989). Agarose chymotrypsin as a catalyst for peptide and amino acid ester synthesis. **Biotechnol. Lett.** 11, 811-816.

- Blanco, R.M., Terreros, P., Fernandez-Perez, M., Otero, C., Díaz-González, G. (2004). Functionalization of mesoporous silica for lipase immobilization characterization of the support and the catalysts. **J. Mol. Catal. B: Enzymatic**. 30(2), 83-93.
- Bloomer, S. (1992). Lipase-catalysed modifications in non-aqueous media, Doctoral Dissertation, Lund University, Lund, Sweden.
- Bloomer, S., Adlercreutz, P., Mattiasson, B. (1992). Facile synthesis of fatty acid esters in higher yields. **Enzyme Microb. Technol.** 14, 89-97.
- Bock, K., Pederson, C. (1983). Carbon – 13 Nuclear Magnetic Resonance spectroscopy of monosaccharides. Stuart-Tipson, R., Horton, D. (Eds). **Adv. Carbohydr. Chem. Biochem.** 41, 27-66.
- Bock, K., Pederson, C., Pederson, H. (1984). Carbon-13 Nuclear Magnetic Resonance data for oligosaccharides. Stuart-Tipson, R., Horton, D. (Eds). **Adv. Carbohydr. Chem. Biochem.** 42, 193 –225.
- Borzeix, F., Monot, F., Vandecasteele, J.P. (1992). Strategies for enzymatic esterification in organic solvents: Comparison of microaqueous, biphasic and micellar systems. **Enzyme Microb. Technol.** 14, 791-797.
- Bosley, J.A., Clayton, J.C., (1994). Blueprint for a lipase support: Use of hydrophobic controlled-pore glasses as model system. **Biotechnol. Bioeng.** 43, 934-938.
- Bousquet-Dubouch, M. P., Graber, M., Sousa, N. Lamare, S., Legoy, M.D. (2001). Alcoholysis catalysed by *Candida rugosa* lipase B in a gas/solid system obeys a Ping-Pong Bi-Bi mechanism with competitive inhibition by the alcohol substrate and water. **Biochem. Biophys. Acta** 1550(1), 90-99.
- Bousquet, M., Willemot, R., Monsan, P. and Boures, E. (1999). Enzymatic synthesis of unsaturated fatty acid glucoside esters for dermo-cosmetic applications. **Biotechnol. Bioeng.** 63(60), 730-736.
- Boyer, V., Stanchev, M., Fairbanks, A.J., Davis, B.G. (2001). Ready protease catalysed synthesis of carbohydrate-amino acid conjugates. **Chem. Commun.** 1908-1909.
- Brady, L., Brzozowski, A.M., Derewenda, U., Derewenda, Z.S., Dodson, G.G., Tolley, S., Turkenburg, J.P., Christiansen, L., Høge-Jensen, B., Nashkov, L., Thim, L., Menge, U. (1990). A serine protease triad forms the catalytic center of triglycerol lipase. **Nature**. 343, 767-770.
- Brink, L.E.S., Tramper, J. (1985). Optimization of organic solvent in multiple biocatalysis. **Biotechnol. Bioeng.** 27, 1259-1269.
- Brzozowski, A.M., Derewenda, U., Derewenda, Z.S., Dodson, G.G., Lawson, D.M., Turkenburg, J.P., Bjorkling, F., Høge-Jensen, B., Patkar, S.A., Thim, L. (1991). A model for interfacial activation in lipases from the structure of a fungal lipase-inhibitor complex, **Nature** 351, pp. 491-494

- Burdock. (1994). In: Fenaroli's Handbook of flavor ingredients. Volume II, 3rd edition, CRC press.
- Buzzini, P., Martini, A., Pagnoni, U.M., Davoli, P. (2003). Production of flavoured volatile organic compounds (VOCs) by *Candida oleophila* GK10, optimisation using factorial design and response surface analysis. **Enzyme Microb. Technol.** 33, 668-675.
- Camacho-Paez, B., Robles, M. A., Camacho, R. F, Esteban-Cerdán, L. and Molina, G. E. (2003). Kinetics of lipase-catalysed interesterification of triolein and caprylic acid to produce structured lipids. **J. Chem. Technol. Biotechnol.** 78(4), 461-470.
- Cambou, B., Klibanov, A.M. (1984a). Lipase-catalyzed production of optically active acids via asymmetric hydrolysis of esters. Effect of the alcohol moiety. **Appl. Biochem. Biotechnol.** 9, 255-260.
- Cambou, B., Klibanov, A.M. (1984b). Comparison of different strategies for the lipase catalyzed preparative resolution of racemic acids and alcohols: Asymmetric hydrolysis, esterification and transesterification. **Biotechnol. Bioeng.** 26, 1449-1454.
- Cameron, P.A., Davison, B.H., Frymier, P.D., Barton, J.W. (2002). Direct transesterification of gases by dry immobilized lipase. **Biotechnol. Bioeng.** 78, 251-256.
- Carrea, G., Ottolina, G., Riva, S. (1995). Role of solvents in the control of enzyme selectivity in organic media. **Trends Biotechnol.** 13, 63-70.
- Chand, S., Adlercreutz, P., Mattiasson, B. (1997). Lipase-catalysed esterification of ethylene glycol to mono and diesters. The effect of process parameters on reaction rate and production. **Enzyme Microb. Technol.** 20, 102-106.
- Chang, S.W. Shaw, J.F., Shieh, C.J. (2003) Optimization of enzymatically prepared hexyl butyrate. **Food Technol. Biotechnol.** 41, 237-242.
- Chapman., Halli. (1982a). Dictionary of organic compounds. 5th edition, Vol 5, pp-5645.
- Chapman., Halli. (1982b). Dictionary of organic compounds. 5th edition, Vol 3, pp-2957.
- Chen, Q.H., He, G.Q., Ali, M.A.M. (2002). Optimization of medium composition for the production of elastase by *Bacillus* sp.EL31410 with response surface methodology. **Enzyme Microb. Technol.** 30, 667-672.
- Chiang, W.D., Chang, S.W., Shieh, C.J. (2003). Studies on the optimized lipase-catalyzed biosynthesis of cis-3-hexen-1-yl acetate in n-hexane. **Proc. Biochem.** 38, 1193-1199.
- Chong-Qian, L., Bo-Gang, L., Hua-Yi, Q., Qi-Lin, L., Feng-Peng, W., Guo-Lin, Z. (2004), Three cyclooctapeptides and one glycoside from *Microtoena prainiana*. **J. Natur. Prod.** 67, 978-982.

- Chowdary, G.V., Divakar. S., Prafulla S.G. (2002). Modeling on isoamyl isovalerate synthesis from *Rhizomucor miehei* lipase in organic media: optimization studies. **World J. Microbiol. Biotechnol.** 18, 179-185.
- Chulalaksananukul, W., Condoret, J.S., Combes, D. (1993). Geranyl acetate synthesis by lipase catalysed transesterification in supercritical carbon dioxide. **Enzyme Microb. Technol.** 15, 691-698.
- Chulalaksananukul, W., Condort, J.S., Combes, D. (1992). Kinetics of geranyl acetate synthesis by lipase catalyzed transesterification in *n*-hexane. **Enzyme Microb. Technol.** 14, 293-298.
- Chulalaksananukul, W., Condort, J.S., Delorme, P., Willemot, R.M. (1990). Kinetic study of esterification by immobilized lipase in *n*-hexane. **FEBS Lett.** 276, 181-184.
- Claon, P.A., Akoh, C.C. (1994a). Lipase catalyzed synthesis of terpene esters by transesterification in *n*-hexane. **Biotechnol. Lett.** 16, 235-240.
- Claon, P.A., Akoh, C.C. (1994b). Effect of reaction parameters on SP435 lipase-catalyzed synthesis of citronellyl acetate in organic solvent. **Enzyme Microb. Technol.** 16, 835-838.
- Clifford, A.A. (1994). In: Supercritical fluids: Fundamentals and applications. Kiran, E., Levelt-Sengers J. M. H., (eds). Kluwer Academic Publishers, Dordrecht. pp- 449-464.
- Crespo, J.S., Queiroz, N., Nascimento, M.G., Soldi, V. (2005). The use of lipases immobilized on poly (ethylene oxide) for the preparation of alkyl esters. **Proc. Biochem.** 40, 401-409.
- Cushman, D.W., Cheung, H.S. (1971). Spectrophotometric assay and properties of the Angiotensin-Converting Enzyme of rabbit lung. **Biochem. Pharmacol.** 20, 1637-1648.
- Cygler, M., Grochulski, P., Kazlauskas, R.S., Schrag, J.D. Bouthillier, F., Rubin, B., Serreqi, A.N., Gupta, A.K. (1994), A structural basis for the chiral preferences of lipases. **J. Am. Chem. Soc.** 116, 3180-3186.
- Dae-Gill, K., Yong-Sup, L., Hyoung-Ja, K., Yun-Mi, L. and Ho-Sub, L. (2003). Angiotensin converting enzyme inhibitory phenylpropanoid glycosides from *Clerodendron trichotomum*. **J. Ethanopharmacol.** 89, 151-154.
- De-Lima, D. P. (1999). Synthesis of Angiotensin-Converting Enzyme (ACE) inhibitors: An important class of antihypertensive drugs. **Quim. Nova.** 22, 375-381.
- Deloffre, L., Sautiere, P.E., Huybrechts, R., Hens, K., Vieau, D., Salzert, M. (2004). Angiotensin Converting enzyme inhibition studies by natural leech inhibitors by capillary electrophoresis and competition assay. **Eur. J. Biochem.** 271, 2101-2106.

- Derewenda, U., Brzozowski, A.M., Lawson, D.M., Derewenda, Z.S. (1992). Catalysis at the interface: The anatomy of a conformational change in a triglyceride lipase. **Biochem.** 31, 1532-1541.
- Derewenda, Z.S., Derewenda, U. (1991). Relationships among serine hydrolases: evidence for a common structural motif in triacylglyceride lipases and esterases. **Biochem. Cell Biol.** 69, 842-851.
- Derewenda, Z.S., Sharp, A.M. (1993). News from the interface: the molecular structure of triacyl glyceride lipases. **Trends Biochem. Sci.** 18, 20-25.
- Divakar, S. (2003a). Lipase catalysed regioselective esterification of protocatechuic aldehyde. **Ind. J. Chem. Section B.** 42B, 1119-1122.
- Divakar, S. (2003b). Porcine pancreas lipase catalysed preparation of oligomers of p-hydroxybenzoic acid and p-aminobenzoic acid. **Ind. J. Chem. Section B.** 42B, 1467-1470.
- Divakar, S., Kiran, K.R., Harikrishna, S., Karanth, N.G. (1999). An improved process for the preparation of esters of organic acids and alcohols. 1243/DEL/99 No. 191078.
- Dixon, M., Webb, E.C. (1979). *Enzymes*. Academic Press. Orlando, FL, USA.
- Donner. (1976). Preparation of porcine pancreatic lipase free of co-lipase activity. **Acta Chem. Section B.** 30(5), 430-434.
- Dordick, J.S. (1981). Enzymatic catalysis in monophasic organic solvents. **Enzyme Microb. Technol.** 11, 194-211.
- Dorm, N., Belafi-Bak, K., Bartha, L., Ehrenstein, U., and Gubicza, L. (2004). Manufacture of an environmental-safe bio lubricant from fusel oil by enzymatic esterification in solvent-free system. **Biochem. Eng. J.** 21, 229-234.
- Duan, G., Ching, C.B., Lim, E. and Ang, C.H. (1997). Kinetic study of enantioselective esterification of ketoprofen with n-propanol catalysed by an lipase in an organic medium. **Biotechnol. Lett.** 19(11), 1051-1055.
- Eigtved, P. (1989). Immobilization of *Humicola* lipase on a particulate, macroporous resin. US Patent. 4,798,793. (CA 111: 170089)
- Engel, K.H., Bohnen, M., Dobe, M. (1991). Lipase catalyzed reaction of chiral hydroxyacid esters. Competition of esterification and transesterification. **Enzyme Microb. Technol.** 13, 655-660.
- Feichte, C., Faber, K., Griengl, H. (1989). Biocatalytic resolution of long-chain 3-hydroxy alkanolic esters. **Tetrahedron Lett.** 30, 551-552.

Ferrer, M., Cruces, M.A., Bernable, M., Ballesteros, A., Plou, F.J. (1999). Lipase catalysed regioselective acylation of sucrose in two solvent mixtures. **Biotechnol. Bioeng.** 65, 10-16.

Ferrer, M., Soliveri, J., Plou, F.J., Cortes, N.L., Duarte, D.R., Christensen, M., Patino, J.L. C., Ballesteros, A. (2005). Synthesis of sugar esters in solvent mixtures by lipases from *Thermomyces lanuginosus* and *Candida antarctica* B, and their antimicrobial properties. **Enzyme Microb. Technol.** 36, 391-398.

From, M., Adlercreutz, P., Mattiasson, B. (1997). Lipase catalyzed esterification of lactic acid. **Biotechnol. Lett.** 19, 315 - 317.

Gargouri, M., Drouet, P., Legoy, M.D. (2002). Synthesis of a novel macrolactone by lipase-catalyzed intra-esterification of hydroxy-fatty acid in organic media. **J. Biotechnol.** 92, 259-266.

Gayot, S., Santarelli, X., Coulon, D. (2003). Modification of flavonoid using lipase in non-conventional media: effect of the water content. **J. Biotechnol.** 101, 29- 36.

Gelo-Pujic, M., Guibe-Jampel, E., Loupy, A., Galema, S.A. Mathe, D. (1996). Lipase catalysed esterification of some α -D- glucopyranosides in dry media under focused microwave irradiation. **J. Chem. Soc. Perkin Trans 1**, 2777-2780.

Ghamgui, H., Karra-Chabouni, M., Gargouri, Y. (2004). 1-Butyl oleate synthesis by immobilized lipase from *Rhizopus oryzae*: a comparative study between *n*-hexane and solvent-free system. **Enzyme Microb. Technol.** 35, 355-363.

Gill, I., Valivety, R. (1997). Polyunsaturated fatty acids: Part 1. Occurrence, biological activities and applications. **Trends Biotechnol.** 15, 401-409.

Gillies, B., Yamazaki, H., Armstrong, D.W. (1987). Production of flavor esters by immobilized lipase. **Biotechnol. Lett.** 9, 709-714.

Gorman, L.A.S., Dordick, J.S. (1992). Organic solvents strip water off enzymes. **Biotechnol. Bioeng.** 39, 392-397.

Goto, M., Hatanaka, C., Masahiro, G. (2005). Immobilization of surfactant-lipase complexes and their high heat resistance in organic media. **Biochem. Engg. J.** 24, 91-94.

Gregory, R. B. (1995). In: Protein-Solvent interaction. Gregory R. B. (ed.), Marcel Dekker publication. pp. 191-264.

Grochulski, P., Bouthillier, F., Kazlauskas, R.J., Serreqi, A.N., Schrag, J.D., Ziomek, E., Cygler, M. (1994). Analogs of reaction intermediates identify a unique substrate binding site in *Candida rugosa* lipase. **Biochem.** 33, 3494-3500.

- Grochulski, P., Li, Y., Schrag, J.D., Bouthillier, F., Smith, P., Harrison, D., Rubin, B., Cygler, M., (1993). Insight into interfacial activation from an open structure of *Candida rugosa* lipase. **J. Biol. Chem.** 268, 12843–12847.
- Grünke, S. (2003). The influence of conductivity on the Karl Fischer titration. **Food Chem.** 82(1), 99-105.
- Gubicza, L., Kabiri-Badr, A., Keoves, E., Belafi-Bako, K. (2000). Large-scale enzymatic production of natural flavour esters in organic solvent with continuous water removal. **J. Biotechnol.** 84, 193-196.
- Gunnlaugsdottir, B., Jaremo, M., Sivik, B. (1998). Process parameters influencing ethanolysis of cod liver oil insupercritical carbon dioxide. **J. Super. Fluids.** 12, 85-93.
- Gutman, A.L., Shapira. (1991). Effect of water on enzymatic activity and stereoselectivity in organic solvents. Trans esterification of a disubstituted malonate diester. **J. Chem. Soc. Chem. Commun.** 1467-1468.
- Güvenc, A., Kapucu, N., Mehmetoglu, I. (2002). The production of isoamyl acetate using immobilized lipases in a solvent-free system. **Proc. Biochem.** 38, 379-386.
- Güvene, A., Kapucu, N., Bayraktar, E., Mehmetoglu, Ü. (2003). Optimization of the enzymatic production of isoamyl acetate with novozyme 435 from *Candida antarctica*. **Chem Eng commun.** 190, 948-961.
- Hahn-Hägardal, B. (1986). Water activity: a possible external regulator in biotechnical processes. **Enzyme Microb. Technol.** 8, 322-327.
- Haines, A.H. (1981) Selective removal of protecting groups in carbohydrate chemistry. **Adv. Carbohydr. Chem. Biochem.** 39, 13 -70.
- Halling, P.J. (1989). Organic liquids and biocatalysts: theory and practice. **Trends Biotechnol.** 7, 50-52.
- Halling, P.J. (1990). Lipase catalyzed modification of fats in organic two-phase systems. **Fat Sci. Technol.** 92, 74-79.
- Halling, P.J. (1992). Salt hydrates for water activity control with biocatalysis in organic media. **Biotechnol. Tech.** 6, 271-276.
- Halling, P.J. (1994). Thermodynamic predictions for biocatalysis in biocatalysis in non-conventional media: theory, dynamics predictions and recommendations for experimental design and analysis. **Enzyme Microb. Technol.** 16, 178-206.
- Hamsaveni, D.R., Prafulla, S.G., Divakar, S. (2001). Optimization of isobutyl butyrate synthesis using central composite rotatable design. **Proc. Biochem.** 36(11), 1103-1109.

- Han, Y., Chu, Y. (2005). The catalytic properties and mechanism of cyclohexane/DBSA/water microemulsion system for esterification. **J. Mol. Cat. A**: 237, 232-237.
- Harikrishna, S., Divakar, S., Karanth, N.G. (2001). Enzymatic synthesis of isoamyl acetate using immobilized lipase from *Rhizomucor miehei*. **J. Biotechnol.** 87(3), 193-201.
- Harikrishna, S., Manohar, B., Divakar, S., Karanth, N.G. (1999). Lipase catalysed synthesis of isoamyl butyrate: optimization by response surface methodology. **J. Am. Oil Chem. Soc.** 76, 1483-1488.
- Harikrishna, S., Manohar, B., Divakar, S., Prapulla, S.G., Karanth, N.G. (2000). Optimization of isoamyl acetate production using immobilized lipase from *Mucor miehei* by response surface methodology. **Enzyme Microb. Technol.** 26, 132-138.
- Hartmann, T., Meyerb, H.H., Scheper, T. (2001). The enantioselective hydrolysis of 3-hydroxy-5-phenyl-4-pentenoic acid ethylester in supercritical carbon dioxide using lipases. **Enzyme Microb. Technol.** 28, 653-660.
- Hirakawa, H., Kamiya, N., Kawarabayashi, Y., Nagamune, T. (2005). Log P effect of organic solvents on a thermophilic alcohol dehydrogenase. **Biochim. Biophys. Acta.** 1748, 94-99.
- Holmberg, K., Lassen, B., Stark, M.B. (1989). Enzymatic glycerolysis of a triglyceride in aqueous and non-aqueous emulsions. **J. Am. Oil Chem. Soc.** 66, 1796-1800.
- Huang, S.Y., Chang, H.L., Goto, M. (1998). Preparation of surfactant-coated lipase for the esterification of geraniol and acetic acid in organic solvents. **Enzyme Microb. Technol.** 22, 552-557.
- Hult, K., Norin, T. (1993). Enantioselectivity of some lipases: control and prediction. **Ind. J. Chem.** 32B, 123-126.
- Humeau, M., Girardin, B., Rovel, A.M. (1998). Effect of the thermodynamic water activity and the reaction medium hydrophobicity on the enzymatic synthesis of ascorbyl palmitate. **J. Biotechnol.** 63, 1-8.
- Hurtley, S.; Service, R.; Szuromi, P. (2001), Cinderella's coach is ready. **Science.** 291, 2337.
- Hyuncheol, O., Dae-Gill, K.C., Hun-Taeg, L., Ho-Sub. (2003). Four glycosides from the leaves of *Abeliophyllum distichum* with inhibitory effects on angiotensin converting enzyme. **Phytother. Res.** 17, 811-813.
- Ison, A.P., Dunill, P., Lilly, M., Macrae, A.R., Smith, C. (1990). Enzymic interesterification of fats: immobilization and immunogold localization of lipase on ion-exchange resins. **Biocatalysis** 3, 329-342.

- Iwai, M., Okumura, S., Tsujisaka, Y. (1980). Synthesis of terpene alcohol esters by lipase. **Agri. Biol. Chem.** 44, 2731-2732.
- Jackson, M.A., King, J.W. (1997). Lipase catalyzed glycerolysis of soybean oil in super critical carbon dioxide. **J. Am. Oil Chem. Soc.** 74, 103-106.
- Janssen, A.E.M., Sijnsnes, B.J., Vakurov, A.V., Halling, P.J. (1999). Kinetics of lipase catalyzed esterification in organic media: correct model and solvent effects on parameters. **Enzyme Microb. Technol.** 24, 463-470.
- Jeon, G.J., Park, O.J., Hur, B.K., Yang, J.W. (2001). Enzymatic synthesis of amino acid-sugar alcohol conjugates in organic media. **Biotechnol. Lett.** 23, 929-934.
- Johnston, C.I. (1992). Renin-angiotensin system: A dual tissue and hormonal system for cardiovascular control. **J. Hypertens.** 10, 13-26.
- Kanwar, L., Goswami, P. (2002). Isolation of a *Pseudomonas* lipase produced in pure hydrocarbon substrate and its application in the synthesis of isoamyl acetate using membrane-immobilised lipase. **Enzyme Microb. Technol.** 31, 727-735.
- Khaled, N., Montet, D., Pina, M., Graille, J. (1991). Fructose oleate synthesis in a fixed catalyst bed reactor. **Biotechnol. Lett.** 13, 167-172.
- Kim, J., Haam, S., Park, D.W., Ahn, I.S., Lee, T.G., Kim, H.S., Kim, W.S. (2004). Biocatalytic esterification of β -methylglucoside for synthesis of biocompatible sugar-containing vinyl esters. **Chem. Engg. J.** 99, 15-22.
- Kim, S.K., Byun, H.G., Park, P.J., Shahidi, F. (2001). Angiotensin I converting enzyme inhibitory peptides purified from bovine skin gelatin hydrolysate. **J. Agri. Food Chem.** 49(6), 2992-2997.
- Kiran, K.R., Divakar, S. (2001). Lipase catalysed esterification of organic acids with lactic acid. **J. Biotechnol.** 87, 109-121.
- Kiran, K.R., Divakar, S. (2002). Preparation of o-palmityl alkyl lactates through lipase catalysis. **World J. microbial. Biotechnol.** 18(2), 121-124.
- Kiran, K.R., Karanth, N.G., and Divakar, S. (2002). Hydrogen ion concentration at the microaqueous phase in lipase catalysed esterification in non-aqueous organic media - steroyllactic acid. *Ind. J. Biochem. Biophys.* 39, 101-105.
- Kiran, K.R., Karanth, N.G., Divakar, S. (1998). An improved enzymatic process for the preparation of fatty acid hydroxyacidester. 1978/DEL/98:187313.
- Kiran, K.R., Karanth, N.G., Divakar, S. (1999). Preparation of steroyl lactic acid catalysed by immobilized lipases from *Mucor miehei* and porcine pancreas optimization using response surface methodology. **Appl. Microbiol. Technol.** 52, 579-584.

- Kiran, K.R., Manohar, B., Divakar, S. (2001). A central composite rotatable design analysis of lipase catalysed synthesis of lauroyl lactic acid at bench-scale level. **Enzyme Microb. Technol.** 29, 122-128.
- Kiran, K.R., Manohar, B., Karanth, N.G., Divakar, S. (2000). Response Surface Methodological study of esterification of lactic acid with palmitic acid catalysed by immobilised lipases from *Mucor miehei* and porcine pancreas. **Z. Lebm. Unt. Fors.** 211, 130-135.
- Kiran, K.R., Suresh-Babu, C.V., Divakar, S. (2001). Thermostability of porcine pancreas lipase in non-aqueous media. **Proc. Biochem.** 36, 885-892.
- Kirk, O., Bjorkling, F., Godfredsen, S.E., Larsen, T.S. (1992). Fatty acid specificity in lipase catalysed synthesis of glucoside esters. **Biocatalysis.** 6, 127-134.
- Kittleson, J.R., Pantaleone. (1994). Enzymic biphasic process for the synthesis of aromatic esters flavoring agents from corresponding carboxylic acid and alcohol by esterification mediated by a lipase from *Candida cylindracea*. U. S. Patent. 5,437,991. (CA 123: 227820)
- Klibanov, A.M. (1986). Enzymes that work in organic solvents. **Chem. Technol.** 16, 354-359.
- Knez, Z., Leitgeb, M., Završnik, D., Lavrie, B. (1990). Synthesis of oleic acid esters with immobilized lipase. **Fat Sci. Technol.** 4, 169-172.
- Krieger, N., Bhatnagar, T., Baratti, J.C., Baron, A.M., De-Lima, V.M., Mitchell, D. (2004). Non-aqueous biocatalysis in heterogeneous solvent systems. **Food Technol. Biotechnol.** 42(4), 279-286.
- Krik, O., Bjorkling, F., Godfredsen, S. E., Larsen, T. S. (1992). Fatty acid specificity in lipase catalysed synthesis of glucoside esters. **Biocatalysis** 6, 127-134.
- Kumar, R., Modak, J., Madras, G. (2005). Effect of the chain length of the acid on the enzymatic synthesis of flavors in supercritical carbon dioxide. **Biochem. Engg. J.** 23, 199-202.
- Kumura, H., Mikawa, K., Saito, Z. (1993). Influence of milk proteins on the thermostability of the lipase *Pseudomonas fluorescens*. **J. Dairy Sci.** 76, 2164-2167.
- Kung, S., Rhee, J. (1989). Effect of solvents on hydrolysis of olive oil by immobilized lipase in reverse phase system. **Biotechnol. Lett.** 11, 37-42.
- Kunz, H. and Kullmann, R. (1992). Metal ion promoted activations of amino acid esters of carbohydrates in the synthesis of peptides. **Tetrahedron Lett.** 33, 6115-6118.
- Kvittengen, L. (1994). Some aspects of biocatalysis in organic solvents. **Tetrahedron.** 50, 8253-8274.

Kvittengen, L., Sjursnes, B., Anthonsen, T., Halling, P.J. (1992). Use of salt hydrate pairs to buffer optimal water level during lipase catalyzed synthesis in organic media. A practical procedure for organic chemists. **Tetrahedron**. 48, 2793-2802.

Laane, C., Boeren, S., Vos, K., Veeger, C. (1987). Rules for optimization of biocatalysis in organic solvents. **Biotechnol. Bioeng.** 30, 81-87.

Laemmli, U. K. (1970). Cleavage of structural proteins during assembly of the head bacteriophage T4. **Nature** 227, 680-685.

Langrand, G., Rondot, N., Triantaphylides, C., Baratti, J. (1990). Short-chain flavor esters synthesis by microbial lipases. **Biotechnol. Lett.** 12, 581-586.

Langrand, G., Triantaphylides, C., Baratti, J. (1988). Lipase catalysed formation of flavor esters. **Biotechnol. Lett.** 10, 549-554.

Lee, S.B. (1995). Enzyme reaction kinetics in organic solvents: A theoretical kinetic model and comparison with experimental observations. **J. Ferm. Bioeng.** 79, 479-484.

Leszczak, J.P., Tran-Minh, C. (1998). Optimized enzymatic synthesis of methyl benzoate in organic medium. Operating conditions and impact of different factors on kinetics. **Biotechnol. Bioeng.** 60(3), 556-561.

Li, G.H., Le, G.W., Yong-Hui, S. Shrestha, S. (2004). Angiotensin I-converting enzyme inhibitory peptides derived from food proteins and their physiological and pharmacological effects. **Nutr. Res.** 24, 469-486.

Liao, H .F., Tsai, W.C., Chang, S.W., Shieh, C.J. (2003). Application of solvent engineering to optimize lipase-catalyzed 1,3-diglycerols by mixture response surface methodology. **Biotechnol. Lett.** 25(21), 1857-1861

Lohith, K., Divakar, S. (2005). Lipase catalysed synthesis of L-phenylalanine esters of D-glucose. **J. Biotechnol.** 117, 49-56.

Lohith, K., Somashekar, B.R., Manohar, B., Divakar, S. (2005). An improved enzymatic process for the preparation of amino acyl esters of disaccharides. Indian patent. (submitted to CSIR patent cell).

Lohith, K., Vijayakumar, G.R., Manohar, B., Divakar, S. (2003). An improved enzymatic process for the preparation of amino acyl esters of monosaccharides. NF-492/03. PCT/03/00466.

Lortie, R., Trani, M., Ergon, F., 1993. Kinetic study of the lipase catalysed synthesis of triolein. **Biotechnol. Bioeng.** 41, 1021-1026.

Loupy, A., Petit, A., Hamelin, J., Texier-Boullet, F., Jacquault, P., Mathe, D. (1998). New solvent free organic synthesis using focused microwaves. **Synthesis** 2, 1213-1234.

- Lowry, O.H., Rosenbrough, N.J., Farr, A.L., Randal, R.J., (1951). Protein measurement with Folin Phenol reagent. **J. Biol. Chem.** 193, 265–275.
- Ma, L., Persson, M., Adlercreutz, P. (2002). Water activity dependence of lipase catalysis in organic media explains successful transesterification reactions. **Enzyme Microb. Technol.** 31, 1024-1029.
- Macedo, G.A., Lozano, M.M.S., Pastore, G.M. (2003). Enzymatic synthesis of short chain citronellyl esters by a new lipase from *Rhizopus* sp. **Electronic J. Biotechnol.** ISSN: 6(1), 0717-3458.
- Macedo, G.A., Pastore, G.M., Rodrigues, M.I. (2004). Optimising the synthesis of isoamyl butyrate using *Rhizopus* sp. lipase with a central composite rotatable design. **Proc. Biochem.** 39, 687-692.
- Malcata, F.X., Reyes, H.R., Garcia, H.S., Hill, J.C.G. (1990). Immobilized lipase reactors for modifications of fats and oils - A review. **J. Am. Oil Chem. Soc.** 67, 890-910.
- Manini, P., Napolitano, A., d'Ischia, M. (2005). Reaction of D-glucose with phenolic amino acids: further insights into competition between Maillard and Pictet-Spengler condensation pathways. **Carbohydr. Res.** 340, 2719 – 2727.
- Manohar, B., Divakar, S. (2002). Application of central composite rotatable design to lipase catalyzed syntheses of m-cresyl acetate. **World J. Microbiol. Biotechnol.** 18(8), 745-751.
- Manohar, B., Divakar, S. (2004a). Application of surface plots and statistical designs to selected lipase catalysed esterification reactions. **Proc. Biochem.** 39(7), 847-851.
- Manohar, B., Divakar, S. (2004b). Porcine pancreas lipase acetylation of beta-cyclodextrin anchored 4-t-butylcyclohexanol. **Ind. J. Chem. Section B.** 43B, 2661-2665.
- Marlot, C., Langrand, G., Triantaphylides, C., Baratti, J. (1985). Ester synthesis in organic solvent catalyzed by lipase immobilized on hydrophilic supports. **Biotechnol. Lett.** 647-650.
- Marty, A., Chulalaksananukul, W., Willemot, R.M., Condoret, J.S. (1992). Kinetics of lipase catalyzed esterification in super-critical CO₂. **Biotechnol. Bioeng.** 39, 273-276.
- Maruyama, T., Nagasawa, S.I., Goto, M. (2002). Enzymatic synthesis of sugar esters in organic solvents. **J. Biosci. Bioeng.** 94(4), 357-361.
- Mestri, S., Pai, J. S. (1994a). Effect of moisture on lipase catalyzed esterification of geraniol palmrosa oil in non-aqueous system. **Biotechnol. Lett.** 17, 459-461.
- Mestri, S., Pai, J.S. (1994b). Synthesis of isoamyl butyrate by lipase by lipase of *Mucor miehei*. **Pafai J.** 2, 24-26.

- Michaud, A., Williams, T.A., Chauvet, M.T., Corvol, P. (1997). Substrate dependence of angiotensin I-converting enzyme inhibition: captopril displays a partial selectivity for inhibition of N-acetyl-seryl-aspartyl-lysyl-proline hydrolysis compared with that of angiotensin I. **Mol. Pharmacol.** 51 1070-1076.
- Miller, C., Austin, H., Posorske, L., Gonzelez, J. (1988). Characteristics of an immobilized lipase for the commercial synthesis of esters. **J. Am. Oil Chem. Soc.** 65, 927-931.
- Mishio, T., Takahashi, K., Yoshimoto, T., Kodera, Y., Saito, Y., Inada, Y. (1987). Terpene alcohol ester synthesis by polyethylene glycol modified lipase in benzene. **Biotechnol. Lett.** 9, 187-190.
- Montgomery, D.C. (1991). Design and analysis of experiments. John Wiley and Sons, New York: pp 542-547.
- Mullally, M.M., Meisel, H. FitzGerald, R. J. (1996). Synthetic peptides corresponding to α -lactalbumin and β -lactoglobulin sequences with angiotensin-I-converting enzyme inhibitory activity. **Biol. Chem.** 377, 259-260.
- Murakata, T., Yusa, K., Yada, M., Kato, Y., Sato, S. (1996). Esterification activity of lipase entrapped in reverse micelles formed in liquefied gas. **J. Chem. Eng. Japan.** 29 (2), 277-281.
- Nagayama, K., Yamasaki, N., Imai, M. (2002). Fatty acid esterification catalyzed by *Candida rugosa* lipase in lecithin microemulsion-based organogels. **Biochem. Eng. J.** 12, 231-236.
- Nakamura, K., Takobe, Y., Kitayama, T., Ohno, A. (1991). Effect of solvent structure on enantioselectivity of lipase-catalyzed transesterification. **Tetrahedron Lett.** 32, 4941-4944.
- Naoe, K., Ohsa, T., Kawagoe, M., Imai, M. (2001). Esterification by *Rhizopus delemar* lipase in organic solvent using sugar ester reverse micelles. **Biochem. Eng. J.** 9, 67-72.
- Ngrek, S. (1947). Synthesizing power of liver lipase. **Acta. Biol. Exptl.** 14, 157-174.
- Noel, M., Combes, D. (2003). Effects of temperature and pressure on *Rhizomucor miehei* lipase stability. **J. Biotechnol.** 102, 23- 32.
- Nogales, J.M.R., Roura, E., Contreras, E. (2005). Biosynthesis of ethyl butyrate using immobilized lipase: a statistical approach. **Proc. Biochem.** 40, 63-68.
- Noureddini, H., Gao, X., Philkana, R.S. (2005). Immobilized *Pseudomonas cepacia* lipase for biodiesel fuel production from soybean oil. **Biores. Technol.** 96, 769-777.
- Orrenius, C., Norin, T., Hult, K., Carrea, G. (1995). The *Candida antartica* lipase B catalysed kinetic resolution of seudenol in non aqueous media of controlled water activity. **Tetrahedron: Asy.** 12, 3023-3030.

- Osorio, N.M., Ferreira-Dias, S., Gusmao, J.H., Da-Fonseca, M.M.R. (2001). Response surface modelling of the production of ω -3 polyunsaturated fatty acids-enriched fats by a commercial immobilized lipase. **J. Mol. Catal. B: Enzymatic**. 11, 677-686.
- Palomo, J.M., Segura, R.L., Mateo, C., Terreni, M., Guisan, J.M., Fernandez-Lafuente, R. (2003). Synthesis of enantiomerically pure glycidol via a fully enantioselective lipase-catalyzed resolution. **Enzyme Microb. Technol.** 33, 97-103.
- Parida, S., Dordick, J.S. (1991). Substrate structure and solvent hydrophobicity control: lipase catalysis and enantioselectivity in organic media. **J. Am. Chem. Soc.** 113, 2253-2259.
- Parida, S., Dordick, J.S. (1993). Tailoring lipase specificity by solvent substrate chemistries. **J. Org. Chem.** 58, 3238-3244.
- Park, O.J., Jeon, G.J., Yang, J.W. (1999). Protease catalysed synthesis of disaccharide amino acid esters in organic media. **Enzyme Microb. Technol.** 25, 455-462.
- Park, O.J., Park, H.G., Yang, J.W. (1996). Enzymatic transesterification of monosaccharides and amino acid esters in organic solvents. **Biotechnol. Lett.** 18, 473-478.
- Patil, D.R., Rethwisch, D.G., Dordick, J.S. (1991). Enzymatic synthesis of sucrose containing liner polyester in nearly anhydrous organic media. **Biotechnol. Bioeng.** 37, 639-646.
- Patridge, J., Harper, N., Moore, B., Halling, P.J. (2001). Enzymes in Nonaqueous Solvents Methods and Protocols In Series: **Methods Biotechnol.** pp - 227-234.
- Perraud, R., Laboret, F. (1989). Optimization of methyl propionate production catalyzed by *Mucor miehei* lipase. **Appl. Microbiol. Biotechnol.** 44, 321-326.
- Peschke, G. (1991) Active components and galenic aspects of enzyme preparations. In: Pancreatic enzymes in health and disease. Lankisch P.G.(ed). Springer, Berlin, pp. 55-64.
- Pleiss, J. Fischer, M. Schmidt, R.D. (1998). Anatomy of lipase binding sites: The scissile fatty acid binding site. **Chem. Phys. Lipid.** 93, 67-80.
- Plou, F.J., Cruces, M.A., Pastor, E., Ferrer, Bernab'e, M., Ballesterose1, A. (1999). Acylation of sucrose with vinyl esters using immobilized hydrolysis: demonstration that chemical catalysis may interfere with enzymatic catalysis. **Biotechnol. Lett.** 21, 635-639.
- Rahman, M.B.A., Md-Tajudin, S., Hussein, M.Z., Rahman, R.N.Z.R.A., Salleh, A.B., Basri, M. (2005). Application of natural kaolin as support for the immobilization of lipase from *Candida rugosa* as biocatalyst for effective esterification. **Applied Clay Sci.** 29,111-116.

- Rantwijk, F., Sheldon, R.A. (2004). Enantioselective acylation of chiral amines catalysed by serine hydrolases. **Tetrahedron**. 60, 501-519.
- Rao, P., Divakar, S. (2001). Lipase catalysed esterification of α - terpineol with various organic acids application of the Plakett- Burman design. **Proc. Biochem**. 36, 1125-1128.
- Rao, P., Divakar, S. (2002). Response surface methodological approach for the *Rhizomucor miehei* lipase- mediated esterification of α - terpineol with propionic acid and acetic anhydride. **World J. Microb. Biotechnol**. 18, 341 - 345.
- Razafindralambo, H., Blecker, C., Lognoy, G., Marlier, M., Wathlet, J. P., and Severin, M. (1994). Improvement of enzymatic synthesis yields of flavor acetates: the example of isoamyl acetate. **Biotechnol. Lett**. 16, 247-250.
- Rees, G.D., Robinson, B.H. (1995). Esterification reactions catalyzed by *Chromobacterium viscosum* lipase in CTAB-based micro-emulsion systems. **Biotechnol. Bioeng**. 45, 344-355.
- Rees, G.D., Robinson, B.H., Stephenson, R.G. (1995). Macrocyclic lactone synthesis by lipases in water-in-oil microemulsions. **Biochim. Biophys. Acta**. 1257, 239-248.
- Reihl, O., Bieme, K.M., Lederer, M.O., Schwach, W. (2004). Pyridinium-carbaldehyde: active maillard reaction product from the reaction of hexose with lysine residues. **Carbohydr Res**. 339, 705 – 714.
- Reimann, A., Robb, D.A., Halling, P.J. (1994). Solvation of CBZ aminoacid nitrophenyl esters in organic media and the kinetics of their transesterification by subtilisin. **Biotechnol. Bioeng**. 43, 1081-1086.
- Riva, S., Chopineau, J., Kieboom, A.P.G., Klibanov, A.M. (1988). Protease catalysed regioselective esterification of sugars and related compounds in anhydrous dimethylformamide. **J. Am. Chem. Soc**. 110, 584-589.
- Rizzi, M., Stylos, P., Riek, A., Reuss, M., (1992). A kinetic study of immobilized lipase catalyzing the synthesis of isoamyl acetate by transesterification in *n*-hexane. **Enzyme Microb. Technol**. 14, 709 -714.
- Romero, M.D., Calvo, L., Alba, C., Daneshfar, A., Ghaziaskar, H.S. (2005a). Enzymatic synthesis of isoamyl acetate with immobilized *Candida antarctica* lipase in *n*-hexane. **Enzyme Microb. Technol**. 37, 42-48.
- Romero, M.D., Calvo, L., Alba, C., Daneshfar, A., Ghaziaskar, H.S. (2003). Enzymatic synthesis of isoamyl acetate with immobilized *Candida antarctica* lipase in *n*-hexane. **Enzyme Microb. Technol**. 37: 42-48.
- Romero, M.D., Calvo, L., Alba, C., Habulin, M., Primožic, M., Knez, Z. (2005b). Enzymatic synthesis of isoamyl acetate with immobilized *Candida antarctica* lipase in supercritical carbon dioxide. **J. Supercrit. Fluids** 33(1), 77-84.

- Rubio, E., Fernandez-Mayorales, A., Klibanov, A.M. (1991). Effect of the solvent on enzyme regio-selectivity. **J. Am. Chem. Soc.** 113, 695-696.
- Sakurai, T., Margolin, A.L., Russell, A.J., Klibanov, A.M. (1988). Control of enzyme enantioselectivity by the reaction medium. **J. Am. Chem. Soc.** 110, 7236-7237.
- Santaniello, E. Ferraboschi, P and Paride Grisenti. (1993). Lipase-catalyzed transesterification in organic solvents: Applications to the preparation of enantiomerically pure compounds. **Enzyme Microb. Technol.** 15, 367-382.
- Sarney, D.B., Barnard, M.J., Mac-Manus, D.A., Vulfson, E.N. (1996). Application of Lipases to the regioselective synthesis of sucrose fatty acid monoesters. **J. Am. Oil Chem. Soc.** 73, 1481-1487.
- Sarney, D.B., Vulfson, E.N. (1995). Application of enzymes to the synthesis of surfactants. **Trends Biotechnol.** 13, 164-172.
- Scharpe, S., Uyttenbroeck, W., Samyn, N. (1997). Pancreatic enzyme replacement. In: Pharmaceutical enzymes -. Lauwers, A. and Scharpe, S. (eds), Marcel Dekker , INC. New York. pp. 187-221.
- Schlotterbeck, A., Lang, S., Wray, V., and Wagner, F. (1993). Lipase catalyzed monacylation of fructose. **Biotechnol. Lett.** 15, 61-64.
- Schrag, J. D., Cygler, M. (1997). Lipases and α/β hydrolase fold. **Methods Enzymol.** 284, 85-107.
- Schrag, J.D., Li. Y., Wu, S., Cygler, M. (1996). Ser-His-Glu triad forms the catalytic site of the lipase from *Geotrichum Candidum*. **Nature.** 351, 761-764.
- Schreier, P. (1997). In: Biotechnology of aroma compounds. Berger RG (ed). **Adv. Biochem. Engg. Biotechnol.** 17, 52.
- Schreier, P., Winterhalter, P. (1993). In: Progress in flavor precursor studies. Allured Carol Stream, USA.
- Scilimati, A., Ngooi, T.K., Sih, C.J. (1988). Biocatalytic resolution of (\pm)-hydroxyalkanoic esters. A strategy for enhancing the enantiomeric specificity of lipase-catalyzed ester hydrolysis. **Tetrahedron Lett.** 29, 4927-4930.
- Segel, I.H. (1993). *In: Enzyme Kinetics.* John-Wiley and Sons, NY, USA.
- Sharma, R., Chisti, Y., Banerjee, U.C. (2001). Production, purification, characterization and applications of lipases. **Biotechnol. Adv.** 19, 627-662.
- Shaw, J.F., Wu, H.Z., Shieh, C.J. (2003). Optimized enzymatic synthesis of propylene glycol monolaurate by direct esterification. **Food Chem.** 81, 91-96.

- Sheldon, R.A. (1996). Chirotechnology: designing economic chiral syntheses. **J. Chem. Tech. Biotechnol.** 67, 1-14.
- Shieh, C.J., Akoh, C.C., Koehler, P.E. (1995). Four-factor response surface optimization of the enzymatic modification of triolein to structured lipids. **J. Am. Oil Chem. Soc.** 72, 619-623.
- Shieh, C.J., Akoh, C.C., Yee, L.N. (1996). Optimized enzymatic synthesis of geranyl butyrate with lipase AY from *Candida rugosa*. **Biotechnol. Bioeng.** 51, 371-374.
- Shieh, C.J., Liao, H.F., Lee, C.C. (2003). Optimization of lipase-catalyzed biodiesel by response surface methodology. **Biores. Technol.** 88, 103-106.
- Shiraki K, Kudou M., Sakamoto R, Yanagihara I., Takagi M . (2004). Amino Acid esters prevent thermal inactivation and aggregation of lysozyme. **Biotechnol Prog.** 21(2), 640-3.
- Soo, E., Salleh, A.B., Basri, M., Noor-zaliha, R., Abdul-rahman, R., and Kamaruddin, K. (2003). Optimization of the enzyme catalyzed synthesis of amino acid - based surfactants from palm oil fractions. **J. Biosci. Bioeng.** 95(4), 361-367.
- Srivastava, S., Madras, S., Modak J. (2003). Esterification of myristic acid in supercritical carbon dioxide. **J. Supercrit. Fluids.** 27, 55- 64.
- Stamatis, H., Xenakis, A., Kolisis, F.N. (1999). Bioorganic reactions in microemulsions: the case of lipases. **Biotechnol. Adv.** 17, 293-318.
- Stamatis, H., Xenakis, A., Menge, V., Kolisis, F.N. (1993). Kinetic study of lipase catalyzed esterification in microemulsion. **Biotechnol. Bioeng.** 42, 931-937.
- Suresh-Babu, C.V., Divakar, S. (2001). Selection of alcohols through Plakett-Burman design in lipase catalyzed syntheses of anthranilic acid. **J. Am. Oil Chem. Soc.** 78(1), 49-52.
- Suresh-Babu, C.V., Karanth, N.G., Divakar, S. (2002). Lipase catalysed esterification of cresols. **Ind. J. Chem. Section B.** 41B, 1068-1071.
- Suzuki, Y., Shimizu, T., Takeda, H., Kanda, K. (1991). Fermentative or enzymatic manufacture of sugar amino acid esters. Japan Patent. 03216194 A2. (CA 116: 127007).
- Szczesna-Antczak, M., Antczak, T., Rzycka, M., Modrzejewska, Z., Patura, J., Kalinowska, H. and Bielecki, S., (2004). Stabilization of an intracellular *Mucor circinelloides* lipase for application in non-aqueous media. **Journal Molecular Catalysis, B, Enzymatic** 29, 155-161.
- Takahashi, K., Saito, Y., Inada, Y. (1988). Lipases made active in hydrophobic media. **J. Am. Oil Chem. Soc.** 65, 911-916.

- Talon, R., Montel, M.C., Berdague, J.L. (1996). Production of flavor esters by lipases of *Staphylococcus warneri* and *Staphylococcus xylosus*. **Enzyme Microb. Technol.** 19:620-622.
- Tamura, M., Shoji, M., Nakatsuka, T., Kinomura, K., Okai, H., Fukui, S. (1985). Methyl 2,3-di-(L- α -amimobutyryl)- α -D- glucopyranoside, a sweet substance and tastes of related compounds of neutral amino acids and D-glucose derivatives. **Agric. Biol. Chem.** 49, 2579 -2586.
- Therisod, M., Klibanov, A.M. (1986). Facile enzymatic preparation of mono acylated sugars in pyridine. **J. Am. Chem. Soc.** 108, 5638-5640.
- Torres, C., Otero, C. (1999). Part 1: Enzymatic synthesis of lactate and glycolate esters of fatty alcohols. **Enzyme Microb. Technol.** 25, 745-752.
- Tramper, J., Vermie, M.H., Beetink, H.H., Von-Stocker, U. (1992). In: Biocatalysis in non-conventional media. Elsevier, Amsterdam.
- Trani, M., Ergan, F., Andre, G. (1991). Lipase catalyzed production of wax esters. **J. Am. Oil Chem. Soc.** 68, 20-22.
- Turner, N.A., Duchateau, D.B., Vulfson, E.N. (1995). Effect of hydration on thermostability of serine esterases. **Biotechnol. Lett.** 17, 371-376.
- Ulbrich, R., Golbik, R., Schelleberger, A. (1991). Protein adsorption and leakage in carrier-enzyme systems. *Biotechnol. Bioeng.* 37, 280-287.
- Valivety, R.H., Halling, P.J., Macrae, A.R. (1993). Water as a competitive inhibitor of lipase-catalysed esterification in organic media. **Biotechnol. Lett.** 15(11), 1133-1138.
- Valivety, R.H., Johannes, L.L., Rakels, L., Blanco, R.M., Johnston, R.M., Brown, L., Suckling, C.J., Halling, P.J. (1990). Measurement of pH changes in an inaccessible aqueous phase during biocatalysis in organic media. **Biotechnol. Lett.** 12, 475-480.
- Valivety, R.H., Johnston, G.A., Suckling, C.J., Halling, P.J. (1991) Solvent effects on biocatalysis in organic systems: equilibrium position and rates of lipase catalyzed esterification. **Biotechnol. Bioeng.** 38: 1137-1143.
- Van-Tol, J.B.A., Odenthal, J.B., Jongejan, J.A., Duine, J.A. (1992). Relation of enzyme reaction rate and hydrophobicity of the solvent. *In: Biocatalysis in non-conventional media.* Tramper J. Vermue M. H., Beetink, H. H., Von-Stocker U. (eds). Elsevier, Amsterdam, 229-235.
- Vecchia, R.D., Sebrao, D., Nascimento, M.G., Soldi, V. (2005). Carboxymethylcellulose and poly (vinyl alcohol) used as a film support for lipases immobilization. **Proc. Biochem.** 40, 2677-2682.

- Verger, R., DeHass, K., Sarda, L., Desnuelle, P. (1969). Purification from porcine pancreas of two molecular species with lipase activity. **Biochem. Biophys. Acta.** 188, 272-282.
- Vermeirssen, V., Van-Camp, J., Verstraete, W. (2002). Optimisation and validation of an angiotensin-converting enzyme inhibition assay for the screening of bioactive peptides. **J. Biochem. Biophys.** 51, 75-87.
- Vermue, M.H., Tramper, J., (1995). Biocatalysis in non-conventional media. Medium engineering aspects. **Pure Appl. Chem.** 67, 345-373.
- Vijayakumar, G.R., Lohith, K., Somashekar, B.R., Divakar, S. (2004). Lipase catalysed synthesis of L-alanyl, L-Leucyl and L-phenylalanyl esters of D-glucose using unprotected amino acids. **Biotechnol. Lett.** 26, 1323-1328.
- Vogel, I. (1961). In: A text book of quantitative inorganic analysis. Potentiometric titrations, 3rd edition, ELBS and Langman group Ltd., London. 944-948.
- Volkin, D.B., Staubli, A., Langer, R., Klibanov, A.M. (1991). Enzyme Thermoinactivation in anhydrous organic solvents. **Biotechnol. Bioeng.** 37, 843-853.
- Vorderwulbecke, T., Kieslich, K., Erdmann, H. (1992). Comparison of lipases by different assays. **Enzyme Microb. Technol.** 14, 631-639.
- Vulfson, E.N. (1994). In: Lipases their structure biochemistry and application, eds. Industrial applications of lipases, Wolley, P., Petersen, SB: Cambridge University Press, New York USA.
- Vulfson, E.N. (1996) Enzymatic synthesis of food ingredients in low water media. **Trends Food Sci. Technol.** 4, 209-215.
- Wei, Y., Schottel, J.L., Derewenda, U., Swenson, L., Patkar, S., Derewenda, Z.S. (1995). A novel variant of the catalytic triad in the *Streptomyces scabies* esterase. **Nat. Struct. Biol.** 2, 218 – 223.
- Welsh, F.W., Williams, R.E. (1990). Lipase-mediated production of ethyl butyrate and butyl butyrate in nonaqueous systems. **Enzyme Microb. Technol.** 12:743-748.
- Welsh, F.W., Williams, R.E., Dawson, K.H. (1990). Lipase-mediated synthesis of low molecular weight flavor esters. **J. Food Sci.** 55, 1679-1682.
- Winkler, F. K., Gubernator, K. (1994). Structure and mechanism of human pancreatic lipase. In: Wooley, P., Peterson, S. B. (Eds). Lipase : Their structure, Biochemistry and Applications. Cambridge University Press, Cambridge. pp- 139-157.
- Winkler, F., D'Arcy, A., Hunziker. (1990) Structure of human pancreatic lipase. **Nature** 343, 771.

- Winkler, F., Gubernator, K. (1986). Structure and mechanism of human pancreatic lipase. In: Lipases. Woolley and Petersen (eds), Cambridge University Press. Cambridge, pp-139-157.
- Wu, J., Ding, X. (2002). Characterization of inhibition and stability of soy-protein derived angiotensin I-converting enzyme inhibitory peptides. **Food Res. Int.** 35, 367-375.
- Wu, J.C, Song, B.D., Xing, A.H., Hayashi, Y., Talukder, M. M. R., and Wang. S. C. (2002). Esterification reactions catalyzed by surfactant-coated *Candida rugosa* lipase in organic solvents. **Proc. Biochem.** 37, 1229-1233.
- Wu, J.Y., Liu, S.W. (2000). Influence of alcohol concentration on lipase-catalyzed enantioselective esterification of racemic naproxen in isooctane: under controlled water activity **Enzyme Microb. Technol.** 26, 124-130.
- Xu, Y., Wang, D., Qing-Mu, X., Ao-Zhao, G., Zhang, K.C. (2002). Biosynthesis of ethyl esters of short chain fatty acids using whole -cell lipase from *Rhizopus Chinesis* CCTCCM 201021 in non aqueous phase. **J. Mol. Cata. B: Enzymatic** 18, 29-37.
- Yadav, G.D., Lathi, P.S. (2004). Synthesis of citronellol laurate in organic media catalyzed by immobilized lipases: kinetic studies. **J. Mol. Cata. B: Enzymatic.** 27, 113-119.
- Yadav, G.D., Devi, K.M. (2004). Immobilized lipase-catalysed esterification and transesterification reactions in non-aqueous media for the synthesis of tetrahydrofurfuryl butyrate: comparison and kinetic modeling. **Chem. Eng. Sci.** 59, 373 - 383.
- Yadav, G.D., Lathi, P.S. (2003). Kinetics and mechanism of synthesis of butyl isobutyrate over immobilised lipases. **Biochem. Eng. J.** 16(3):245-252.
- Ye, P., Xu, Z.K., Wang, Z.G., Wu, J., Deng, H.T., Seta, P. (2005). Comparison of hydrolytic activities in aqueous and organic media for lipases immobilized on poly (acrylonitrile-co-maleic acid) ultrafiltration hollow fiber membrane. **J. Mol. Cata. B: Enzymatic.** 32, 115-121.
- Zaidi, A., Gainer, J.L., Carta, G., Mrani, A., Kadiri, T., Belarbi, Y., and Mir, A. (2002). Esterification of fatty acids using nylon-immobilized lipase in *n*-hexane: kinetic parameters and chain length effects. **J. Biotechnol.** 93, 209-216.
- Zaks, A., Dodds, D.R. (1997). Applications of biocatalysts and biotransformations to the synthesis of pharmaceuticals. **Drug Dev. Today.** 2, 513 -531.
- Zaks, A., Klibanov, A.M. (1984). The effect of water on enzyme reaction in organic media. **J. Biol. Chem.** 263, 8017-8021.
- Zaks, A., Klibanov, A.M. (1985). The effect of water on enzyme activity in organic media. **Proc. Natl. Acad. Sci. USA.** 82, 3192-3196.

Zaks, A., Klivanov, A.M. (1986). Substrate specificity of enzymes in organic solvents vs. water is reversed. **J. Am. Chem. Soc.** 108, 2767-2768.

Zaks, A., Klivanov, A.M. (1988). The effect of water on enzyme action in organic media. **J. Biol. Chem.** 263, 8017-8021.

Zhang, T., Yang, L., Zhu, Z. (2005). Determination of internal diffusion limitation and its macroscopic kinetics of the transesterification of CPB alcohol catalyzed by immobilized lipase in organic media. **Enzyme Microb. Technol.** 36, 203-209.

Zhou, G.W., Li, G.Z., Xu, J., Sheng, Q. (2001). Kinetic studies of lipase-catalyzed esterification in water-in-oil microemulsions and the catalytic behavior of immobilized lipase in MBGs. **Colloids and Surfaces A: Physicochem. Eng. Aspects.** 194, 41-47.

Zhu K, Jutila A, Tuominen E.K.J, Patkar SA, Svendsen A, Kinnunen PK. (2001). Impact of the tryptophan residues of Humicola lanuginosa lipase on its thermal stability. **J Biochim Biophys Acta** 1547, 329-38.

Zoser. (2005). Anti-cancer composition comprising proline or its derivatives as anti-tumor antibody. WO2005 120495. European patent A61K39/395C3. (CA 144: 35316).